TABLE DES MATIÈRES

Page

LISTE DES TABLEAUX

Page

LISTE DES FIGURES

LISTE DES ABRÉVIATIONS, SIGLES ET ACRONYMES

d	distance inter électrodes
E	champ électrique dans le cas où r<<d
I_c	courant de conduction
U_0	amplitude de la tension appliquée
U(t)	tension appliquée
I(t)	courant induit
r_p	rayon de courbure de la pointe
t	temps
T°	température
T_v	température de transition vitreuse
T_f	température de fusion
Y	module de Young
ε_0	permittivité du vide =8,85418782 × 10-^{12} m^{-3} kg^{-1} s^4
ε'	partie réelle de la permittivité diélectrique
ε'	partie imaginaire de la permittivité diélectrique
ε_r	permittivité relative
α	paramètre d'échelle
β	paramètre de forme
n	nombre d'échantillon testé
r_i	nombre d'échantillon claqué

Acronymes

ASTM	American Society for Testing and Materials
ATR	Attenuated Total Reflexion
CRSNG	Conseil de recherches en sciences naturelles et en génie du Canada
DC	Décharges couronne
DMT	Diméthyle téréphtalate
DP	Décharges partielles
DSC	Differential Scanning Calorimetry
HT	Haute tension
IR	Infrarouge
IEC	International Electrotechnical Commission
IEE-STD930	IEE guide for Statistical Analysis of Electrical Insulation Breakdown Data.
MEB	Microscopie électronique à balayage
PEN	Polyéthylène Naphthalate
PET	Polyéthylène Téréphtalate
TGA	Thermogravimetric analysis

INTRODUCTION

Aujourd'hui, le développement des composites à base de matériaux recyclés est devenu une préoccupation primordiale étant donné les bénéfices économiques et environnementaux soulevés par l'utilisation des matériaux recyclés. Les travaux proposés dans ce manuscrit s'inscrivent dans le cadre d'une étude sur la caractérisation diélectrique des matériaux composites à base de thermoplastiques recyclés destinés à la fabrication de supports mécaniques des bougies d'allumage dans le domaine d'automobile ou à toute autre application en électronique ou en électrotechnique pour laquelle les propriétés diélectriques doivent être examinées. Les résultats obtenus par cette étude pourront être exploitées pour améliorer les recettes existantes afin de concevoir des pièces convenables pour des applications diélectriques, plus particulièrement dans le domaine de l'automobile.

L'objectif global du projet est d'évaluer la fiabilité des composites fabriqués à base de matrice recyclée et de vérifier la possibilité de les utiliser pour des applications électriques telles que le support mécanique des systèmes haute tension dans le domaine de l'automobile. La figure ci-dessous illustre un support mécanique de bougie d'allumage fabriqué par le Groupe Lavergne à partir d'un composite à base de matériau recyclé renforcé de renforts inorganiques.

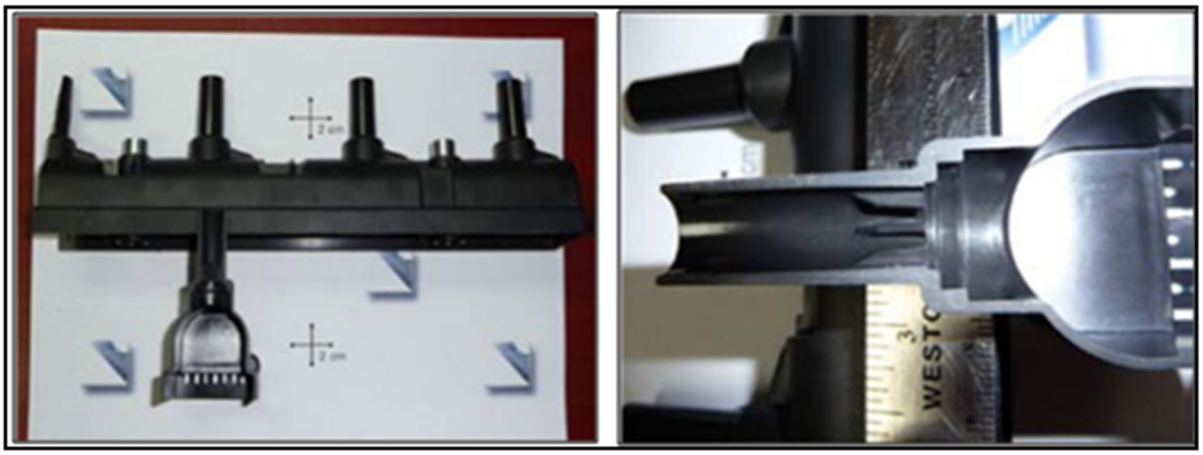

Figure 0 1.1 Support pour le système d'allumage fabriqué à partir du PET recyclé
Tirée d'Éric David (2009, p. 20)

Parmi la diversité des matériaux thermoplastiques utilisés en industrie, le projet se focalisera sur le polyéthylène téréphtalate (PET) recyclé et le polyéthylène Naphthalate (PEN). Des

renforts inorganiques comme les fibres de verre courtes et le mica permettent d'améliorer certaines propriétés des polymères thermoplastiques. Cependant, cette amélioration est accompagnée par une diminution du champ de rupture et de l'endurance diélectrique de ce matériau(Roy et al., 2005). Certains plastifiants ont été également incorporés en vue d'améliorer la structure de la surface et de faciliter la mise en œuvre des composites. La figure ci-dessous illustre la structure chimique des deux polyesters employés lors de cette étude.

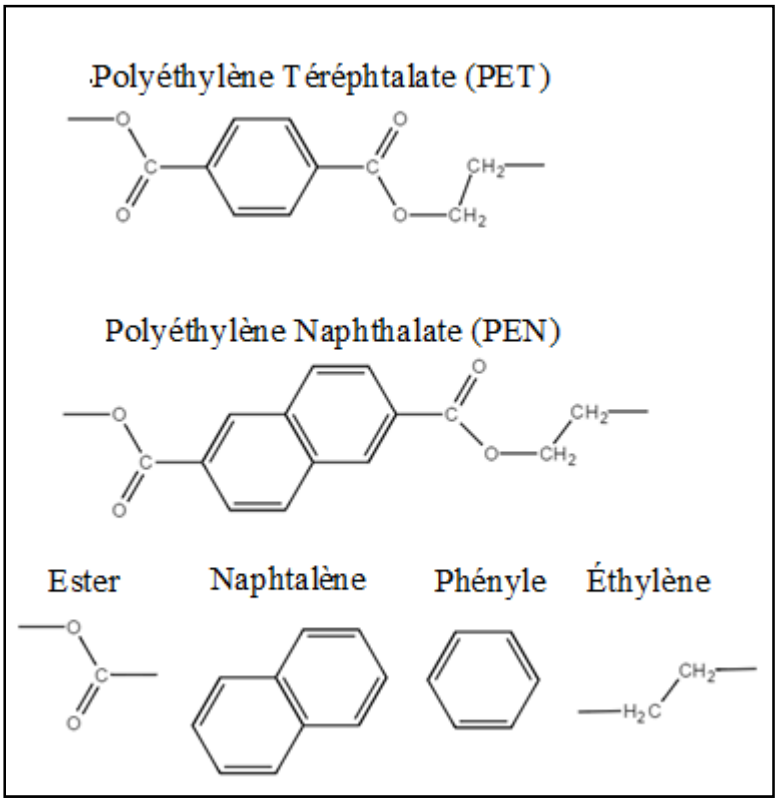

Figure 0 1 Structure chimique du PET et PEN

La fiabilité d'un système isolant dépend de certains facteurs qui sont liés particulièrement à sa composition et aux conditions d'application dans lesquelles il doit opérer. Dans notre étude, ce matériau composite à base de matériau recyclé renforcé de fibres de verre courtes et de mica est considéré comme un mélange hétérogène possédant une interface matrice-renforts assez complexe. Ainsi, chaque composant joue un rôle primordial dans la dégradation des composites soumises à certaines contraintes électriques et thermiques. En effet, les différentes mesures réalisées sur les propriétés diélectriques, comme la rigidité diélectrique et l'endurance

estimée à partir des essais de vieillissement accéléré sous effet couronne, ont été jugées également nécessaires pour confirmer la fiabilité des sources du PET recyclé. L'interface polymère-renforts qui correspond aux surfaces de contact entre la matrice et les différents renforts compte parmi les facteurs contribuant à la dégradation des composites. En effet, l'impact des différents renforts (fibres de verre et mica) sur les propriétés diélectriques telles que la permittivité complexe du matériau doit être pris en considération durant cette étude. Dans ce contexte, il serait donc opportun de s'intéresser à l'état de l'interface renforts-matrice qui est généralement un moyen pertinent pour investiguer la fiabilité des composites.

La problématique de notre étude se situe principalement au niveau de la confirmation de la fiabilité des sources recyclées provenant du recyclage de cartouches d'encre et de bouteilles fabriquées en PET. Notre solution se base essentiellement sur l'étude approfondie des différentes propriétés du PET recyclé. Des méthodes de caractérisation sous contraintes électriques et thermiques extrêmement sévères permettront de comprendre le comportement des matériaux candidats, à la fois au niveau de l'endurance et au niveau de la réponse diélectrique. Le polyester polyéthylène Naphthalate qui est un matériau ayant une structure chimique très proche du PET joue le rôle du matériau concurrent dans notre étude permettra ainsi de valider la fiabilité du PET recyclé.

Pour atteindre notre objectif la démarche décrite ci-dessous sera adoptée :

Dans un premier chapitre, une revue de littérature détaillée sur les plastiques et leurs utilisations dans l'industrie automobile sera présentée. Nous présenterons également une revue sur les polymères renforcés par des matières inorganiques. Cette partie sera complétée par quelques définitions et notions de base sur les propriétés thermiques et diélectriques les plus importantes dans le cas des polymères. Après avoir établi un état de l'art sur la théorie des milieux effectifs et les lois des mélanges, une synthèse bibliographique sur les travaux antérieurs effectués sur l'étude de la réponse diélectrique par différentes méthodes numériques et théoriques sera faite.

Le deuxième chapitre est entièrement consacré à la présentation des matériaux fournis et les différentes méthodes utilisées pour l'évaluation de la fiabilité des sources de PET recyclé. Nous commençons d'abord par une description des différents matériaux étudiés. Nous verrons par la suite les diverses techniques expérimentales optées pour l'étude des propriétés thermiques et diélectriques. Une attention particulière sera accordée aux procédés de vieillissement électriques, thermiques et combinés.

Nous présenterons dans le troisième chapitre, les effets du vieillissement électrothermique sur le polyéthylène téréphtalate recyclé (RPET) et ses différents composites. Une comparaison entre un composite à base du PET recyclé et son concurrent le PET vierge (provenant de l'industrie pétrochimique) sera établie.

Dans le quatrième chapitre, nous étudierons la relation entre la réponse diélectrique et les propriétés thermiques du PET recyclé et du PEN. L'effet de l'ajout des renforts inorganiques (particulièrement les flocons de mica) sur les pertes diélectriques et la permittivité complexe sera abordé.

Nous traitons dans le cinquième chapitre les effets du vieillissement thermique sur les propriétés diélectriques (notamment la rigidité et les pertes diélectriques) et les propriétés thermiques (principalement la cristallisation et la transition vitreuse) des polymères d'études ainsi que leurs composites.

Dans le sixième chapitre, nous verrons la modélisation de la permittivité complexe dans le domaine fréquentiel d'un composite biphasique en 2D. Nous verrons également la modélisation 3D d'un système hétérogène.

Enfin, les principales conclusions et perspectives tirées lors de cette recherche seront abordées. Sur la base de nos constatations, la fiabilité des ressources du PET recyclé sera confirmée.

Notre objectif principal est d'étudier la possibilité d'utiliser des composites à base de matériaux recyclés pour la fabrication des pièces pour des applications diélectriques. Plus précisément, le projet se concentrera sur l'étude de la fiabilité des composites à base de Polyéthylène Téréphtalate (PET) recyclé renforcés de fibre de verre courte et mica pour la fabrication des pièces pour des applications électriques comme le support du système d'allumage dans les moteurs à combustion interne dans le domaine d'automobile. Du Polyéthylène Naphthalate (PEN) qui possède une température de transition vitreuse supérieure à celle du PET sera également caractérisée afin de déterminer la possibilité d'augmenter la performance des composites par l'ajout de ce polyester au composite.

Le travail envisagé consiste à caractériser les propriétés diélectriques des matériaux composites à base de résine de PET et de PEN, et plus particulièrement au niveau de la réponse diélectrique et de l'endurance. L'investigation servira à ajuster les formulations existantes tout en respectant les conditions de service surtout que ces composites doivent opérer sous contraintes électriques et thermiques extrêmement sévères. Pour atteindre cet objectif axé essentiellement sur l'amélioration des recettes existantes pour le développement des composites à base de matériaux recyclés opérant sous contraintes électriques et dans un intervalle de température allant jusqu'à 140°C, notre recherche sur ce sujet s'articulera autour des points suivants :

- **Sur le plan pratique et industriel**

1. Caractérisation diélectrique des matériaux candidats et vérification de plusieurs paramètres. Cette vérification comprend les points suivants :

- L'évaluation de la possibilité d'ajouter une quantité de PEN au PET afin d'améliorer les propriétés diélectriques des composites ;
- La vérification de la fiabilité des sources du PET recyclé.
- L'analyse de l'effet des différents renforts sur les propriétés diélectriques et thermiques.

2. Perfectionnement du banc d'essai des mesures d'endurance sous effet couronne afin d'effectuer des tests de vieillissement accéléré jusqu'à la rupture diélectrique des échantillons.

3. Étude de l'endurance des matériaux soumis à des contraintes électriques ou/et thermiques.

- **Au niveau de la recherche scientifique**

- Des mesures de permittivité complexe des deux polymères d'études ainsi que leurs composites avant et après exposition aux décharges partielles.
- La modélisation de la réponse diélectrique des différents composites fournis et caractérisation de l'interface matrice-renforts qui joue un rôle indispensable dans les mécanismes de rupture.

CHAPITRE 1

ÉTUDE BIBLIOGRAPHIQUE

1.1 Introduction

Dans les principaux domaines d'application de la haute tension, les composites à base de matrice thermodurcissable ont longtemps dominés comme isolation électrique et thermique, en grande partie pour leur résistance à la détérioration causée par les décharges électriques et d'autre part pour leur résistance à la haute température. Cependant, le développement de nouveaux matériaux à base de matrice thermoplastique afin de remplacer ces matériaux classiques est devenu de plus en plus répandu. Ces matériaux innovateurs sont devenus les matériaux prometteurs dans plusieurs secteurs d'industrie grâce à leurs propriétés, particulièrement le faible coût et la possibilité d'utiliser des ressources recyclées. Ces bénéfices ont grandement ouvert de nombreux marchés notamment dans l'industrie automobile, construction et aéronautique.

La maîtrise des procédés de fabrication, la caractérisation des produits et le contrôle de qualité sont les paramètres essentiels permettant non seulement l'innovation de matériaux plus performants mais aussi à moindre coût. En effet, de nombreux avantages sont offerts par l'utilisation des composites à base de matrice thermoplastique notamment la possibilité d'utiliser des matières recyclables, l'ajustement des propriétés selon leur application et la facilité de la mise en forme. En outre, l'utilisation des ressources recyclées contribue surtout à la réduction de l'impact négatif sur l'environnement.

Le développement de nouveaux matériaux composites plus performants suscite beaucoup d'intérêt dans plusieurs secteurs d'industrie. En effet, la demande de nouveaux matériaux fabriqués à partir de ressources recyclées est en pleine croissance et le développement des composites à base des matériaux recyclés occupe une grande partieau niveau de la recherche. Cependant, le développement ne nécessite pas seulement la maîtrise des procédés de

fabrication mais aussi la connaissance des différentes propriétés des composites qui restent parfois mal connues, la raison pour laquelle la connaissance des propriétés des composites nécessitent la prédiction par modélisation ce qui permettra de prédire les propriétés effectives d'un matériau composite à partir de la connaissance des propriétés des différentes phases.

L'objectif générique de ce projet est d'acquérir une meilleure compréhension des propriétés diélectriques de matériaux composites à base de Polyéthylène téréphtalate (PET) recyclé tant au niveau de la réponse diélectrique qu'au niveau de l'endurance et la rigidité diélectrique. L'étude de la réponse diélectrique permet de caractériser l'interface matrice/renforts, qui est généralement responsable de la rupture diélectrique, et d'autre part d'améliorer les modèles existants en utilisant par exemple des modèles à paramètres variables.

Les matériaux composites ont trouvé des applications dans différents secteurs notamment en industrie aéronautique, automobile et bâtiment. En effet, le développement des composites est devenu, aujourd'hui, d'une nécessité évidente offrant des avantages permettant d'obtenir des matériaux convenables pour certaines applications que les matériaux classiques ne peuvent pas l'être(Lan & Pinnavaia, 1994; Quintanilla, Rodríguez-Cabello, Jawhari, & Pastor, 1994; Sahu & Broutman, 1972; Willems, 1995).

1.2 Les polymères et l'industrie automobile

1.2.1 L'industrie automobile

Les composites à base de résines polymères sont omniprésents en industrie automobile. De nos jours, leurs utilisations augmentent de plus en plus grâce à leurs multiples avantages. Les résines polymères les plus populaires sont les thermoplastiques. Grâce à la possibilité du recyclage, ces matériaux sont devenus les matériaux d'intérêt à l'heure actuelle. En effet, le recyclage de ces matériaux offre une préservation des matières premières, une protection de l'environnement contre la pollution ainsi qu'une économie importante pour les fabricants.

Dans le domaine de l'industrie canadienne, la fabrication des pièces d'automobile en matière plastique s'est amplifiée au quart de sa totalité au cours de ces dernières années. Dans le secteur d'automobile, plus de 10% des composants des véhicules sont fabriqués à base de matériaux plastiques pur renforcés par des additifs. Ils sont présents dans l'aménagement intérieur comme à l'extérieur ou au niveau du moteur : les sièges, les ceintures de sécurités, les phares, les fixations, les tableaux de bord, le collecteur d'air qui permet d'optimiser le débit d'air, le support mécanique des bougies d'allumage ainsi que d'autres accessoires. L'utilisation du plastique résulte en une baisse de la consommation du carburant et conséquemment en une diminution de l'émission des gaz à effet de serre. En effet, une réduction d'environ 100kg du poids total d'un véhicule permet de réduire sa consommation de carburant d'environ 0.2l aux 100 km et de baisser ses émissions de CO_2 d'environ 10g/km (MIT, 2008).

Le support mécanique des bougies d'allumage qui est un composant important du système d'allumage des moteurs à combustion interne sert à fixer fermement les bougies d'allumage et à les protéger. Quant aux bougies, elles servent à provoquer l'étincelle entre le carburant et le gaz dans un moteur à combustion interne. Une bougie usée peut évidemment entrainer une surconsommation du carburant dans le moteur d'automobile. Au cours de l'allumage, des décharges électriques surviennent au niveau du moteur à combustion interne. Ainsi, le support sera assujetti aux décharges, ce qui peut entrainer la détérioration du matériau. Le support devrait résister non seulement aux contraintes électriques mais également aux contraintes thermiques. En augmentant la température d'opération du support, il sera donc possible d'élever la température du fonctionnement des moteurs et ainsi réduire sa consommation de carburant en augmentant l'efficacité du moteur.

Le support mécanique des bougies d'allumage compte parmi les composants d'automobile fabriqués à base des résines polymériques renforcées de fibres de verre et de mica. Ces composites offrent une large liberté de design et permettent de réduire globalement le coût et le poids par rapport aux plastiques classiques notamment si le composite est conçu à base de thermoplastique recyclé. En effet, les manufacturiers d'automobile sont très influencés par la nouvelle tendance de réduire au maximum le coût de fabrication tout en respectant la fiabilité

des véhicules. C'est la raison pour laquelle, plusieurs recherches ont été effectuées sur l'élaboration de nouveaux composites à base de matériaux recyclés (Adhikary, Pang, & Staiger, 2008; Bentchikou, 2008; Lei, Wu, Yao, & Xu, 2007; Singleton, Baillie, Beaumont, & Peijs, 2003). La figure 1.1 présente un support de bougies d'alimentation d'un un moteur d'automobile.

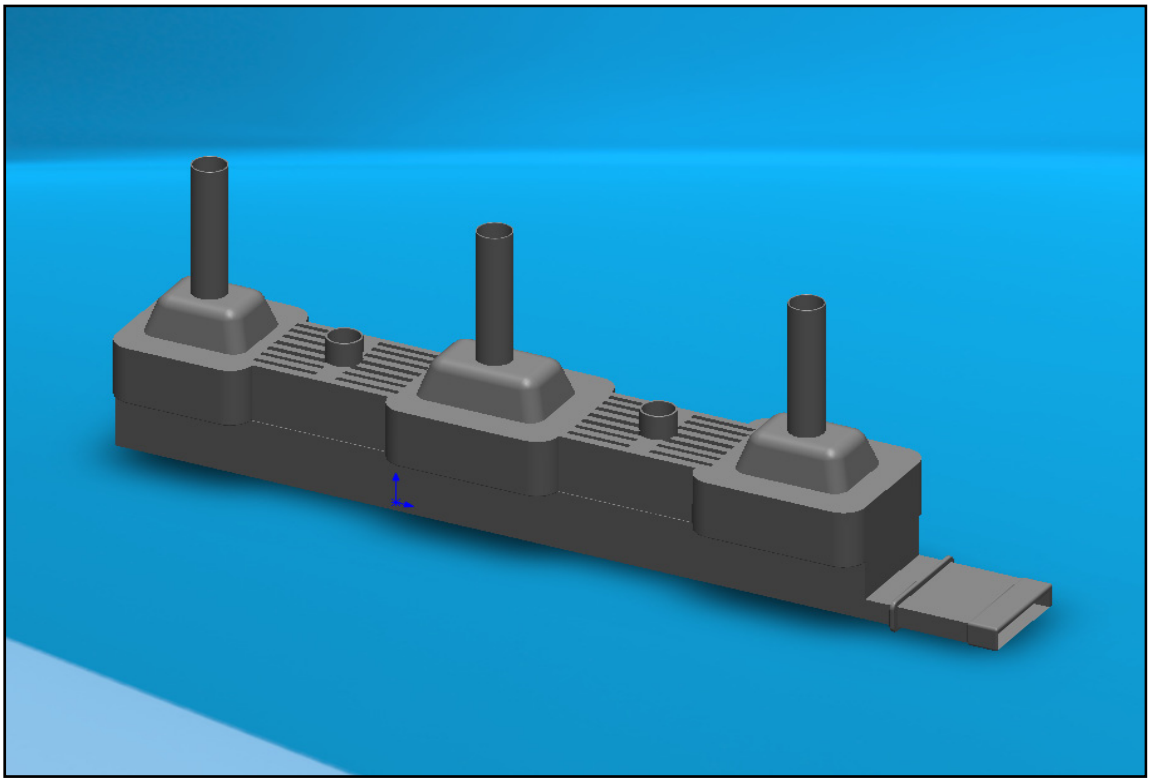

Figure 1.1 Support pour le système d'allumage

1.2.2 Les polymères

Les plastiques, appelés polymères en science des matériaux, sont des matériaux obtenus par polymérisation. Ce processus permet de convertir un monomère ou un ensemble de monomère en une macromolécule dite polymère. Ils sont fréquemment employés comme matrice dans les composites destinés à différentes applications. Ces polymères sont classés selon leurs natures en trois distinctes catégories, les thermodurcissables, les thermoplastiques et les élastomères.

Les thermoplastiques comme les thermodurcissables sont largement utilisés en plusieurs secteurs d'industrie.

Le Polyéthylène téréphtalate connu sous l'abréviation PET est un polymère issu habituellement par polycondensation de l'acide téréphtalique et l'éthylène glycol, une réaction chimique au cours de laquelle on obtient du polyéthylène téréphtalate et deux molécules d'eau. Le Polyéthylène Naphthalate est produit également par polycondensation d'acide naphtalène-2,6-dicarboxylique ou d'un dérivé fonctionnel de celui-ci, tel que le 2,6-dicarboxylate de diméthylnaphtalène avec de l'éthylène glycol dans des conditions réactionnelles appropriées en présence d'un catalyseur(Sakamoto & Sato, 1988).La figure 1.2 illustre la méthode de synthèse du PET et de PEN par polycondensation.

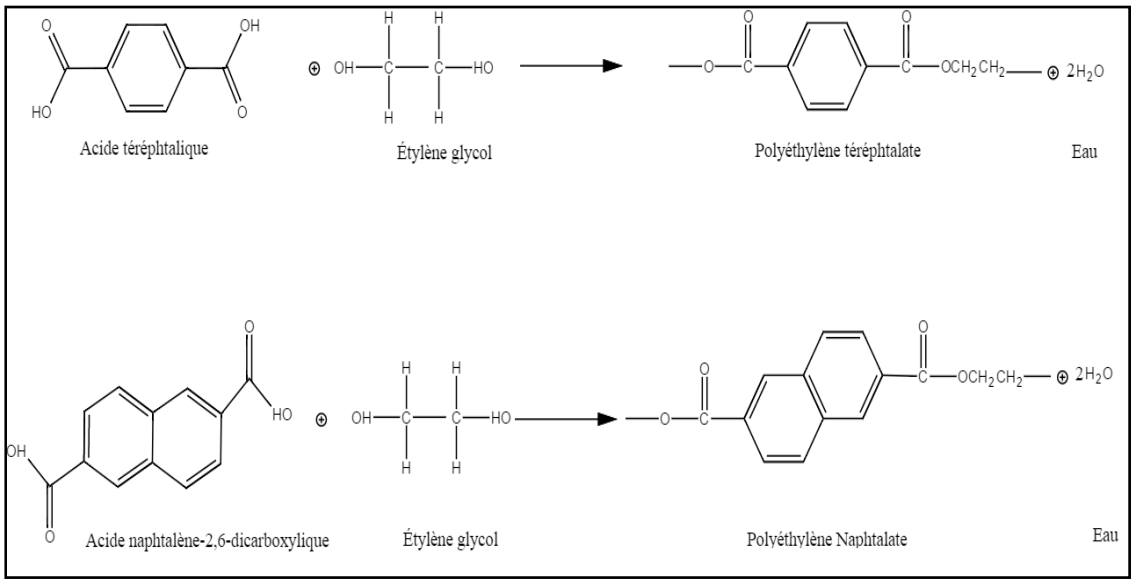

Figure 1.2 Méthode de synthèse du PET et PEN par polycondensation

1.3 Les composites

Les matériaux composites sont indispensables dans les domaines de l'industrie aéronautique, de l'automobile, de la construction ou des applications électrotechniques. Certains composites peuvent atteindre un certain niveau de performance grâce aux propriétés améliorées que les

éléments de base comme la matrice et les renforts ne possèdent pas séparément. C'est ainsi que la conception préliminaire de ces matériaux permet de comprendre et de contrôler également le comportement d'un matériau en fonction de son domaine d'utilisation.

1.3.1 Les thermoplastiques et le recyclage

Le recyclage n'est pas une invention moderne du 19^{e} siècle. Cette notion existait déjà il y a longtemps sous le nom de réutilisation, et n'a cessé de se développer surtout à l'échelle industrielle. En effet, ce concept omniprésent dans le secteur industriel suscite actuellement beaucoup d'intérêt en partie à cause des bénéfices économiques et d'autre part à cause de la diminution remarquable des effets nuisibles sur l'environnement. La fiabilité et la qualité des sources de matières recyclables sont primordiales. La question qui se pose alors est de savoir si les matières plastiques recyclées gardent réellement leur performance après le recyclage. Plusieurs facteurs doivent intervenir pour répondre à cette question. En effet, le bon tri constitue la phase initiale d'un recyclage crédible et adéquat. La seconde phase est le processus de recyclage. Cette phase constitue un facteur critique de l'ensemble des opérations notamment dans le recyclage des matières plastiques.

Les thermoplastiques issus des déchets peuvent être recyclés plusieurs fois en conservant relativement leur performance sans altérer leurs propriétés de façon importante. Certains types de thermoplastiques nécessitent un procédé de recyclage différent des autres matières. Le PET utilisé pour la fabrication des bouteilles de boissons gazeuses est considéré comme le thermoplastique le plus recyclé dans l'industrie de recyclage des matériaux plastiques. Ce matériau d'ingénierie a prouvé sa performance et fiabilité pour ses applications usuelles(Sulyman, Haponiuk, & Formela, 2016).Une attention particulière a été portée aux différents processus de recyclage du PET dans certaines études(Awaja & Pavel, 2005; Fregoso-Infante, Vega-Rangel, & Figueroa-Gomez-Crespo, 2011;Pietrasanta, 1996).

1.3.2 Les renforts inorganiques

Le concept de renfort est apparu après de nombreuses tentatives faites pour réduire le coût des matières plastiques destinées à certaines applications. En effet, plusieurs types de matières peu couteuses ont été introduits afin d'élaborer des matériaux plastiques à moindre coût. Certaines charges peuvent affecter considérablement leurs propriétés comme elles peuvent améliorer significativement d'autres propriétés. C'est ainsi que la conception des matériaux plastiques renforcés convenables à certaines applications a commencé. La conception permet de prédire les propriétés finales d'un matériau afin d'assurer la fiabilité et la performance nécessaire à l'application pour laquelle ce matériau est destiné.

Certains renforts sont utilisés principalement pour améliorer les propriétés des polymères, notamment les propriétés mécaniques. Ils peuvent être classés selon leur nature en trois catégories : les renforts inorganiques, organiques et métalliques. Ils peuvent être classés également selon leur structure en fibres courtes ou longues, en particules, en tissu, en mât ou en voile. Comme elles peuvent être différenciées selon leur composition chimique, on compte ainsi les fibres A, C, D, E, R et S. Les fibres de verre sont parmi les renforts inorganiques les plus utilisées en industrie. Ces renforts se classent parmi les fibres utilisées afin d'améliorer les propriétés mécaniques des polymères thermoplastiques (voir figures 1.3). Par exemple l'addition de 10% de fibres de verre résulte en une augmentation significative du module élastique et de la résistance à la traction du polypropylène(Mebarki, 2012; Richardson & Sauer, 1976). De plus, le traitement des fibres de verre assure une meilleure adhésion avec le polymère (Etcheverry & Barbosa, 2012). Plusieurs types de fibres de verre sont utilisés comme renforts inorganiques pour différents polymères. Les fibres de verre (type E) conviennent aux applications d'usage général. Ces fibres se distinguent par une haute résistance thermique et offrent de bonnes propriétés d'isolement électrique.

Des flocons ou paillettes de mica comptent également parmi les renforts inorganiques utilisées, surtout pour des applications dans des isolations électriques. Ces renforts donnent en effet une excellente stabilité diélectrique et thermique en plus de l'amélioration de la rigidité

diélectrique. Ils peuvent également améliorer la conductivité thermique des polymères qui sont généralement des résines de faible conductivité thermique.

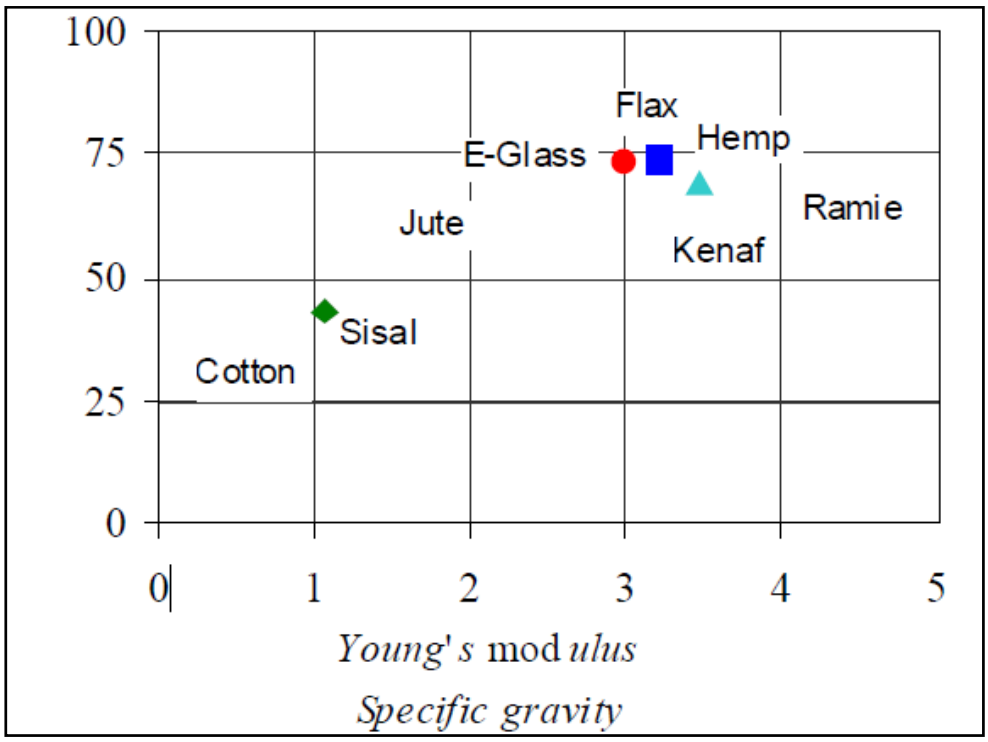

Figure 1.3 Module élastique et la résistance à la traction pour différents types de fibres
Tirée (Mueller & Krobjilowski, 2004)

1.4 Les propriétés thermiques

1.4.1 La transition vitreuse

La transition vitreuse compte comme la plus importante phase thermique d'un polymère. C'est le stade où les zones amorphes du polymère passent de l'état caoutchouteux à l'état solide vitreux avec le refroidissement. La transition vitreuse est considérée comme la phase thermique la plus intéressante d'un polymère et est en effet spécialement critique dans le procédé de mise en œuvre des polymères thermoplastiques. C'est un stade où les zones amorphes passent de l'état souple caoutchouteux à l'état solide vitreux (avec le refroidissement). Au cours de la transition vitreuse, la mobilité des chaines polymériques augmente significativement. Cette

phase est caractérisée par une température qu'on appelle la température de transition vitreuse (T_v) Cette température ne dépend pas seulement de la structure chimique du polymère mais aussi de certains facteurs thermodynamiques tels que la vitesse du chauffage et le refroidissement ainsi que la pression exercée au cours du procédé de mise en œuvre. La densité et la distribution des chaines moléculaires sont également des facteurs structuraux significatifs, dans le contrôle de la température de transition vitreuse.

L'analyse enthalpique différentielle est la technique la plus couramment utilisée en milieu industriel ou académique pour la recherche et la détermination de la transition vitreuse. Les mesures se font typiquement selon la norme ASTM-E1356 (Standard Test Method for Assignment of the Glass transition temperature by Differential Scanning Calorimetry). Cette grandeur est déterminée à partir du milieu du saut de la capacité calorifique. Au cours de la transition vitreuse, des changements significatifs peuvent apparaître au niveau des propriétés d'un polymère. En effet, la transition vitreuse d'un matériau polymère s'accompagne toujours d'un changement significatif de son comportement mécanique (Lawrence & Robert, 1994). En plus, le décalage du pic de relaxation des pertes diélectriques est particulièrement associé à la transition vitreuse du polymère (McCrum, Read, & Williams, 1967).

1.4.2 La fusion

La fusion est un processus thermodynamique permettant de modifier la structure des chaines moléculaires. Pendant ce processus, la chaleur absorbée fournit l'énergie au matériau qui passe à l'état de fondu. Ce paramètre, appelé enthalpie de fusion, est nécessaire pour le passage de l'état solide ordonné à l'état liquide désordonné. Ce changement s'effectue à une température qu'on appelle la température de fusion (T_f). Cette température reste pratiquement stable pendant la fusion du polymère. Cette grandeur est déterminée comme le maximum du pic endothermique.

1.5 La morphologie et la cristallisation

1.5.1 La morphologie

Les polymères thermoplastiques semi-cristallins ont une morphologie complexe combinant à la fois des zones cristallines hautement ordonnées appelées sphérolites et des zones amorphes désordonnées. La cohésion de l'ensemble polymérique est favorisée par des liaisons secondaires faibles pouvant être facilement détruites avec une faible croissance d'énergie thermique. Ces liaisons peuvent également se reformer lorsque le thermoplastique est refroidi. C'est ainsi qu'il revient à son état vitreux d'origine.

1.5.2 La cristallisation

La cristallisation des polymères est un processus très complexe. Cette transformation entièrement thermodynamique permet aux conformations des chaines moléculaires de s'organiser afin de former une structure ordonnée. Bien qu'on parle d'une distribution ordonnée des chaines moléculaires, seulement une partie de ces chaines conserve en effet son emplacement dans les zones amorphes. C'est d'ailleurs ainsi qu'un polymère semi-cristallin se forme et la notion du taux de cristallinité s'applique. Les propriétés polymériques dépendent fortement du taux de cristallinité. Ce paramètre défini comme étant la fraction des zones cristallines du polymère par rapport au même polymère 100% cristallin peut être contrôlé par certains facteurs thermodynamiques du procédé de la mise en forme comme la température, la vitesse et le temps de refroidissement ou mécaniques tel que le degré d'étirage et le taux de cisaillement (Avenas, 1978). Bien que de nombreuses études sur l'effet des paramètres de la mise en forme aient été faites, aucune formule générale ou loi quantitative permettant le contrôle total du taux de cristallinité des polymères n’existe à ce jour.

1.5.3 La cristallisation froide

La cristallisation froide s'observe dans un polymère amorphe ayant la tendance de se cristalliser sous l'effet d'une contrainte thermique ou dynamique. Ce processus est caractérisé par un pic endothermique qui apparaît après la transition vitreuse. En effet, les chaînes moléculaires sont relativement rigides mettant en évidence leur mobilité. Au-delà de la transition vitreuse, l'énergie thermique fournie au polymère offre une certaine mobilité aux chaînes permettant ainsi un réarrangement (réorganisation) partiel dans les zones cristallines. La figure 1.4 illustre un thermographe d'un échantillon de PET recyclé représentant une cristallisation froide.

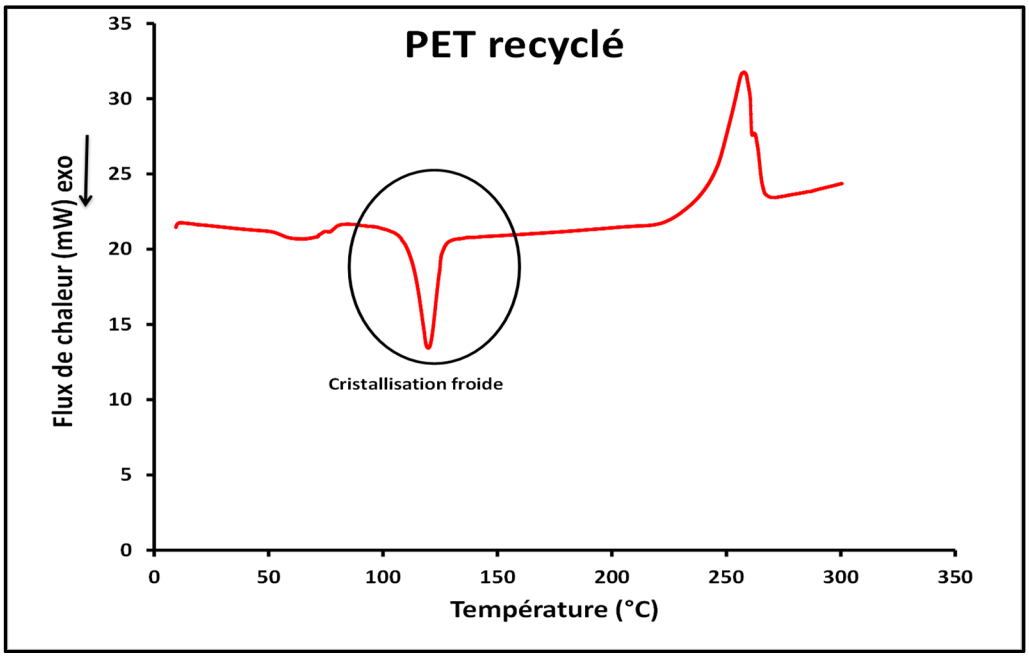

Figure 1.4 Thermographe d'un échantillon de PET recyclé

1.6 Les propriétés diélectriques

Un matériau composite est un ensemble de deux ou plusieurs constituants ayant des propriétés supérieures à celles des composants. Le succès dans le secteur des matériaux composites à base de résine thermoplastique est tributaire d'une série de facteurs comme la possibilité de développer des composites ayant des propriétés très diverses dépendamment des caractéristiques des différents constituants. L'interface polymère-renforts qui correspond aux

surfaces de contact entre le polymère et les différents renforts joue un rôle primordial lors du vieillissement des composites soumis à des contraintes électriques et thermiques sévères. Ce qui rend l'interprétation des mécanismes de relaxation interfaciale dans un composite un concept important et nécessaire pour investiguer la qualité de l'interface matrice-renforts et un moyen efficace pour la conception des matériaux ayant les propriétés convenables pour certaines applications diélectriques.

Dans cette partie, nous rappellerons brièvement les concepts de base qui vont nous permettre plus tard d'effectuer l'analyse de la réponse diélectrique des matériaux composites et notamment l'interprétation du spectre de la permittivité diélectrique complexe.

1.6.1 Concept de polarisation

Un matériau diélectrique possède peu ou pas de charges libres, ce qui limite la circulation du courant électrique à travers le matériau. Toutefois, sous l'action d'un champ électrique, les charges présentes dans le diélectrique commencent à se déplacer localement et le concept de polarisation est ainsi apparaît. La polarisation qui est une caractéristique physique est exprimée en C/m^2. On peut distinguer quatre types de polarisation : électronique, ionique, dipolaire et interfaciale.

La polarisation électronique est créée par le déplacement des électrons par rapport au noyau. La polarisation électronique s'observe dans tous les matériaux diélectriques à des fréquences très élevées, supérieures à 10^{15} Hz en un temps de réponse très court soit de l'ordre de 10^{-15}s.

La polarisation ionique (atomique) est due à la création des dipôles sous l'effet d'un champ électrique appliqué. Ce phénomène manifeste dans le domaine de l'infrarouge soit à des fréquences autour de 10^{13} Hz et en un temps de réponse court d'environ 10^{-13}s.

La polarisation dipolaire (par orientation) apparait dans les domaines de fréquences Radio soit à des fréquences supérieures à 10^{13}Hz. Ce type de polarisation est relié à l'orientation des

molécules sous l'effet d'un champ électrique appliqué. L'orientation des molécules dépend fortement de la force d'interaction entre ces molécules.

La polarisation interfaciale est habituellement observée à des fréquences très basses (d'environ 10^{-1} à 10^{2} Hz) dans les interfaces des milieux hétérogènes ou même d'un milieu homogène possédant de forte densité d'interfaces. La figure 1.5illustre les différents types de polarisation.

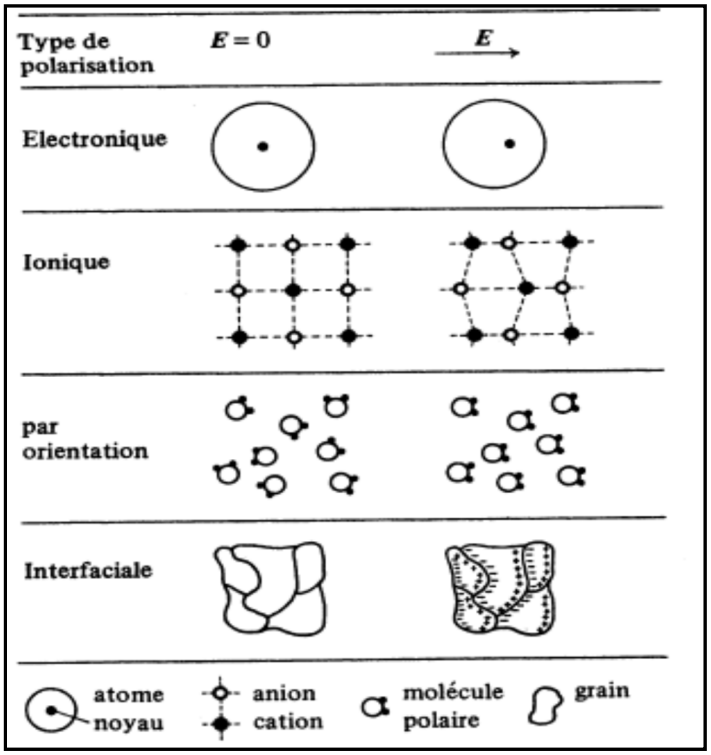

Figure 1.5 Différents mécanismes de polarisation
Tirée d'Éric David (2009)

1.6.2 La permittivité complexe et la relaxation des matériaux

Contrairement aux conducteurs, les diélectriques ont l'aptitude de permettre au champ électrique de les pénétrer, vu qu'ils sont caractérisés par une faible conductivité et une permittivité modérée. La permittivité ε qui est une caractéristique physique qui dépend de la

fréquence est définie comme le rapport entre le déplacement D et le champ électrique appliqué E.

$$\vec{D} = \varepsilon\varepsilon_0 \vec{E} \qquad (1.1)$$

où ε_0 est la permittivité du vide. Elle est égale à 8,85 x 10^{-12} F/m.

La permittivité diélectrique ou la constante diélectrique sous sa forme complexe est définie par

$$\hat{\varepsilon} = \varepsilon' - i\varepsilon''(\omega) \qquad (1.2)$$

où ε' est la permittivité réelle qui dépend du milieu. Elle caractérise la capacité du matériau à stocker de l'énergie électrique. La constante ε'' qui la partie imaginaire de la permittivité représente les pertes diélectriques (perte de l'énergie électrique stockée) reliées aux charges libres ou liées.

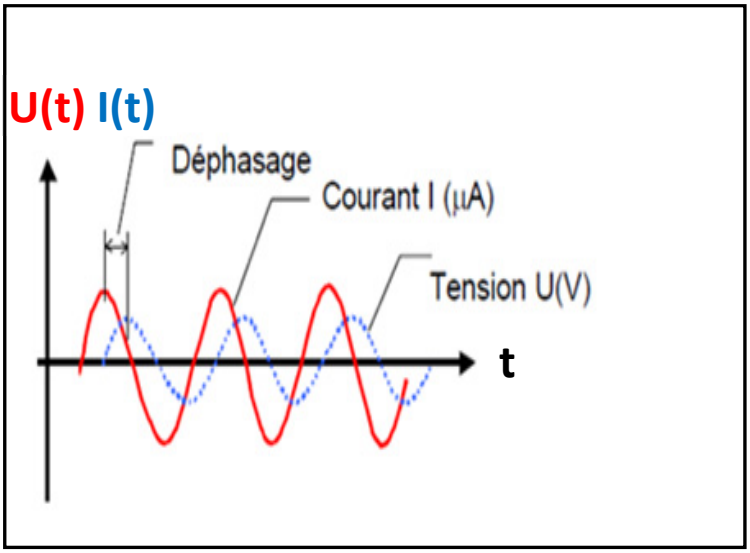

Figure 1.6 La tension, le courant et le déphasage entre la tension appliquée et le courant

Ces grandeurs peuvent être mesurées expérimentalement grâce à la spectroscopie diélectrique qui sert à enregistrer l'amplitude de la tension sinusoïdale appliquée sur le diélectrique et le déphasage entre cette tension et le courant qui le traverse tel qu'il est illustré par la figure 1.6. La figure 1.7 illustre la variation de la permittivité réelle et imaginaire sous forme de courbes isochrones dans le cas d'un échantillon en PET amorphe.

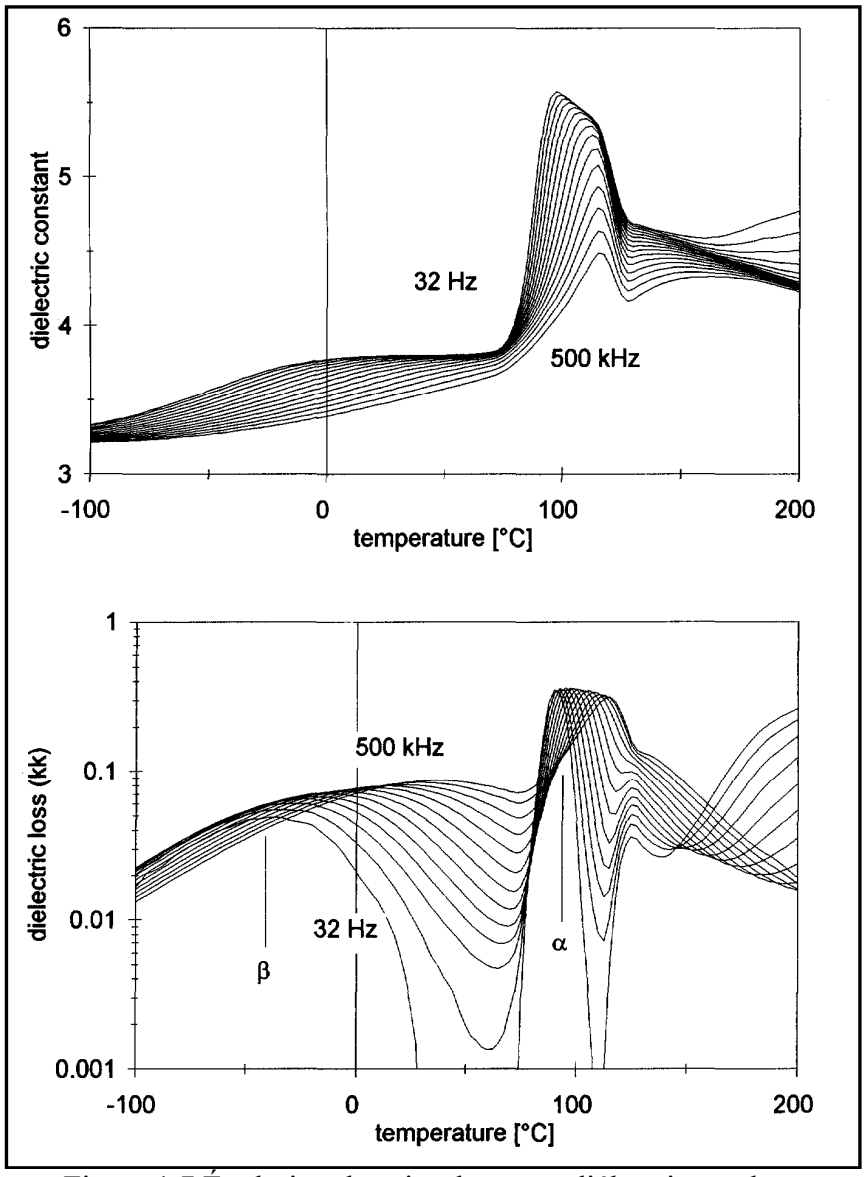

Figure 1.7 Évolution des pics de pertes diélectriques dans le cas d'un échantillon en PET amorphe
Tirée de (Willems, 1995)

1.6.3 La rigidité diélectrique

La rigidité diélectrique compte parmi les paramètres importants d'une isolation électrique. Cette grandeur exprimée en kV/mm est définie comme étant le champ électrique maximal qu'un isolant peut supporter avant qu'une décharge électrique ne se produise. En industrie d'installation et de fabrication d'équipements électriques, elle est mesurée pour évaluer le comportement d'un isolant soumis à un champ électrique. Dans un système électrique, il est très important que la rigidité diélectrique d'un matériau isolant soit la plus élevée possible afin d'éviter la probabilité du claquage qui se produit principalement à cause de la dégradation des isolants ou parfois à cause d'autres facteurs comme l'humidité, la température ou même la poussière qui peuvent contribuer à l'amorçage de la rupture. La figure1.8 illustre la rigidité diélectrique du PET recyclé renforcé de 20% de fibres de verre. Celle-ci est présenté sous forme d'un diagramme statistique appelé diagramme de Weibull.

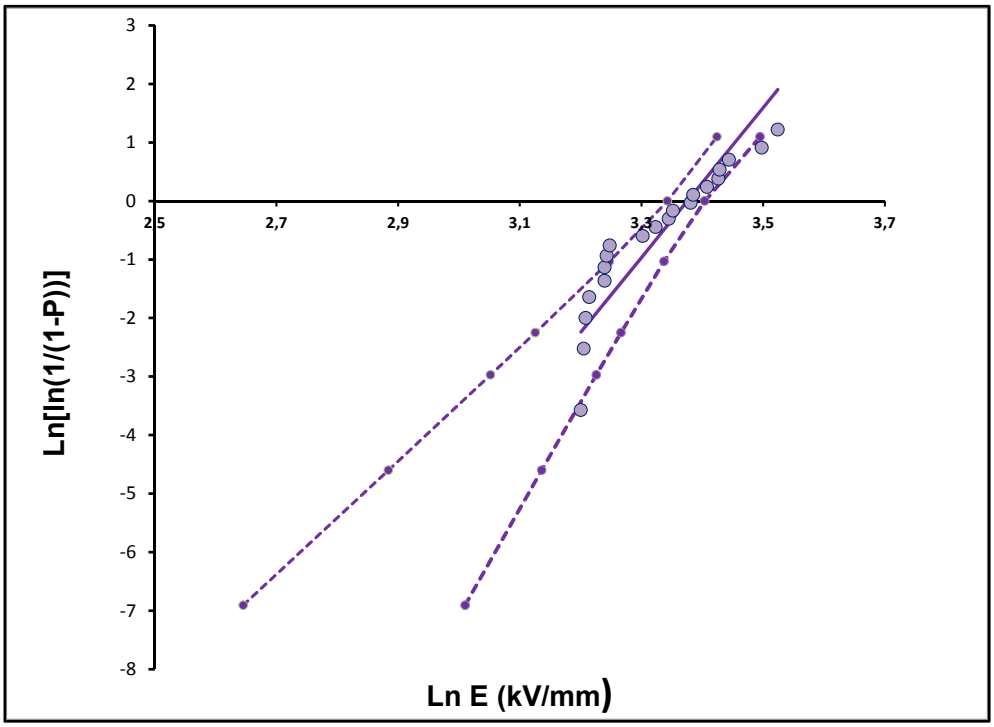

Figure 1.8 Rigidité diélectrique du PET recyclé renforcé de 20% de fibres de verre sous forme de diagramme de Weibull

1.7 Théorie de milieu effectif et lois des mélanges

1.7.1 Théorie du milieu effectif et la permittivité effective complexe

La permittivité diélectrique effective des milieux hétérogènes peut être définie en utilisant la densité d'énergie du milieu sous la forme (Beran, 1968):

$$\langle \widehat{D_k} \rangle = \varepsilon_0 \hat{\varepsilon} \langle \widehat{E_k} \rangle \tag{1.3}$$

où $\langle \widehat{E_k} \rangle$ est la valeur moyenne du vecteur-phaseur du champ, $\langle \widehat{D_k} \rangle$ est le vecteur-phaseur du déplacement diélectrique, $\hat{\varepsilon}$ est la permittivité effective complexe d'un milieu hétérogène et ε_0 est la permittivité du vide. Elle est égale à 8,85 x 10^{-12} F/m.

La permittivité complexe du milieu biphasique exprimée selon la théorie de Maxwell-Garnette du milieu effectif s'écrit (Serdyuk, 2004) :

$$\hat{\varepsilon} = \frac{\upsilon_1 \widehat{\varepsilon_1} \langle \widehat{E_1} \rangle + \upsilon_2 \widehat{\varepsilon_2} \langle \widehat{E_2} \rangle}{\langle \widehat{E} \rangle} \tag{1.4}$$

où $\langle \widehat{E_1} \rangle$ et $\langle \widehat{E_2} \rangle$ sont les vecteurs-phaseurs du champ électrique appliqué sur les deux phases (matrice et inclusions), υ_1 et υ_2 sont les fractions volumiques des deux phases et $\langle \widehat{E} \rangle$ est le vecteur-phaseur du champ électrique moyen donné par :

$$\langle \widehat{E} \rangle = \upsilon_1 \langle \widehat{E_1} \rangle + \upsilon_2 \langle \widehat{E_2} \rangle \tag{1.5}$$

Dans le cas d'une particule ellipsoïdale ayant une permittivité $\widehat{\varepsilon_2}$ incluse dans une matrice ayant une permittivité $\widehat{\varepsilon_1}$, le ratio du champ électrique à l'intérieure et à l'extérieure de la phase minoritaire peut être donné par (Banhegyui, 1986) :

$$\frac{\langle\widehat{E_2}\rangle}{\langle\widehat{E_1}\rangle} = \sum_{k=1}^{3} \frac{\cos^2\alpha_k}{1 + \left(\frac{\widehat{\varepsilon_2}}{\widehat{\varepsilon_1}} - 1\right) A_k} \tag{1.6}$$

où A_k sont les facteurs de dépolarisation qui dépendent de la géométrie de l'inclusion et de la direction du champ appliqué et les α_k représentent les angles entre le champ appliqué et les $k^{éme}$ axes de l'ellipsoïde.

L'équation ci-dessus représente l'approximation du champ moyen. Dans le cas d'inclusions orientées de façon aléatoire, en utilisant les équations 4, 5 et 6 on obtient (Banhegyui, 1986);

$$\hat{\varepsilon} = \frac{(1-\upsilon_1)\,\widehat{\varepsilon_1} + \frac{\upsilon_2\widehat{\varepsilon_2}}{3}\sum_{k=1}^{3}\frac{\widehat{\varepsilon_1}}{\widehat{\varepsilon_1} + (\widehat{\varepsilon_2} - \widehat{\varepsilon_1})A_k}}{1 - \upsilon_2 + \frac{\upsilon_2}{3}\sum_{k=1}^{3}\frac{\widehat{\varepsilon_1}}{\widehat{\varepsilon_1} + (\widehat{\varepsilon_2} - \widehat{\varepsilon_1})A_k}} \tag{1.7}$$

Pour des particules sphériques :

$$\begin{cases} A_1 = A_2 = A_3 = {}^1/_3 \\ \cos^2\alpha_1 = \cos^2\alpha_2 = \cos^2\alpha_3 = 1/3 \end{cases}$$

Dans ce cas, on aura donc

$$\frac{\langle\widehat{E_2}\rangle}{\langle\widehat{E_1}\rangle} = \frac{3\widehat{\varepsilon_1}}{2\widehat{\varepsilon_1} + \widehat{\varepsilon_2}} \tag{1.8}$$

Pour des particules cylindriques, ayant leur axe principal perpendiculaire à la direction du champ

$$\begin{cases} A_1 = A_2 = {}^1/_2 \; et \; A_3 = 0 \\ \cos^2\alpha_1 = 1 \; et \; \cos^2\alpha_2 = \cos^2\alpha_3 = 0 \end{cases}$$

Dans ce cas, on aura donc

$$\frac{\langle \widehat{E_2} \rangle}{\langle \widehat{E_1} \rangle} = \frac{2 * \widehat{\varepsilon_1}}{\widehat{\varepsilon_1} + \widehat{\varepsilon_2}} \tag{1.9}$$

Pour un système diélectrique de n composantes la relation suivante est valable (Banhegyui, 1986);

$$\hat{\varepsilon} = \widehat{\varepsilon_n} + \sum_{i=1}^{n} \upsilon_i (\widehat{\varepsilon_i} - \widehat{\varepsilon_n}) \frac{\langle \widehat{E_I} \rangle}{\langle \widehat{E} \rangle} \tag{1.10}$$

1.7.2 Lois de mélange

De nombreux modèles, essentiellement empiriques, basés sur la loi des mélanges existent dans la littérature. Ces modèles visent à exprimer la permittivité effective d'un milieu multiphasique en fonction de la permittivité et la fraction volumique de chaque composant. On peut citer, la loi de Looyenga, les limites de Wiener et la loi de Böttcher.

- Loi de Looyenga (Merrill, Diaz, LoRe, Squires, & Alexopoulos, 1999) est donnée par

$$(\hat{\varepsilon})^{1/3} = (\upsilon_2)(\widehat{\varepsilon_1})^{1/3} + (1 - \upsilon_2)(\widehat{\varepsilon_2})^{1/3} \tag{1.11}$$

- Les limites de Wiener (Merrill et al., 1999) expriment les deux situations limites pour lesquelles les phases sont soit complètement perpendiculaires au champ électrique (en série) ou soit complétement parallèles au champ électrique (en parallèle) :

$$\frac{1}{\hat{\varepsilon}(\text{phases en série})} = \frac{1-\upsilon_2}{\widehat{\varepsilon_1}} + \frac{\upsilon_2}{\widehat{\varepsilon_2}} \qquad (1.12)$$

$$\hat{\varepsilon}(\text{phases en paralelle}) = \upsilon_1\widehat{\varepsilon_1} + \upsilon_2\widehat{\varepsilon_2} \qquad (1.13)$$

- Loi de Böttcher (Merrill et al., 1999)

$$\frac{\hat{\varepsilon} - \widehat{\varepsilon_2}}{3\hat{\varepsilon}} = \upsilon_2 \frac{\hat{\varepsilon}_1 - \hat{\varepsilon}_2}{\hat{\varepsilon}_1 + 2\hat{\varepsilon}} \qquad (1.14)$$

Où υ_1 et υ_2 sont les fractions volumiques des deux phases, $\hat{\varepsilon}_1$ et $\hat{\varepsilon}_2$ sont les permittivités complexes des deux phases. Toutefois, ces lois ont des limitations vu qu'elles n'intègrent pas tous les paramètres reliés à la structure du mélange ni la notion des interactions entre les inclusions.

1.7.3 Synthèse bibliographique sur les travaux effectués sur l'étude de la réponse diélectrique par différentes méthodes

La réponse diélectrique d'un matériau composite permet d'interpréter son comportement électrique dans une certaine gamme de fréquences. Parmi les propriétés diélectriques, la

permittivité complexe est une caractéristique intéressante pour évaluer le comportement d'un composite dans un système électrique. Un grand nombre de travaux ont été porté sur l'étude des propriétés diélectriques des composites, particulièrement en ce qui concerne leur endurance aux décharges partielles. Cependant peu d'études ont été reportées sur la détermination de la permittivité complexe des milieux hétérogènes notamment ceux capables de fournir des prédictions pour la permittivité complexe effective des hétéro-structures. Dans ce contexte, nous proposons dans cette section une description des études antérieures qui ont été menées.

(Banhegyi, 1986) a présenté des méthodes théoriques pour le calcul des propriétés diélectriques des mélanges hétérogènes. L'étude n'était pas du type critique, mais plutôt un regroupement des différentes formules et théories permettant de calculer la permittivité diélectrique complexe et plus précisément les théories de champ moyen, et les équations intégrales de frontière. L'auteur a classé les formules en deux catégories selon le type de composite. Une comparaison entre les résultats obtenus par les deux méthodes a abouti à la conclusion qu'il y a une différence entre les valeurs obtenues surtout dans le cas des composites contenants des inclusions sphériques. L'auteur a suggéré de faire une description détaillée de la microstructure de l'ensemble matrice-inclusion comme la forme et la distribution des inclusions et les fluctuations de concentration afin de les intégrer dans l'ensemble des équations.

(Tuncer, Gubański, & Nettelblad, 2001) ont effectué une simulation en 2D de la permittivité effective d'un composite hétérogène biphasique (diélectrique/conducteur) dont les inclusions sont infiniment longues. Les résultats obtenus par la méthode des éléments finis pour des composites à faibles concentrations d'inclusion ont été similaires à ceux calculés par d'autres modèles analytiques basés sur la loi des mélanges comme celui de Wiener et de Steeman. Toutefois, l'augmentation de la concentration des inclusions entraîne une différence significative entre les valeurs comparées. En 2002, les mêmes auteurs (Tuncer, Serdyuk, & Gubanski, 2002) ont démontré la dépendance des propriétés des constituants, leurs concentrations et les arrangements géométriques à la réponse diélectrique des matériaux composites.

Une procédure pour les calculs numériques des paramètres effectifs dépendant de la fréquence d'un matériau composite à structure stochastique en trois dimensions a été développée par (Serdyuk, Podoltsev, & Gubanski, 2004). Les résultats obtenus par l'analyse numérique des propriétés diélectriques réalisée dans la gamme de fréquences de 1 MHz à 1 kHz ont été confrontés aux paramètres obtenus expérimentalement ainsi que les résultats obtenus par les équations de Maxwell-Garnett et celles de Bergman.

Une revue très détaillée sur la prédiction de la réponse diélectrique des milieux hétérogènes a été publiée par (Brosseau & Beroual, 2003). Les auteurs ont présenté des études numériques en deux dimensions (2D) et trois dimensions (3D) sur deux composites dans lesquels les inclusions gardent une forme, une taille et une orientation fixe dans un réseau périodique carré (2D) ou cubique (3D). Les auteurs ont également montré l'importance de l'approche de calcul ab-initio pour caractériser avec plus de précision l'interface des milieux hétérogènes périodiques dans la limite quasi-statique et de fournir des prédictions très précises pour la permittivité complexe effective des hétéro structures. Les auteurs ont également confronté les résultats obtenus à d'autres modèles existants dans la littérature.

Plus récemment, (Myroshnychenko & Brosseau, 2009) ont utilisé la simulation par éléments finis à partir de l'approche ab-initio afin d'étudier les propriétés diélectriques d'un système percolation- continuum à deux dimensions où des disques circulaires sont distribués de façon aléatoire à travers une matrice hôte. L'étude a été réalisée en fonction de plusieurs facteurs physiques caractérisant les structures hétérogènes, particulièrement la fraction surfacique de l'inclusion et le degré d'impénétrabilité caractérisé par le paramètre λ.

1.8 Conclusion

Pour aborder ce chapitre, nous avons rappelé quelques définitions et notions de base sur les l'industrie automobile et le recyclage. Nous avons vu également, les polymères thermoplastiques ainsi que les différentes propriétés thermiques et diélectriques importantes

dans le cas des polymères destinés aux applications électriques. Un rappel sur le concept de polarisation ainsi que la permittivité effective ont été également abordés suivis d'une synthèse bibliographique sur la modélisation numérique de la permittivité diélectrique effective.

L'objectif du prochain chapitre sera de faire une description des différents matériaux composites à base de PET recyclé et PEN renforcés de charges inorganiques. Les différentes méthodes et équipements qui ont été utilisés lors de cette étude afin de valider la fiabilité des ressources du PET recyclé seront également présentés.

CHAPITRE 2

METHODOLOGIE D'ANALYSE

2.1 Introduction

Pour connaitre le comportement d'un matériau opérant dans certaines conditions et soumis à certaines contraintes, une caractérisation doit être faite convenablement. Pour cela, il existe des essais et des mesures normalisées auxquelles il faudrait se conformer. Nous consacrons ce chapitre à une description détaillée des différents matériaux retenus pour notre étude. Les diverses techniques d'investigation employées pour la caractérisation des propriétés thermiques et diélectriques seront également présentées. Nous commençons d'abord par une description sommaire des différents matériaux candidats. Nous passerons ensuite à la présentation des différentes techniques utilisées pour la caractérisation. Chaque technique sera suivie d'un exemple montrant le type de données recueillies après les mesures.

Dans cette section, nous proposons une description des matériaux candidats ainsi que les différentes techniques expérimentales qui seront employées afin de caractériser les différents matériaux retenus pour notre étude. Comme première partie, nous devrons caractériser les matériaux candidats. Une dissection des différents matériaux fournis semble nécessaire afin de préparer des échantillons (découpage, polissage, nettoyage à l'éthanol et revêtement d'or) pour mieux caractériser leur microstructure.

Les matériaux composites à base de Polyéthylène téréphtalate recyclé (PET) et Polyéthylène Naphthalate (PEN) qui serviront à réaliser notre étude, ont été préparés par la compagnie Groupe Lavergne selon le procédé d'injection à partir des granules de PET et PEN recyclé, des flocons de mica et des fibres de verre courtes (voir figure 2.1). Les matériaux ont été injectés sous forme de disques de 101 mm de diamètres et 1,6 mm d'épaisseur.

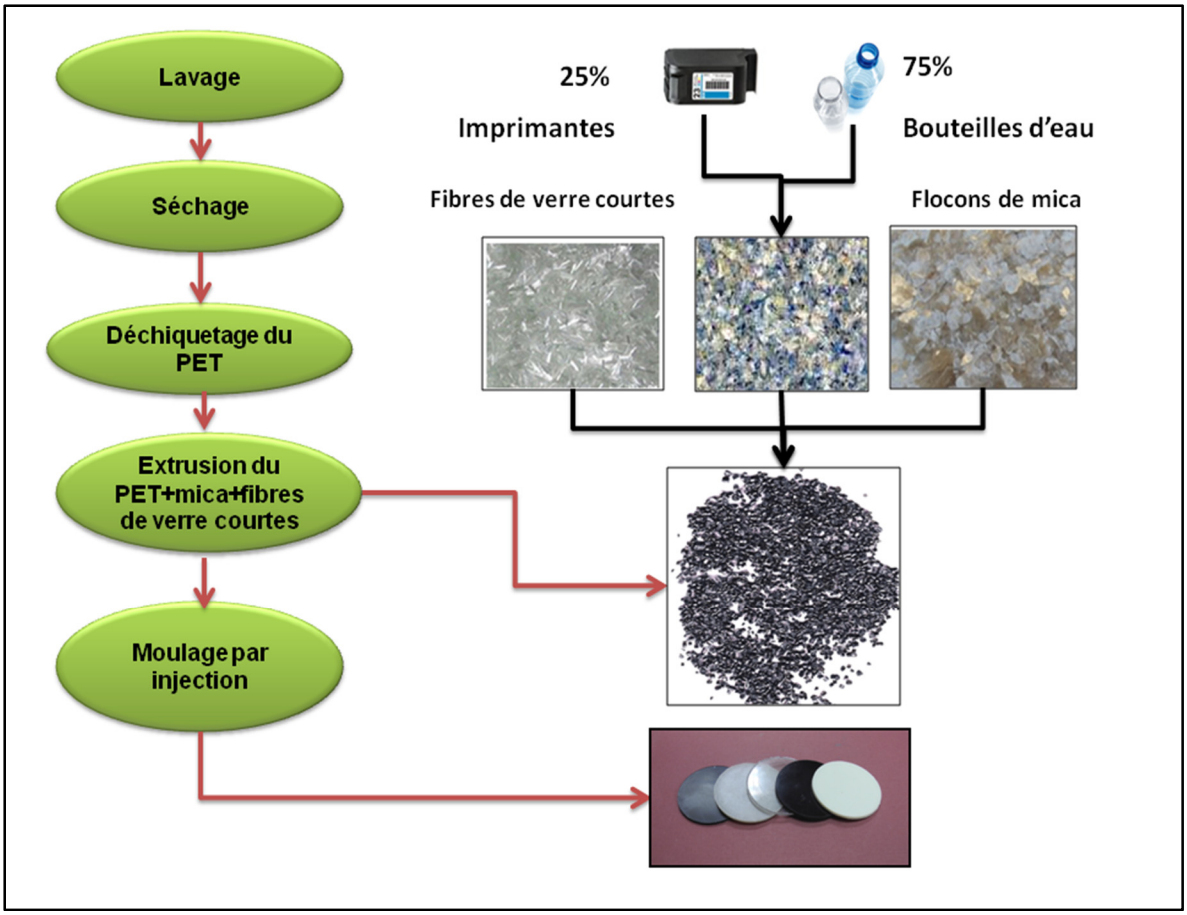

Figure 2.1 Les étapes d'élaboration des échantillons testés (cas du PET recyclé renforcé des fibres de verre et du mica (RPET-GF-LM1)

La série des matériaux fournis inclut une famille de composites nommée RPETGFLM1. Ce sont des composites à base de PET, renforcés de 25% de fibre de verre et 15% de mica. Le RPET-GF-SM1 qui comprend 25% et 15% de mica se diffère du RPET-GF-LM1 par la taille des flocons de mica utilisés selon le tableau ci-dessous. Le VPET-GF2 est une résine polyester thermoplastique à base de polyéthylène téréphtalate vierge provenant de l'industrie pétrochimique renforcé de 30% de fibres de verre. Ce composite permettra de comparer la fiabilité des ressources de PET recyclé au niveau des propriétés diélectriques. Le VPET-GF2 qui est une résine à base de PET pur renforcé de 30% de fibre de verre est le composite le plus convenable d'être comparé au RPET-GF2. Des échantillons en PEN ainsi qu'en PEN renforcé par 20% de fibres de verre seront testés également et ce, d'une part pour vérifier l'effet des renforts sur les propriétés diélectriques de ce polyester et d'une autre part pour confronter les

résultats à ceux obtenus par son concurrent, le PET recyclé. Le tableau 2.1 illustre une description sommaire des matériaux candidats incluant les proportions des principales constituantes.

Tableau 2.1 Description sommaire des différents matériaux

Matériaux	Désignation	Fibres de verre (% m)	Mica (% m)	Autres
PET recyclé non renforcé	RPET	0%	0%	PET recyclé
PET recyclé renforcé de fibres de verre et de mica	RPET-GF-LM1	25%	15% Grand flocons	PET recyclé
PET recyclé renforcé de fibres de verre et de mica	RPET-GF-SM1	25%	15% Petit flocons	PET recyclé
PET recyclé renforcé de mica	RPET-M	0%	15%	PET recyclé
PET recyclé renforcé de fibres de verre	RPET-GF1	20%	0%	PET recyclé
PET recyclé renforcé de fibres de verre	RPET-GF2	30%	0%	PET recyclé
PET non recyclé renforcé de fibres de verre	VPET-GF2	30%	0%	PET non recyclé
PEN non renforcé	PEN	0%	0%	100% PEN
PEN renforcé de fibres de verre	PEN-GF	20%	0%	PEN à 20% Fibre de verre

Le noir de carbone a été incorporé en faibles quantités dans ces composites afin de rendre le matériau opaque et diminuer la dégradation causée par les rayonnements ultraviolets. Le noir de carbone qui a été introduit avec une concentration de 0.01% par rapport à la matrice thermoplastique ne peut influencer les propriétés diélectriques des composites, plus précisément, la conductivité électrique. En effet, le pourcentage de noir de carbone nécessaire pour atteindre le seuil de percolation est insuffisant. Ainsi, on peut obtenir l'opacité du polymère en évitant la percolation. Par conséquent, la conductivité électrique du mélange demeure proche de celle de la matrice pour une telle concentration.

2.2 Les techniques et moyens de caractérisation

L'objectif principal de cette section est de définir les différents moyens et méthodes ayant servi à notre caractérisation. La caractérisation comprend l'inspection de la qualité de la dispersion des renforts au niveau de la matrice grâce à l'observation optique et microscopique. Elle comprend également l'analyse des propriétés thermiques par l'analyse thermogravimétrique (TGA) ainsi que la calorimétrie différentielle à balayage (DSC). Cette caractérisation inclut également des mesures diélectriques par spectroscopie diélectrique et des essais de rigidité diélectrique. Différents types de vieillissement ont été adoptés dans notre étude (électrique, thermique et électrochimique). Pour chaque technique d'analyse, le principe sera décrit et le dispositif expérimental sera présenté. Nous verrons aussi quelques résultats relatifs aux différentes analyses.

2.3 Préparation des échantillons

Plusieurs méthodes ont été adoptées pour le découpage et la préparation pour la caractérisation. Elles dépendent essentiellement du type de caractérisation. Le dispositif le plus adéquat à utiliser pour préparer des coupes convenables à l'inspection morphologique est le microtome. Cet appareil permet d'obtenir avec précision des surfaces lisses convenables pour réussir à avoir des images claires surtout lorsqu'il s'agit de faire des coupes à travers un matériau ayant des particularités à inspecter, comme par exemple une perforation due au claquage. Pour les

échantillons destinés aux mesures de spectroscopie diélectrique, le découpage a été effectué grâce une couronne dentée qu'on a placée à l'extrémité d'une perceuse électrique. Les échantillons obtenus sont des disques de 40 mm de diamètre.

2.4 Caractérisation morphologique

Cette partie a pour but de résumer brièvement en revue la technique d'observation de la morphologie des matériaux d'étude grâce à la microscopie.

2.4.1 Microscopie électronique à balayage (MEB)

La microscopie électronique à balayage est une technique d'observation de la topographie des surfaces ou également la détermination de la composition chimique. Cet outil indispensable en sciences des matériaux permet l'obtention d'image en haute résolution. Son principe réside essentiellement dans le balayage de la surface d'un échantillon par un faisceau d'électrons incidents produit par effet thermoélectrique à l'aide d'un filament.

L'observation a été effectuée avec un microscope Hitashi S4700. La tension d'accélération était de 5kV. Les échantillons ont été coupés sous azote avec un microtome cryogénique ensuite couvert d'une mince couche d'or grâce à un métalliseur haute-résolution (Emitech K575X) avant l'observation. Il permet de réaliser des dépôts de couche très fine afin de rendre la surface des échantillons conductrice. La microstructure et la morphologie d'un échantillon en PET recyclé renforcé de 20% de fibres de verres sont représentées par la figure2.2. Les images obtenues révèlent une bonne dispersion des renforts inorganiques (les fibres de verre) ainsi que la qualité de la surface.

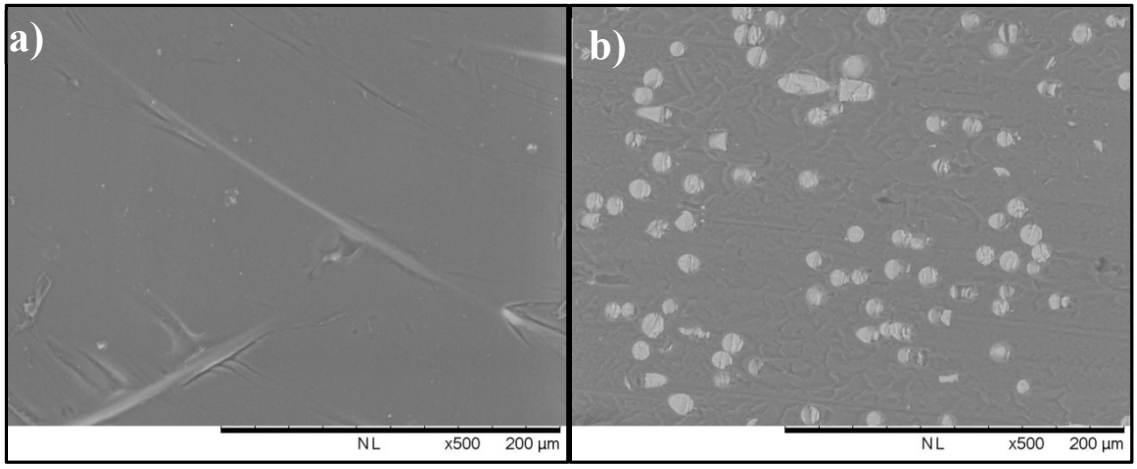

Figure 2.2 Morphologie a) de la surface et b) d'une coupe d'un échantillon de PET recyclé renforcé de 20% de fibres de verre (x500)

2.4.2 Microscopie optique (MO)

Un microscope optique à caméra couleur a été également utilisé pour caractériser la morphologie. Cette technique a été employée en particulier pour confirmer la rupture diélectrique après les tests de claquage ou dans le cas des échantillons ayant subis des tests d'érosion. La figure 2.3illustre un échantillon de PET recyclé renforcé de 15% de mica après la rupture diélectrique et la figure 2.4présente un échantillon après un test de vieillissement sous effet couronne à haute température d'un échantillon de PET recyclé renforcé de fibre de verre et de mica.

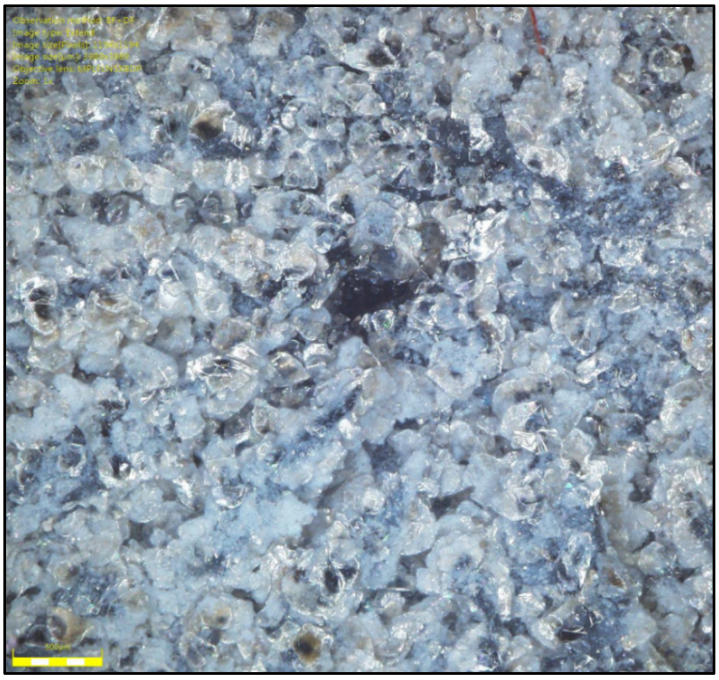

Figure 2.3 PET recyclé renforcé de 15% de flocons de mica après un test de claquage (x100)

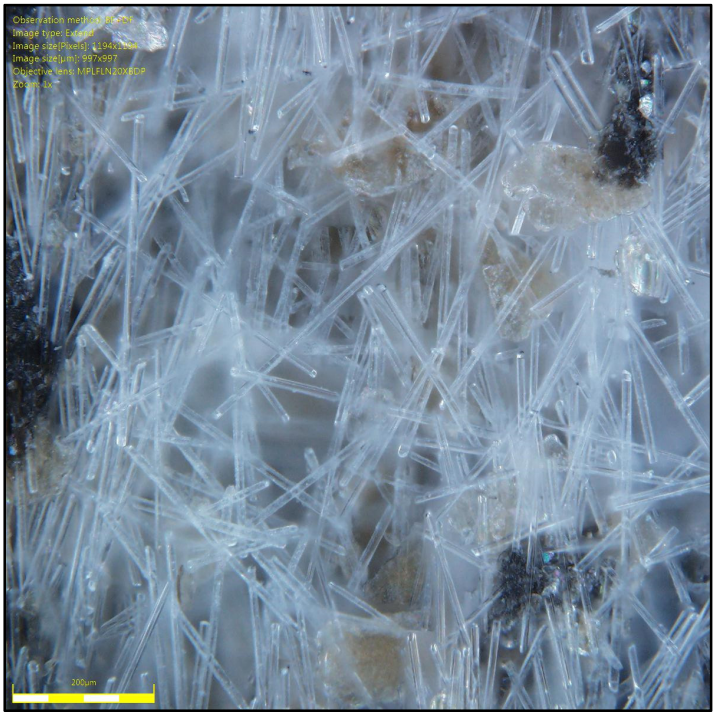

Figure 2.4 PET recyclé renforcé de fibres de verre et de mica (PETGFLM1) après un test de vieillissement sous effet couronne à haute température(x100)

2.5 Analyse thermique

L'analyse de certains changements au niveau du comportement diélectrique des matériaux ayant subi des transformations structurales ou ayant été sous certaines contraintes requiert une explication ou une corrélation avec d'autres changements au niveau des propriétés structurales ou thermiques comme la cristallisation ou la transition vitreuse. L'étude des propriétés des différents composites a été réalisée par l'analyse thermogravimétrique (TGA) et la calorimétrie à balayage différentiel (DSC).

2.5.1 Analyse thermogravimétrique (TGA)

L'analyse thermogravimétrique est une procédure d'analyse thermique servant à mesurer le taux du changement de masse pendant le chauffage ou le refroidissement et en fonction du temps (s) ou de la température (^oC) sous atmosphère contrôlée. Cette technique expérimentale permet de fournir des connaissances importantes sur le type de dégradation et de mesurer le taux de perte en masse de l'humidité, les plastifiants et les résidus. Cette analyse est généralement menée conformément aux standards précis tels que la norme ASTM-E1131. Les résultats obtenus sont recueillis sous forme de thermogramme montrant les différentes étapes de dégradation et incluant les diverses températures pour lesquelles des pertes de masse de l'échantillon ont eu lieu. La figure 2.5 montre le schéma du principe de l'appareil TGA.

Certaines mesures ont été faites entre 50 et 600^oC grâce à un analyseur thermogravimétrique Perkin Elmer et selon la norme ASTM-EP131-03. L'analyse a été réalisée dans les conditions inertes (N_2) avec une vitesse de balayage de $10^oC.min^{-1}$ en utilisant des échantillons de 5 ±0.3 mg. La figure 2.6 montre la variation de la masse en fonction de la température d'un échantillon de PET recyclé et un échantillon de PEN.

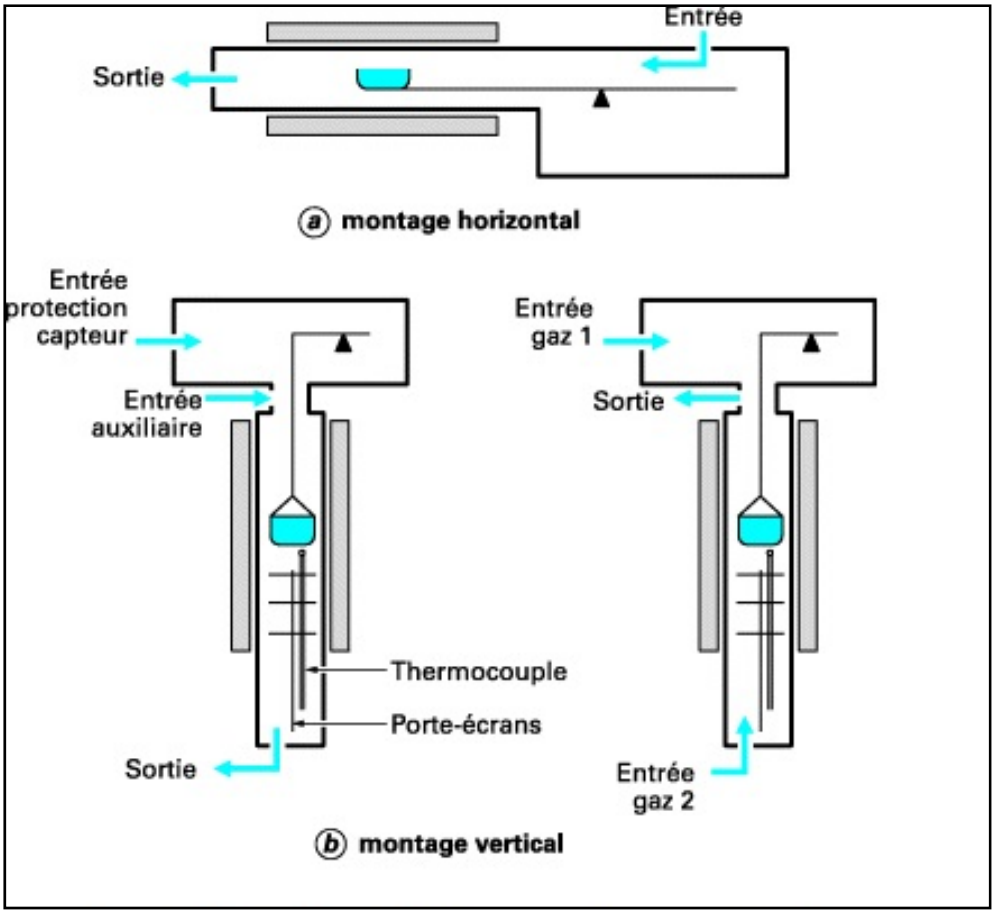

Figure 2.5 Schéma de principe de l'appareil de TGA
Tirée du (Emmanuel WIRTH, 2014)

La courbe représentée par la figure 2.6 révèle deux parties bien claires. Au début de cette mesure, le PET a perdu environ 3% de sa masse totale vers 390ºC. Tandis que le PEN n'a perdu que 2%. Une décomposition d'environ 77% a été observée entre 300 et 470°C pour le PET et de 70% pour le PEN. Un résidu de 15% et de 20% a été noté vers 530ºC pour le PET recyclé et PEN respectivement. Ce résidu correspond à l'acide carbonyle et les noyaux du benzène pour le PET et le naphtalène pour le PEN (Papageorgiou, 2014). Le PEN résiste mieux à la dégradation thermique que le PET recyclé.

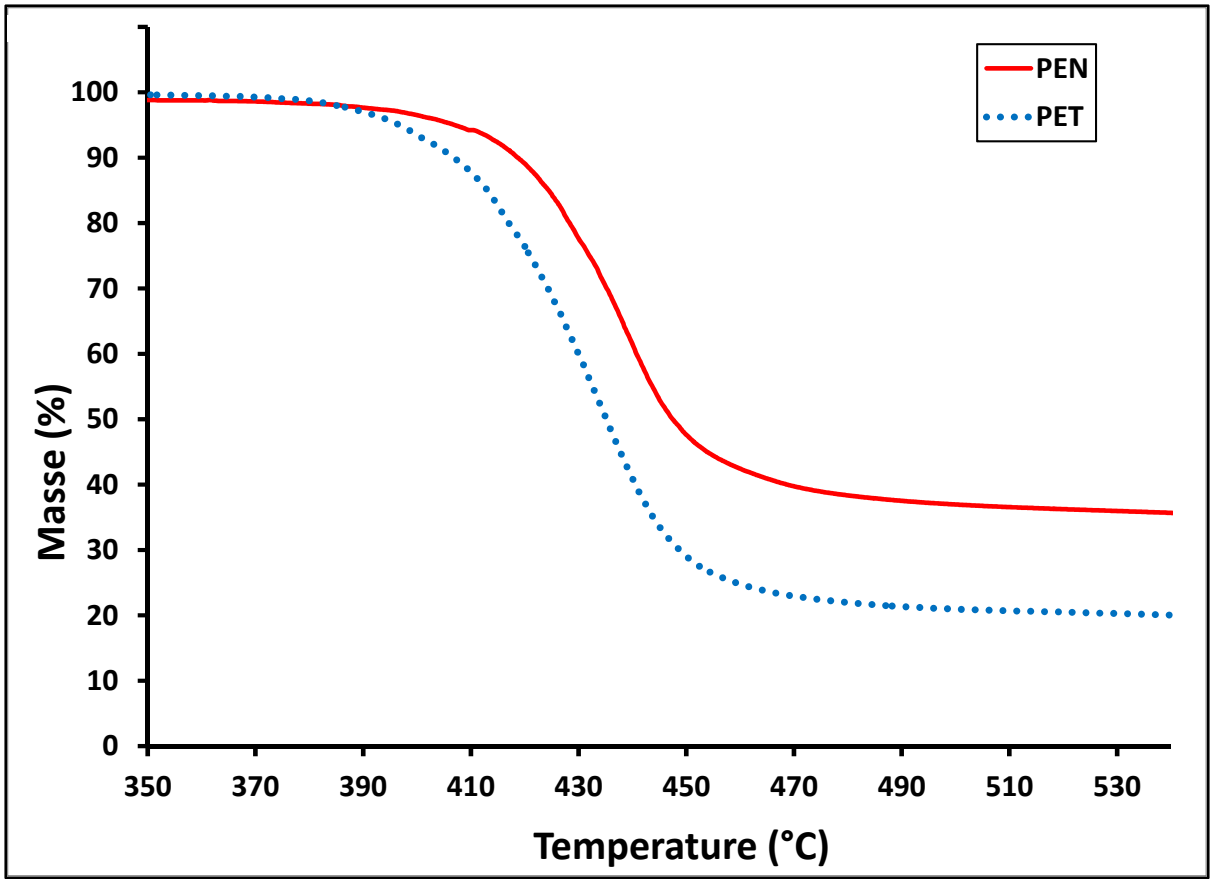

Figure 2.6 Courbes de dégradation thermique pour le PET recyclé et le PEN

2.5.2 Calorimétrie différentielle à balayage (DSC)

La calorimétrie différentielle à balayage est une technique de mesure qui a été conçue principalement pour fournir des connaissances concernant plusieurs propriétés thermiques d'un matériau. En effet, cette technique permet de déterminer les différentes températures à lesquelles les principales transitions de phase se produisent lorsqu'un matériau est soumis à un programme de température sous atmosphère contrôlée. Son principe consiste à mesurer la variation du flux de chaleur absorbée ou dégagée par l'échantillon en fonction du temps ou de la température. L'appareil est équipé de deux cellules de mesure, l'une est considérée comme référence et l'autre sert à renfermer l'échantillon. La figure 2.7 illustre un schéma du principe de l'appareil de DSC.

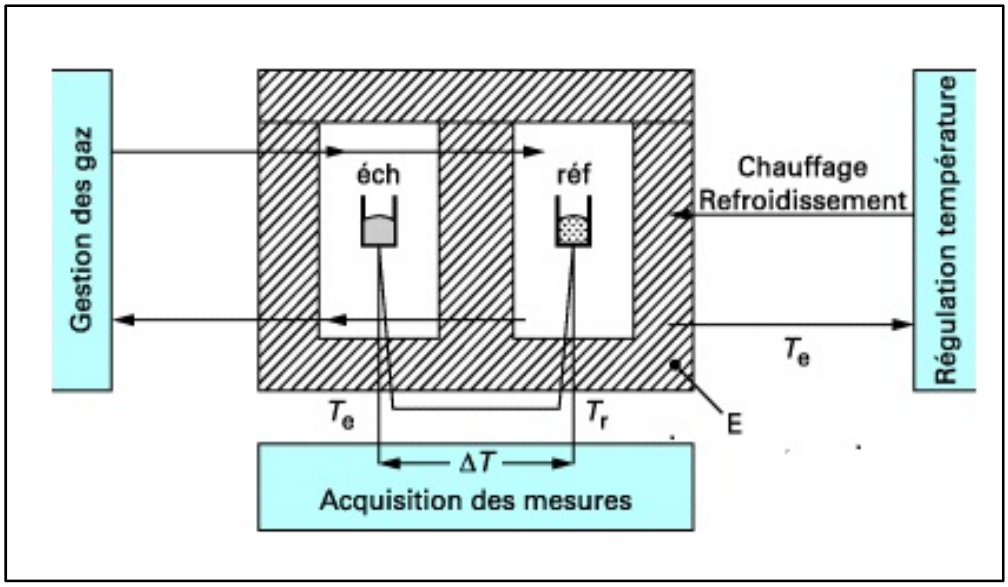

Figure 2.7 Schéma de principe de l'appareil de DSC
Tirée de (Jean GRENET, 2010)

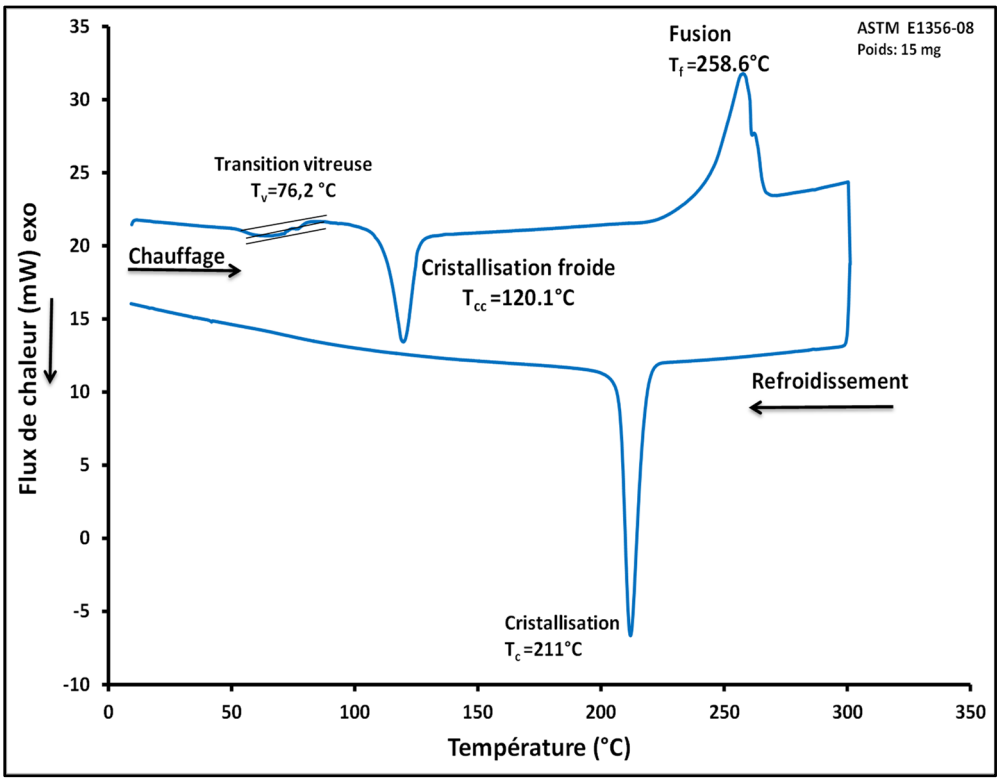

Figure 2.8 Analyse enthalpique différentielle du Polyéthylène téréphtalate recyclé

Les résultats recueillis d'une mesure DSC sont illustrés à la figure 2.8 sous forme de données de la variation de flux de chaleur en fonction de la température (ºC). Le matériau étudié est du PET recyclé, un thermoplastique semi-cristallin. Les données reportées concernent une mesure calorimétrique qui a été utilisé avec un analyseur Perkin Elmer Diamond sous atmosphère inertes (N_2) selon la procédure (ASTME1356-08, 2014). Ces essais ont été menés entre 0 et 300ºCavec une vitesse de balayage de 10ºC en utilisant un échantillon d'environ 15mg± 0,3 pour lesquels on a caractérisé la transition vitreuse, le point de fusion et le degré de cristallisation.

Le spectre obtenu révèle la présence d'un saut de capacité calorifique à 76ºC. Un pic endothermique est identifié entre 235 et 270ºC avec un maximum de 258,6ºC, ce qui correspond à la température de fusion. Un pic endothermique est observé entre le saut et le pic endothermique de fusion. Ce pic situé entre 105 et 130ºC avec un minimum de 120ºCet correspond à la cristallisation froide. Lorsque le PET a atteint sa phase de cristallisation dans le cycle de refroidissement, un pic exothermique a été observé entre 200 et 210ºC.

2.6 Caractérisation diélectrique

2.6.1 Mesures par spectroscopie diélectrique

La spectroscopie est une technique de caractérisation non destructive permettant de contrôler la qualité des isolants électriques et de diagnostiquer le type de polarisation. Cette technique permet de mesurer certains paramètres diélectriques, les plus importants sont les pertes diélectriques et la permittivité réelle. La figure 2.9 illustre le principe de la spectroscopie diélectrique.

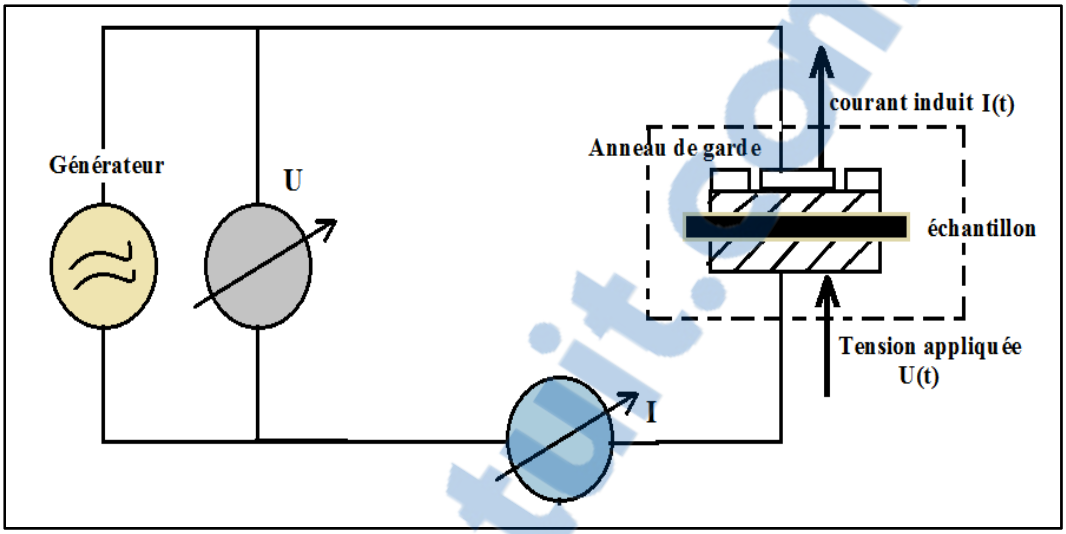

Figure 2.9 Schéma du principe de la spectroscopie diélectrique

Dans le domaine fréquentiel, si l'on exerce une tension nominale $U^* = U_0 \sin \omega t$, la réponse résulte en un courant induit possédant la même pulsation angulaire que la tension mais déphasé avec un angle φ:

$$I^*(\omega) = I_0 \sin(\omega t + \varphi) \tag{2.1}$$

Ainsi l'impédance complexe est déduite par le rapport des grandeurs U^*et I^*comme :

$$Z^*(\omega) = \frac{U^*(\omega)}{I^*(\omega)} \tag{2.2}$$

La permittivité sous sa forme complexe s'écrit :

$$\varepsilon^*(\omega) = \frac{1}{i\omega Z^*(\omega)} \tag{2.3}$$

avec

$$\varepsilon^*(\omega) = \varepsilon'(\omega) - i\varepsilon''(\omega) \qquad (2.4)$$

Le facteur de dissipation qui est une propriété diélectrique reliée aux pertes diélectriques dues à la polarisation et/ou au transport de charges est égal au quotient de partie réelle du courant et la partie imaginaire. L'angle δ représente l'angle complémentaire de l'angle du déphasage entre le courant traversant l'isolant et la tension appliquée U, tel qu'il illustré par la figure 2.10.

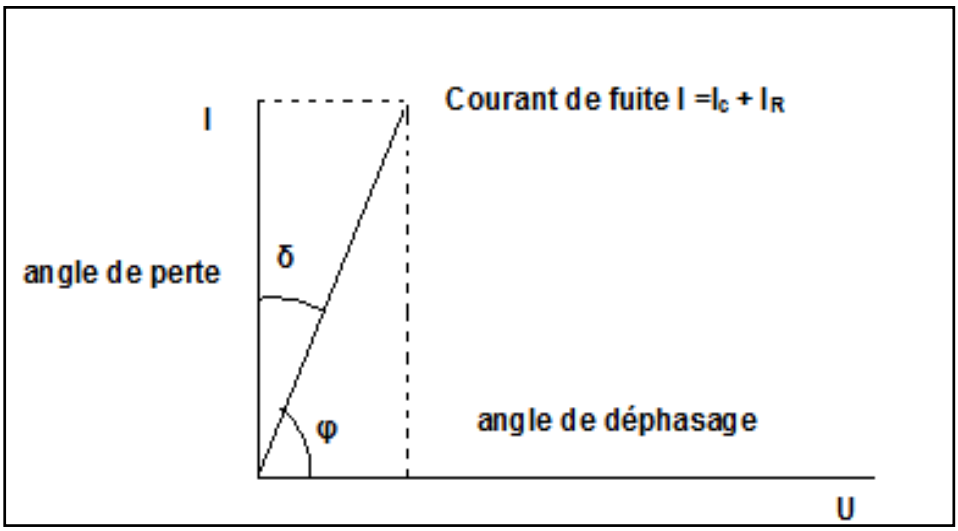

Figure 2.10 Courant et tension dans un diagramme de phase

Les mesures ont été menées dans l'air, à l'aide d'un spectromètre diélectrique Novocontrol dans un large domaine de fréquence allant de 10^{-2} à 10^5 Hz pour des températures allant de la température ambiante à des températures proches de la température de transition vitreuse du matériau et par saut de 5°C pour chaque spectre isotherme. Quelques exceptions ont été faites au niveau du pas ou de l'intervalle de température pour certains matériaux. L'échantillon a été inséré entre deux électrodes circulaires (géométrie plan-plan), aux bornes auxquelles une tension de 3V a été appliquée. L'ensemble géométrie-échantillon a été placé dans une cellule de mesure piloté par le logiciel « Windeta » qui nous a permis d'enregistrer l'ensemble des paramètres mesurés. Les électrodes utilisées se présentent sous forme de disque de 40 mm de diamètre et 2 mm d'épaisseur. La figure 2.11illustre les électrodes utilisées pour effectuer les mesures.

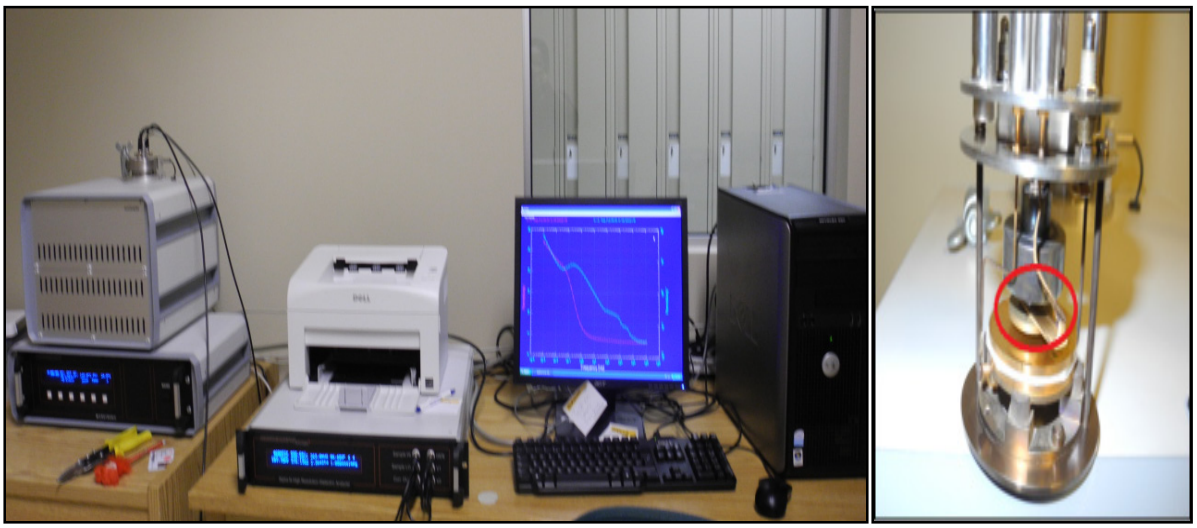

Figure 2.11 Banc d'essai des mesures de spectroscopie et le porte échantillon

Le banc d'essai servant à effectuer les mesures de spectroscopie diélectrique est illustré par la figure 2.11. Les résultats obtenus ont été utilisés pour tracer des courbes 2D ou 3D. La figure 2.12 illustre des courbes représentant la permittivité imaginaire dans le cas du PET recyclé. Ces mesures ont été réalisées dans une bande de fréquences entre 10^{-2} à 10^{5} Hz à tous les 5°C dans une gamme de températures allant de 70 à 90 °C, ce qui représente l'intervalle de température de la transition vitreuse du matériau.

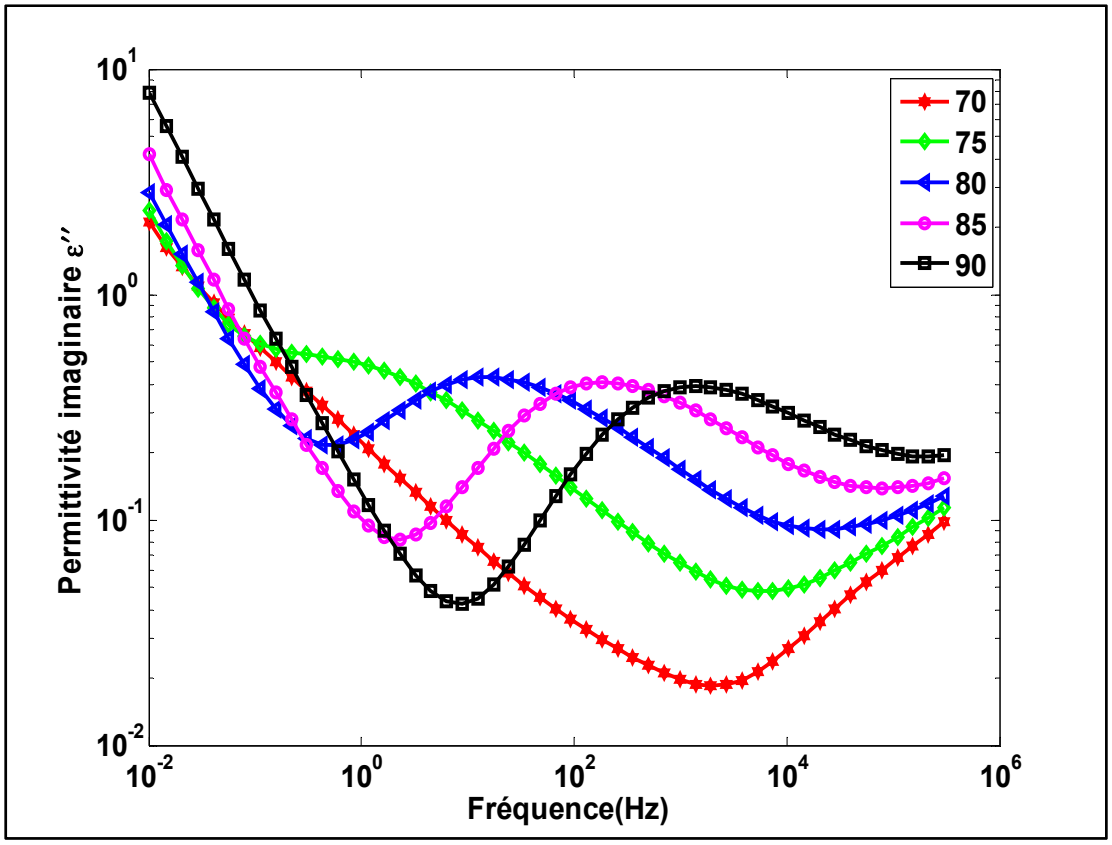

Figure 2.12 Courbes de la permittivité imaginaire dans le cas du PET recyclé

2.6.2 Mesures de rigidité diélectrique par claquage

Le test de claquage est une méthode de diagnostic destructive utilisée pour caractériser la rigidité diélectrique des matériaux. La rupture diélectrique, connue également sous l'appellation claquage, est un phénomène destructif irréversible dans les isolations solides. Ce type de mesure est basé sur l'application d'un fort champ électrique jusqu'à la rupture. En effet, il permet d'obtenir le champ électrique pour lequel un échantillon peut claquer. Il est important de reconnaître que les tests doivent respecter certaines normalisations.

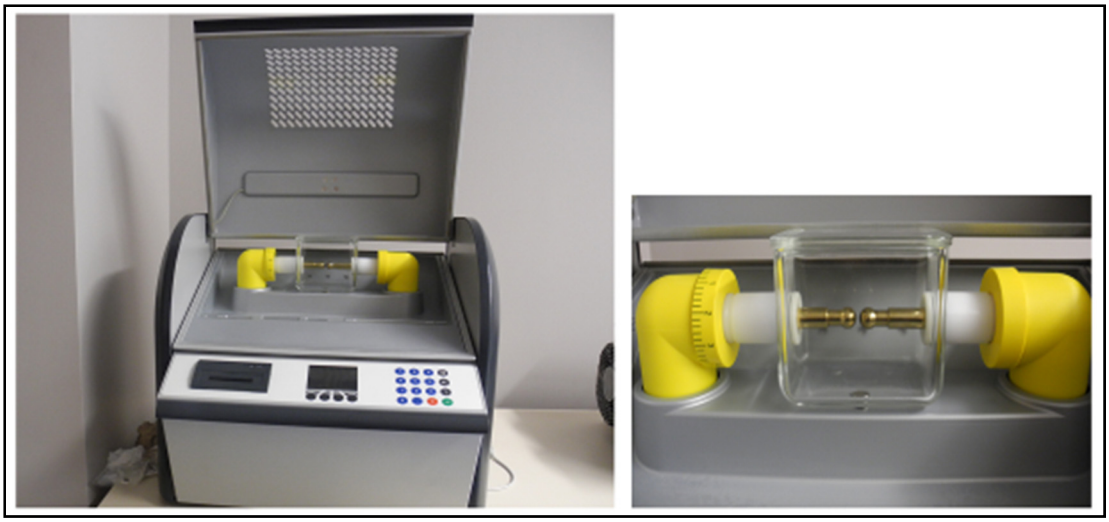

Figure 2.13 Testeur d'huile, Bauer DTA 100

Les mesures ont été réalisées à l'aide d'un testeur d'huile, Bauer DTA 100 illustré par la figure 2.13. Les échantillons ont été placés entre deux électrodes sphériques de 12,5 mm de diamètre. Les tests ont été effectués dans de l'huile minérale dégazée (Luminoil) afin d'éviter le contournement des échantillons. Des mesures à courts termes ont été réalisées sur un grand nombre d'échantillons (jusqu'à 24) selon la norme(ASTMD149, 2004). Il s'agit d'appliquer une tension croissante avec une vitesse typique jusqu'à la rupture. Le champ de claquage se calcule en divisant la tension pour laquelle l'échantillon a claqué par l'épaisseur du même échantillon. Les résultats obtenus ont été traités selon la distribution de Weibull à deux paramètres (voir figure 2.14). L'expression de la distribution de Weibull à deux paramètres est donnée par

$$P(E) = 1 - exp\left[-\left(\frac{E}{\alpha}\right)^{\beta}\right] \tag{2.5}$$

$P = 1\text{-}\exp\left[-\left(\frac{E}{\alpha}\right)^{\beta}\right]$ où P(E) représente la probabilité de la rupture et E est la rigidité diélectrique expérimentale. Le facteur de forme β indique la dispersion des données tandis que le paramètre d'échelle α désigne indiquant la rigidité diélectrique de l'échantillon pour une probabilité d'échec de 63,2%.

Les estimateurs de α et β seront calculées en utilisant la méthode de régression pondérée des moindres carrées pour chaque échantillon. La détermination des probabilités d'occurrence de chaque mesure a été faite grâce à la fonction F (i, n) donnée par la formule suivante

$$F(i,n) = \frac{i - 0.44}{n + 0.25}\, x100\% \qquad (2.6)$$

$F(i,n) = \frac{i-0.44}{n+0.25} x100\%$ où n est le nombre des échantillons testés et i désigne le rang des données dans l'ordre croissant. Il est a noté que les paramètres des mesures doivent être mis en ordre du plus petit au plus grand.

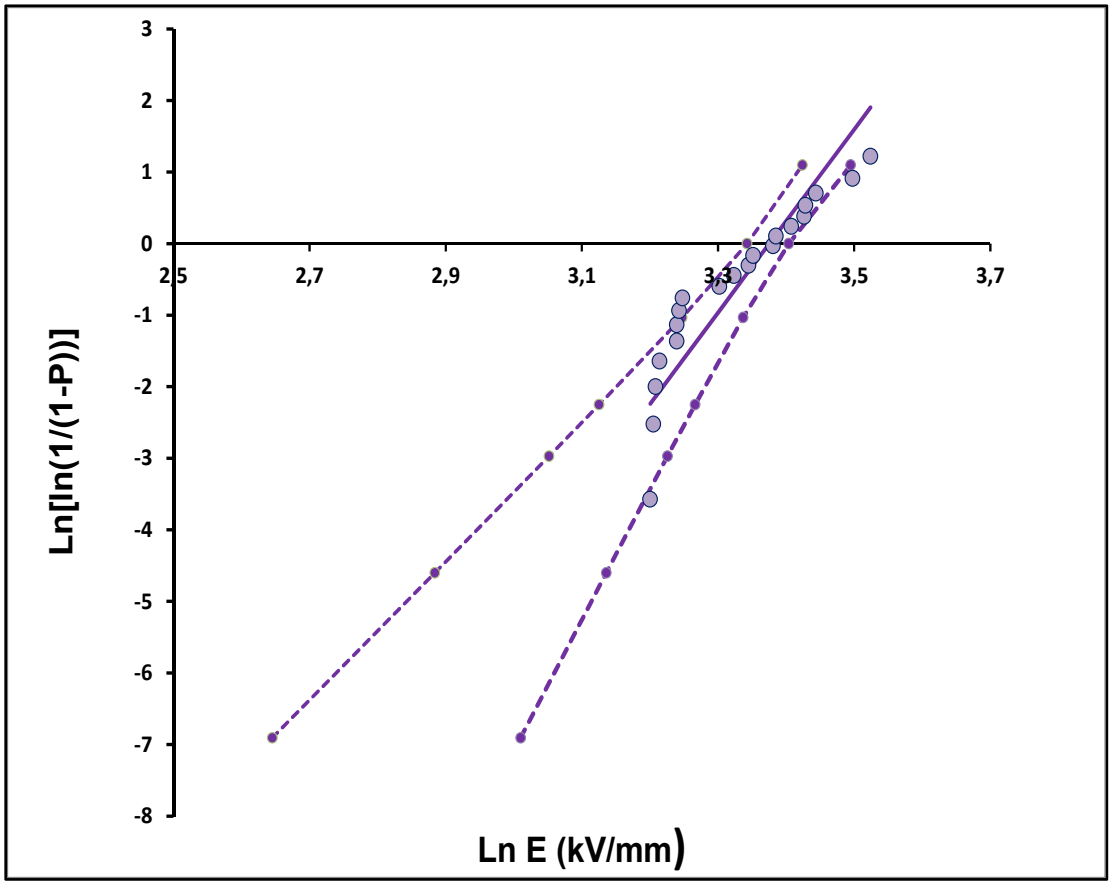

Figure 2.14 Rigidité diélectrique du PET recyclé renforcé de 20% de fibres de verre

2.7 Processus du vieillissement des isolants électriques

2.7.1 Introduction

Le vieillissement des isolants électriques est un processus complexe qui est défini comme étant la dégradation graduelle se produisant sous l'effet de certaines contraintes (Tanaka, 2002). Différents types de contraintes thermiques, électriques, mécaniques ou même environnementales peuvent contribuer individuellement ou combinées à la réduction de la durée de vie des composants en service. Durant notre étude, différents processus de vieillissement seront adoptés afin d'évaluer l'endurance à la dégradation sous contraintes électriques, thermiques ou combinées. Le vieillissement des isolants électriques peut entrainer des changements structuraux, électriques et morphologiques. Par conséquent, quelques propriétés seront altérées. Les pertes diélectriques augmentent et la rigidité diélectrique diminue (L. Dissado, Mazzanti, & Montanari, 1997).

2.7.2 Vieillissement thermique

Le vieillissement thermique des matériaux composites à base de matrice polymérique est défini comme étant la perte partielle ou totale des propriétés initiales des composants principaux d'un composite soumis à des fortes contraintes thermiques. Ce processus est considéré comme un phénomène irréversible prenant en compte la limitation de la durée de vie d'un système fabriqué à partir de ce composite. Des réactions moléculaires amorcée par la chaleur peuvent susciter des changements importants au niveau de certaines propriétés thermodynamiques telle que la transition vitreuse, la cristallinité et la fusion du composite. On peut s'attendre également à certains changements au niveau des propriétés mécaniques (Bárány, Földes, & Czigány, 2007) et particulièrement structurales (Quintanilla et al., 1994).

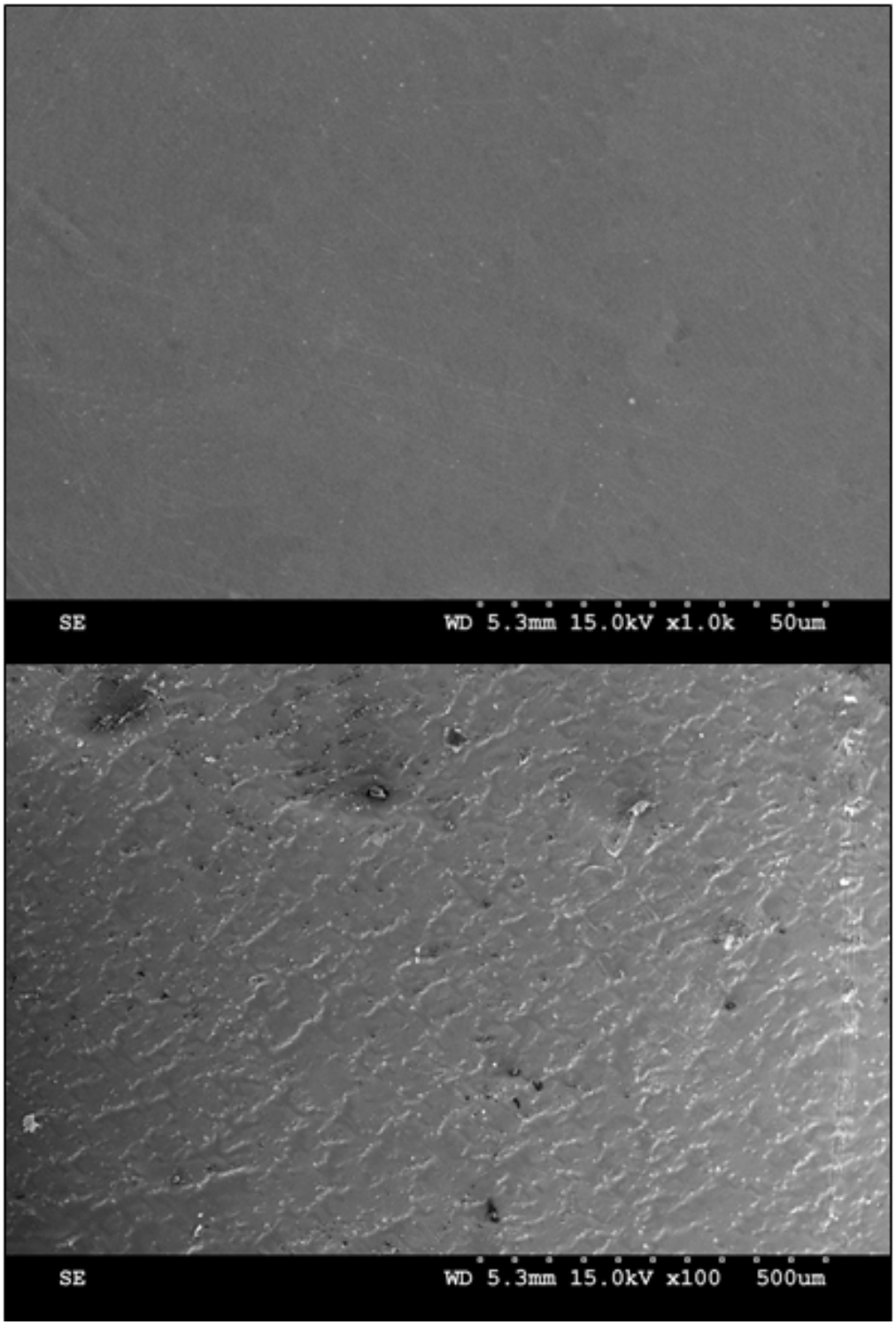

Figure 2.15 Microscopie électronique pour un échantillon du PET recyclé avant et après vieillissement à 200 °C pendant 360 heures (x100)

Certains polymères comme le PET, PEN et le PVC deviennent opaques après leur vieillissement thermique. En effet, un thermoplastique semi-cristallin a la tendance de se déformer sous l'effet de la chaleur (Duguet, Pariente, & Conort, 2005). Cette propriété d'opacité est un phénomène réversible et le polymère peut récupérer sa transparence lorsqu'il est chauffé au-dessus de son point de fusion, si ce polymère n'a pas été renforcé par des charges inorganiques (Degallaix, 2007). Le comportement diélectrique des matériaux composites vieillis semble mettre en jeu quelques modifications qui se distinguent particulièrement par une forte diminution des pertes diélectriques tandis que la rupture diélectrique semble être un facteur moins important (Bellomo, Lebey, Oraison, & Peltier, 1995). Cependant, la rigidité diélectrique, qui est une propriété physique liée au champ électrique appliqué, dépend également de la nature de l'ensemble des éléments formant le composite (matrice et renforts). Par conséquent, la dégradation d'un système due aux contraintes thermiques cause un changement structural qui peut entrainer une baisse ou hausse du champ électrique nécessaire à la rupture diélectrique. Afin de valider cette hypothèse, plusieurs tests ont été effectués. La figure 2.15 illustre un échantillon de PET recyclé avant et après vieillissement thermique à 200 °C pendant 360 heures. Plus de détails sont représentés par l'article 2 dans le chapitre 4.

2.7.3 Vieillissement accéléré par effet couronne

La durée de vie d'un système d'isolation électrique opérant sous contraintes électriques est contrôlée par plusieurs facteurs. La qualité de l'isolant ainsi que l'amplitude des contraintes électriques contribuent en grande partie au vieillissement de ces isolations. Certains systèmes d'isolation sont soumis à des décharges électriques pré-disruptives que l'on nomme décharges couronnes. L'effet couronne est un phénomène électrique extrêmement complexe et très fréquent dans les isolations électriques. Ce phénomène électrique connu principalement dans les bobines de grandes machines tournantes et dans les câbles et lignes haute tension se manifeste par l'initiation d'une décharge électrique au voisinage d'une pointe, surface ou cavité dans un milieu diélectrique. Le phénomène se produit dans les systèmes d'isolation où la tension appliquée dépasse la tension-seuil menant à l'ionisation du milieu gazeux (l'air) et

provoquant des décharges partielles pouvant à plus ou moins long terme entrainer la rupture du système d'isolation.

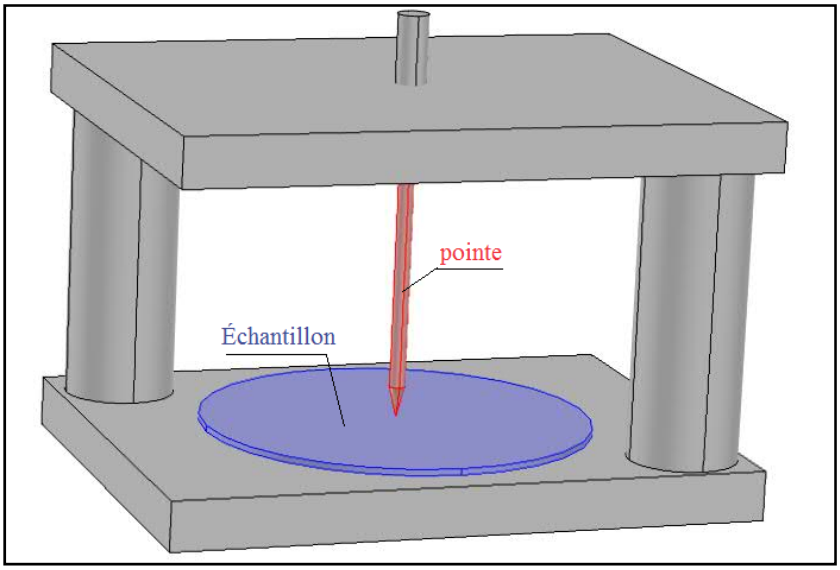

Figure 2.16 Cellule de mesure avec pointe ayant un rayon de courbure de 1mm

Afin d'examiner l'endurance des matériaux de notre étude, un système de vieillissement accélère sous effet couronne a été adopté. Tel qu'illustré par la figure ci-dessous, le système comprend trois parties principales, la cellule de mesure, la source d'alimentation et le système d'affichage des décharges partielles (couronnes). La cellule de mesure comprend deux plaques parallèles reliées par des tiges en polyimide, la plaque inférieure est mise à la terre, la plaque supérieure permet de tenir la pointe traversant son centre à partir d'un perçage. La figure 2.16 illustre la géométrie pointe –plan qui sera utilisée pour effectuer les essais de vieillissement accéléré.

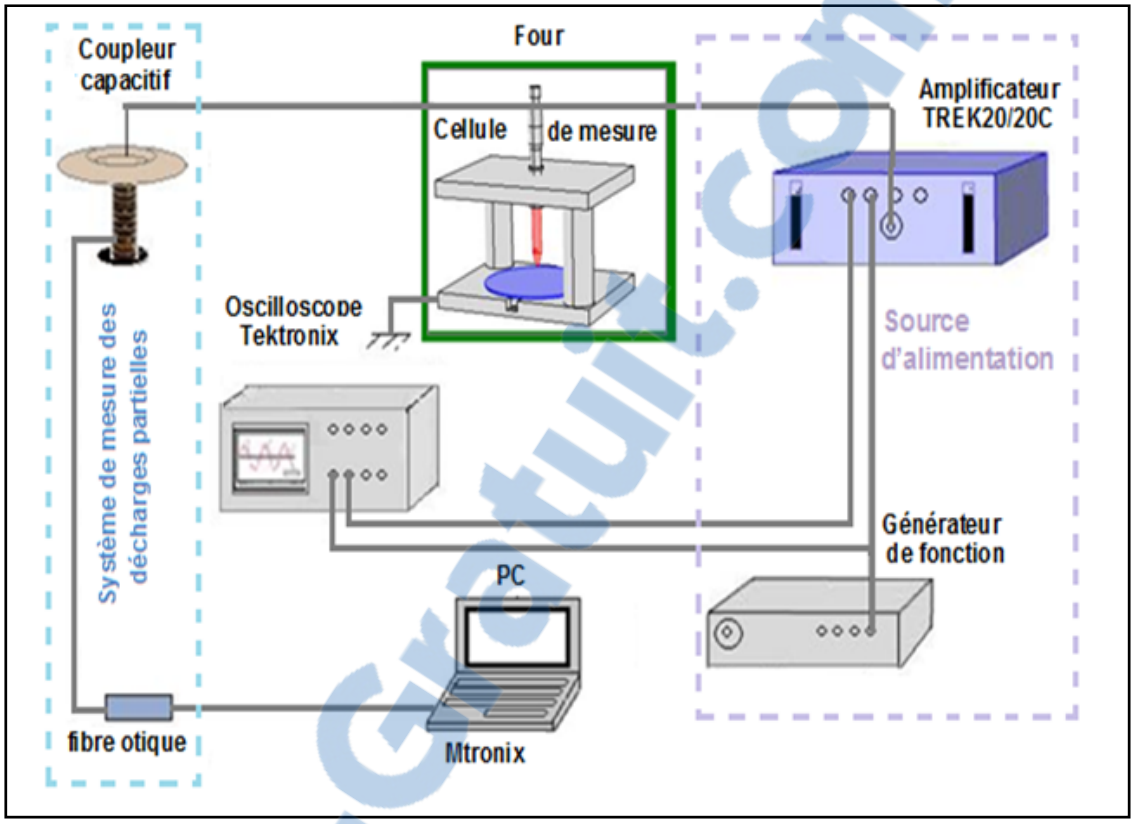

Figure 2.17 Schéma synoptique du banc d'essai pour les mesures d'endurance
Tiré de Mebarki et *al*. (2012)

Le système d'alimentation comprend un générateur permettant de fournir une tension sinusoïdale. La tension de sortie est par la suite élevée grâce à l'amplificateur capable d'offrir un gain de 1000V/V. Les décharges couronnes sont détectées par un moniteur de courant « PEARSON » de type transformateur de courant et affichées à l'aide d'un oscilloscope TEKTRONIX. L'essai consiste essentiellement à appliquer sur la pointe une tension constante (par exemple 7kV rms) afin d'estimer la durée de vie des matériaux sous étude dans des conditions de vieillissement sous décharges et sous température contrôlée. Le dispositif expérimental réalisé à l'ÉTS et qui a été adopté pour ce type de mesure est illustré par la figure 2.17. Plus de détails sont représentés par l'article 1 dans le chapitre 3.

2.7.4 Vieillissement combiné (électrothermique)

La principale cause de défaillance d'un système électrique opérant à haute température est la dégradation causée par les contraintes électriques et thermiques auxquelles ces composants sont exposés. La combinaison de contraintes électriques et thermiques peut accélérer le processus de vieillissement et minimiser ainsi la durée de vie du système ou même causer sa rupture diélectrique. Dans ce cas, la cellule de mesure du type pointe-plan sera placée dans une enceinte climatique(four) permettant de réaliser des essais à des températures allant de la température ambiante jusqu'à 200ºC. C'est ainsi que les contraintes électriques et thermiques seront combinées.

2.8 Conclusion

Le présent chapitre avait comme objectif de présenter les diverses méthodes qui ont été utilisées pour valider la performance des échantillons fabriqués à partir des ressources du PET recyclé. Des caractérisations morphologiques, diélectriques et thermiques ont été également réalisées sur les différents matériaux composites à base de PET recyclé renforcés de fibre de verre et mica. Les mesures effectuées ont permis également d'examiner l'effet de l'ajout des renforts à la matrice (PET recyclé et le PEN).

Le chapitre suivant sera consacré à l'étude de la dégradation sous effet couronne. Les effets du vieillissement électrothermique sur le polyéthylène téréphtalate recyclé (RPET) et ses différents composites sera faite surtout sur les propriétés diélectriques comme la rigidité et la permittivité. On verra également une comparaison entre le PET recyclé et son concurrent le PET vierge (provenant de l'industrie pétrochimique).

CHAPITRE 3

ARTICLE I: Characterization of the Dielectric Endurance of Reinforced Recycled PET Using Electro-Thermal Aging Test

Fouzia Mebarki and Éric David

Département de génie mécanique École de Technologie Supérieure (ÉTS), 1100 Notre-Dame Ouest, Montréal QC, Canada H3C 1K3

Article publié dans le journal : IEEE Transactions on Dielectrics and Electrical Insulation, Décembre 2015.DOI: 10.1109/TDEI.2015.005194

ABSTRACT

This paper presents the advantages of dielectric characterization by electro-thermal aging testing in the durability analysis of reinforced recycled polyethylene terephthalate (PET), as compared to short-term dielectric breakdown strength measurements. Dielectric breakdown strength measurements were carried out at room temperature according to ASTM D149-a, while electro-thermal aging tests were conducted in air at different constant temperatures ranging from 140 to 170 °C, using an experiment setup comprising a cell test arranged in a point-to-plane configuration, with a very small air gap of 50±1 µm. The tests were conducted at an AC voltage of amplitude 7 kV rms on eight different reinforced recycled PET samples. The degradation of recycled PET-based composites during exposure to corona discharges at elevated temperatures was characterized by optical microscopy and scanning electron microscopy (SEM). The main goal of this study is to characterize and to determine the relationship between the addition of different inorganic reinforcements, such as mica and glass fibers, to a recycled PET matrix, as well as the resistance to dielectric failure during electro-thermal aging. The effect of plasticizers on the dielectric endurance of recycled PET-based composites was also investigated. Results obtained showed that glass fibers contribute to the enhancement of the resistance to dielectric failure. Our experiments also revealed that the dielectric behaviour of these composites can be affected by the presence of plasticizers. In

addition, the size of additives such as mica can greatly improve the resistance to the dielectric breakdown caused by electro-thermal aging.

3.1 Introduction

Dielectric characterization plays an important role in the improvement of recipes used in manufacturing insulation systems in the electrical and electronic fields. One of the most common problems affecting insulation systems is aging caused by electrical and thermal stresses, which can eventually degrade insulating materials to the point where they are no longer reliable under normal operating conditions.

In a variety of applications, the use of thermoplastic polymer in place of thermosets is constantly on the rise. Among thermoplastic polymer resins, Polyethylene Terephthalate (PET) is one of the best promising candidate polyesters thanks to its excellent mechanical and chemical properties, which remain stable in a relatively large range of temperatures, in addition to having good processability. PET also exhibits good electrical insulating properties, which makes it a suitable material for insulation systems in electrical and electronic applications. One of such applications is the mechanical support for the HV terminal system feeding the spark plugs of internal combustion engines.

The mechanical supports of engine ignition systems used in the automotive industry are subjected to high dielectric and thermal stresses. While the ideal operating temperature of an automobile engine is typically around 90 °C, it can nevertheless achieve temperature variations taking it up to 140 °C. In addition, temperatures in North America can get down to -40 °C in winter, and as a result, this application requires materials with a good dielectric endurance for a wide range of temperatures going from -30 to over 150 °C.

Polyethylene Terephthalate is a recyclable polyester that retains its good electrical and mechanical characteristics. Although recycling plastics involves significant costs, it is still

relatively cheaper than using virgin PET. The treatment and recycling of plastics from post-consumption components requires a good knowledge and understanding of the chemistry and physics of polymers as well as their manufacturing processes(Awaja & Pavel, 2005). PET can be recycled chemically, by complete depolymerisation, to recover terephthalic acid (TPA) monomers, Dimethyl Terephthalate (DMT), and Monoethylene Glycol (MEG), or by partial polymerization, to recover oligomers. It can also be done by mechanical separation from other components based on their density differences.

The problem of aging or deterioration of insulation materials under combined thermal and electrical stresses has been widely covered in the literature, and several improvements of the dielectric endurance have been proposed (164, 1991; Bahadoorsingh & Rowland, 2008; L. A. Dissado & Fothergill, 1992; Montanari, Mazzanti, & Simoni, 2002; Simoni, 1999). Some studies mainly related to the introduction of additives such as mica and other reinforcements, including nano-sized particles were also reported (Haq & Omranipour, 2011; Hong, 2005; Roy et al., 2005). Mica is used as the primary barrier to erosion caused by partial discharges (Shields & Kemp, 2000) while other conventional fillers, such as short or long glass fibers, are incorporated to improve the mechanical properties(Jarukumjorn & Suppakarn, 2009; Kalaprasad, Joseph, & Thomas, 1997).

This type of reinforcement is commonly used to manufacture components in electrical and electronic devices and automotive parts. However, few studies have been conducted on the thermal and mechanical properties of recycled Polyethylene Terephthalate-based composites(Corradini et al., 2009), and fewer still on their dielectric properties. Some studies examining the dielectric properties of thermoplastic PET have been reported (Adhikari, Hepburn, & Stewart, 2011; Beauguitte, Yahyaoui, Notingher, Agnel, & Kieffel, 2012;Neagu, Pissis, Apekis, & Ribelles, 1997). To our knowledge, no reports have been published dealing with comparative studies of the dielectric properties and the dielectric endurance of recycled and virgin PET reinforced with inorganic materials such as mica and glass fibers.

The main objectives of the current study were to verify the reliability of recycled PET composites, and secondly, to investigate the role of each additive in the resistance to the

dielectric degradation caused by both electric and thermal stresses. Our investigation of dielectric breakdown caused by electro-thermal aging was also aimed at discussing the dielectric breakdown mechanism and the effect of some reinforcements added to recycled PET, as well as its impact on the performance and durability of thermoplastic insulation materials.

3.2 Materials

Eight different PET-based materials were used to investigate the relationship between the composite formulation and the electro-thermal endurance, as well as the use of recycled PET as the polymeric matrix on the dielectric endurance under thermal stresses. Materials were compounded and supplied by the Lavergne Group in Montreal, Canada. A brief description of the different materials investigated in this studied is given in Table 3.1.

The glass fiber and large platelet mica-filled recycled PET (RPET_GF_LM2) contains almost twice as much plasticizer as the glass fiber and small platelet mica-filled recycled PET (RPET_GF_LM1). RPET_GF1 and RPET_GF2 are two recycled glass fiber-filled PET without plasticizers, but RPET_GF2 also contains almost twice as much glass fiber as RPET_GF1. The RPET is a recycled PET with plasticizers and without inorganic reinforcements, while the recycled mica-filled PET with plasticizers (RPET_M) contains the same amount of mica as the other recycled PET filled with mica and glass fibers.

Tableau 3.1 Brief description of the different materials

Sample identification	Composite	Additional information
RPET	Recycled PET with plasticizers	Material without inorganic reinforcements
RPET_M	Recycled mica-filled PET with plasticizers	RPET_LM contains the same amount of mica as the other recycled PET filled with mica and glass fiber
RPET_GF1	Recycled glass fiber-filled PET without plasticizers	RPET_GF2 contains almost twice as much glass fiber as RPET_GF1
RPET_GF2	Recycled glass fiber-filled PET without plasticizers	VPET_GF2 contains almost the same amount of glass fiber as RPET_GF2
VPET_GF2	Virgin glass fiber-filled PET without plasticizers	
RPET_GF_SM1	Recycled glass fiber and small platelet mica-filled PET with a small quantity of plasticizers	Glass fiber /Mica ratio 2:1
RPET_GF_LM1	Recycled glass fiber and large platelet mica-filled PET with a small quantity of plasticizers	Glass fiber /Mica ratio 2:1
RPET_GF_LM2	Recycled glass fiber and large platelet mica-filled PET with plasticizers	Glass fiber /Mica ratio 2:1

3.3 Experimental setup and test procedure

The setup used in our previous investigation (Mebarki & David, 2012) was modified by adding of a programmable timer controller capable of measuring the time to dielectric breakdown under exposure to partial discharges at elevated temperatures.

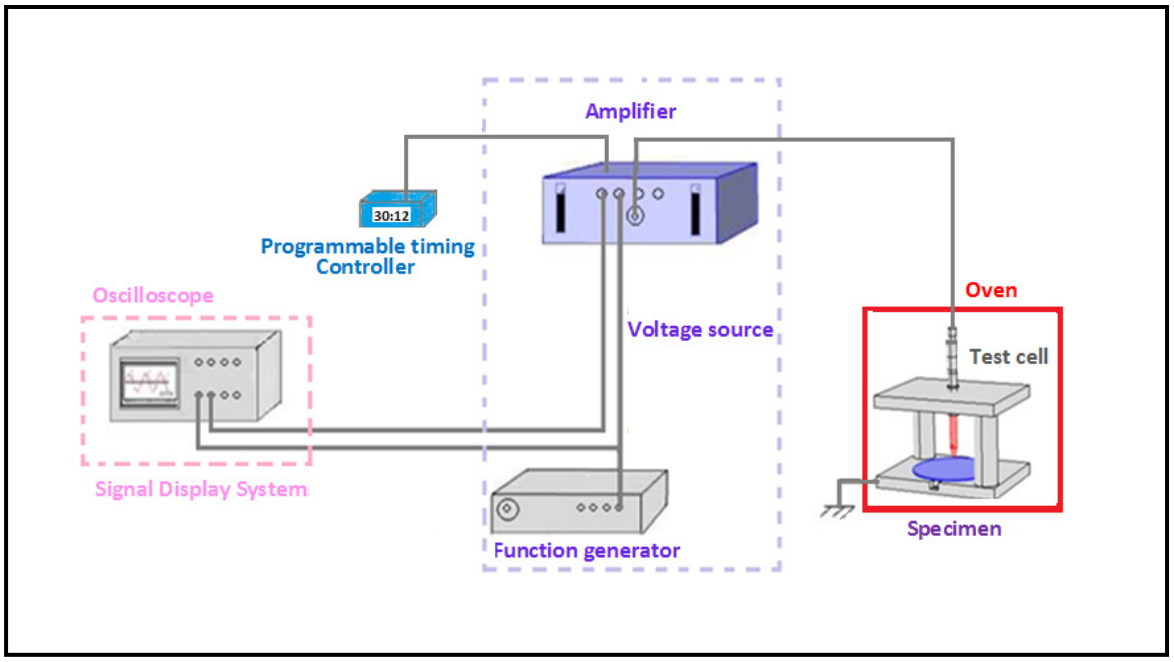

Figure 3.1 Schematic diagram of the experimental system

The tests were conducted in air at different constant temperatures ranging from 140 to 170 °C and at 300 Hz AC voltage of around 7 kV rms; the test cell was arranged in a point-to-plane configuration, with a very small air gap of 50±1 µm between the point electrode and the flat surface of the disk-shape sample. Figure3.1 shows a schematic diagram of the experimental system used for the current investigation.

It was possible to measure accurately the breakdown time using a programmable timer controller which was connected to the high-voltage amplifier. Once the breakdown occurred, an electrical signal was sent to the timer, which automatically stopped.

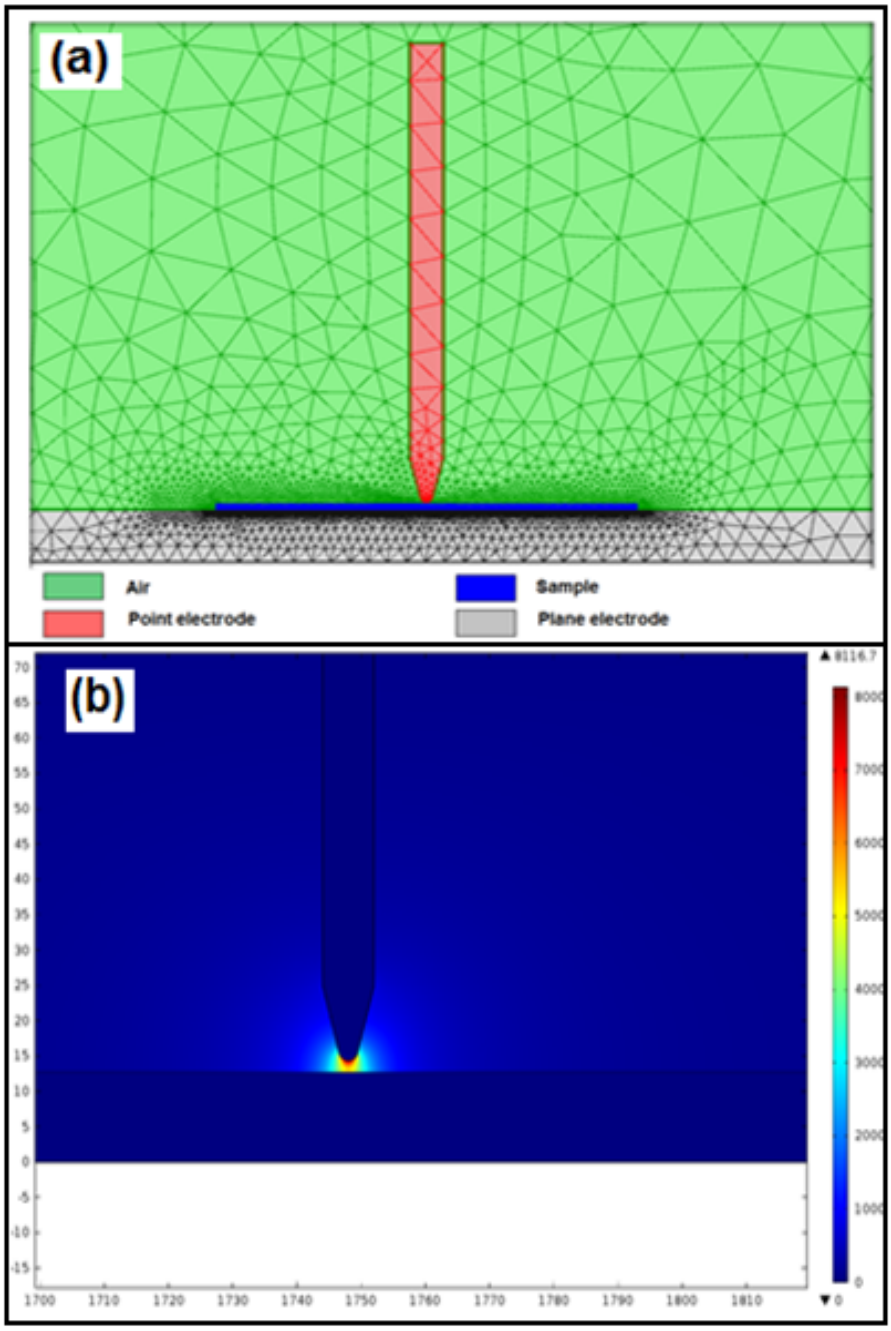

Figure 3.2 a) Geometry used for FEM analysis; b) electrical field distribution with a potential difference of 7 kV rms between the point electrode and the plane electrode (Comsol Multiphysics).

The magnitude of the electrical field along the electrode axis, E, at the tip of the point electrode can be evaluated using the well-known hyperbolic approximation given by (Mason, 1981):

$$E = \frac{2 * U}{r * ln\left[1 + \frac{4 * d}{r}\right]} \quad (3.1)$$

where U is the applied voltage, r is the tip radius and d is the distance between the needle tip and the plane electrode.

In the presence of an insulator close to the tip of the electrode, the distribution of the electrical field can be computed using numerical techniques such as the finite element methods (FEM), as shown in Figure 3.2a.; with a radius of curvature of 1 mm and an applied voltage of 7 kV rms, the numerical simulation yielded an electrical field of 29.1 kV/mm at the electrode tip, as shown in Figure 3.2b.

3.4 Results and discussion

3.4.1 Structure and morphology

The microstructural degradation caused by the electro-thermal aging of reinforced recycled PET was examined by both scanning electron microscopy (SEM) and optical microscopy. To observe the breakdown path, specimens were carefully cut in order to allow the observation of the perforation caused by dielectric breakdown. The cut surfaces were polished to a smooth finish surface free from scratches. Two grades of polishing sandpapers were consecutively used: 800 Grit followed by 1000. Once the specimen was polished, it was cleaned with methanol. A thin gold layer measuring approximately 20 nanometers was applied using a plasma coater for the observation with the SEM.

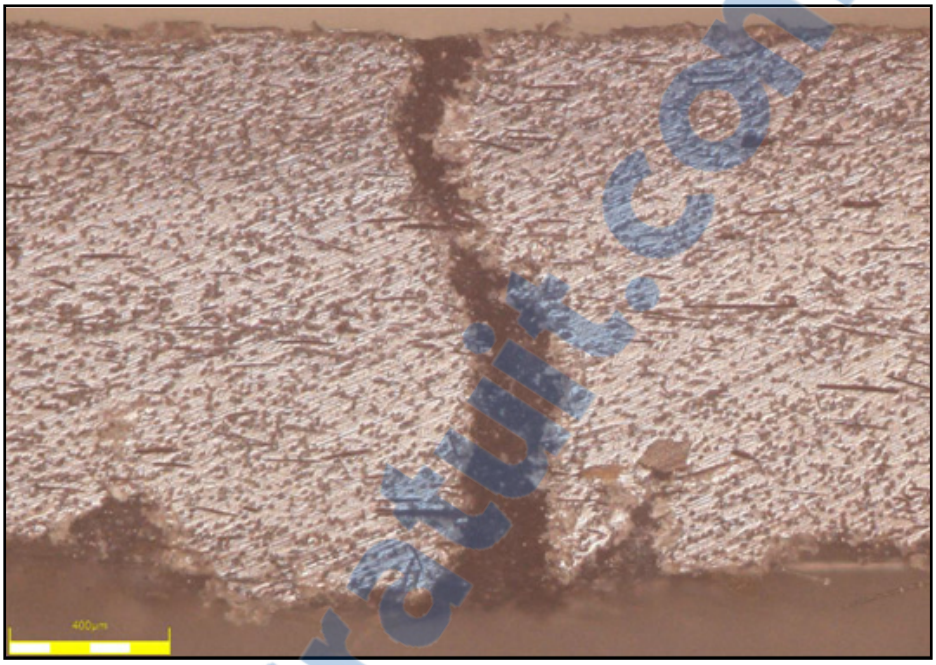

Figure 3.3 Photograph (X69) showing a cross-section of the eroded area and the breakdown path through a specimen (RPET_GF_SM1) tested at 140 °C).

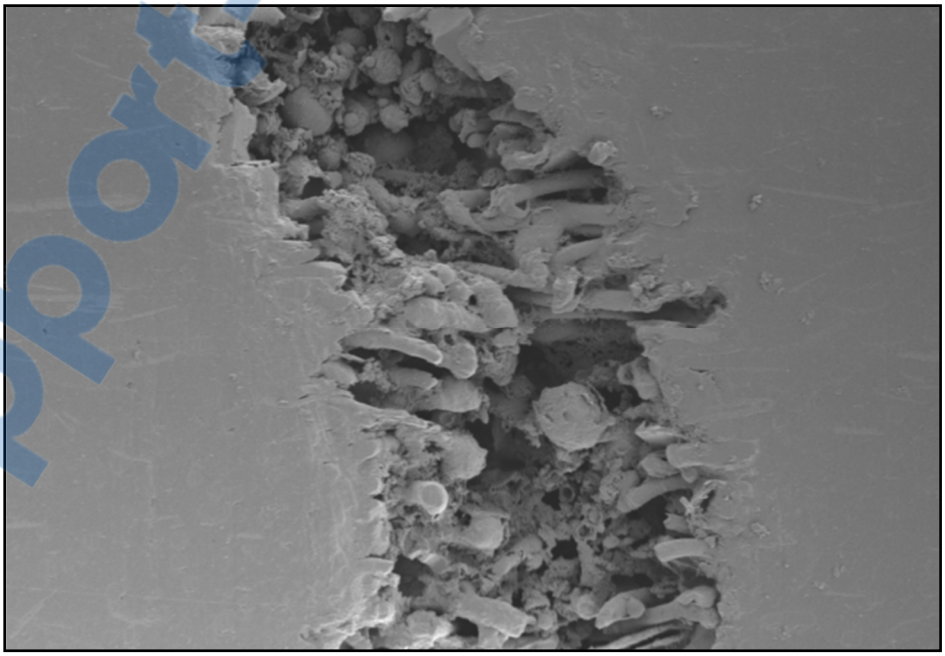

Figure 3.4 SEM image showing a part of the breakdown path of a specimen (RPET_GF_SM1) tested at 170 °C (X200).

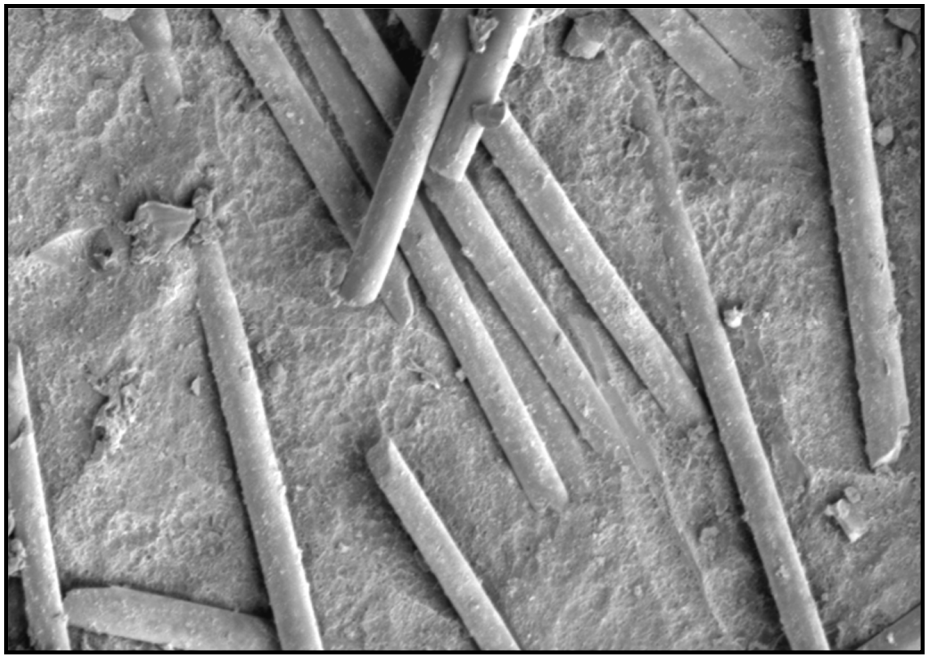

Figure 3.5 SEM image of the eroded area caused by electro-thermal aging of a specimen (RPET_GF_SM1) (X500).

The microscopic examination shown in Figure 3.3 (optical) and Figure 3.4 (electronic) revealed the tortuous breakdown path, suggesting a zigzag type pre-breakdown treeing mechanism. A SEM image taken from an eroded area caused by the electro-thermal aging of a specimen is shown in Figure3.5. As can be seen, inorganic reinforcements did not seem to be affected by electro-thermal aging, while the resin was eroded away. Photographs taken by optical microscope revealed the deterioration steps of recycled PET reinforced with mica under thermal and electrical stresses (see Figure 3.6).

The steps of the electro-thermal aging process as observed by SEM and optical microscopy are schematically depicted in Figure 3.7. The first step in the electro-thermal aging process is the softening of the polymeric matrix. The degradation process starts with the aging of the matrix, leading to surface erosion as the partial discharge activity continues. As shown in the figure, the polymeric matrix continues to be eroded away while inorganic materials such as glass fibers and mica platelets remain relatively unaffected. After a certain aging time, the combined thermal and electrical stresses embrittle the matrix and a final perforation or breakdown occurs.

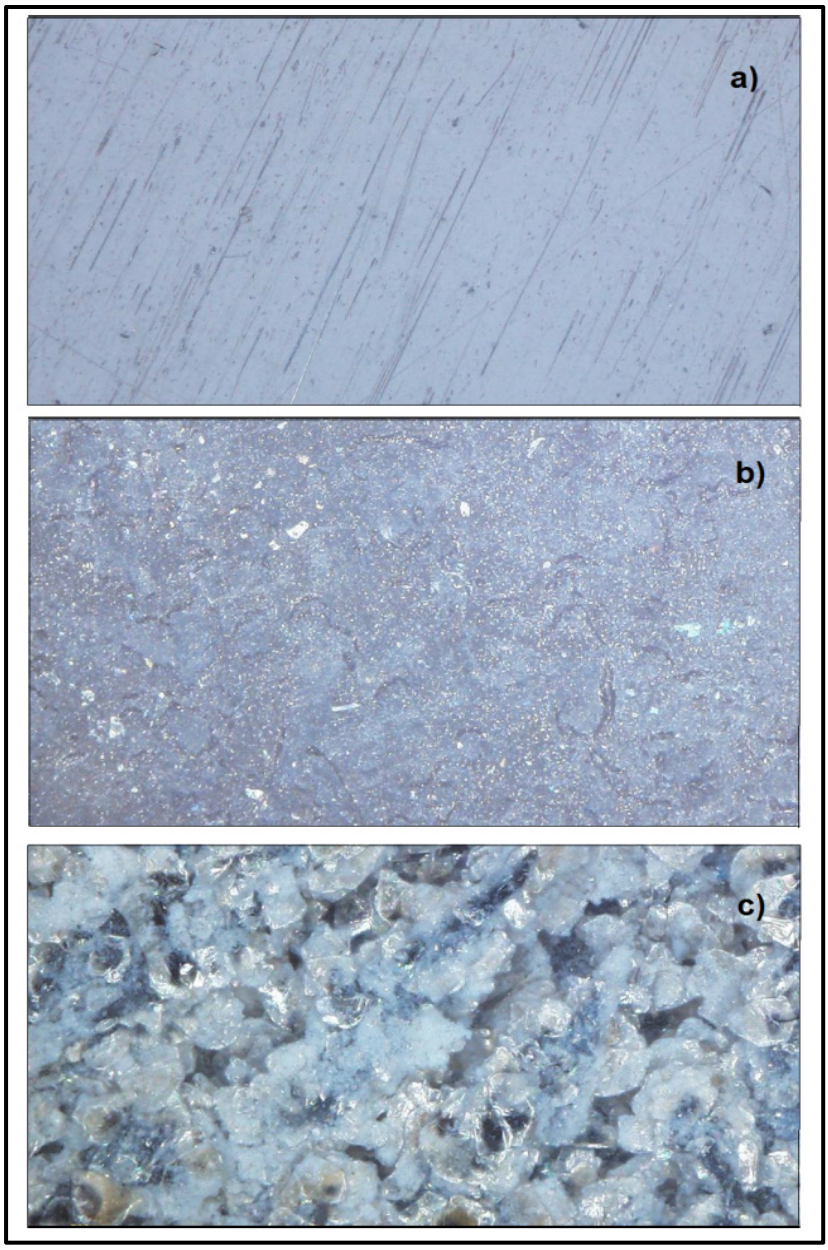

Figure 3.6 Optical microscope images (X69) of the deterioration steps of a recycled PET reinforced with mica under thermal and electrical constraints: a) non-eroded specimen; b) specimen eroded for 5 hours, and c) specimen eroded for 60 hours.

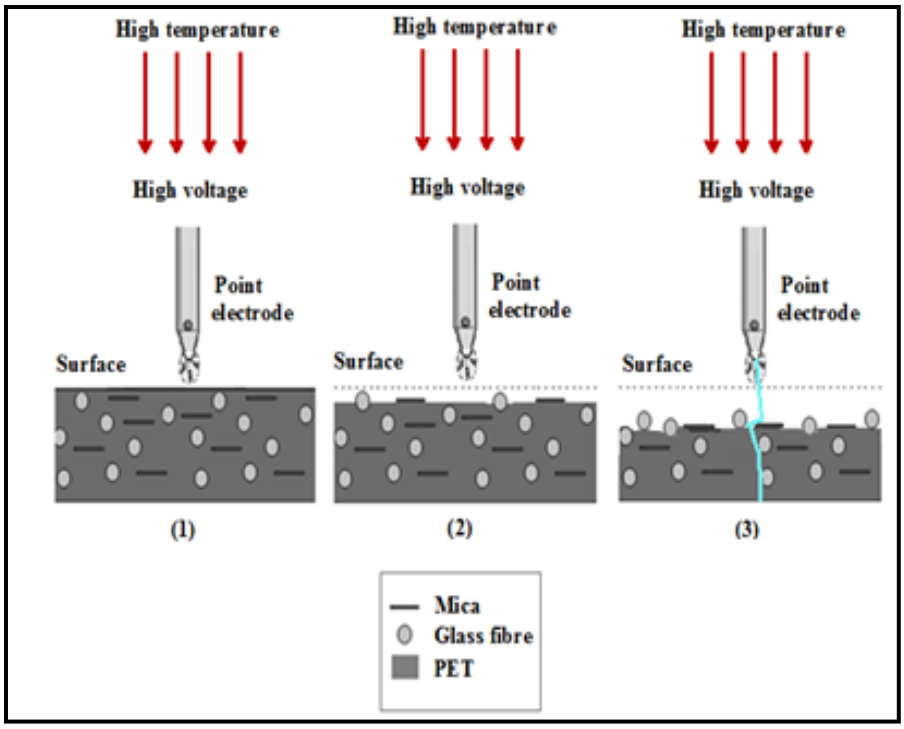

Figure 3.7 Steps in electro-thermal aging process

3.4.2 Dielectric failure statistical analysis

In order to quantify the dielectric endurance and the dielectric strength of the various materials listed in Table 3.1, two different types of tests were performed on different sets of specimens, namely, a short-term breakdown test and an electro-thermal endurance test under corona discharges. The data obtained were analyzed with the aid of the two-parameter Weibull distribution according to the IEEE Standard 930 (Montanari et al., 2002)whereby the cumulative probability of failure is given by the following equation:

$$F(x) = 1 - exp\left[-\left(\frac{x}{\alpha}\right)^{\beta}\right] \tag{3.2}$$

where β is the Weibull shape factor, α is the scale factor corresponding to 63.2% failure probability, and x is either an electrical field or a time to breakdown (electric field in the case of short-term breakdown tests and time to breakdown in the case of endurance tests). The 90% confidence bounds were obtained using the weighted least squares regression technique, as recommended in (ASTMD149, 2004).

3.4.3 Short term breakdown tests

Single measurement tests were carried out on four different recycled PET-based composites (RPET, RPET_M, RPET_GF1 and RPET_GF_SM1, in accordance with ASTM D149-97a (2004) [20] on twenty specimens of each material. All tests were performed under identical conditions at room temperature, with spherical electrodes 12.5 mm in diameter, and using mineral oil as the surrounding medium.

Tableau 3.2 Weibull distribution parameters.

Sample identification	Weibull distribution parameters at 140°C			
	B	α_l (h)	α (h)	α_u(h)
RPET_GF1	12.8	28.3	29.2	30.1
RPET_GF_SM1	13.5	30	31.1	31.9
RPET	10.1	31	32.3	33.5
RPET_M	14.8	33.7	34.6	35.2

Table 3.2 summarizes the dielectric breakdown strength data for each tested material. These parameters were calculated as recommended in [19]. The parameters αu and αl denote the upper and lower limits of the 90% confidence interval for the scale parameter α. As was reported in our previous studies, and as can be seen in Figure 8, all materials exhibit a roughly similar behaviour, having dielectric breakdown strength values (scale parameter) with

overlapping or nearly overlapping confidence bounds (not shown in Figure 8). RPET_GF1 and RPET_M composites show the lowest and the highest scale factor values respectively, while RPET_GF_SM1 and RPET composites have quite similar values of breakdown strength. Therefore, we can conclude that addition of glass fibers reinforcements does not increase the material breakdown strength during short term test (and possibly decreases it) while the addition of mica fillers improves it.

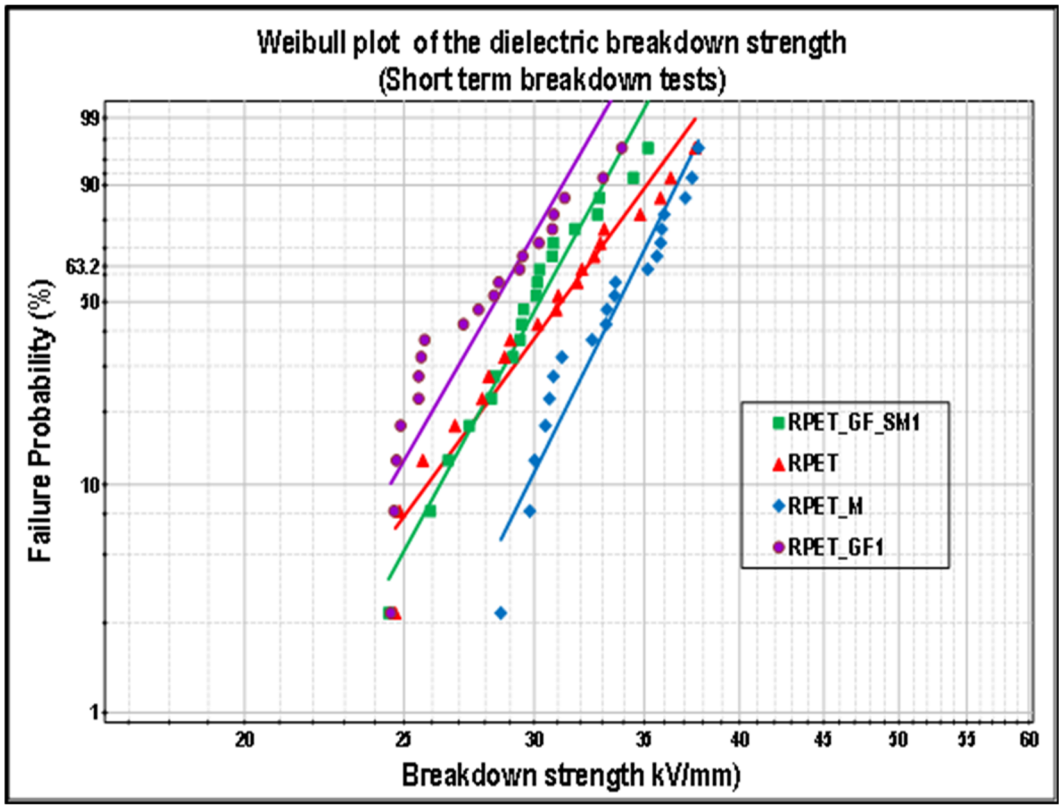

Figure 3.8 Dielectric breakdown strength of four types of recycled PET materials

3.4.4 Endurance tests

For this type of test, the aging temperature and voltage were kept constant until the breakdown of each sample occurred. For each tested condition, only five specimens of each material were tested since the duration of the test imposes a practical limit on the number of tested specimens. The time-to-failure data obtained for the various tested materials were also processed using the

two-parameter Weibull distribution according to the IEEE Standard 930. The resulting Weibull probability plots for each set of data are shown in Figures 3.9 to 3.13.

3.4.5 Effect of plasticizers

The influence of plasticizers on the resistance to dielectric failure caused by electro-thermal aging on three different types of recycled PET-based composite materials was investigated. The resulting Weibull probability plots for each set of values obtained at 140 and 170 °C are shown in Figures 3.9 and 3.10, respectively.

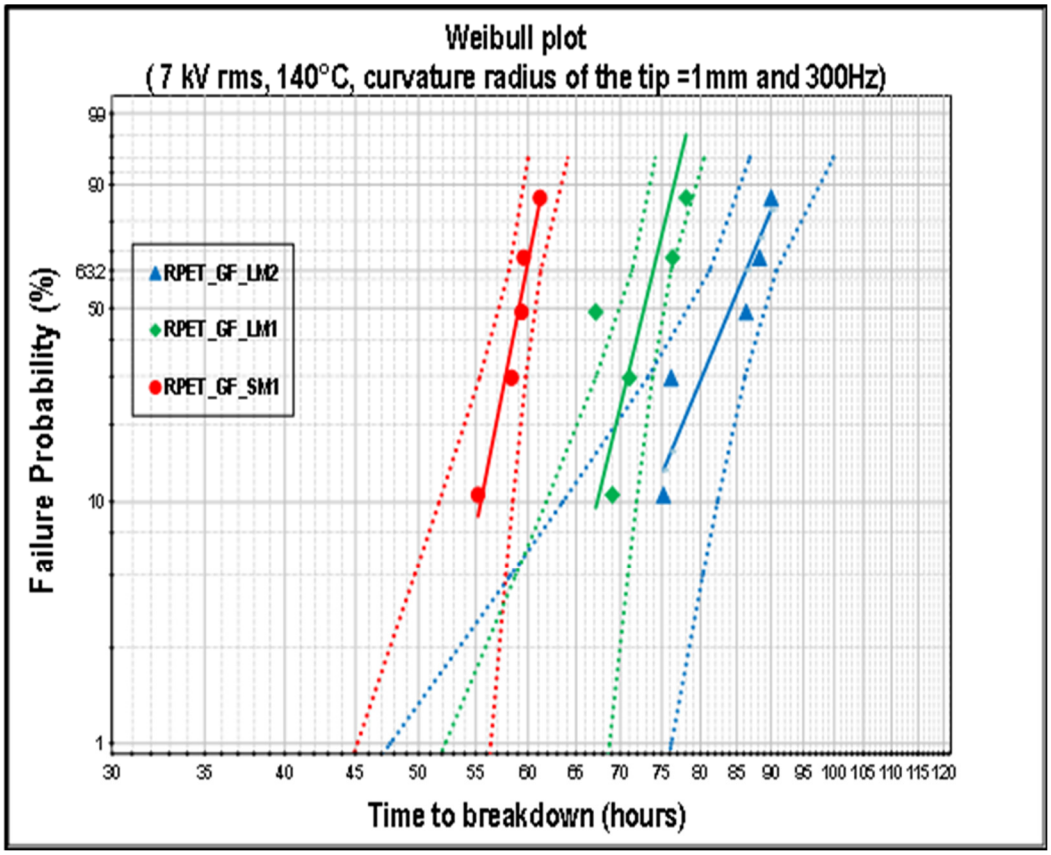

Figure 3.9 Effect of plasticizers on the time-to-breakdown Weibull distributions of three different types of recycled PET-based composites at 140 °C and 7 kV rms

Specimens of the material RPET_GF_SM1 that were produced using the lowest percentage of plasticizers have the lowest average time to breakdown, 59.8 hours at 140°C, as compared to

the other materials, RPET_GF_LM1 and RPET_GF_LM2, which have a time to breakdown of 73.9 and 86.3 hours, respectively. At 170 °C, specimens of the material RPET_GF_LM2 and RPET_GF_LM1 have an average time to breakdown of 65.3 and 50.1 hours, respectively. Therefore, it could be concluded, comparing sample RPET_GF_LM1 and RPET_GF_LM2 (see Figure3.10) that the addition of plasticizers enhances the dielectric endurance at high temperature for reinforced recycled PET.

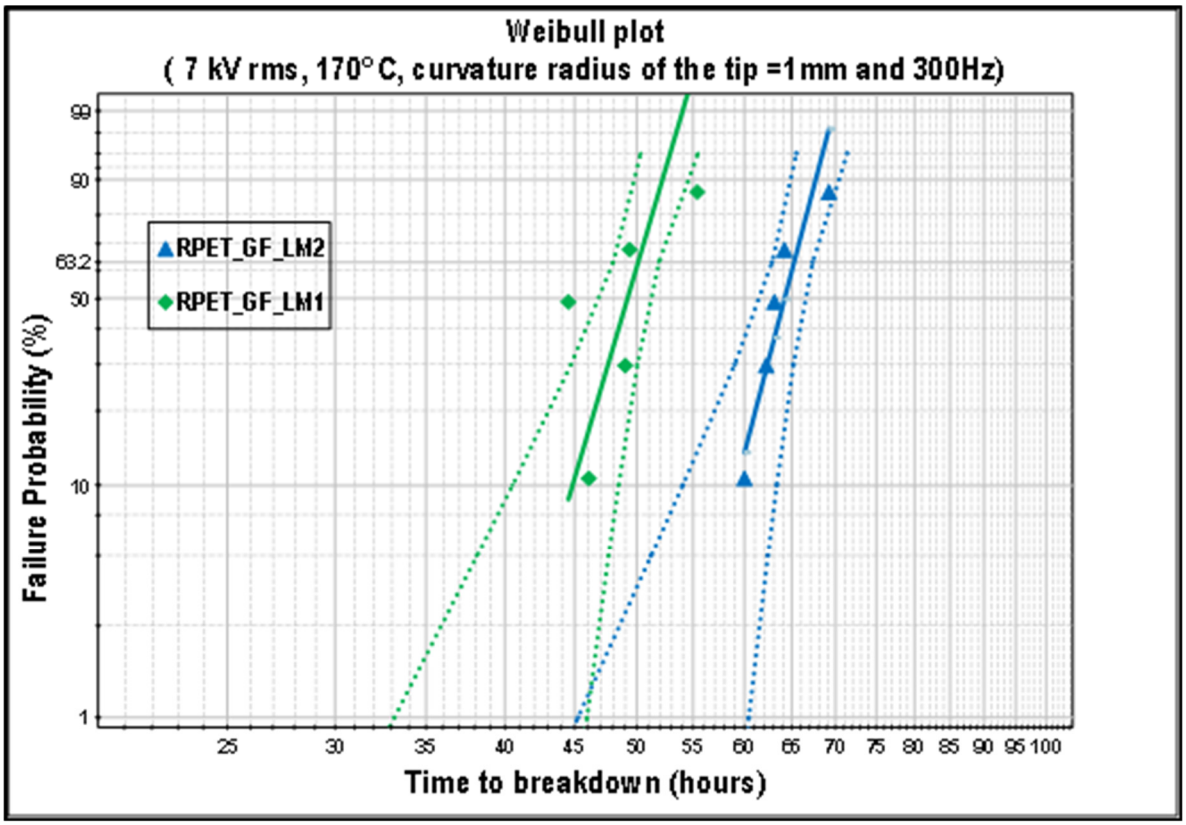

Figure 3.10 Effect of plasticizers on the time-to-breakdown Weibull distributions of three different types of recycled PET-based composites at 170°C and 7 kV rms

3.4.6 Effect of the amount of glass fibers

Figure 3.11 shows the comparison between the RPET_GF1 and RPET_GF2 materials. It can be seen that the composite containing the higher amount of glass fibers (RPET_GF2) showed an improved performance as compared to a material containing a small amount of glass fibers.

It was also reported in (Poh, 2004)that glass fibers can improve thermal properties of recycled PET.

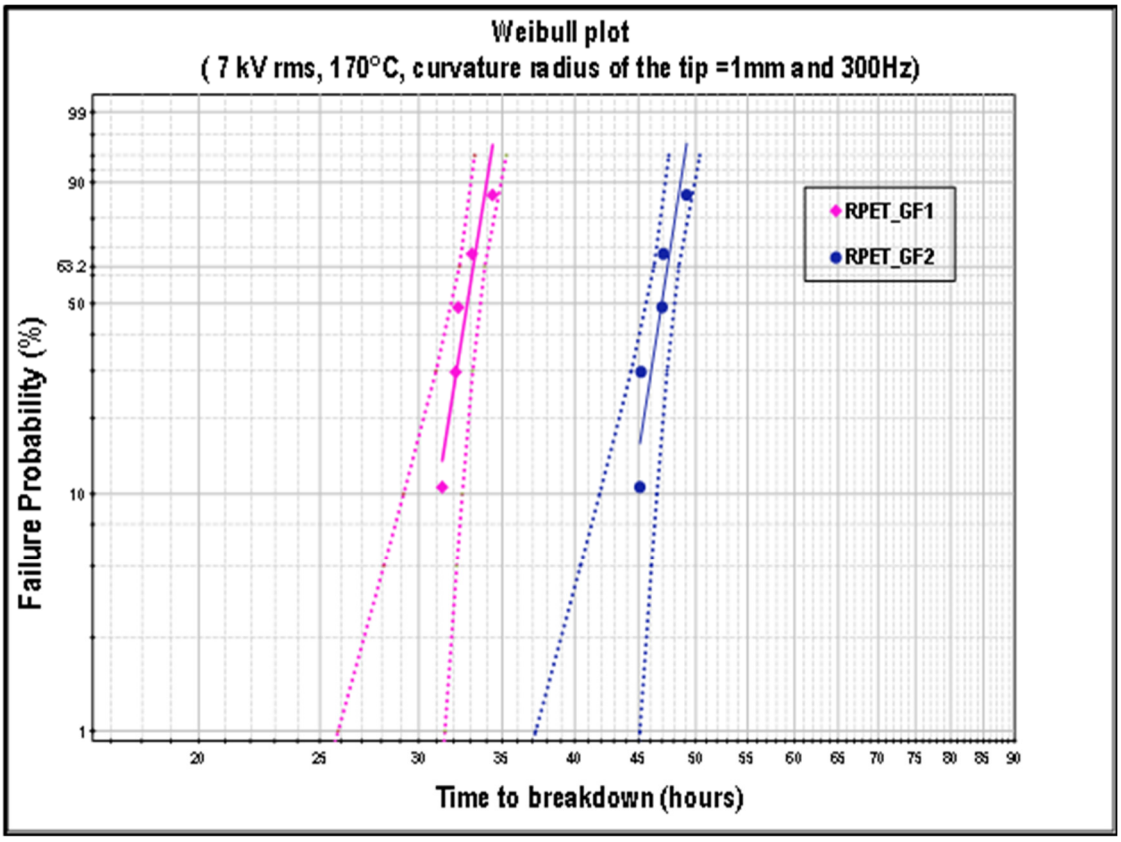

Figure 3.11 Effect of the amount of glass fibers on the time-to-breakdown Weibull distributions of RPET_GF1 and RPET_GF2 materials at 170 °C.

3.4.7 Effect of mica platelets sizes

Figure 3.12 shows the data obtained from the time-to-breakdown Weibull distributions of two different types of recycled PET materials at 170 °C and 7 kV rms. The RPET_GF_LM1 has a higher resistance to dielectric breakdown than that of RPET_GF_SM1. This higher resistance can be attributed to the size of mica platelets. The composite containing the higher mica platelets size shows the best result for the endurance test, with an average time to breakdown of 86.3 hours at 140 °C and 65.3 hours at 170 °C (see Tables 3 and 4). This behavior is attributable to the improved electric and thermal properties due to the formation of large surface dielectric barriers.

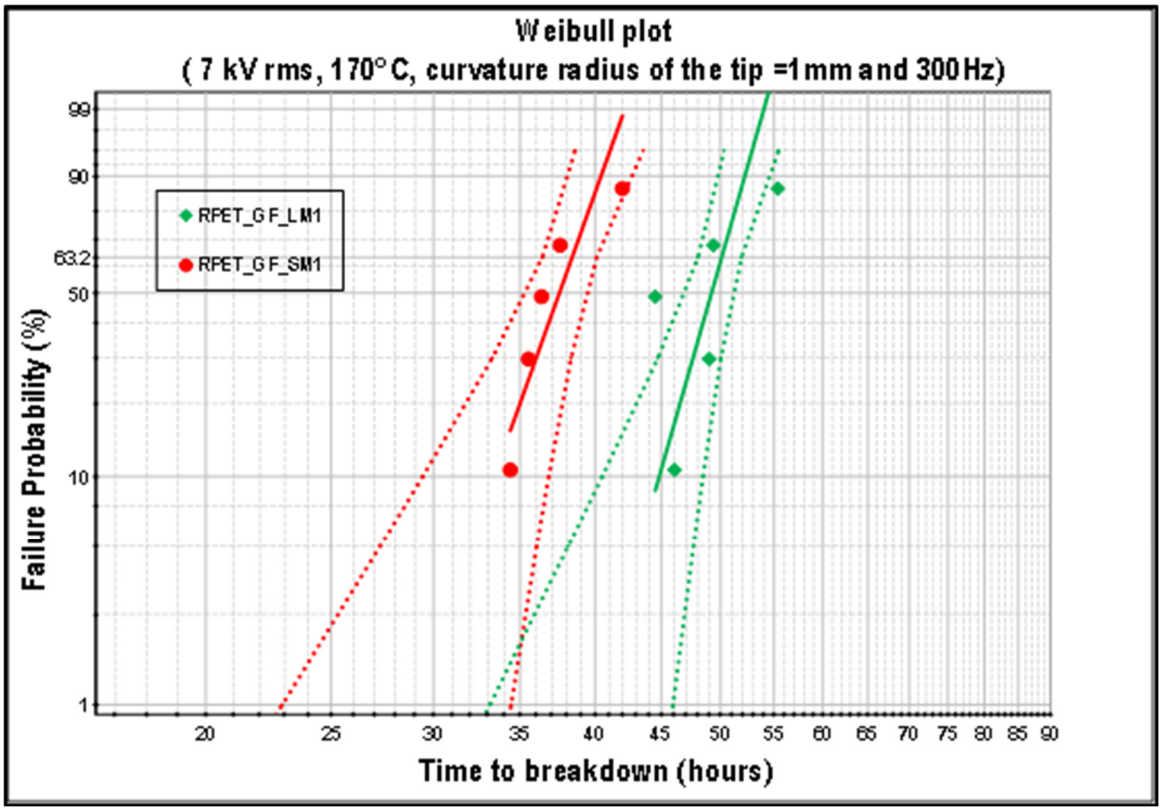

Figure 3.12 Effect of mica platelet sizes on the time-to-breakdown Weibull distributions of two different types of RPET-based composites at 170 °C and 7 kV rms.

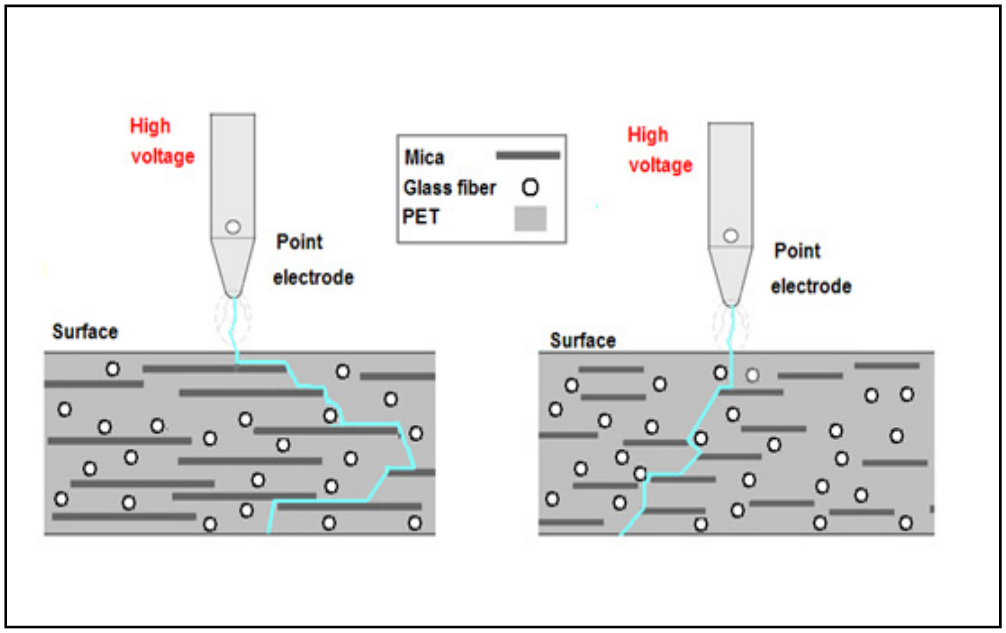

Figure 3.13 Schematic comparison of the possible breakdown path for the two different types of mica platelets

Figure 3.13 illustrates a schematic comparison of the possible breakdown path for the two different types of mica platelets showing the need for a longer path in the case of the large mica platelets.

3.4.8 Recycled PET reliability

The reliability of the recycled PET resources for use as dielectric materials has been investigated using two PET-based composites; one manufactured using recycled PET, and the other with industrial (virgin) PET. As we can see in Figure 3.14, for similar glass fiber loads, the recycled PET-based material exhibits a similar dielectric performance as its virgin counterpart. Therefore, it can be concluded that there is no downgrade of the dielectric properties from the use of recycled material for PET.

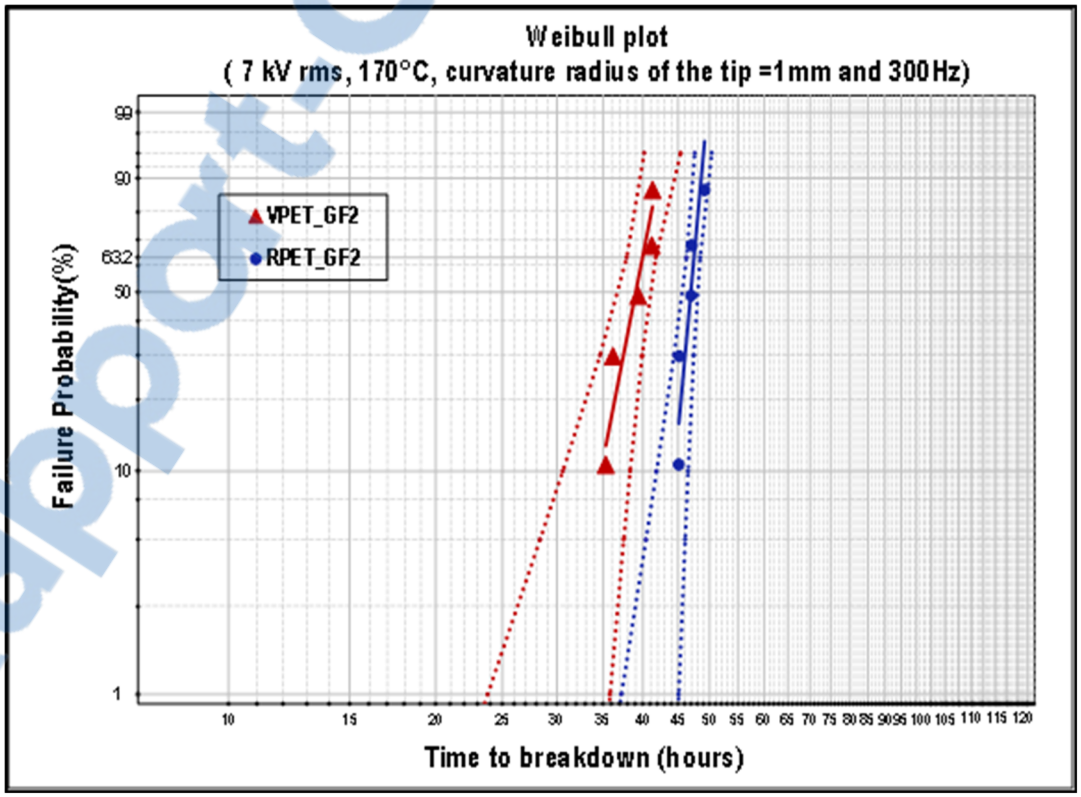

Figure 3.14 Time-to-breakdown Weibull distributions showing the reliability of recycled PET resources.

3.4.9 The non-filled Recycled PET

Unlike the reinforced recycled PET, the non-filled recycled PET starts to deform and shrink at 140 °C when in contact with the lower plate of the measuring cell. As a result, it was difficult to accurately determine the air gap value. Therefore, the non-filled recycled PET was only tested at 110 °C. Figure 3.15 shows the data obtained from the time-to-breakdown Weibull distributions of the non-filled recycled PET at 110 °C and 7 kV rms.

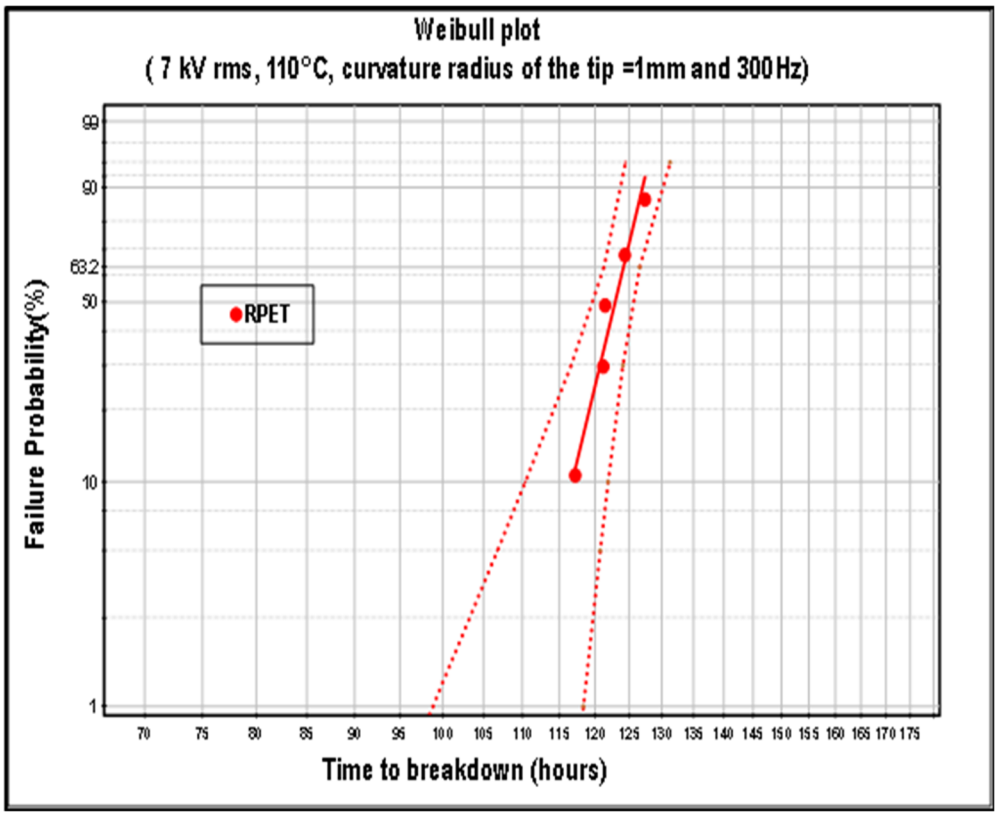

Figure 3.15 Time-to-breakdown Weibull distributions of RPET at 110°C and 7 kV rms

Tables 3.3 and 3.4 summarize the dielectric time to failure for each tested material under electro-thermal aging at 140 and 170 °C. The high values of the shape parameter translate near Gaussian type distribution with a rather low dispersion. As an objective mean to claim enhanced dielectric endurance from one sample to the other, the non-overlapping rule of the confidence bonds was used. Accordingly, it can be seen that the PET composites reinforced by large mica platelets, and

with the highest amount of plasticizers shows the best dielectric performance, as the mica platelet acts as a dielectric barrier and the plasticizer improves the material processability decreasing the number a voids and frozen internal stresses.

Tableau 3.3 Weibull distribution parameters at 140 °C

Sample identification	Weibull distribution parameters at 140 °C			
	B	α_l (h)	α (h)	α_u (h)
RPET_GF_SM1	29.7	58.1	59.8	61.3
RPET_GF_LM1	24.1	71.4	73.9	76.2
RPET_GF_LM2	14.1	81.2	86.3	90.8

Tableau 3.4 Weibull distribution parameters at 140 °C

Sample identification	Weibull distribution parameters at 170 °C			
	B	αl (h)	α (h)	αu (h)
RPET_GF_SM1	16.2	36.4	38.4	40.1
RPET_GF_LM1	20.2	48.0	50.1	51.1
RPET_GF_LM2	22.2	62.9	65.3	67.3
VPET_GF	16.1	37.9	39.9	41.5
RPET_GF	34.4	46.3	47.5	48.5
RPET_M	33.8	59.4	60.9	62.2

3.5 Conclusion

An investigation of the dielectric endurance of recycled PET-based composites has been presented in this paper. This material is a good candidate for manufacturing electrical and electronic devices and automotive parts, such as the mechanical support for internal combustion engine ignition systems. In this experimental study, the following results were obtained:

- The most prominent limitation that currently exists in dielectric characterization by dielectric short-term breakdown testing is the difficulty in comparing materials which are somewhat similar in their compositions and which yield approximately similar results.
- An analysis of the resistance to dielectric failure of the recycled PET under electro-thermal aging reveals that the time to breakdown decreases when thermal and electric stresses are combined.
- Additional plasticizers can enhance the processability and the adhesion of the reinforcement fillers to the PET matrix, and accordingly improve resistance to the electro-thermal aging of reinforced recycled PET.
- The addition of mica, especially large platelet mica, greatly improves the dielectric endurance of the recycled PET.
- Increasing the amount of glass fibers contributes to the enhancement of the resistance to dielectric failure at high temperature.
- Microstructural characterization has shown that the trajectory of the breakdown path is influenced by the presence of inorganic fillers, especially mica.

Dielectric characterization by electrical and thermal aging may support the optimization of existing composite recipes. This leads to the continuous improvement of the quality of materials used to produce electrical insulation systems.

ACKNOWLEDGMENT

The authors are grateful to Patrick Lachance and Doru Davinscu from the Lavergne Group, which kindly supplied the materials used for this study. Great thanks to the National Sciences and Engineering Research Council of Canada (NSERC) for its financial support. The authors also wish to thank Michel Drouin for his technical help.

CONFLICT OF INTERESTS

The authors declare that there is no conflict of interests regarding the publication of this paper.

CHAPITRE 4

ARTICLE II: DielectricCharacterization of thermally-aged RECYCLED POLYETHYLENE terephtalate and polyethylene naphthalate reinforced with inorganic fillers

Fouzia Mebarki and Éric David

Département de génie mécanique École de Technologie Supérieure (ÉTS), 1100 Notre-Dame Ouest, Montréal QC, Canada H3C 1K3

Article soumis et accepté dans le journal : Polymer Engineering & Science le 10 Septembre 2016. Article ID: PES-16-0801

ABSTRACT

In order to assess the influence of the operating temperature on the dielectric properties of recycled Polyethylene Terephthalate (PET) and PET) and Polyethylene Naphthalate (PEN) reinforced with inorganic fillers, a dielectric and thermal investigation was undertaken. Specimens were thermally aged at several temperatures between 90 and 200 °C for 360 hours. The effect of thermal aging time on dielectric and thermal properties was also investigated. The dielectric response and breakdown strength properties were evaluated. Differential scanning calorimetry (DSC) measurements showed that the degree of crystallinity and the glass transition temperature increased with aging temperature and duration. The data obtained showed that these materials exhibited a good resistance to thermal aging at temperatures below 140 °C. Furthermore, it was found that the dielectric strength of the recycled PET and PEN and their composites decreased considerably for temperatures of over 170 °C.

4.1 Introduction

During the past few decades, considerable attention has been devoted to the development of new insulating materials suitable for electric and electronic parts. The majority of insulating materials used in high voltage devices used to be restricted to thermoset composites, specifically mainly epoxy resin-based composite materials. However, these thermosets are gradually being replaced by thermoplastic ones. The benefits of thermoplastic composites include lower weight, lower costs, recyclability and faster processing cycles, which make them the ideal materials used in electric and electronic devices, as compared to thermoset composites. Thermoplastic materials must possess high resistivity, low dielectric constants and, for some applications, good endurance to electrical discharges. In addition, they must exhibit a good resistance to thermal aging.

In the automotive industry domain, polyethylene terephthalate (PET) is used to manufacture certain parts, such as the fixture and the mechanical support for spark plugs. In such applications, this mechanical support is subjected to hard thermal and electric stresses. It must operate at a high voltage at over -40 to 110 °C temperature range. Increasing the operating temperature of these materials allows a corresponding increase in the operating temperature of internal combustion engines, thus improving their efficiency through reduced fuel consumption.

Polyethylene terephthalate (PET) is a popular thermoplastic used in a variety of areas thanks to its excellent characteristics, which remain relatively stable over a wide range of operation temperatures. It is a polyester with a melting temperature of 267 °C and a glass transition temperature between 67 and 80 °C, and has a dielectric constant value of approximately 3.1. PET has attracted a lot of attention over the years, and several studies have been reported on the analysis of its morphological, thermal, mechanical and dielectric properties (Alves, Mano, & Ribelles, 2002; Awaja & Pavel, 2005; Badia, Vilaplana, Karlsson, & Ribes-Greus, 2009; Fox, Moad, Van Diepen, Willing, & Cook, 1997; Lu & Hay, 2001; Miyairi, 1986; Neagu et al., 1997; Ward, 1962). When reinforced with inorganic fillers such as mica and glass fibers, this polyester may represent the most promising thermoplastic for some automotive parts.

Polyethylene Naphthalate (PEN) is also semi-crystalline polyester, with a higher glass transition temperature (112-120 °C) and a higher melting temperature (268 to 270 °C) as compared to PET. Its relative permittivity is about 3.3 at room temperature, and at a frequency of 103 Hz, and its dielectric breakdown voltage is higher than that of PET. Because of its good thermal and barrier properties, as well as its high cost, PEN is mainly used as a high performance engineering polymeric material in advanced mechanical and electrical applications, such as special packaging and bottling susceptible to oxidation, as well as for the miniaturization of capacitors. Fig. 4.1 presents a schematic diagram of both materials (PET and PEN) employed in this study. They are chemically similar, but a naphthalene ring in PEN replaces the benzene ring in PET, increasing the structural stiffness of the former (Lechat, Bunsell, Davies, & Piant, 2006).

PEN and PET can also be mixed together, and their blends used in different applications, especially in electric and electronic devices, thanks to their unique thermal and dielectric properties, which can remain stable over a wide temperature domain (Bedia, Murakami, Kitade, & Kohjiya, 2001; Fermeglia et al., 2006; Ghadami, Ehsani, & Khonakdar, 2015; Kyotani, Pudjiastuti, & Saeed, 1999; Patcheak & Jabarin, 2001). Several works have reported on comparison studies between PET and PEN. Adding PEN to PET can alter some of the combined thermal, chemical and mechanical properties. Morphological inspections report that in PET/PEN blends, the morphologies changed from PET type to PEN type, with increasing PEN content (Yoshioka, Tsuji, Kawahara, & Kohjiya, 2003). To further enhance the oxygen barrier and thermal stability properties, the core layer may further include a copolymer or blend of PEN (Collette, Schmidt, & Krishnakumar, 1999). Several studies have reported on the significant mechanical properties of the PEN polymer, which make it a more suitable substrate material for various applications. Based on their creep behavior (and relative cost), PEN appear to be suitable alternative substrates to PET (Weick & Bhushan, 1995). Other studies report that phosphorus containing copolyesters of both PET and PEN exhibit better flame retardancy, higher char yield, and thermal stability than homopolymers of PET and PEN(C. S. Wang, Shieh, & Sun, 1998). Moreover, dielectric permittivity has been found to be related to crystallinity growth in both PET and PEN polymers (Bellomo & Lebey, 1996), and the β* dielectric process in the copolymers (PEN/PET) has been found to shift to higher frequencies

isothermally (or to lower temperatures isochronally), with increasing terephthalic acid content (Bravard & Boyd, 2003). Few studies about the characterization of thermally-aged virgin PET have been published (Morel, Dung, & Joly, 1980; Ulrych, Polanský, & Pihera, 2014). In a recent paper by Wang et al. (W. Wang et al., 2015), color changes and changes in the dielectric response of virgin PET as a function of thermal aging was reported, and the results were in good agreement with our findings.

Thermal aging is a convenient test that may be used to predict the operating temperature of various materials, and in this particular case of dielectrics, used for electric and electronic applications. It is certainly one of the most widely used assessment tests and has been the subject of a number of reports in recent decades. Several studies confirm that prolonged exposure to high temperatures causes significant changes in thermal, chemical, electrical, and mechanical properties. Indeed, the degradation in the surface region is believed to be responsible for the embrittlement of aged material (Eriksson, Boydell, Eriksson, Månson, & Albertsson, 1997) and they may exhibit a faster reduction in elongation at break and melting peak temperature (Budrugeac & Segal, 1998). Moreover, a significant reduction of molecular weight has been reported after thermal degradation occurs in polyethylene samples containing pro-oxidants (Chiellini, Corti, D'antone, & Baciu, 2006). It has also been confirmed that some changes in the crystallinity and the electrical resistivity were found after thermal aging of some materials (Hamasha et al., 2012). Other studies have demonstrated that the sensitivity to partial discharges (PD) (Farahani, Gockenbach, Borsi, Schafer, & Kaufhold, 2010)and changes in some mechanical properties such as elongation at break and tensile strength may occur in polymeric insulation systems due to the aging process (Budrugeac & Segal, 1998; Farahani et al., 2010).

This work aims to provide an understanding of the dielectric properties of composite materials manufactured with recycled PET resin, in terms of dielectric response and dielectric endurance. To the best of our knowledge, no work has reported on the correlation between dielectric properties and thermal aging performed on recycled PET or PEN and their composites. This new knowledge will improve existing recipes for making recycled PET-based composites reinforced by glass fibers and mica, in order to obtain materials that are easy to process, and

that have the desired electrical and thermal properties. The purpose is not only to use low-cost and low-weight recyclable materials, but also to enhance the performance of internal combustion engines while reducing the fuel rate. In order to assess the reliability as well as the condition of recycled PET resources, some accelerated thermal aging tests were conducted on different recycled PET reinforced with mica and glass fibers. In addition, the thermal and dielectric endurance of PEN and glass fiber-filled PEN was investigated in order to evaluate the possibility of using a blend of recycled PET and PEN to form polymer composites that can be used in automotive engines.

4.2 Materials and samples preparation

Seven different materials, including polymers and polymer composites, were used in this investigation. They were provided by the Lavergne Group, Montreal, Canada, in the form of disks measuring 100 mm in diameter and 1.6 mm in thickness. These materials were first extruded into pellets, and then injection-molded at 110 °C into the previously mentioned disk shape samples. Two different micrometric reinforcements, consisting of short glass fibers 3 mm in length and 10.5 µm in diameter, as well as mica platelets 89~254 µm in diameter, were used to form composites. As is well known, glass fibers are the most commonly used reinforcements to enhance mechanical strength (Etcheverry & Barbosa, 2012; Richardson & Sauer, 1976;Stipho, 1998). Mica platelets constitute a high voltage dielectric barrier in polymeric insulation materials. Mica fillers are often applied to enhance both resistance to partial discharges and dielectric breakdown strength (Mebarki & David, 2015; Shields & Kemp, 2000;Sreekanth, Bambole, Mhaske, & Mahanwar, 2009). Fig.4.1 illustrates the morphology of both fillers used.

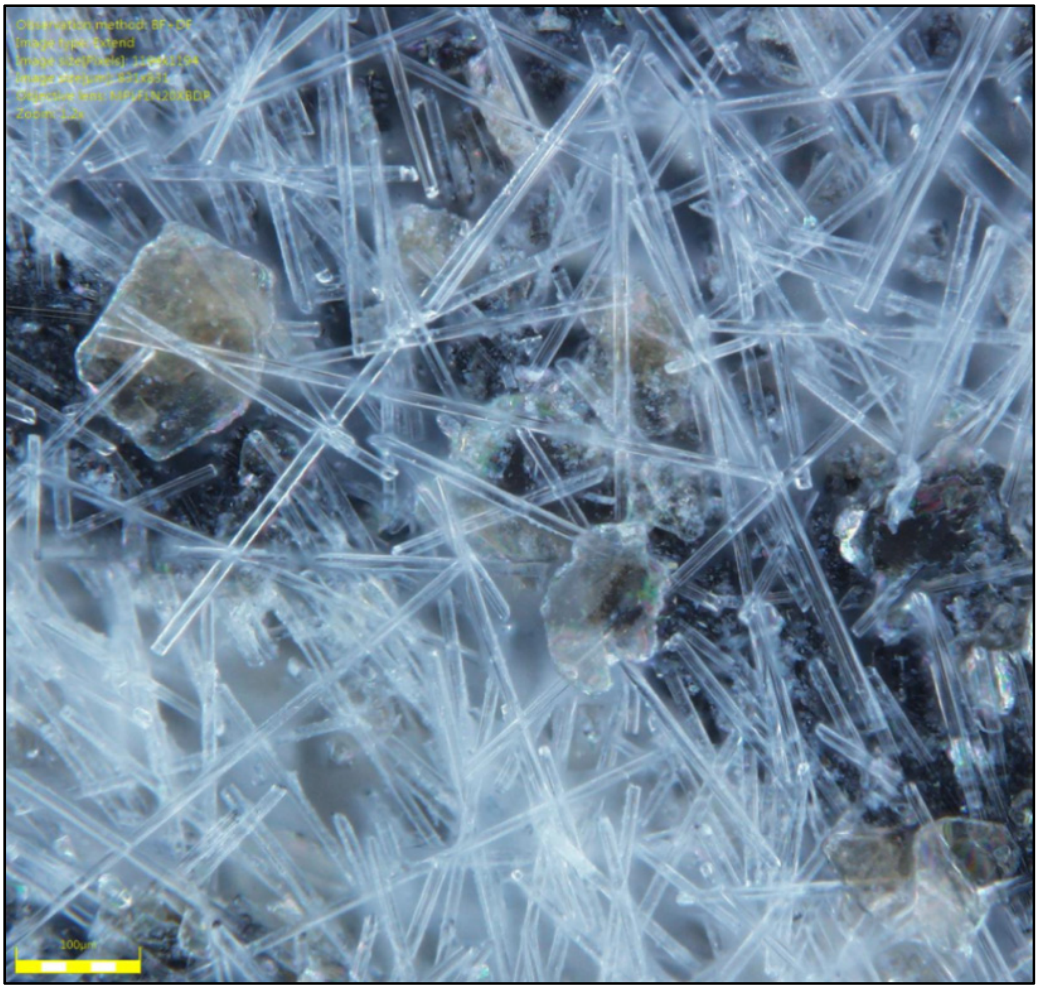

Figure 4.1 Morphology of the glass fibers and mica platelets
used to form the composites of our study (500x)

RPET stands for Recycled PET without inorganic reinforcements and having a density of 1.35 g/cm^3, and PEN is a virgin Polyethylene Naphthalate (with a density of 1.43 g/cm^3), also without inorganic fillers. RPET-GF and the PEN-GF were recycled PET and virgin PEN filled with short glass fibers, respectively. The recycled mica-filled PET used contained the same amount of mica as the other recycled PET filled with mica and glass fiber. RPET-M material is recycled PET reinforced with only large mica platelets, while the RPET-GF-M composite is a recycled PET reinforced with large mica platelets and glass fibers. A brief description of the different materials used in this investigation is given in Table 4.1.

Tableau 4.1 Brief description of the different materials

Specimen identification	Material	Additional information
RPET	Recycled PET	Recycled PET without inorganic reinforcements
PEN	PEN	PEN without inorganic reinforcements
PEN-GF	Glass fiber-filled PEN	PEN filled with glass fibers
RPET-M	RPET reinforced with only mica	Containsonly mica platelets
RPET-GF-M	RPET reinforced with mica platelets and glass fibers	Approx. twice as much glass fibers as mica platelets
RPET_GF	Glass fiber-filled recycled PET	RPET_GF contains almost the same amount of glass fiber as PEN-GF
VPET-GF	Glass fiber-filled virgin PET	RPET_GF contains almost the same amount of glass fiber as VPET-GF

In order to evaluate the effect of the operating temperature on the dielectric properties of recycled PET reinforced with glass fibers or mica, or both of them, a dielectric and thermal analysis of different recycled PET-based composites was undertaken. In addition, specimens of PEN and PEN reinforced with only glass fibers were also investigated in order to compare recycled PET and PEN as well as to evaluate the possibility of using a blend of recycled PET with PEN to form polymer composites for electric applications such as dielectric materials. Some specimens were kept unaged to serve as a reference, while others were thermally-aged in an oven at several constant temperatures between ranging 90 and 200 °C for 360 hours. The effect of the thermal aging time on dielectric and thermal properties was also investigated at 170 °C by using aging times of 360 and 720 hours.

4.3 Characterization

Microstructural analysis was performed on some unaged samples and samples aged at different constant temperatures between 140 and 200 °C, and for different constant durations of 360 and 720 hours, using scanning electron microscopy (SEM). The SEM used in this study was an SU-70 from Hitachi. It is characterized by a secondary electron image of 1.0 nm/15kV and a magnification between 20x and 80,000x. In our study, an accelerating voltage of 3kV was used. Two different magnifications, 10,000x and 50,000x, were used, but only one of them was presented in this paper. Details were better observed with the 10,000x magnification. Before observation under the SEM, the specimens were coated with a very thin layer of gold (20 nm).

Differential scanning calorimetry (DSC) tests were conducted in a dry nitrogen atmosphere according to the ASTM procedure. The DSC run were conducted at a scanning rate of 10°C/ min from 0 to 300 °C using samples of about 15 mg for which the glass transition, melting point and crystallization degree were characterized. The crystallinity degree was measured by following equation (Chen et al., 2014).

$$x_c = 100\frac{\Delta H_m - \Delta H_{cc}}{\Delta H_m^0 * \emptyset} \tag{4.1}$$

where ΔH_m is the enthalpy of fusion of the semi-crystalline polymer, ΔH_{cc} is the enthalpy of polymer cold crystallization obtained by DSC measurement, Ø is the weight fraction of the matrix specimen, and ΔH_m^0 is the enthalpy of fusion of the 100% crystalline polymer (117.6 J/g and 103.4 J/g are values used for the PET and PEN polymers).

The dielectric response was evaluated in the frequency domain using broadband dielectric spectroscopy (BDS), leading to the computation of the real and the imaginary parts of the complex permittivity. The BDS measurements were carried out in the frequency domain in a 10^{-2} to 10^5 Hz frequency window, and at the room temperature, with an upper and a lower

circular electrode 40 mm in diameter. The rms value of the applied voltage was 1V. The frequency dependency of the complex permittivity ε* can be written as:

$$F(t) = \quad 1 - \exp\left[\left(\frac{t}{\alpha}\right)^{\beta}\right] \tag{4.2}$$

where β is the Weibull shape factor, α is the scale factor, corresponding to 63.2% of failure probability, and t is the time or voltage to breakdown of the distribution.

The dielectric breakdown strength (DBS) of unaged and thermally-aged specimens was evaluated using an AC breakdown voltage set-up. Specimens were inserted between two stainless steel spherical electrodes with a 12.7 mm diameter. The thickness of the specimens lay between 1.62 and 1.67 mm. All dielectric breakdown tests were carried out under the same conditions, at room temperature, in a thoroughly degassed mineral oil using the short-time procedure described in the ASTM-D149 for which a 60 Hz sinusoidal wave voltage was applied at a ramp rate of 0.5 kV/s until the specimen breakdown voltage was reached. Data obtained were analyzed with the aid of the two-parameter Weibull distribution according to the IEEE Standard 930 (Std-930, 2004). The cumulative probability of failure is given by the following equation:

$$\varepsilon^*(\omega) = \varepsilon'(\omega) + j\varepsilon''(\omega) \tag{4.3}$$

Where ε' is the real part, ε" is the imaginary part and ω=2πf is the angular frequency.

4.4 Results and discussion

4.4.1 Visual inspection

Figure 4.2a shows the gradual color changes of the recycled PET and PEN as a function of thermal aging temperature (90, 140, 170 and 200 °C). A visual inspection of the recycled PET and PEN samples after thermal aging shows that there is no effect on specimens aged at 90 °C in the case of PEN, with PEN color remaining unaffected by aging at this temperature. However, the color of RPET changes from transparent to opaque at 90 °C and higher temperatures. Furthermore, although no mechanical measurements were done, it was obvious that thermal aging leads to a significant decrease in the mechanical properties as the sample became more brittle after aging, particularly the unfilled recycled PET and PEN, as compared to their composites. Nevertheless, PEN seemed to be more resistant than recycled PET. It should be noted that in the 120 to 160 °C range, PEN is significantly stiffer and stronger, with a modulus almost twice that of PET (Rand & Richter, 2014). Figure 4.2b illustrates the effect of the aging duration on the gradual color changes of some materials after thermal aging at 170 °C for aging times of 0, 320 and 720 hours. Composites filled with mica or glass fibers or both seemed to be more resistant to thermal aging since they are less prone to fracturing. It should also be noted that the samples' thickness increases with increasing aging temperature and duration.

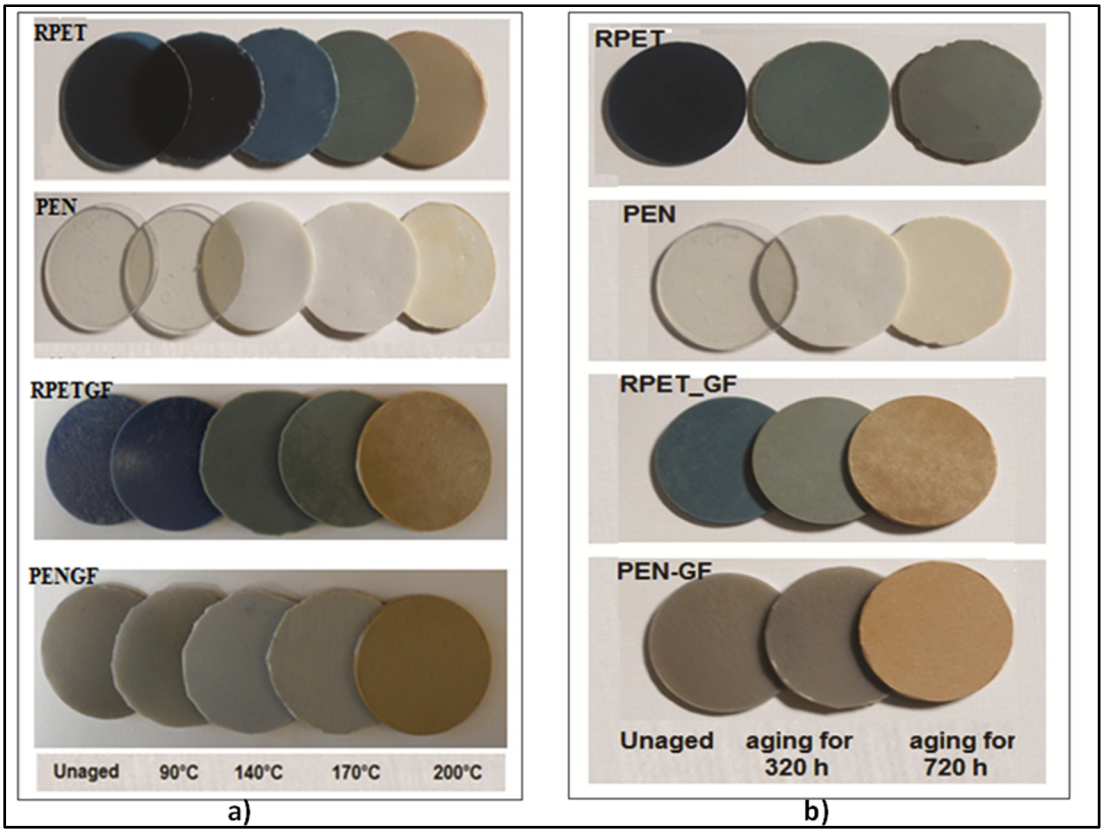

Figure 4.2 Gradual color changes of some samples aged a) for 320 hours at different constant temperatures, and b) at 170 °C for different constant durations

4.4.2 Microstructure and morphology

The microstructural analysis results of some unaged and aged samples at different constant temperatures between 140 and 200 °C are given in Figures 4.3 to 4.5. According to Figure 4.3, no significant change was observed at 140 °C. However, a slight morphological change was seen for the aged PEN after thermal aging at 170 °C. The most prominent surface change was observed after thermal aging at 200 °C. As shown in Figure 4.4, similar surface morphological changes could be observed in the recycled PET polymer. Minor morphological changes were observed at 140 °C. Nevertheless, changes were more obvious for specimens aged at 170 and 200 °C. The effect of thermal aging on surface morphological changes for the recycled PET reinforced with both mica and glass fibers can be observed in Figure 4.5. This composite seems

to be more resistant to thermal aging than the unfilled polymers. As we can see, the surface changes for the composites are only significant for specimens aged at 200 °C.

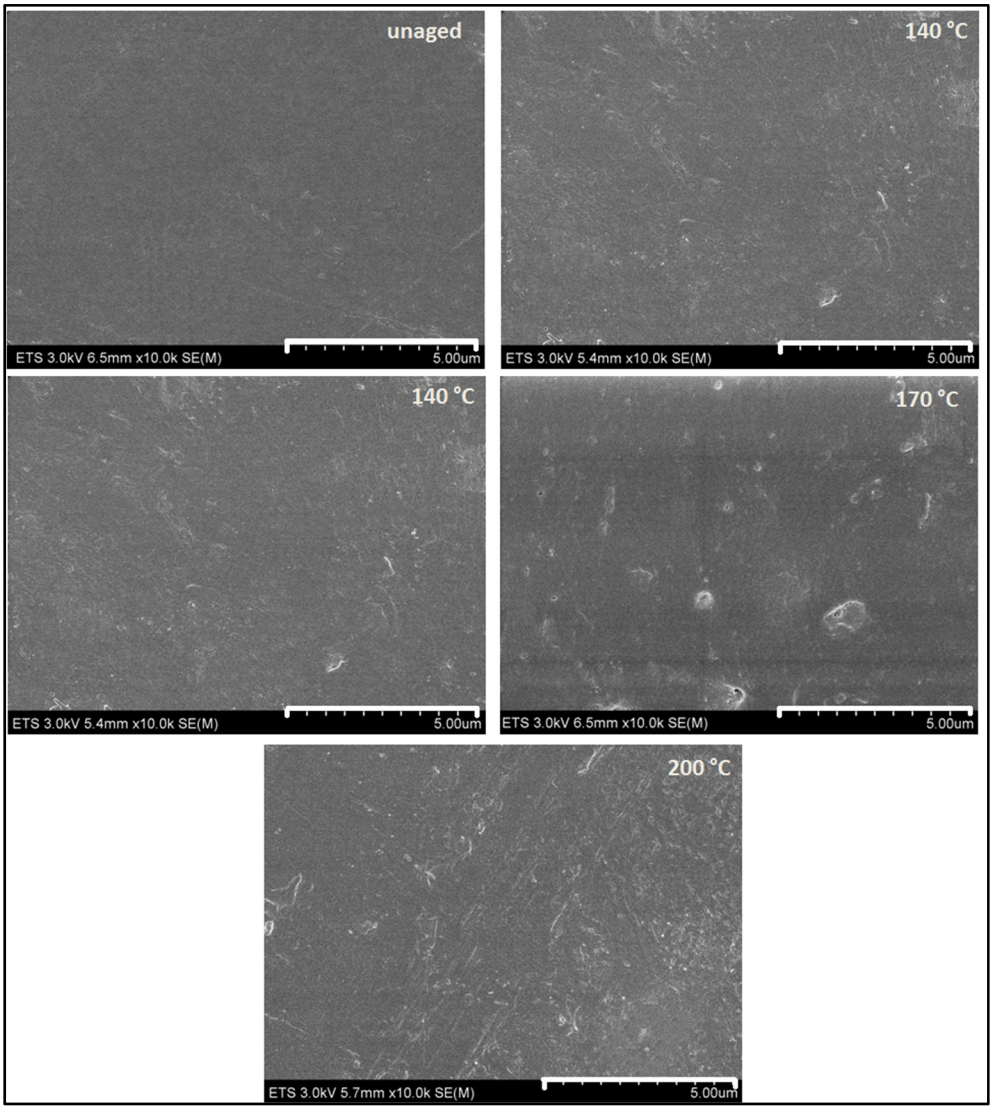

Figure 4.3 SEM images showing effect of the aging temperature on surface PEN (10 000X)

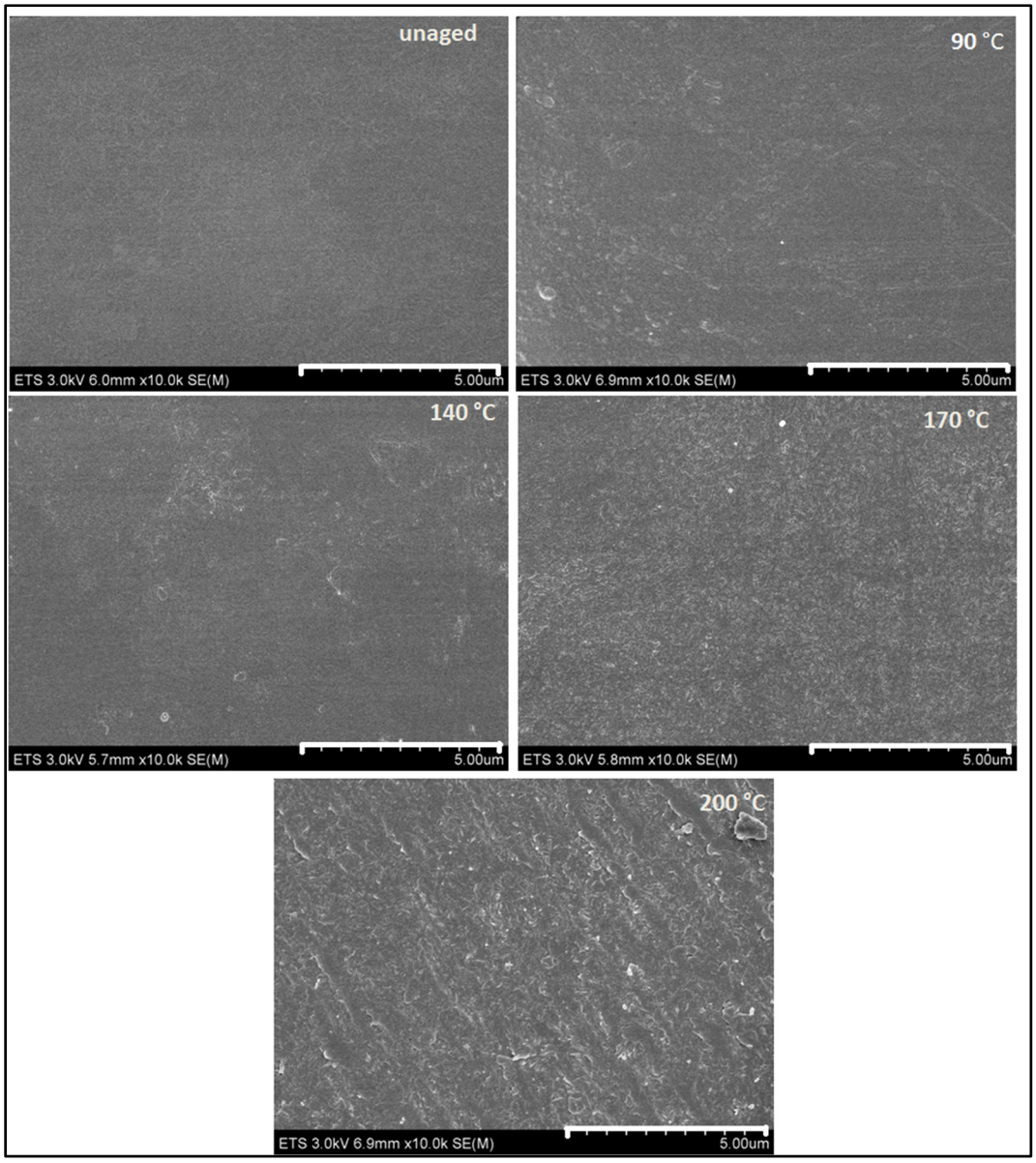

Figure 4.4 SEM images showing effect of the aging temperature on surface RPET (10 000X)

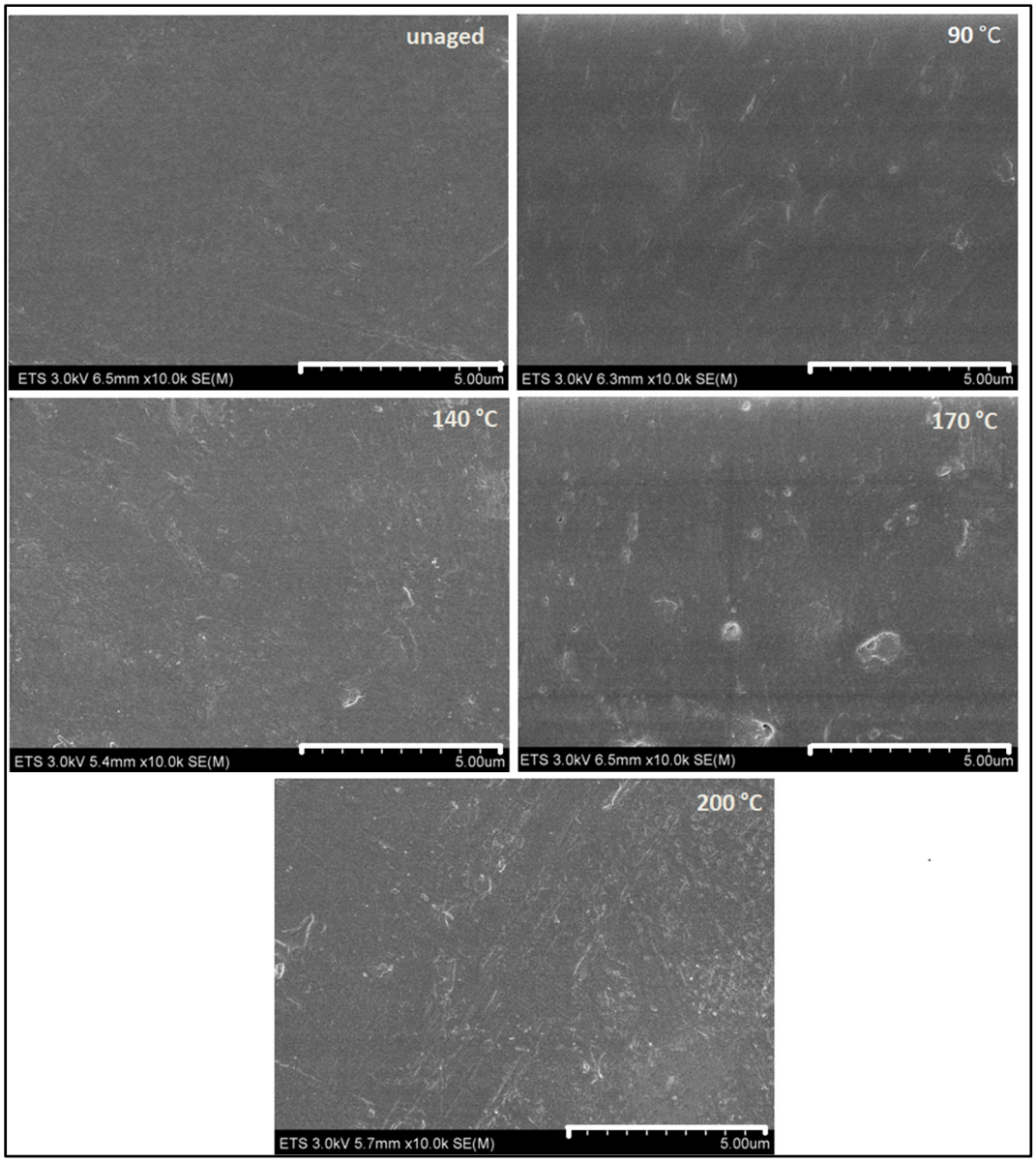

Figure 4.5 SEM images showing effect of the aging temperature on surface RPET-GF-M (10 000X)

4.4.3 Thermal analysis

The DSC curves of the thermally-aged recycled PET and PEN, at four aging temperatures (90, 140, 170 and 200 °C), for 360 hours, are respectively given in Figures 4.6a and 4.6b. It can be noted that the degree of crystallization can be determined by the DSC curves using the area

under the endothermic peaks and the extrapolated value of the heat of fusion for the pure polymer.

The unaged recycled PET exhibits a specific heat jump at about 71 °C, which is characteristic of the glass transition, followed by the cold crystallization peak at 120 °C. The curve also shows an endothermic peak at around 256 °C, corresponding to melting. With the increase of aging temperature, the cold crystallization peak disappeared completely, indicating structural changes associated with the nucleation and crystallization growth rate in the polymer (Abdi, Khemici, & Doulache, 2015; de la Fuente, 2009; Zhu & Ma, 1997). In the case of the recycled PET, the glass transition temperature increases with aging temperature from 76.2 to 102 °C (not clear for aging temperature of 170 and 200 °C). Furthermore, the degree of crystallinity given in Table 3 increases with the thermal aging temperature from 17 to 43%. Besides, for aging temperatures of 140 and 170 °C, a relatively small peak appears at 160 and 215 °C, respectively. For the aging temperature of 200 °C, this peak shifts to 230 °C, and becomes sharper. This phenomenon can be ascribed to both the reduction of the molecular mobility of the amorphous phase and to the cross-linking effect of the crystals occurring during thermal aging, especially in case of recycled PET and its composites(W. Wang et al., 2015; Wei & Hsueh, 1989).

As is well known for the PEN thermogram, the glass transition can be clearly observed at around 120 °C, followed by an exothermic peak centered at around 189 °C (the cold crystallization peak). At higher temperatures, an endothermic peak is observed at around 270 °C, which corresponds to the melting temperature of PEN polyester. A similar thermal behavior to PET was observed for the PEN polymer. Indeed, the glass transition temperature was found to increase from 114 to 154 °C upon thermal aging at 140 °C. Furthermore, the degree of crystallinity increased from 13 to 48%, as indicated in Table 4.2. Unlike what was observed for the recycled PET, the cold crystallization peak of the PEN polymer disappeared only for thermal aging at 170 °C. Thus, the cold crystallization peak disappears only if the aging temperature is higher than the glass transition temperature, which allows segmental motions in polyester.

Tableau 4.2 Glass temperature and calculated degree of crystallinity as a function of aging temperature

Agingtemperature	RPET polymer			PEN polymer			RPET-GF-M composite		
	Tg (°C)	Tf (°C)	Xc (%)	Tg (°C)	Tf (°C)	Xc (%)	Tg (°C)	Tf (°C)	Xc (%)
Unaged	76.2	256.9	17.1	114	270.6	13.1	*	250.1	30.7
90 °C	100.1	257.3	42.5	118	270.1	16.3	*	251.8	37.3
140 °C	101.9	259.5	43.4	154	270.5	44.6	*	250.9	36.4
170 °C	*	259.5	43.1	*	269.7	48.5	*	250.9	36.5
200 °C	*	257.2	43.4	*	269.1	48.4	*	249.1	35.7

In order to investigate the influence of additives on the thermal properties of the recycled PET polymer, a DSC analysis was performed on the unaged composites. Figure 4.7b shows the corresponding DSC curves. Similar curves and glass transition temperatures were obtained for the unaged recycled PET and its composites. An endothermic peak at around 257 °C, corresponding to the melting, was observed. However, the cold crystallization peak was observed in the case of the recycled PET, the glass fiber-filled recycled PET, and the mica-filled recycled PET, but not for the recycled PET reinforced with both mica and glass fibers. Furthermore, this peak is more apparent in the unfilled recycled PET. This behavior could be explained by assuming that in the case of the cold crystallization process of the composite, the reinforcements participate in the nucleation process and affect the crystallinity rate of the composite.

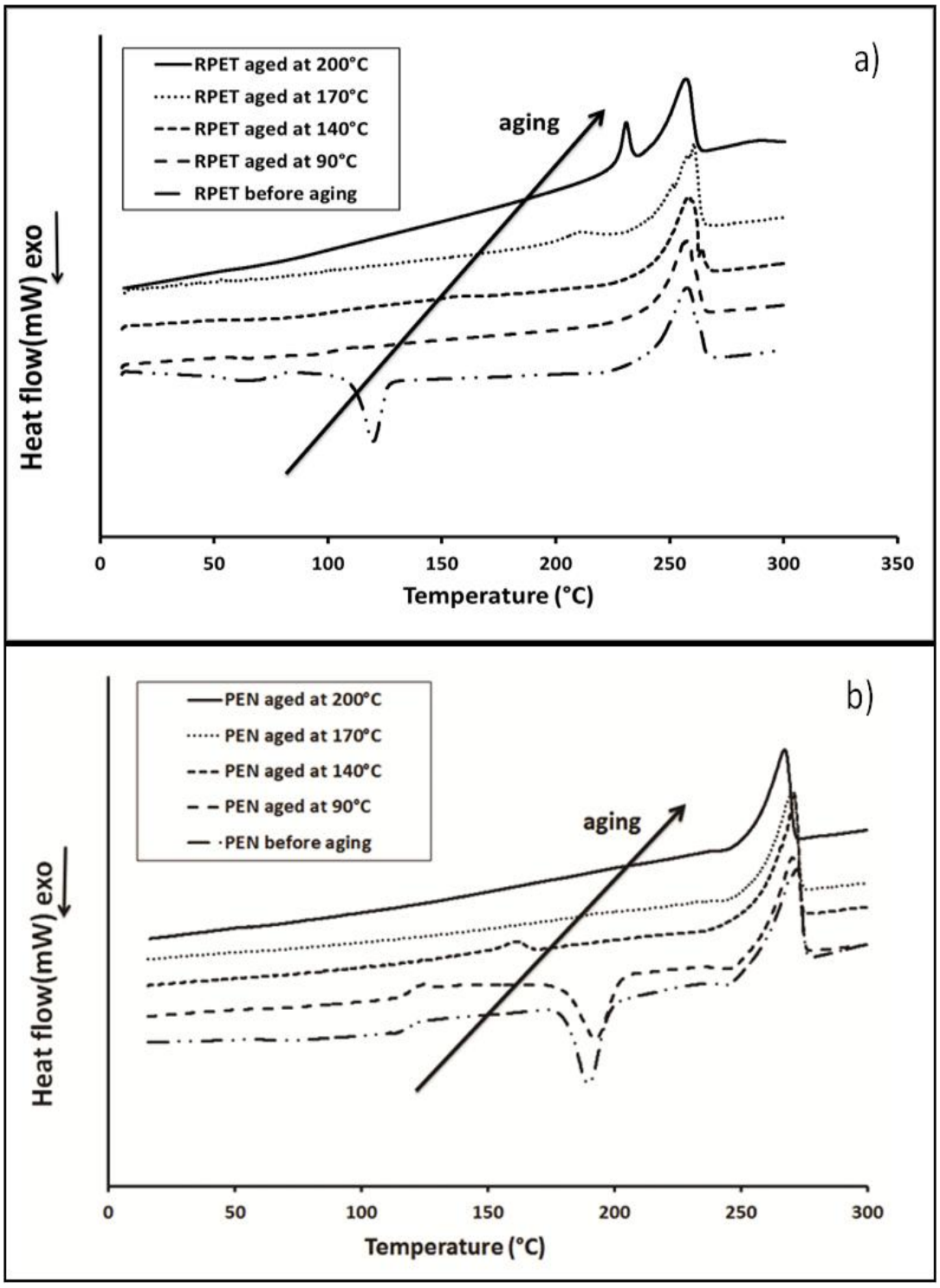

Figure 4.6 DSC scans recorded at 10 °C/min between 0 and 300 °C for a) thermally-aged recycled PET at different aging temperatures for 360 hours, and b) thermally-aged virgin PEN at different aging temperatures for 360 hours

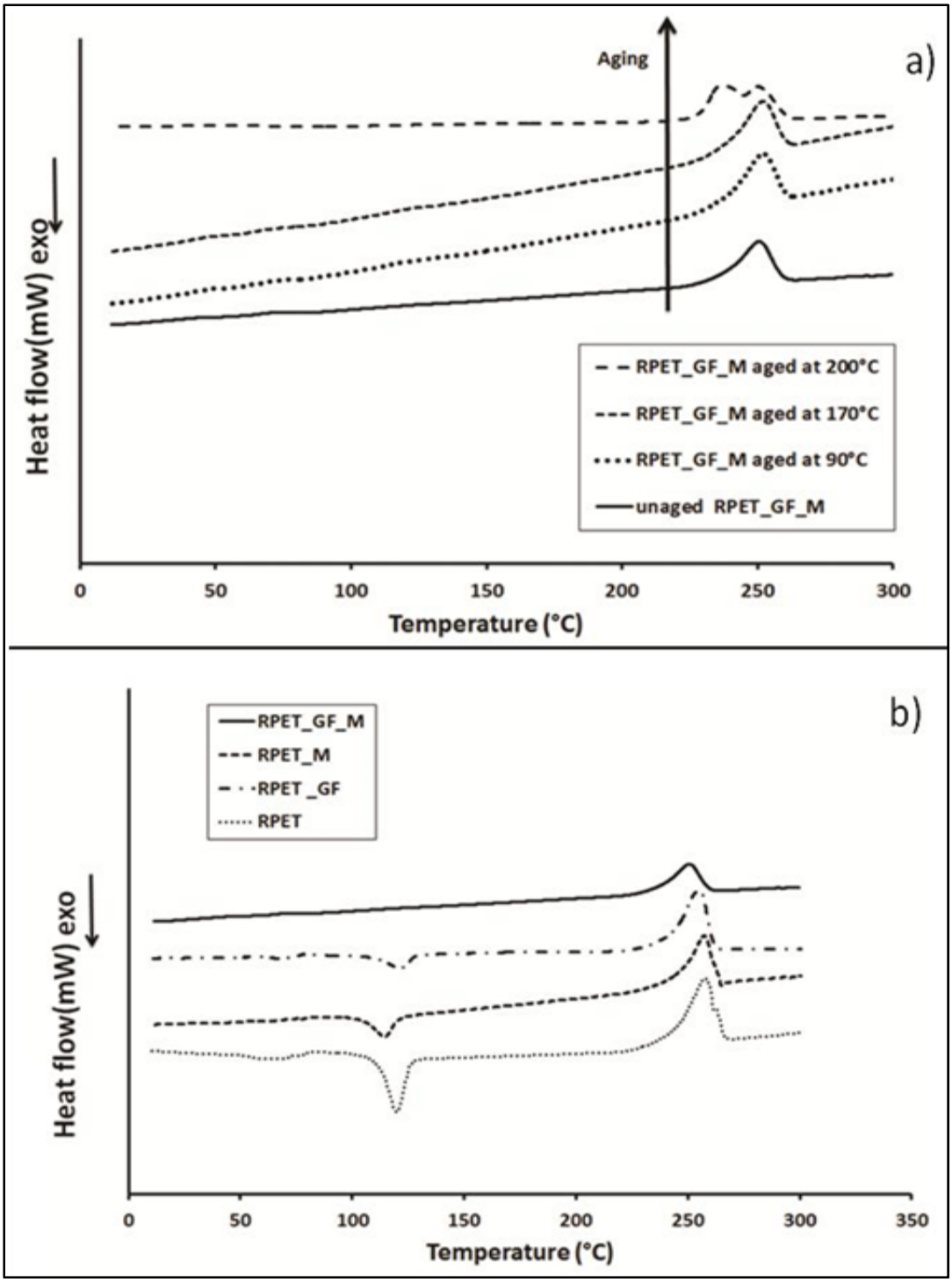

Figure 4.7 DSC scans recorded at 10° C/min between 0 and 300 °C for a) the unaged RPET and its composites, and b) the increase in the crystallinity versus aging temperature as shown by DSC measurement

Figure 4.7b shows the DSC curves of the thermally-aged recycled PET filled with mica and glass fibers (RPET-GF-M), at three aging temperatures (90, 170 and 200 °C) for 360 hours. For the unaged composite, the endothermic peak corresponding to the melting is clear at around 250 °C. After thermal aging up to 170 °C, the composite also manifested a similar behavior as the unaged one. However, a double melting point peak (at around 230 and 249 °C, respectively) was observed after thermal aging at 200 °C. This behavior is mainly attributed to the increase in the crystalline surface (C. S. Wang et al., 1998). Consequently, the contribution of the inorganic reinforcements to this behavior cannot be neglected since the crystallinity growth is more pronounced when both additives are added.

4.4.4 Dielectric failure statistical analysis

Figures 4.8 to 4.10 show the dielectric breakdown Weibull distributions of several types of unaged materials and materials aged at different constant temperatures between 90 and 200 °C, and for aging times of 0, 360 and 720 hours. The scale (α) and the shape (β) parameters as well as the 90% confidence bounds (not shown in the figures) were obtained using the weighted least squares regression technique, as described in the IEEE Standard. These statistical parameters for each sample are listed in Tables 3 and 4. The goal of this section is to evaluate whether the dielectric breakdown strength was significantly reduced after thermal aging for recycled PET and its composites, since it was reported that no significant change was observed for the virgin PET after thermal aging (Bellomo et al., 1995). In our study, dielectric breakdown strength data obtained for the set of materials indicate different dielectric behaviors.

Figure 4.8 shows the dielectric breakdown data before and after thermal aging at 200 °C for 360 hours for the unfilled recycled PET, compared to the mica-reinforced recycled PET, glass fiber-reinforced recycled PET, and the recycled PET reinforced with both mica and glass fibers. The results show that for the unaged samples, the recycled PET exhibits a similar breakdown strength value as the recycled PET filled with mica or glass fibers, similarly to what was reported in a previous study (Mebarki & David, 2015; Mebarki & David, 2012). The breakdown field at percentile 63.2for the unaged unfilled recycled PET (33.4 kV/mm) was near equal to materials reinforced with glass fibers or mica (33.6 and 36.1 kV/mm). The unaged recycled

PET filled with both mica and glass fibers seemed to be the worst performing material, with a slightly lower dielectric strength of 30.8 kV/mm. However, the unfilled recycled PET was found to perform worse than the composites materials after 360 hours of thermal aging at 200 ºC, as shown in Figure 8b. Accordingly, the contribution of inorganic fillers, which are not significantly affected by thermal aging, to the enhancement of the failure resistance of recycled PET-based composites after thermal aging, especially mica, was confirmed.

The study of the thermal aging effect on the materials breakdown strength was performed as a function of temperature and time. The effect of aging temperature for a constant aging time is presented by part a) of Figures 4.9 and 4.10, while the effect of aging time at a constant temperature is illustrated in part b) of the same figures. Tables 4.3 and 4.4 list the statistical parameters calculated from the two-parameter Weibull distribution for unaged samples and samples aged for 360 hours at different constant temperatures, from 90 to 200 °C (Table 4.3) and for different aging times at 170ºC (Table 4.4).We notice that the RPET-GF-M is the least sensitive material to thermal aging. For example, at a temperature of 140 °C, the breakdown strength decreases by not more than few % as a function of aging time or as a function of temperature up to 200ºC for the same aging times. A similar behavior was observed for the RPET-M. In the case of the unfilled recycled PET and RPET-GF materials, the dielectric breakdown strength was observed to decrease rapidly at the onset of thermal aging. For temperatures below 200 °C, unfilled PEN behaves better than the unfilled recycled PET. However, for an aging temperature equal to 200 °C, the unfilled PEN degrades rapidly, and has almost the same dielectric breakdown strength than PET (~26.8 kV/mm) after 360 hours of aging. Recycled PET or PEN filled with glass fibers have the same behavior, with their breakdown strength decreasing noticeably after 360 hours of aging, from 33.6 to 30.4 kV/mm for the RPET-GF material, and from 41.6 to 30.7 kV/mm in the case of PEN-GF.

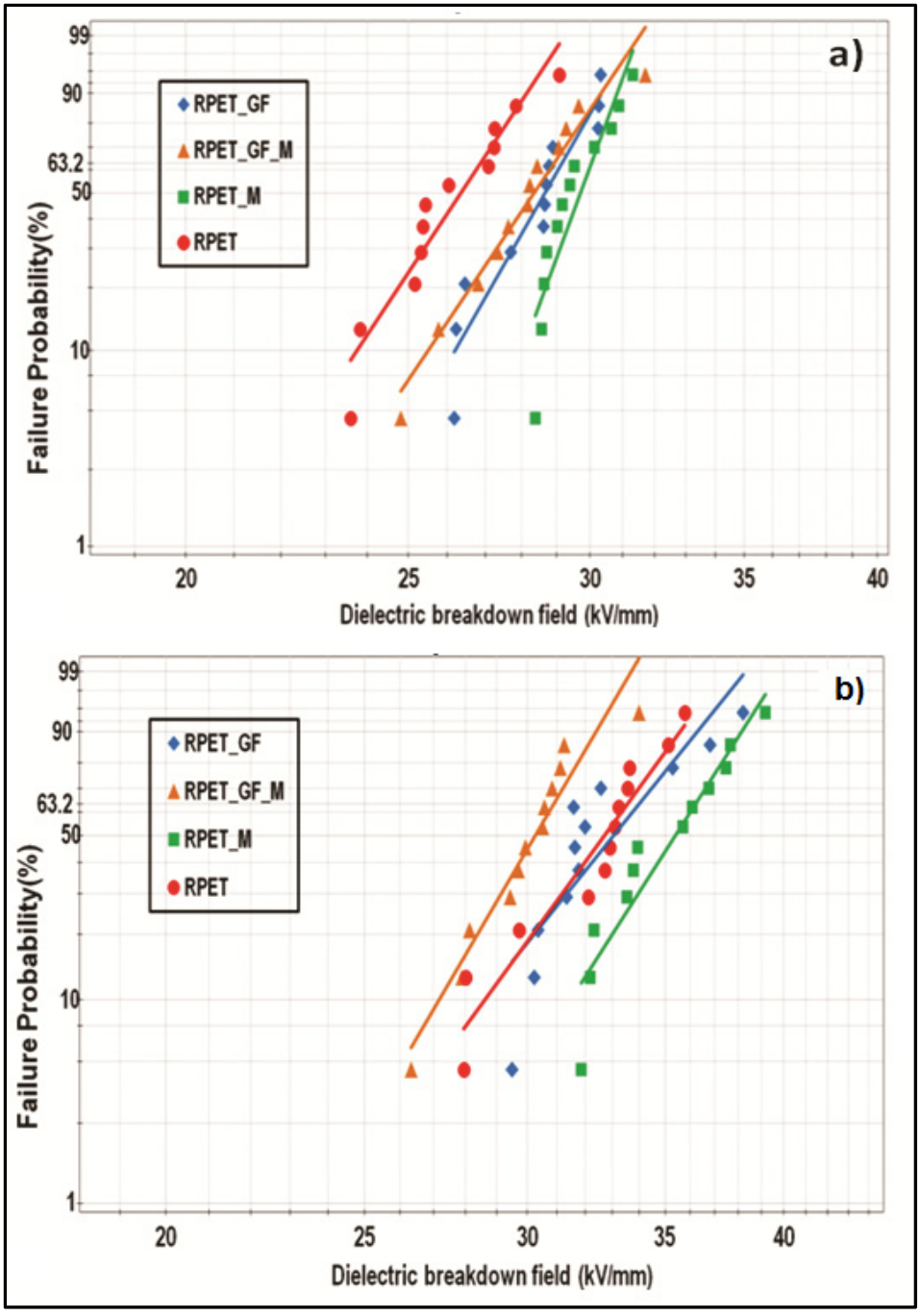

Figure 4.8 Dielectric breakdown strength of different kinds of materials: a) before aging, and b) after thermal-aging for 360 hours at 200 °C

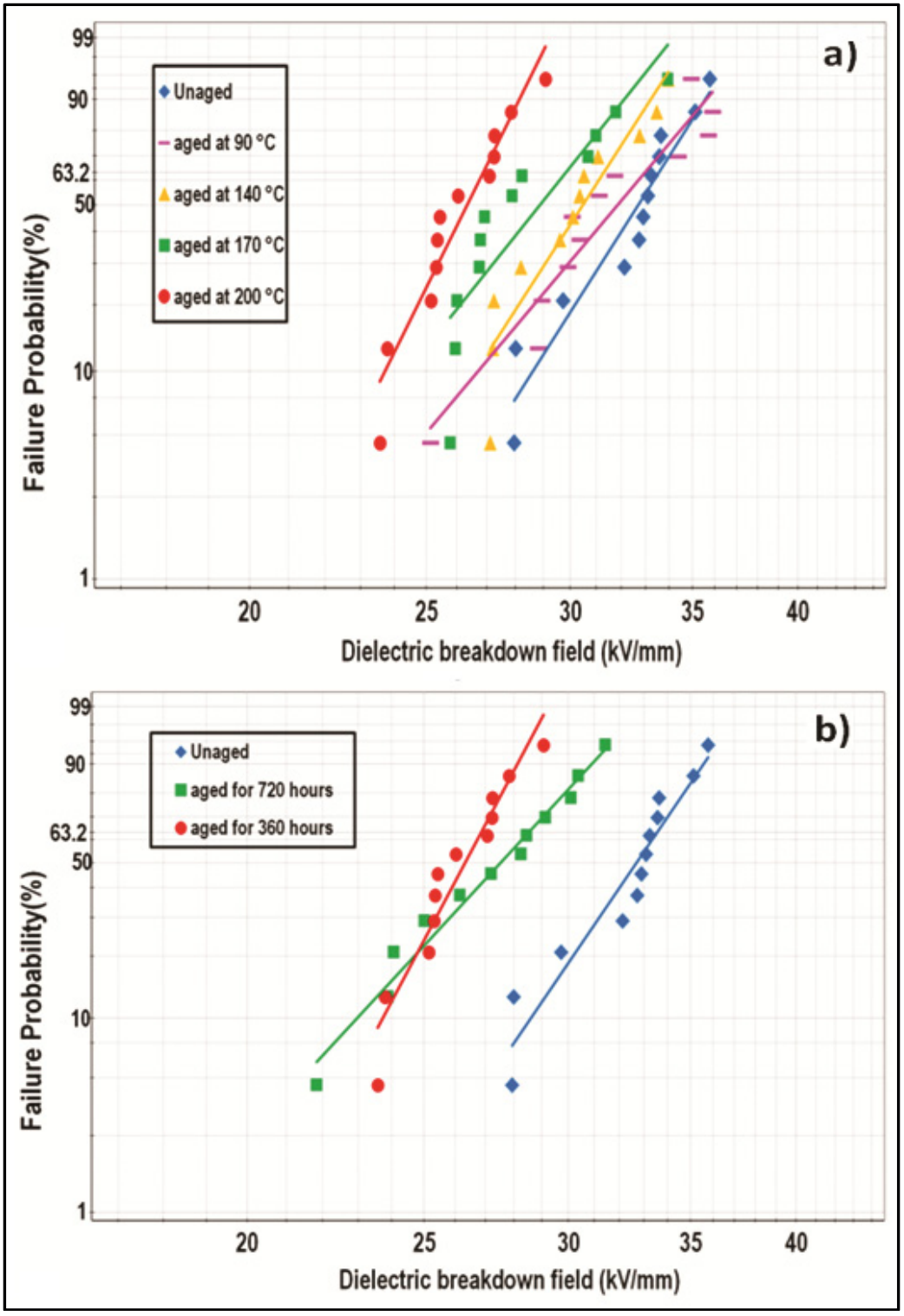

Figure 4.9 Dielectric breakdown strength of the recycled PET a) thermally -aged for 360 hours at different constant temperatures, and b) thermally-aged at 170 °C for different constant durations

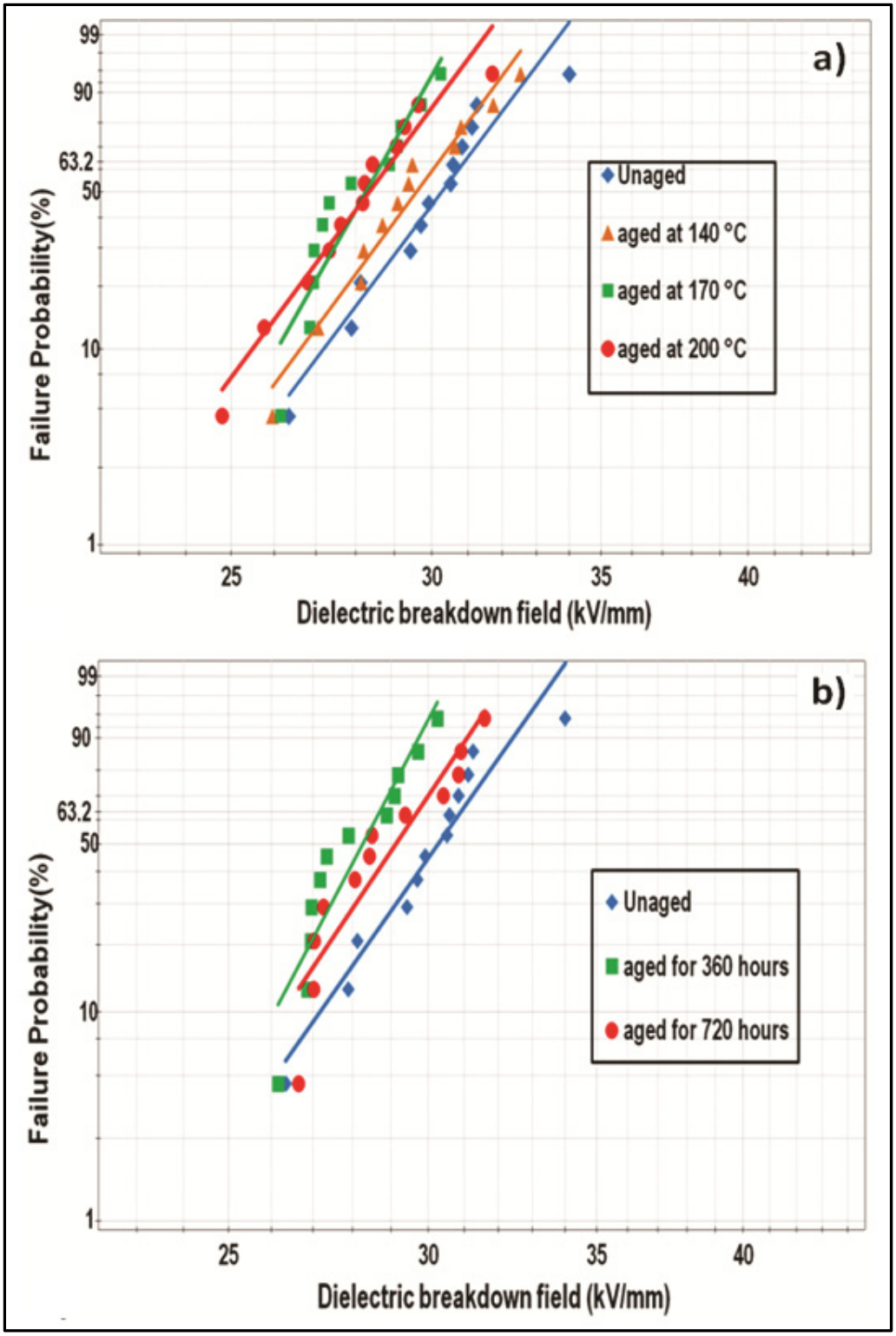

Figure 4.10 Dielectric breakdown strength of RPET-GF-M composite
a) 360 hours at different constant temperatures, and
b) at 170 °C for different constant durations

Tableau 4.3 Breakdown parameter (scale factor and shape factor) calculated from the two-parameter Weibull for unaged samples and samples aged for 360 h at different temperatures

Material	**Unaged samples**		**Samples aged at 90 °C**		**Samples aged at 140 °C**		**Samples aged at 170 °C**		**Samples aged at 200 °C**	
	α	B	α	β	A	β	α	β	α	β
RPET	33.4	16.2	32.9	11	31.2	13	29.5	10.2	26.8	16.2
RPET-GF	33.6	12.1	33.1	8.2	32.8	12	30.4	12.5	29.1	21.4
RPET-M	36.1	14.6	35.4	12.3	34.4	12.3	33	19.6	30	28.7
RPET-GF-M	30.8	18.1	34.5	10.1	30.1	16.4	28.6	20.9	28.9	17.3
PEN	36.2	12.3	37.3	13	33	9	33.5	8.2	26.8	22
PEN-GF	41.6	10.1	41	4.8	35.3	8.2	30.7	12.4	29.9	17.7

In general, the experimental results showed that inorganic reinforcements, mainly mica, have an important effect on maintaining the dielectric breakdown strength of recycled PET-based composites after thermal aging at high temperatures. The effect is suspected to be mostly due to the improved resistance to erosion due to corona discharge provided by the mica reinforcement, since for rather thick samples; the dielectric breakdown during a short-time test is strongly related to the occurrence of partial discharges in the surrounding medium. Also, it shows that the PEN tends to have a similar behavior as the recycled PET when thermally-aged at temperatures greater than 170 °C.

Tableau 4.4 Breakdown parameter and its 95% confidence interval (CI) calculated from the two-parameter Weibull distribution for unaged samples and samples aged at 170 °C for different durations

Material	Unaged samples				Samples aged for 360 hours				Samples aged for 720 hours			
	α_l	A	α_u	β	α_l	α	α_u	β	α_l	α	α_u	β
RPET	32.4	33.4	34.4	16.2	28	29.5	30.9	10.2	27.1	28.5	29.9	10.1
RPET-GF	32.1	33.6	34.9	12.1	29.1	30.4	31.6	12.5	28.1	29.7	31.2	10
RPET-M	34.8	36.1	37.3	14.6	32.1	33	33.8	19.6	30.2	31.3	32.3	15.1
RPET-GF-M	27.2	28.1	28.9	16.5	27.9	28.6	29.3	20.9	28.7	29.6	30.5	16.4
PEN	34.7	36.2	37.7	12.3	31.4	33.5	35.6	8.2	28	29.3	30.6	12
PEN-GF	39.4	41.6	43.6	10.1	29.4	30.7	31.9	12.4	30.6	31.5	32.3	17.8

4.4.5 Dielectric response analysis

Figure 4.11a illustrates the 3D plot of the imaginary part of the recycled unaged PET as a function of frequency for temperatures between 30 and 100 °C. The dielectric response of the unaged recycled PET shows the presence of the usual dielectric relaxation mechanisms in the 10^{-2} to10^{5} frequency range, the α and β processes. Most amorphous and semi-crystalline polymers show a sub-glassy β relaxation at low temperatures and high frequencies, which is associated with the local chain motion and an α process, which is related to the dynamic glass transition at high temperatures and low frequencies (Kremer & Schönhals, 2012). In addition, at low frequencies and high temperatures, the contribution of the direct conductivity to the dielectric response is clear. The behavior of the real and imaginary parts of the complex permittivity of the unaged recycled PET and its three composites were compared in order to evaluate the effects of reinforcements such as mica and glass fibers on the dielectric response of the recycled PET.

Figure 4.12 illustrates the overall behavior of the real and imaginary parts of the unaged recycled PET and its composites. A decrease in the β-peak and an increase in the α-peak of the imaginary part ε" were observed when the recycled PET was filled with both mica and glass fibers. It can be noted that α and β peaks are less pronounced for the reinforced recycled PET as compared to the recycled PET, mostly translating the simple fact that there is a smaller amount of polymer in the composite material. These results are also consistent with DSC analysis, which already confirmed the contribution of the inorganic fillers to the nucleation and crystallization growth, as well as to the molecular chains' motion.

The presence of a broad and small peak was observed at room temperature in the region between 10^1 and 10^4 Hz in the case of the recycled PET filled with mica and the recycled PET reinforced with both mica and glass fibers (Paquin, St-Onge, & Wertheimer, 1982). Such a peak is not present in the case of the glass fiber-filled recycled PET. This indicates the presence of interfacial interactions between the recycled PET resin and the mica platelets. This behavior could be explained by assuming that the inorganic fillers are slightly more conductive then the host matrix, which leads to the accumulation of charge carriers at the interfaces between the matrix and the reinforcements. With glass fibers being less conductive than the mica platelets, the interfacial contribution due to the short glass fibers occurred at much lower frequencies, and consequently, cannot be distinguished from the other low frequency contributions to the dielectric response, as can be seen in Figure 4.12, particularly in part b). The complete dielectric response of the mica/PET composite is shown in Figure 4.11b) in the form of a 3D plot clearly showing the interfacial relaxation peak, which is shifting toward high frequencies as the temperature increases, and consequently, the mica platelets' conductivity also increases.

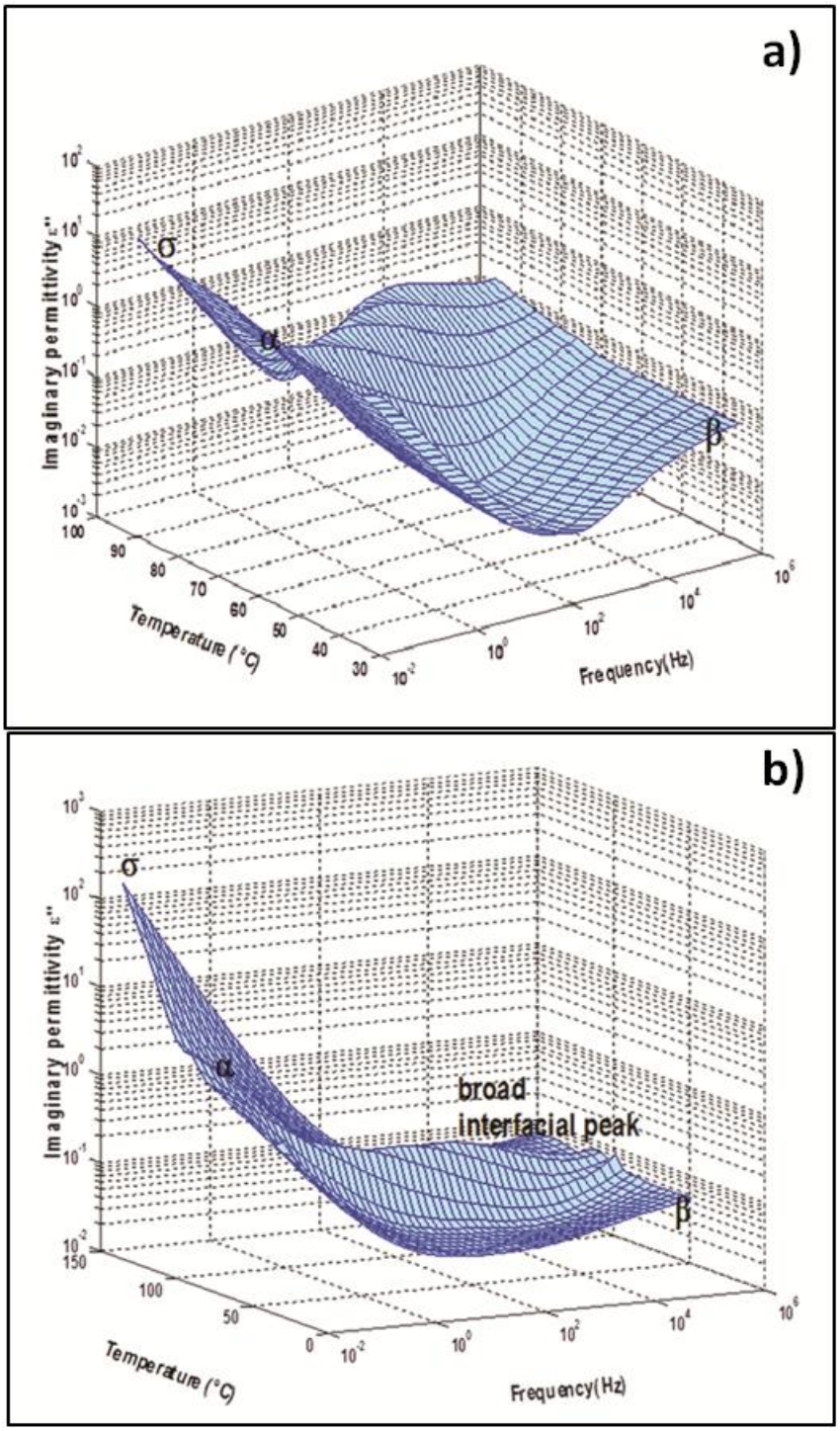

Figure 4.11 3D plot of the imaginary part of a) the unaged PET, and b) the mica-reinforced PET as a function of frequency at temperatures ranged between 30 and 100 °C

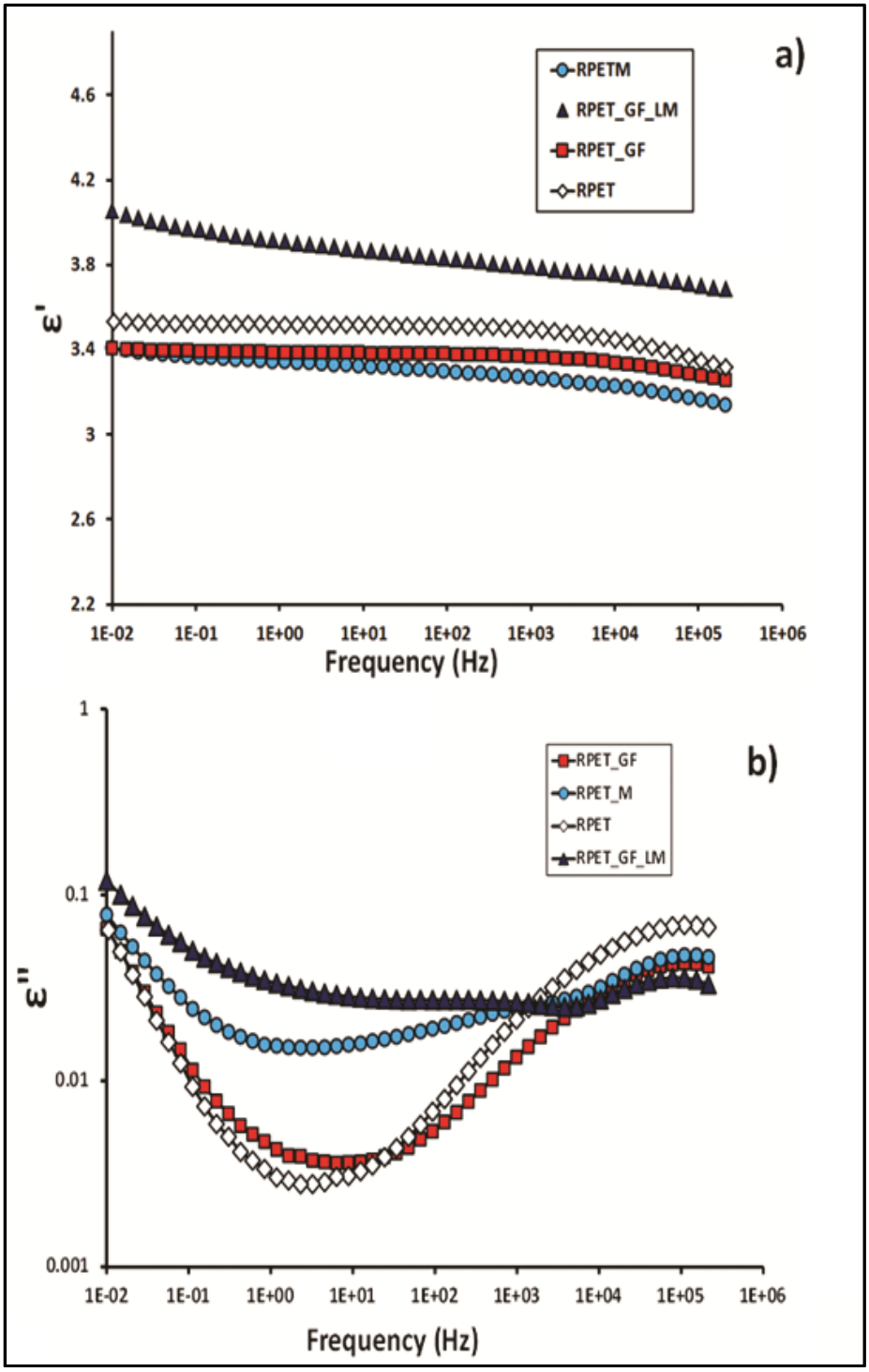

Figure 4.12 Spectra of the a) real part of permittivity, and b) the imaginary part as a function of frequency of four kinds of unaged materials

Similar to the recycled PET, no significant change was found when the glass fibers were added, except maybe for a slight increase in the low frequency dielectric losses, in the material dielectric response was found due to the inclusion of the glass fibers. PEN is known to exhibit a β* relaxation, which is located between the α and β peaks, denoting the Naphthalene ring motion. This peak was found to clearly appear in the measurements obtained at room temperature.

The dielectric frequency spectra of recycled PET and recycled PET-based composites (RPET-GF-M) obtained after different aging times and temperatures are shown in Figures 4.13a and 4.13b, respectively. In the case of recycled PET (Figure 4.13a) and reinforced recycled PET (Figure4.13b), no major or systematic change was observed in the dielectric response due to aging. All imaginary parts, ε", of recycled PET or recycled PET-based composites diagrams represent a typical shape of the PET polymer, with its dielectric relaxation processes, the α and β relaxation peaks. The α-relaxation is associated with the glass transition of the amorphous regions (segmental motions), whereas the β-relaxation is related to the molecular fluctuations (local motion of the carbonyl group). For dielectric measurements conducted at room temperature, only a fraction of the α-peak was observed in the vicinity of 10^{-2} Hz, while it can clearly be observed at higher temperatures in the low frequency range. Similarly, only the low frequency wing of the β-relaxation peak located between 10^4 and 10^5 Hz can be observed. The β-relaxation peak can be fully observed at higher frequencies or lower temperatures.

A careful observation of the imaginary part permittivity ε" shows a slight decrease in the β-peak intensity when the thermal aging temperature is increased. It can be noted that the three composites have a similar dielectric response. The general trend points to a slight decrease of the β-peak intensity when the thermal aging temperature is increased (this change can also be translated into a decrease in the real part of the complex permittivity at low frequencies (W. Wang et al., 2015)).

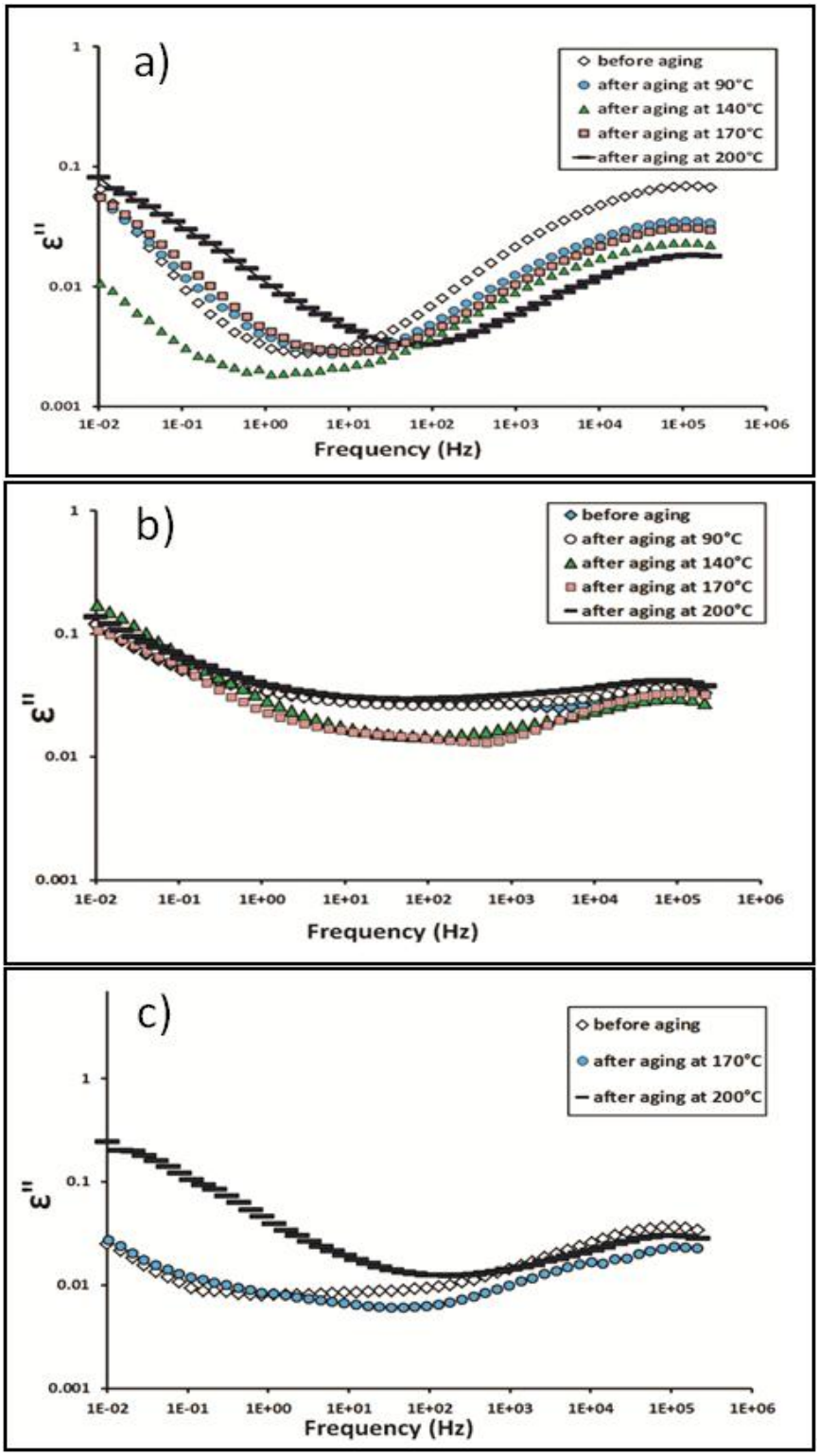

Figure 4.13 Imaginary part of the complex permittivity versus Frequency at different aging temperatures of the a) Recycled PET, b) (RPET-GF-M) composite, and c) the VPET-GF

In order to evaluate the dielectric behavior as a function of aging of the virgin PET, glass fiber-filled virgin PET was used. As observed in Figure 4.13c, a significant increase of the imaginary part (ε") of the complex permittivity (or the dielectric losses) was found after thermal aging at 200 °C, particularly in the low frequency portion of the spectrum. This could be due to an increase of the α-relaxation peak or the contribution of charge fluctuation, leading to electrode polarization or possibly a combination of both. It can be concluded that, overall, the recycled PET-based composite exhibited a similar dielectric behavior as its virgin counterpart. Similarly to PET, no major change in the loss part of the complex permittivity was found after thermal aging of the PEN at four aging temperatures (90, 140, 170 and 200 °C) for 320 hours.

4.5 Conclusion

Changes in the morphology and crystallinity of recycled PET and PEN reinforced with inorganic fillers, such as mica and glass fibers were found in relationship with the material dielectric behavior after thermal aging from 90 to 200 °C. Their dielectric endurance in terms of dielectric strength and real permittivity was found to be reduced after thermal aging, mainly at temperatures below 200 °C. Moreover, PEN, while exhibiting significant dielectric strength, tends to behave similarly to the recycled PET once it is thermally aged at temperatures greater than or equal to 170 °C, thus limiting its operating temperature.

Recycled PET reinforced with both mica and glass fibers can be considered to be the least sensitive to thermal aging among the tested materials. In fact, both inorganic reinforcements, especially mica platelets, contribute significantly to the enhancement of the dielectric strength of recycled PET during thermal aging at high temperatures. It can be noted that unlike glass fibers, the mica platelets lead to the appearance of an interfacial relaxation peak between the recycled PET resin and the mica platelets. In addition to their conductivity, the fillers' shape and hydrophilicity can affect the magnitude and the frequential position of this relaxation process occurring at the interface between the matrix and the reinforcements. Furthermore, the presence of mica platelets leads to a certain adhesion or compatibility between the recycled PET and the mica platelet fillers.

A significant decrease of the mechanical properties (embrittlement) can be observed after thermal aging, mostly for the unfilled recycled PET and PEN, as compared to their composites. It is worth mentioning that a successful characterization of thermally-aged recycled PET-based composites needs to be completed in the future with a mechanical analysis.

ACKNOWLEDGMENT

Financial support of this work by the National Sciences and Engineering Research Council of Canada (NSERC) is gratefully appreciated. The authors would like to express their sincere appreciation to Patrick Lachance and Doru Davinscu from Lavergne Group that kindly supplied materials used for this investigation.

CONFLICT OF INTERESTS

The authors declare that there is no conflict of interests regarding the publication of this paper.

CHAPITRE 5

ARTICLE III: DIELECTRIC AND STRUCTURAL RECYCLED PET AND PEN BASED COMPOSITES

Fouzia Mebarki and Éric David

Département de génie mécanique École de Technologie Supérieure (ÉTS), 1100 Notre-Dame Ouest, Montréal QC, Canada H3C 1K3

Article soumis dans le journal « Transactions on Electrical and Electronic Materials» en Mars 2017. Numéro de confirmation: 17-0026

ABSTRACT

Because of its good mechanical, thermal and dielectric properties, Polyethylene Terephthalate (PET) is one of the most used polymers in engineering applications, including in electric and electronic devices. However, Polyethylene Naphthalate (PEN) has excellent thermal properties that can remain almost constant in a large temperature domain, and as a result, performs better than PET. The main purpose of this work is to assess the dielectric performance of recycled PET reinforced with inorganic fillers, in terms of dielectric strength and dielectric losses, and to compare it with its counterpart PEN composite. In order to estimate the dielectric behavior of recycled PET (RPET) reinforced with short glass fibers or mica platelets, a dielectric investigation of different recycled PET-based composites was carried out. Specimens of PEN and glass fiber-reinforced PEN were also used in this investigation. All materials were first extruded into pellets, and then injection-molded at 110 °C into disk-shaped samples. A microstructural analysis was performed using scanning electron microscopy (SEM). Differential scanning calorimetry (DSC) analysis was carried out on several samples using a Perkin-Elmer DSC apparatus at a heating rate of 10 °C/min under inert atmosphere. In addition, thermogravimetric analysis (TGA) of the different samples was conducted according to the ASTM E1311 standard. To complete this study, FTIR characterization was also carried out.

Further, the real and the imaginary parts of the complex permittivity were investigated using Broadband Dielectric Spectroscopy (BDS) over a large temperature range and for a large frequency window, in order to assess the possible interfacial interaction between the inorganic fillers and the RPET or PEN polymer matrix. Dielectric breakdown measurements were carried out at room temperature in thoroughly degassed oil using a high voltage source at 0.5kV/s as per ASTM D-149. The dielectric breakdown data was analyzed using the two-parameter Weibull distribution function. Both matrix and reinforcements type were found to affect the crystallinity rate in composites. In addition, glass fibers have a significant slowdown in the PEN composite's cold crystallization process. The type or form of the inorganic reinforcement can affect the interfacial interactions between the matrix (recycled PET) and the inorganic fillers. Moreover, the dielectric breakdown during the short-time measurement of the glass fiber PEN-based composites was found to be higher as compared to the PEN polymer. Moreover, the dielectric breakdown during the short-time measurement of the glass fibers PEN based composites was found to be higher as compared to the PEN polymer.

5.1 Introduction

Polyethylene terephthalate (PET) and Polyethylene naphthalate (PEN) are polyesters that are very similar in chemical structure (see Figure 5.1). The only difference between them lies in the presence of a phenyl rigid aromatic ring in the repeating unit in naphthalene. Consequently, PEN has much longer chains, and thus, higher viscosity (Calderas, Sanchez-Solis, Maciel, & Manero, 2009). Both thermoplastics are known for their excellent barrier, mechanical and thermal properties, which are maintained relatively intact over a large temperature range(MacDonald et al., 2007). However, PEN exhibits markedly better temperature endurance and shrinkage resistance as compared to PET (MacDonald, 2004). The superior properties characterizing PEN make it a high-performance engineering polymeric material (Fang, Wegener, Wirges, Gerhard, & Zirkel, 2007; Lillwitz, 2001;Van Den Heuvel & Klop, 2000).

Both PET and PEN polymers form an essential component of various sectors, with applications in packaging, automotive parts, electric and electronic industries. Polyethylene terephthalate is considered as the most recyclable plastic in the world. It is transformed into pellets or flakes that can be used to manufacture several valuable products, as well as into polyester fibers for clothing and carpeting. Polyethylene naphthalate is suitable for advanced applications, particularly those relating to the production of special packaging susceptible to oxidation; it is also widely used in the miniaturization of capacitors and in flexible printed circuit boards. Several studies have carried out comparisons between PEN and PET or their respective blends (Gonzalez, Barankin, Guschl, & Hicks, 2008; Laskarakis, Gravalidis, & Logothetidis, 2004; Rueda & Varkalis, 1995;Sellarès et al., 2012).

It is well known that polymer properties can be significantly enhanced through the incorporation of inorganic fillers (Hassan, 2012; Lee et al., 2005). Most such reinforcements can increase stiffness, or at least maintain strength (Rothon, 2002). Mica platelets are frequently used as a dielectric barrier, and therefore provide an enhanced dielectric breakdown strength and partial discharge resistance for the polymer (Debnath, De, & Khastgir, 1988; F. Mebarki 2016). Glass fibers constitute one of the most commonly used inorganic fillers (Bansal & Doremus, 2013), and a specific amount of them can greatly improve certain thermal (F. Mebarki 2016; Panthapulakkal & Sain, 2007) and mechanical properties of some polymers, particularly the fracture resistance (Laura, Keskkula, Barlow, & Paul, 2002; Stipho, 1998). Several works have shown that a high mechanical and thermal performance of some polymers is essentially due to morphological changes they undergo if a strong interaction between the polymer and the reinforcements exists (Fu, Lauke, Mäder, Yue, & Hu, 2000; Gan, Cao, Song, & Wang, 2001; Li & Liu, 2007; S.-H. Wu et al., 2001). Nevertheless, no applied research works have assessed the effects of inorganic reinforcements on the dielectric properties of recycled PET and PEN thermoplastic polymers, although some findings have shown this to be a significant factor to consider in changing the dielectric properties of some polymers (Akram, Javed, & Rizvi, 2005; Paul & Thomas, 1997).

These materials, particularly the recycled PET-based composites, are intended to replace the virgin PET composite used to manufacture mechanical supports for spark plugs in the

automotive industry. Using recycled PET helps reduce environmental impacts, and provides economic and commercial benefits. Using recycled resources requires a better understanding of their properties, particularly when they are supposed to operate under severe thermal and electric conditions. Incorporating both organic and inorganic fillers of nanometric or micrometric dimensions can greatly enhance these properties. On the other hand, though, these same properties are altered following incorporation of inorganic reinforcements such as glass fibers into recycled PET or PEN polymers; essentially, that is why we studied the morphological, thermal and dielectric properties. To the best of our knowledge, this is the first time a comparative study has been carried out between the recycled PET filled with inorganic fillers and one of its counterpart PEN composites in order to gain a better understanding of thermal and dielectric behavior (in terms of dielectric strength and dielectric losses).

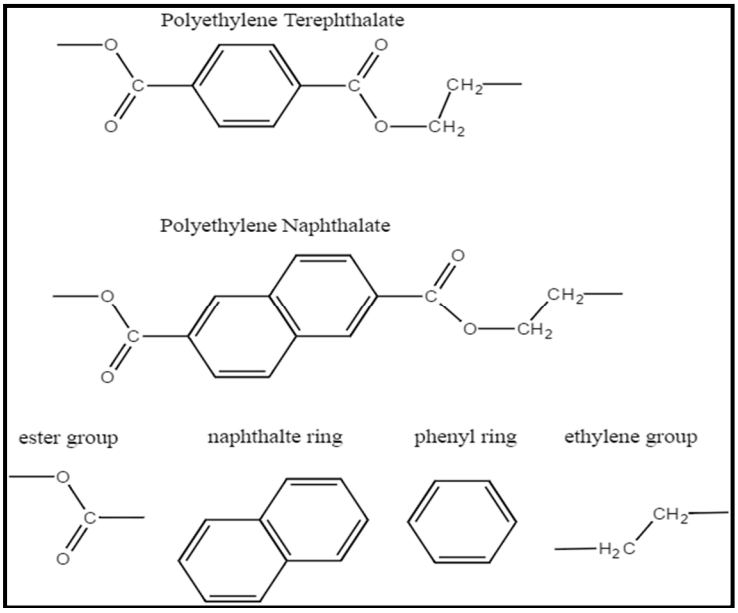

Figure 5.1 Chemical structure of PET and PEN repeating units

5.2 Experimental

Two types of polyester materials were investigated in this study. The PEN was a virgin thermoplastic, while the PET used in this investigation came from recycled sources, such as recycled water bottles and ink cartridges. E-type short glass fibers and/or mica platelets were used as reinforcements. The glass fibers had a 10.5 μm diameter and a length of 3 mm, while

the mica flakes were medium platelets (89~254 μm). Materials were first extruded into pellets, and then injection-molded at a mold temperature of 110 °C into disk-shaped samples. Since PEN is more viscous than PET, the extrusion process for the PEN polymer was more complicated than that for the recycled PET material. All materials were compounded by Lavergne Group, Montreal, Canada, in the form of disks measuring about 1.6 mm in thickness and 100 mm in diameter. More details on the tested composites are given in Table 5.1.

Tableau 5.1 Description of the tested materials

Specimen	Material	Additional information
RPET	Unfilled recycled PET	No fillers was added
RPETM	Mica filled recycled PET	15% of mica was added to the polymer
RPETGF	Glass fiber-filled recycled PET	20% of glass fibers was added to the polymer
RPETGF2	Glass fiber-filled recycled PET	Almost twice as much glass fiber as in RPET-GF was added to the polymer
RPETGFM	Glass fiber- and mica-filled recycled PET	It contains the same amount of glass fibers as RPETGF and the same amount of mica as RPETM
PEN	Unfilled virgin PEN	No fillers was added
PENGF	Glass fiber-filled PEN	20% of glass fibers was added to the polymer

The morphology of the recycled PET and PEN polymers and their composites was observed using a scanning electron microscope (SEM), with an accelerating voltage of 15 kV. In order to prevent charging in the electron beam, all samples used for the SEM observation were coated with a very thin gold layer (20 nm), using a gold sputtering apparatus before scanning microscopy. In order to assess the thermal behavior of the different materials, a differential scanning calorimetry analysis (DSC) was carried out using a Perkin Elmer thermal analyzer. Samples of approximately 15 mg were placed and then encapsulated in standard aluminum

pans. The samples were then heated from room temperature to 200 °C at a heating (or cooling) rate of 10 °C/min, under a nitrogen atmosphere to prevent oxidation. Three replicates of each material were used for each measurement performed. Cold crystallization and melting temperatures were taken as the peak maxima and the glass transition temperatures from the half-extrapolated heat capacity temperature (ASTME1356-08, 2014).

A thermogravimetric analysis (TGA) of the different samples was conducted according to the ASTM E1311 standard, using a Perkin Elmer thermal analyzer. Samples of 6.5 ±0.2 mg were placed in platinum pans, whereas the reference platinum pan was kept empty during the measurement run. Thermogravimetric measurements were performed on heating from 50 to 900 °C at 10 °C/min and under inert atmosphere (nitrogen).

FTIR spectroscopy provides information about the polymer chemical structure, and the FTIR spectra of all materials were recorded over the 400–4000 cm^{-1} range. These spectra were acquired by the attenuated total reflectance (ATR) method, using a Perkin Elmer STA8000 FTIR spectrometer. The resolution of the instrument was 2 cm^{-1}. Only smooth specimens were used in order to ensure a good contact with the crystal. All specimens were first cleaned, and then placed between the crystal and the mirror before being pressed directly.

Dielectric response measurements of polyethylene terephthalate (PET) and polyethylene naphthalate (PEN) disks and their composites were carried out using frequency domain dielectric spectroscopy in the 10^{-2} to 10^{5} Hz frequency range. Sample surfaces were covered by a silver sheet and inserted between two electrodes 40 mm in diameter. The frequency dependency of the complex permittivity ε^* can be written in the form:

$$\varepsilon^*(\omega) = \varepsilon'(\omega) - j\varepsilon''(\omega) \tag{5.1}$$

where ε' is the real part, ε" is the imaginary part, and $\omega=2\pi f$ is the angular frequency.

The relaxation processes, whether dipolar or interfacial in nature, can usually be fitted using the empirical Havriliak-Negami (H-N) equation. In the general case for which more than one relaxation process can be detected, the use of the HN model leads to the following equation for the complex permittivity:

$$\varepsilon^*(\omega) = \varepsilon_\infty + \sum_{i=1}^{n}\left[\frac{\Delta\varepsilon_i}{(1+(j\omega\tau_i)^{\alpha_i})^{\beta_i}}\right] \tag{5.2}$$

where ε^* is the complex dielectric permittivity, ε_∞ the high frequency permittivity, $\Delta\varepsilon_i$ the dielectric relaxation strength of the i^{th} process, n the relaxation process number, and τ_i the relaxation time of the i^{th} relaxation process. The shape parameters α_i and β_i respectively describe the symmetric and asymmetric broadening of the relaxation peak ($0<\alpha<1$ and $\beta>0$). Since charge transport mechanisms, and ultimately, electronic conductivity must be considered at low frequency, an additional term taking these phenomena into account can be added to the previous equation, yielding:

$$\varepsilon^*(\omega) = \varepsilon_\infty + \sum_{i=1}^{n}\left[\frac{\Delta\varepsilon_i}{(1+(j\omega\tau_i)^{\alpha_i})^{\beta_i}}\right] + \frac{\sigma_0}{\varepsilon_0(j\omega)^s} \tag{5.3}$$

where σ_0 is the electrical conductivity when s = 1, ε_0 is the vacuum permittivity (8.85 x10^{-12} F/m), and s is a fitting parameter. Using the preceding expression, the real and imaginary parts of the dielectric permittivity can be separately expressed as:

$$\varepsilon'(\omega) = \varepsilon_\infty + \sum_{i=1}^{n}\left[\frac{\cos(\beta_i\varphi_i)}{\left[1+2[\omega\tau_i]^{\alpha_i}\sin\left[\frac{\pi(1-\alpha_i)}{2}\right]+[\omega\tau_i]^{2\alpha_i}\right]^{\beta_i/2}}\Delta\varepsilon_i\right] + \frac{\sigma_0}{\varepsilon_0(\omega)^s}\cos\left[\frac{\pi s}{2}\right] \tag{5.4}$$

$$\varepsilon''(\omega) = \sum_{i=1}^{n}\left[\frac{\sin(\beta_i\varphi_i)}{\left[1 + 2[\omega\tau_i]^{\alpha_i}\sin\left[\frac{\pi(1-\alpha_i)}{2}\right] + [\omega\tau_i]^{2\alpha_i}\right]^{\beta_i/2}}\Delta\varepsilon_i\right] + \frac{\sigma_0}{\varepsilon_0(\omega)^s}\sin\left[\frac{\pi s}{2}\right] \tag{5.5}$$

where

$$\varphi_i = \operatorname{arctag}\left[\frac{\left[[\omega\tau_i]^{\alpha_i}\cos\left[\frac{\pi(1-\alpha_i)}{2}\right]\right]}{\left[1 + [\omega\tau_i]^{\alpha_i}\sin\left[\frac{\pi(1-\alpha_i)}{2}\right]\right]}\right] \tag{5.6}$$

The dielectric breakdown strength of the different recycled PET and PEN, as well as their composites, were measured at room temperature in a thoroughly degassed mineral oil using an AC breakdown voltage set-up according to the short-term procedure described in the ASTM-D149 (ASTMD149, 2004). At least twelve measurements were performed for each material, and the obtained results were analyzed using the two-parameter Weibull distribution according to the IEEE Standard 930 The cumulative probability of failure, F(t), is given by the following equation.

$$F(t) = 1 - \exp\left[\left(\frac{t}{\alpha}\right)^{\beta}\right] \tag{5.7}$$

where β is the shape parameter, α is the scale parameter, corresponding to 63.2% of failure probability, and t is either an electrical field or a time to breakdown depending on the type of test.

5.3 Results and discussion

5.3.1 Structure and morphology

Figure 5.2 shows the SEM images of the surface of the glass fiber composites from both polymers, the PEN and the recycled PET. Figures 5.3 and 5.4 displayed the cross-section SEM images for the PEN and RPET polymers and their composites.

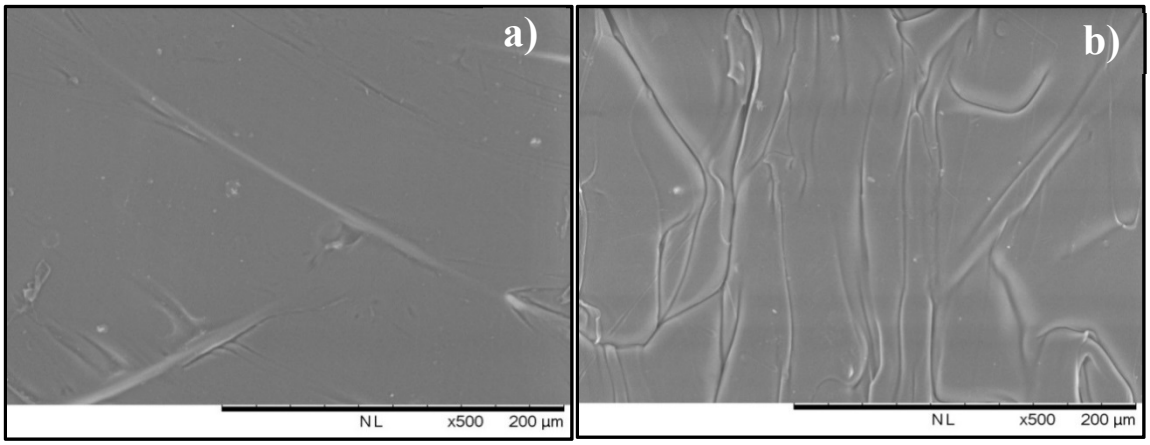

Figure 5.2 Surface SEM images (X500) of a) the recycled PET filled with glass fibers; b) PEN filled with glass fibers

According to the microscopic observations, a good dispersion of the glass fiber reinforcements in the polymer matrix was observed mainly in the cross-section image of the PEN polymer composite. Furthermore, in most cases, surface SEM images reveal more micro-defects in the glass fiber-filled RPET than in the PEN composite; defects were also present close to the glass fiber reinforcements. Consequently, in contrast with the recycled PET, the PEN polymer would appear to have better adhesion to and compatibility with the glass fiber fillers. Furthermore, the PEN composite has a better surface finish as compared to the glass fiber-filled RPET composite.

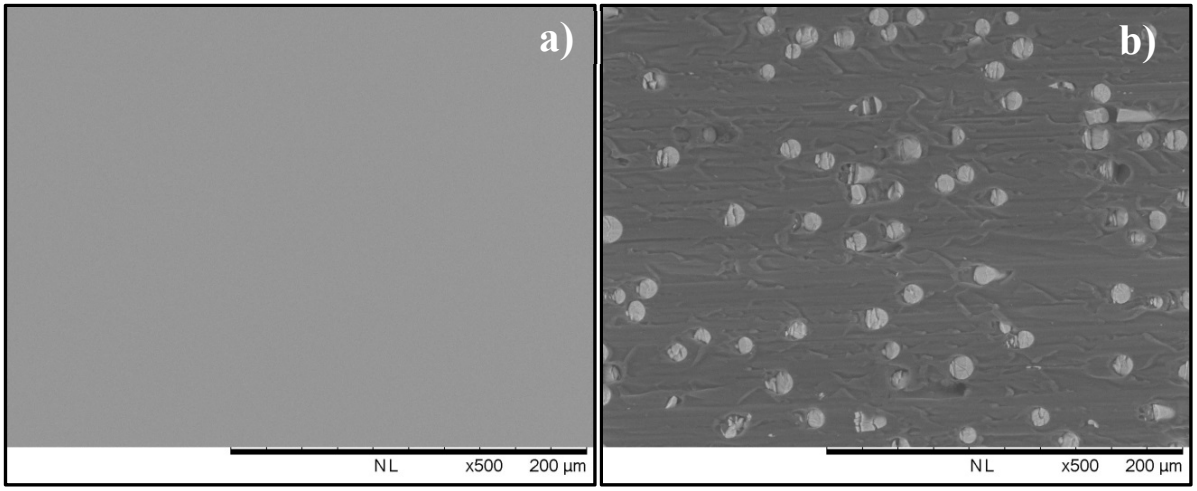

Figure 5.3 Cross-section SEM images(X500) of a) the unfilled PEN; b) PEN reinforced by glass fibers (PEN-GF)

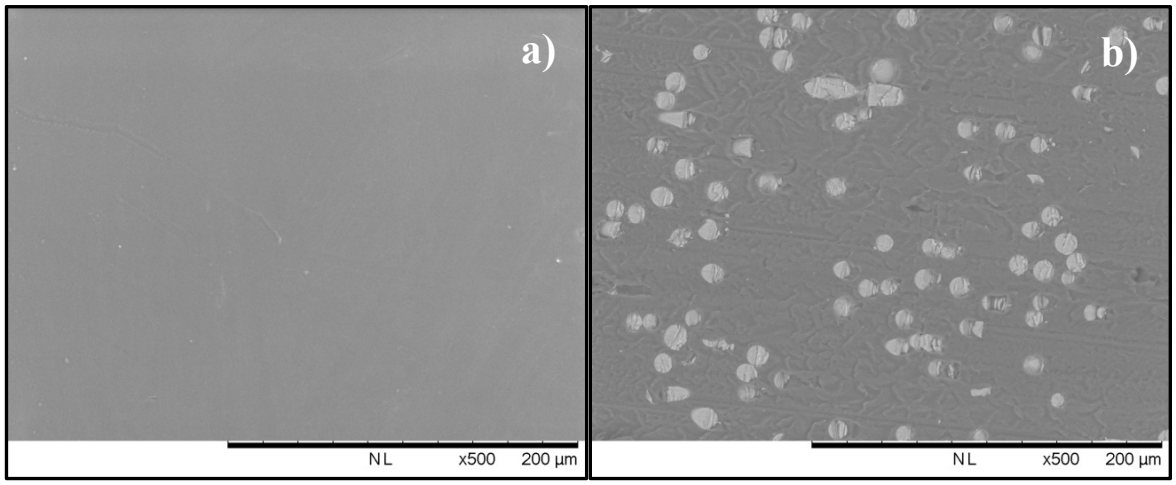

Figure 5.4 Cross-section SEM images (X500) of a) the unfilled recycled PET b) recycled PET reinforced by glass fibers (RPET-GF)

5.3.2 DSC analysis

Figure 5.5 presents the DSC curves of the unfilled recycled PET polymer and its composites, RPET-GF and RPET-M. The RPET polymer exhibits a heat enthalpy jump at about 78 °C, corresponding to the glass transition, followed by a typical cold crystallization peak at 119 °C and an endothermic peak at around 255 °C, corresponding to the main melting peak. A similar thermal behavior with regard to the unfilled RPET polymer was observed for both the RPET filled with glass fibers or with mica. No significant change was observed for the melting

process. However, the cold crystallization peak becomes less obvious in the composites and occurs almost at (or close to) the same temperature of the unfilled recycled PET one. Furthermore, the crystallinity rate increases with the addition of inorganic reinforcements. In fact, we recently reported that a crystallization rate growth was observed in recycled PET and PEN polymers when inorganic fillers such as mica and glass fibers were added (F. Mebarki 2016).

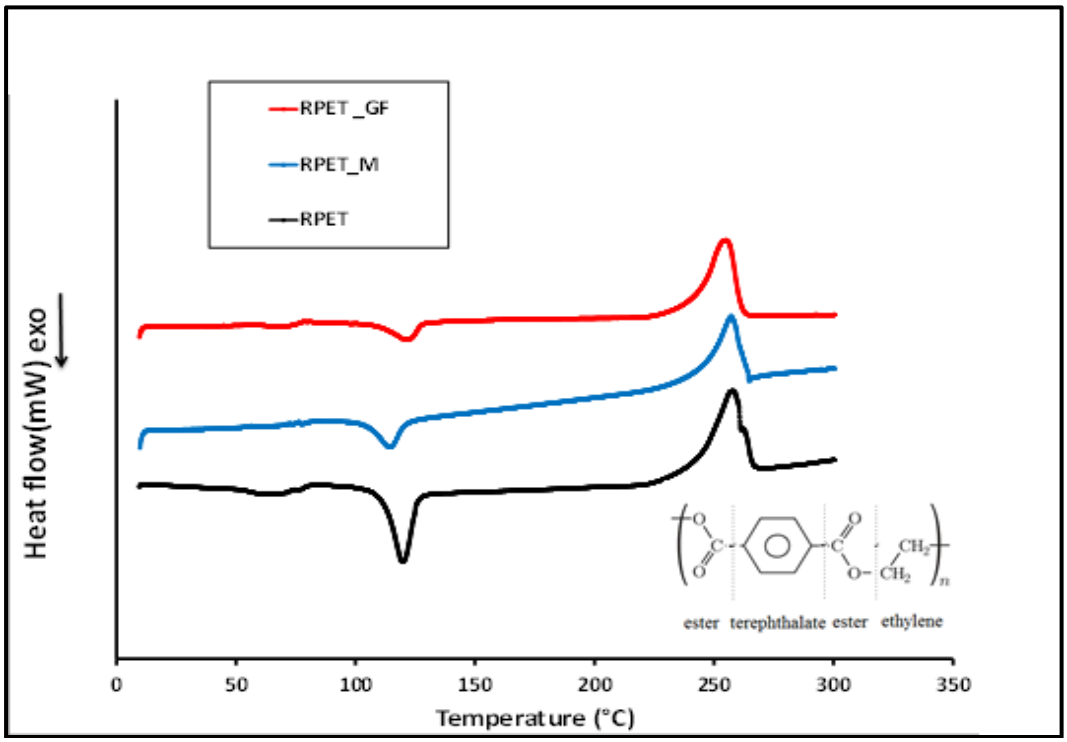

Figure 5.5 DSC curves of the unfilled RPET polymer and the glass fiber RPET material

Figure 5.6 displays the DSC heating curves of the unfilled PEN polymer and the glass fiber-filled PEN material. Both materials showed a heat enthalpy jump, which is characteristic of the glass transition temperature, at a temperature of 120 °C and a melting peak at around 269 °C (the melting point remained practically constant). Both materials show an exothermal peak (the typical cold crystallization) just after the glass transition temperature. This peak was observed at a temperature close to 176 °C for the composite whereas it was found at around 190 °C for the PEN polymer. Such behavior can be explained by the structural rearrangement

occurring during the transition from the amorphous to the crystalline phase, which takes place at a much lower temperature in the PEN-based composite than in the unfilled PEN polymer, thus illustrating the role of the glass fiber fillers in the PEN matrix. Some fillers may act as nucleons in the matrix (Sanchez-Solis, Garcia-Rejon, & Manero, 2003). Thus, in contrast with PET, the presence of the larger asymmetric rigid ring in the PEN polymer could be the main reason for the slowdown in the cold crystallization of the PEN when it is reinforced with glass fibers.

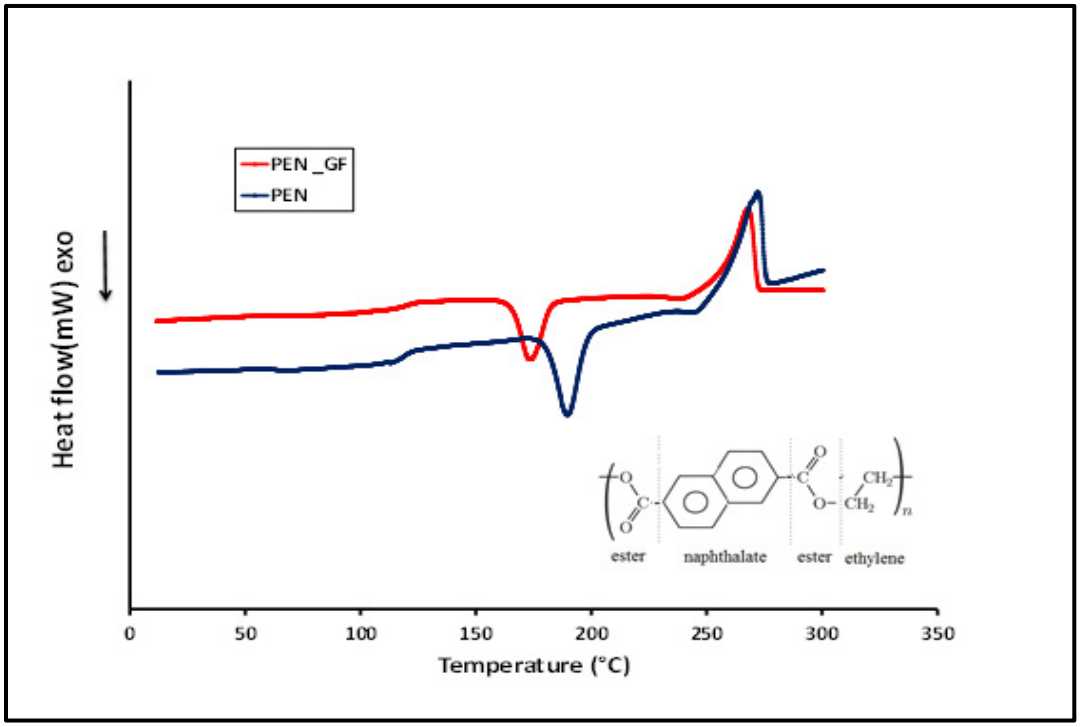

Figure 5.6 DSC curves of the unfilled PEN polymer and the glass fiber PEN material

As indicated in Table 5.2, the degree of crystallinity increased from 13.8 to only 21.8% when glass fibers were added to the PEN polymer. Nevertheless, it increased from 17.1 to 37.7% when the RPET was filled with glass fibers, and only from 17.1 to 19.7% when mica platelets were added. Consequently, both type of matrix and the type of reinforcements were found to affect the crystallinity rate in composites. No significant change was detected for the glass transition and the melting temperature of the recycled PET polymer when the glass fiber

content was increased. However, the crystallization rate appeared to be slightly higher when the glass fibers amount was almost doubled.

Tableau 5.2 Results from DSC analysis

Material	T_g(°C)	T_{cc}(°C)	T_m(°C)	T_c(°C)	X_C(%)
RPET	78.4	119.2	255.2	201.9	17.1
RPETM	79.1	114.2	256.8	218.9	19.7
RPETGF	75.5	120.3	254.4	208.5	37.7
RPETGF2	74.3	----	255.3	210.9	40.6
PEN	119.8	190.4	269.1	207.9	13.8
PENGF	113.3	176.6	268.5	213.5	21.8

5.3.3 TGA analysis

Figures 5.7 and 5.8 present the thermogravimetric tests on heating of several materials from 350 to 540 °C under nitrogen atmosphere. All samples had similar degradation behaviors, and the thermal decomposition was characterized by one step with a different maximal mass loss rate. It is worth mentioning that PET undergoes a more rapid thermal degradation than does the PEN. The PET resin starts to degrade at about 348 °C, while with the PEN polymer, it is at 378 °C; the residue achieved at 530 °C is about 20% for the PET and 36% for the PEN. The non-stability observed confirms the presence of mass loss even after 600 °C. The residues are obviously associated with the segment corresponding to the benzene ring in the case of the PET, and of naphthalene ring, for the PEN (Papageorgiou, Tsanaktsis, & Bikiaris, 2014). In addition, the PET polymer tends to decompose more rapidly than its composites. However, a composite with a 35% glass fiber content degrades at a much higher rate than do the other composites. The presence of both inorganic fillers has a greater effect on the PET thermal resistance. A similar behavior can be observed for PEN glass fiber composites.

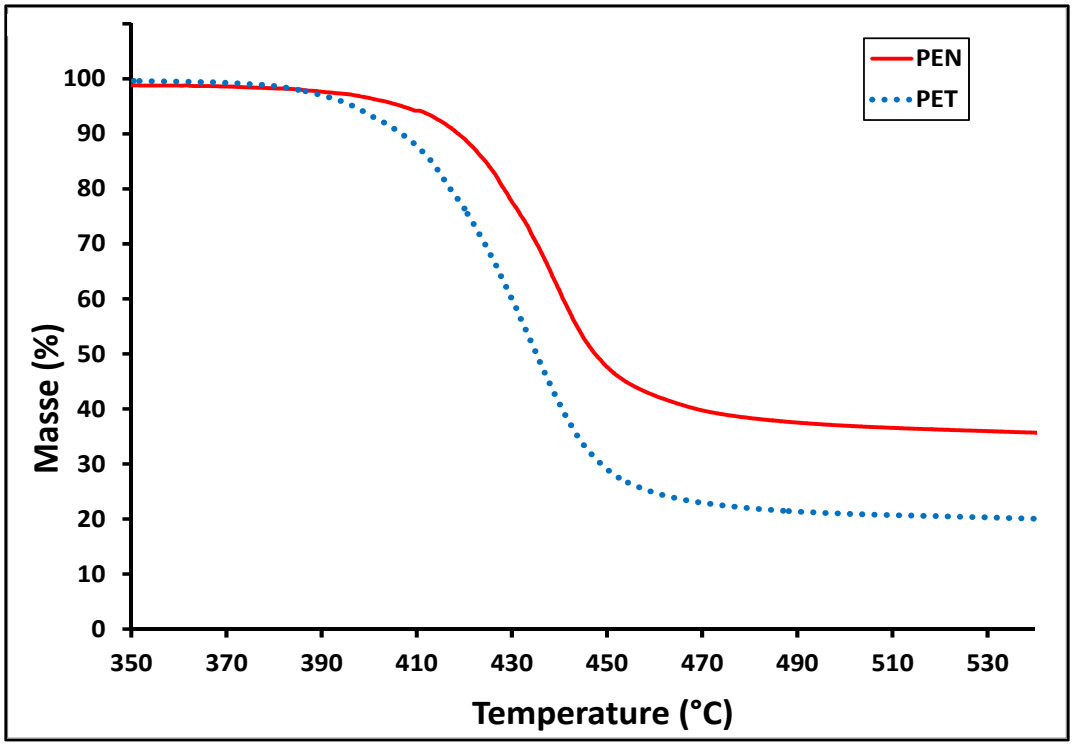

Figure 5.7 TGA curves under nitrogen condition for PET and PEN

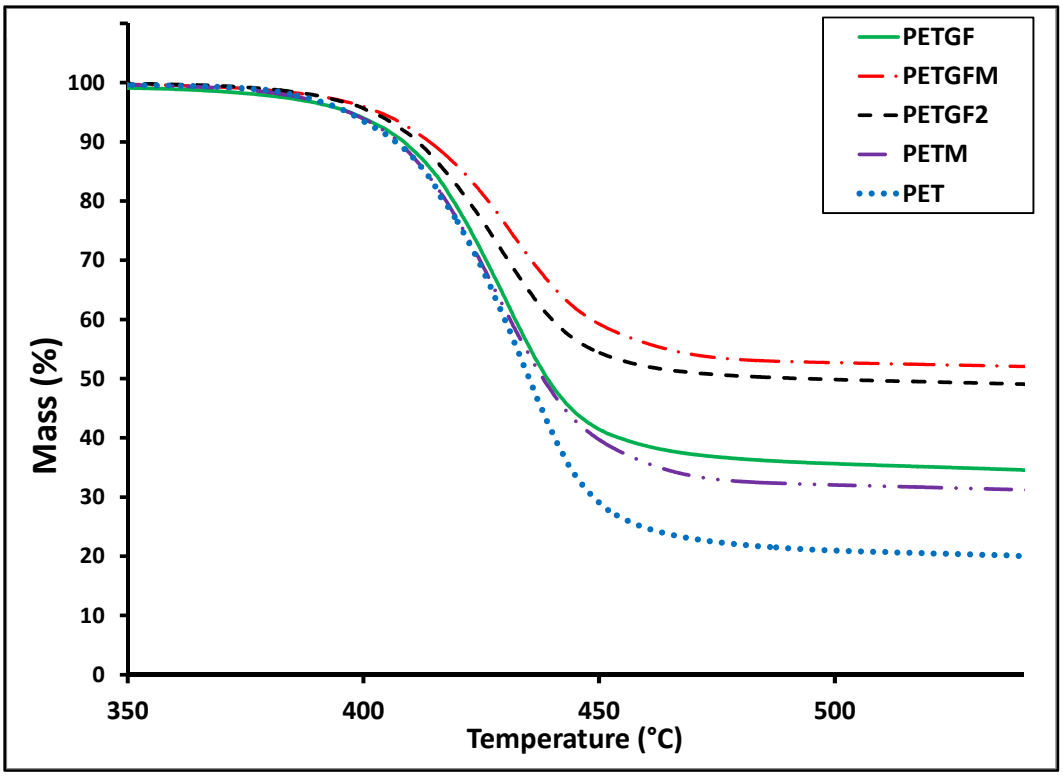

Figure 5.8 TGA curves under N_2 condition for PET, PEN and their composites

5.3.4 FTIR spectroscopic analysis

FTIR spectroscopy was used to determine some possible molecular structure changes in recycled PET and PEN polymer groups when inorganic reinforcements were added. A decrease in intensity and a shift in the wavenumber of some bands can be observed for the recycled PET and its composites in Figure5.9. As can be seen, the intensity of most peaks decreases for both composites mainly for the ester carbonyl bond stretching (1780-1650 cm^{-1}), the ester group stretching (1235 cm^{-1}), the methylene group at 1090 cm^{-1} and the aromatic bands at 1016 and 725 cm^{-1} (Miyake, 1959). Such behavior may be attributed to the structural changes occurring, particularly the crystallization rate when recycled PET is filled with inorganic fillers. Particular attention should be paid in the case of the carbonyl band at 1720 cm^{-1} as it decreased greatly in intensity for both RPET composites, which indicates that the C=O content (the acetyl groups in PET) is enhanced by adding inorganic fillers such as mica or glass fibers.

Due to the presence to the rigid ring, the molecular structure of the PEN polymer is more complicated than that of the recycled PET, and a higher number of absorption peaks was found. Figure 5.10 provides the FTIR spectrum of the PEN and of the PEN filled with glass fibers. The bands of the PEN polymer spectra at 2965 and 2919 cm^{-1} correspond to the bands of the recycled PET at 2957 and 2910 cm^{-1}, which is characteristic of the antisymmetric and symmetric vibrations of the CH_2(Ouchi, Hosoi, & Shimotsuma, 1977). The main absorption bands in the unfilled PEN spectra were assigned as follows: the intense band at 1715 cm^{-1}, which corresponds to the C=O stretching vibration; the bands at 1250 and 1270 cm^{-1}, which are assigned to the stretching vibration of the C=O, and the bands at 1180 and 1135 cm^{-1}, which correspond to the naphthalene ring. We can see that the intensity of the 1450 cm^{-1} band decreased greatly, indicating a significant change in the surface crystallinity of the glass fiber-filled PEN (Pastore & Kiekens, 2000; Quintanilla, Alonso, Rodríguez-Cabello, & Pastor, 1996). In general, a remarkable decrease in the intensity peaks was observed over the 800–2000 cm^{-1} range, indicating significant changes in the rearrangement in the molecular chain, particularly in the crystallinity rate.

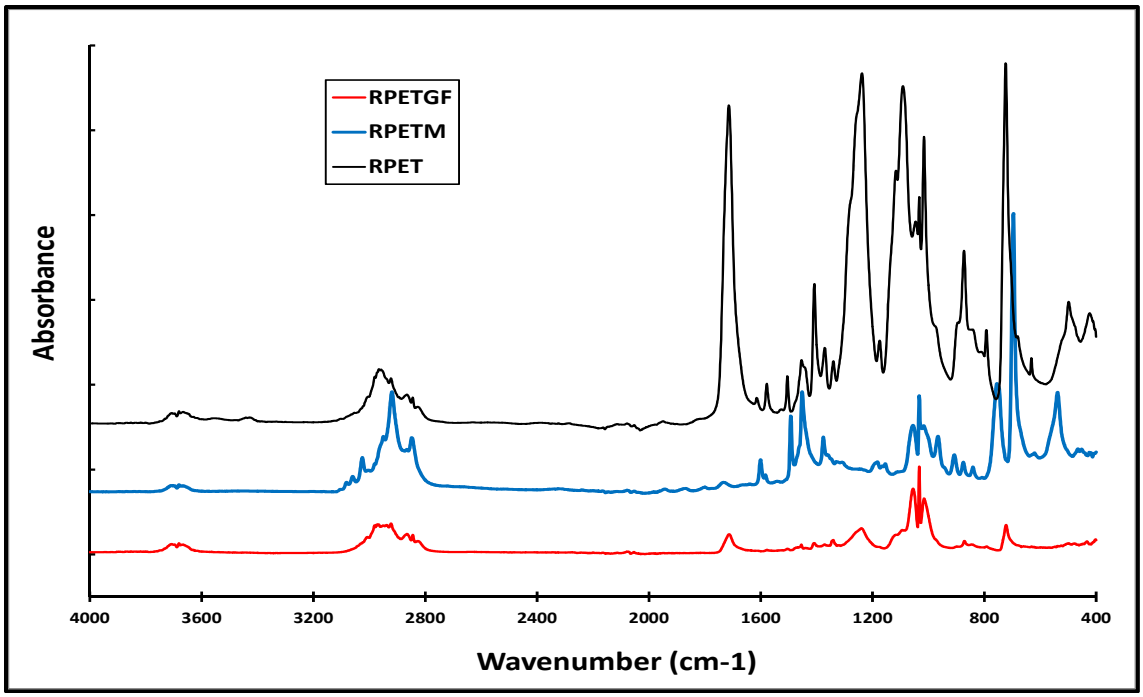

Figure 5.9 The FTIR spectrum of recycled PET and its composites

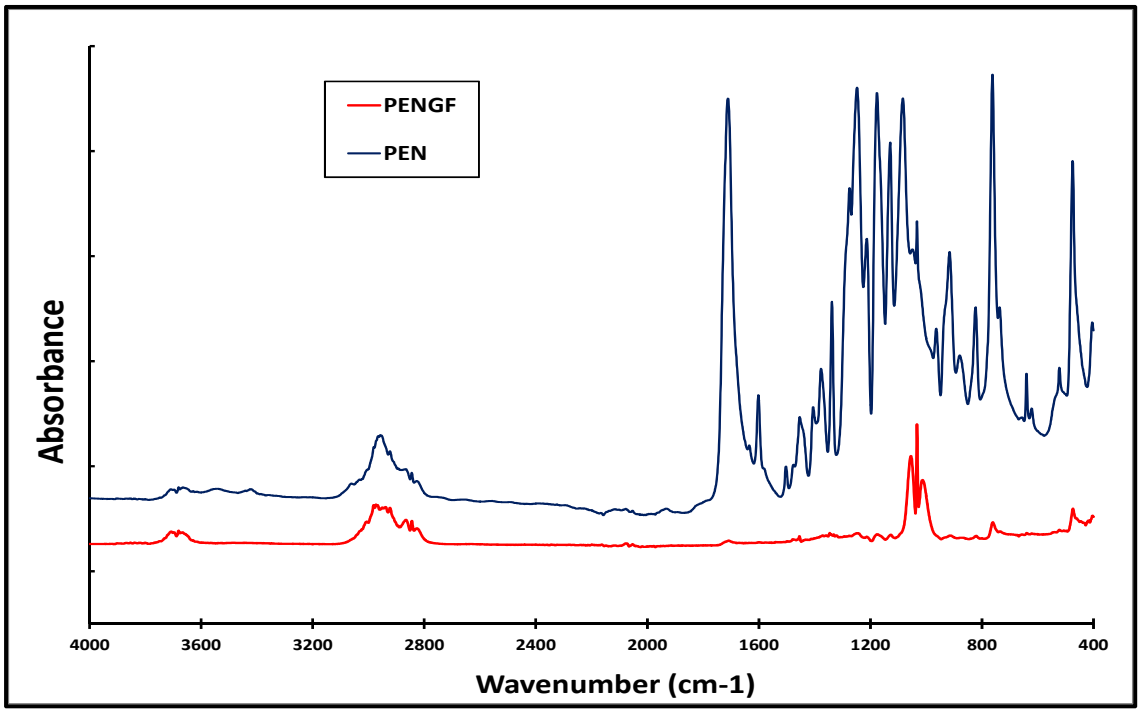

Figure 5.10 The FTIR spectrum of PEN and its composites

5.3.5 Dielectric spectroscopy analysis

In order to assess the effects of inorganic reinforcements such as mica and glass fibers on the dielectric response of the unfilled recycled PET and its composites, the behavior of the real (ε') and imaginary parts (ε") of the complex permittivity was investigated over a wide frequency domain at different temperatures. The dielectric response of the unfilled PEN and the glass fiber-filled PEN polymer was studied as well. It should be noted that semi-crystalline polymers such as polyesters (PET and PEN) have a strong tendency to crystallize (Kremer & Schönhals, 2012). Consequently, the dielectric spectroscopy measurements were mainly restricted to temperatures below 95 °C, for the PET, and 140 °C, for the PEN. Some exceptions were made for the case of the mica-filled recycled PET. It should be mentioned that similar dielectric spectroscopy analyses of the PET polymer have also been reported in some studies (Ménégotto, Demont, & Lacabanne, 1999; Ulrych et al., 2014). Nevertheless, no dielectric studies have been conducted specifically on PET or PEN reinforced with inorganic fillers. For all materials, only a limited fraction of the β-relaxation peak was observed since the measurements only covered the frequency range from 10^{-2} to 10^{5} Hz.

Figures 5.11 to 5.14 illustrate the isothermal plots of the real (ε') and the imaginary (ε") parts of the complex permittivity as a function of frequency at different temperatures ranging from 30 to 90 °C for the recycled PET and the glass fiber-filled RPET (RPETGF), respectively. In order to clarify the changes occurring from adding mica platelet reinforcements to the recycled PET, the imaginary parts (ε") of the complex permittivity for the PETM composite are represented by three distinct spectra, depending on the temperature window (Figures 5.16 to 5.18). The first spectrum corresponds to the results for the 30 to 70 °C; temperature region; the second spectrum illustrates the results in the 75 to 95 °C temperature region, and the last one gives results obtained for temperatures above 100 °C.

Regarding the dielectric imaginary part in Figure 5.12, two relaxation peaks, α and β, were found. The α-relaxation associated with the glass transition is the most visible relaxation above the glass transition temperature. A limited fraction of the β-relaxation peak was observed. As

expected, the α-relaxation was found to be shifting toward high frequencies as the temperature increased, and a step-like in the real permittivity, which corresponds to the relaxation peak in the imaginary part (Kremer & Schönhals, 2012), was observed (see also the spectra related to the real (ε') part of the complex permittivity, and presented in Figures 5.11, 5.13 and 5.15). As seen in Figure 5.14, in the case of the PETGF, the intensity of the α-relaxation was lower, which simply indicated that there was less PET, and the contribution of this peak was superimposed with an interfacial peak in the 1 to 100 Hz frequency window. A broad interfacial peak was also clearly identified in the case of the mica-filled recycled PET in the 10^0 to 10^4 frequency range and at different constant temperatures between 30 and 70 °C (see Figure 5.16). The contribution of charge fluctuations seemed to be lower when the glass fibers were added, as compared to unfilled PET and mica platelet-filled PET.

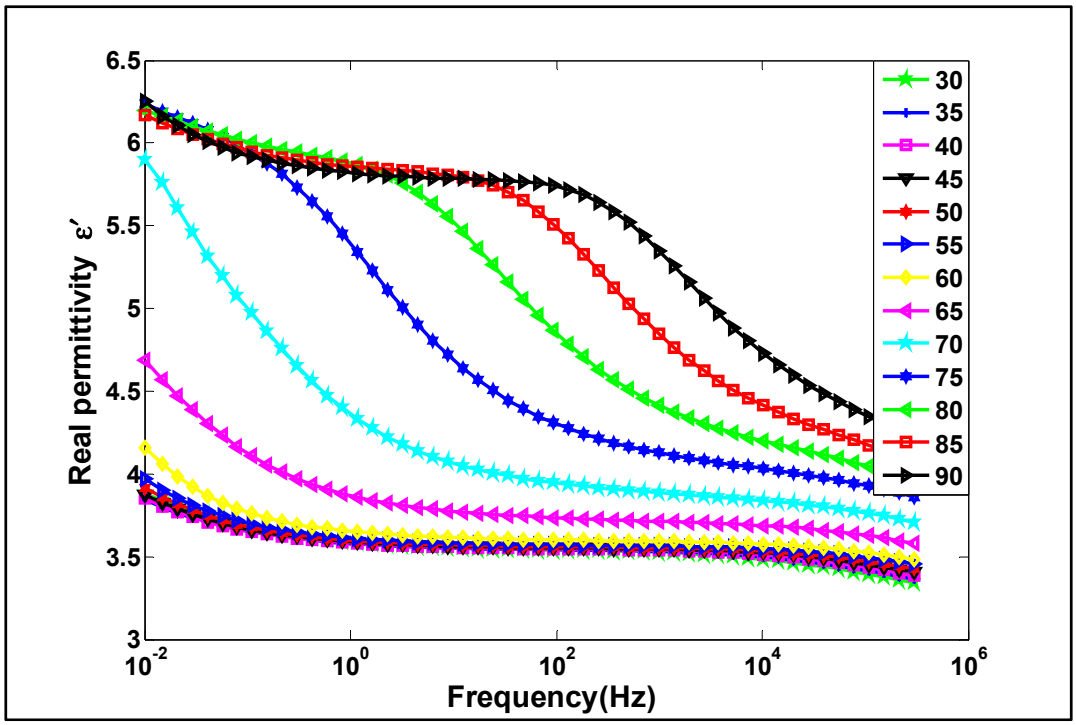

Figure 5.11 2D plot of the dependence of the real permittivity (ε') of the recycled PET polymer on frequency at different temperatures

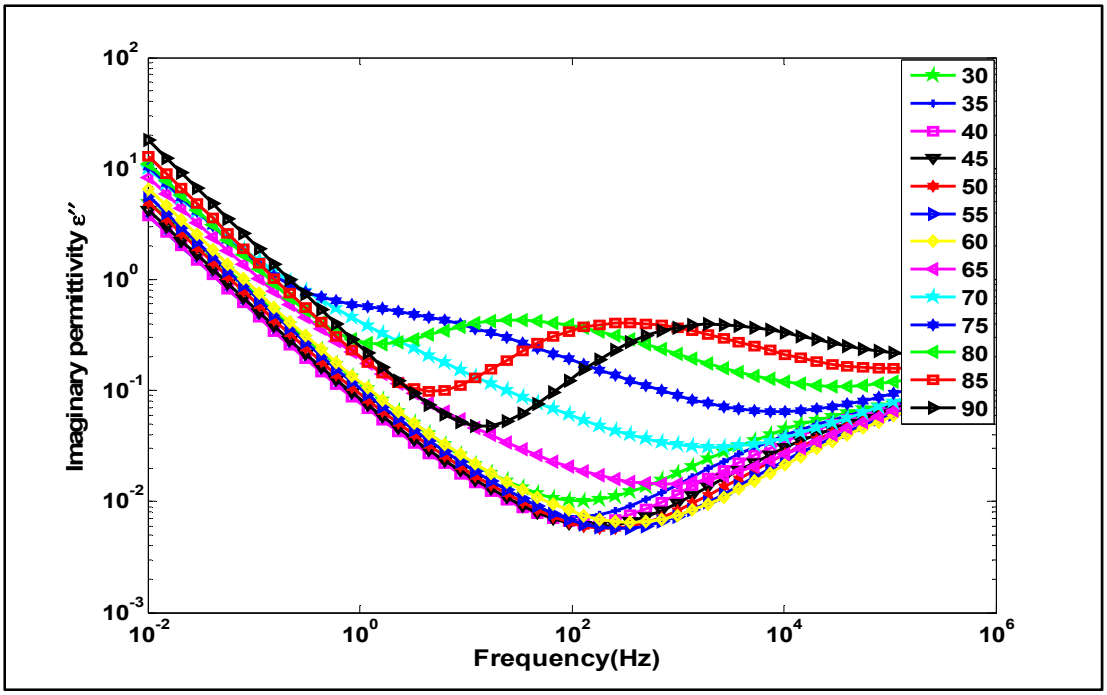

Figure 5.12 2D plot of the dependence of the imaginary permittivity (ε") of recycled PET polymer on frequency at different temperatures

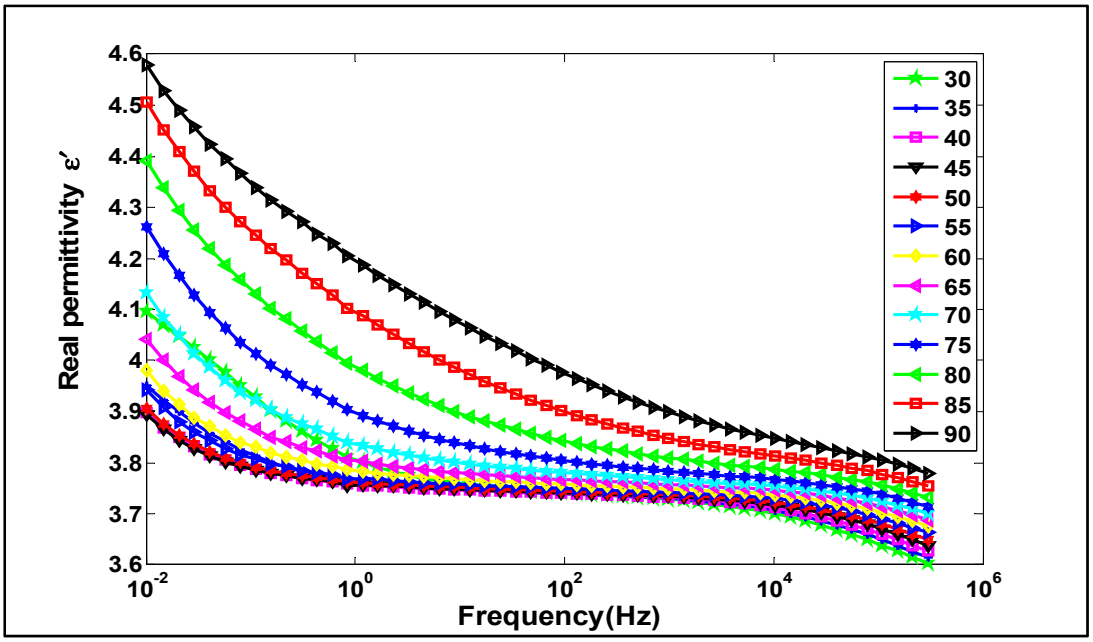

Figure 5.13 2D plot of the dependence of the real permittivity (ε') of the recycled PETGF composite on frequency at different temperatures

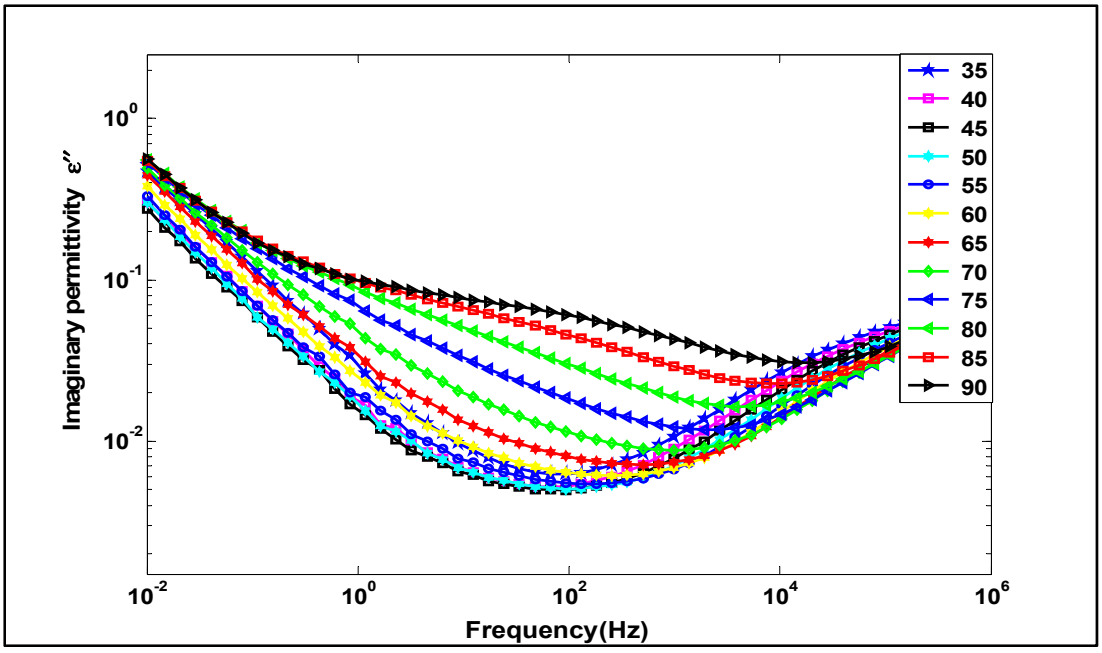

Figure 5.14 2D plot of the dependence of the imaginary permittivity (ε") of the recycled PETGF composite on frequency at different temperatures

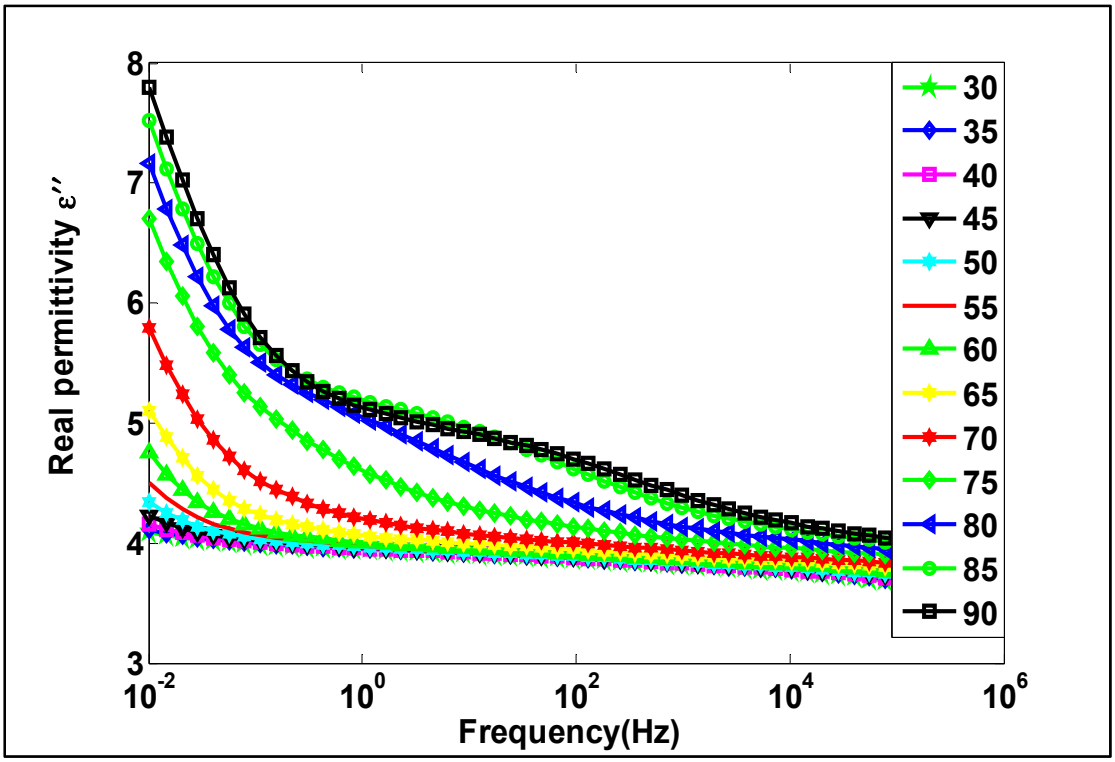

Figure 5.15 2D plot of the dependence of the real permittivity (ε') of the recycled PETM composite on frequency at different temperatures

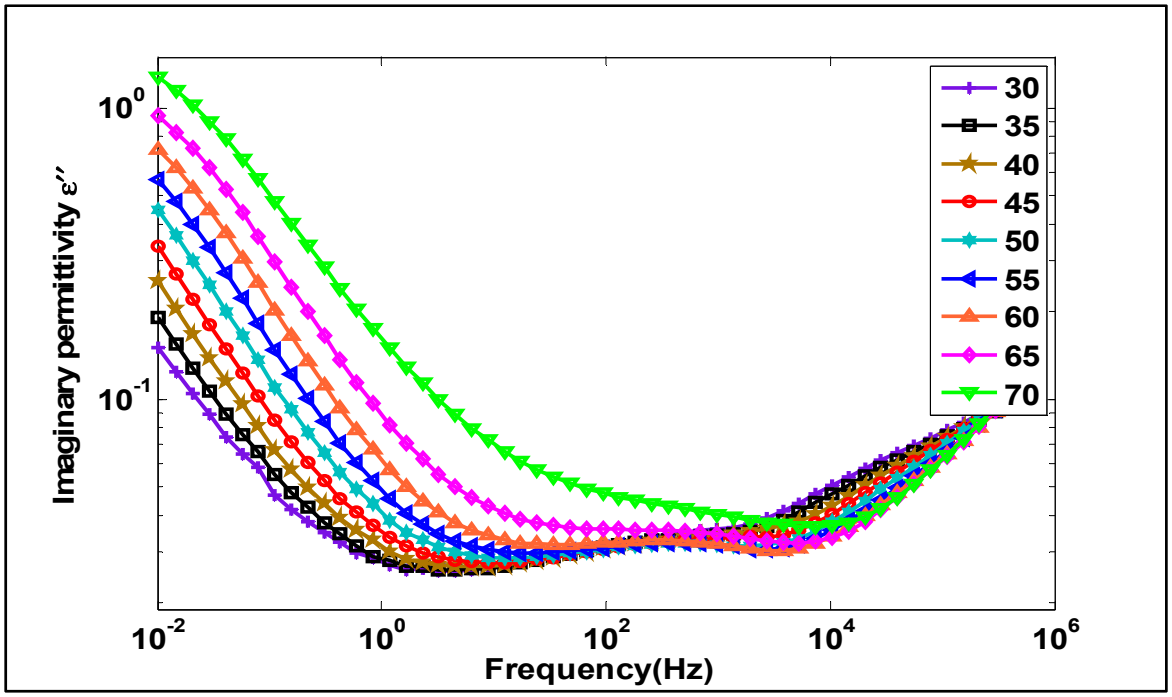

Figure 5.16 2D plot of the dependence of the imaginary permittivity (ε") of the recycled PETM composite on frequency at different constant temperatures between 30 and 70° C

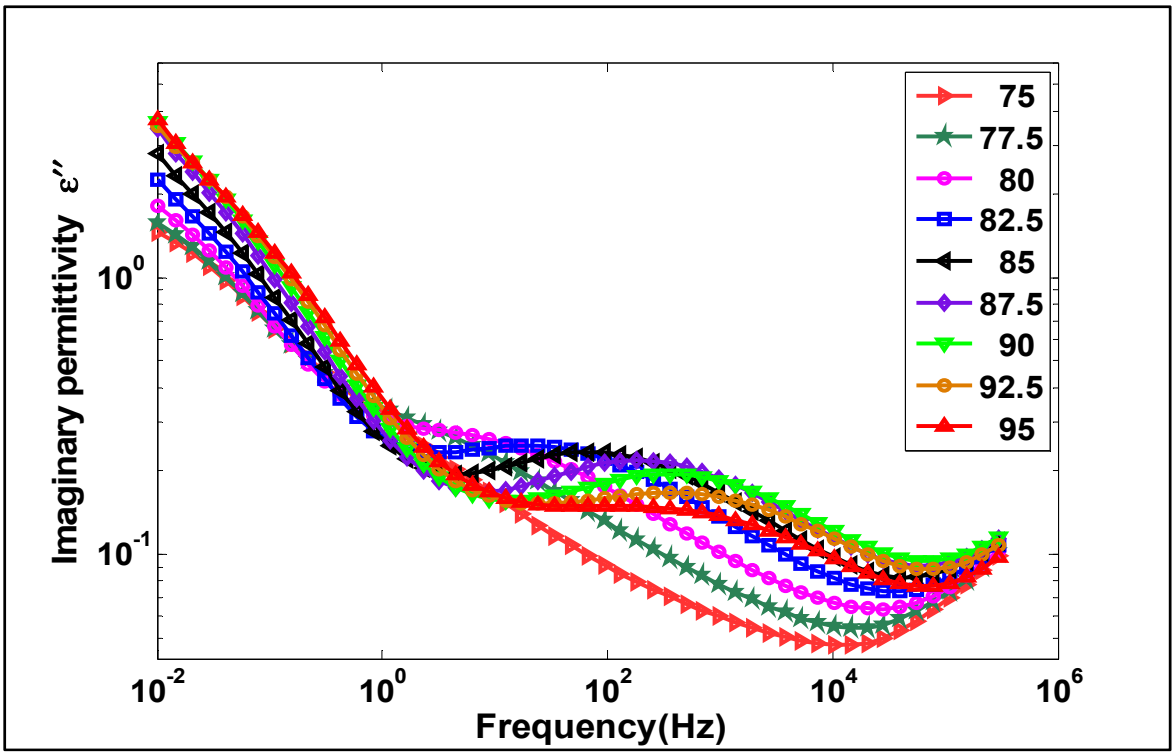

Figure 5.17 2D plot of the dependence of the imaginary permittivity (ε") of the recycled PETM composite on frequency at different constant temperatures between 75 and 95 °C

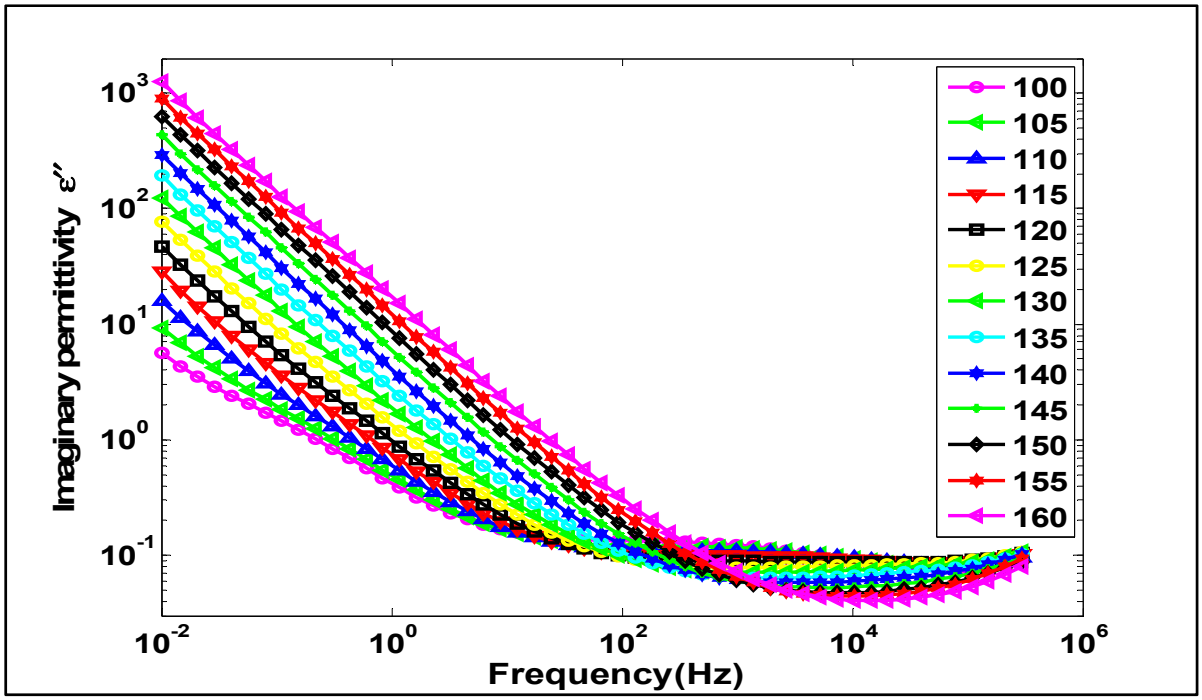

Figure 5.18 2D plot of the dependence of the imaginary permittivity (ε") of the recycled PETM composite on frequency at different constant temperatures between 100 and 160 °C

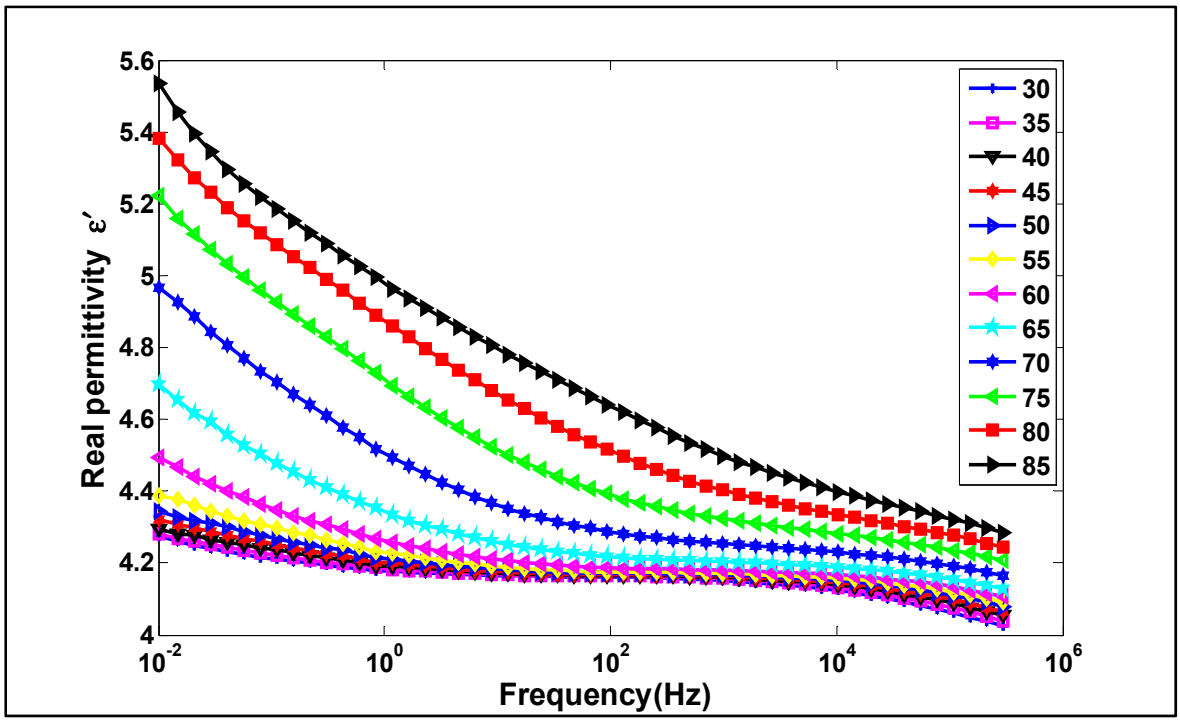

Figure 5.19 2D plot of the dependence of the real permittivity (ε') of the recycled PETGF2 composite on frequency at different temperatures

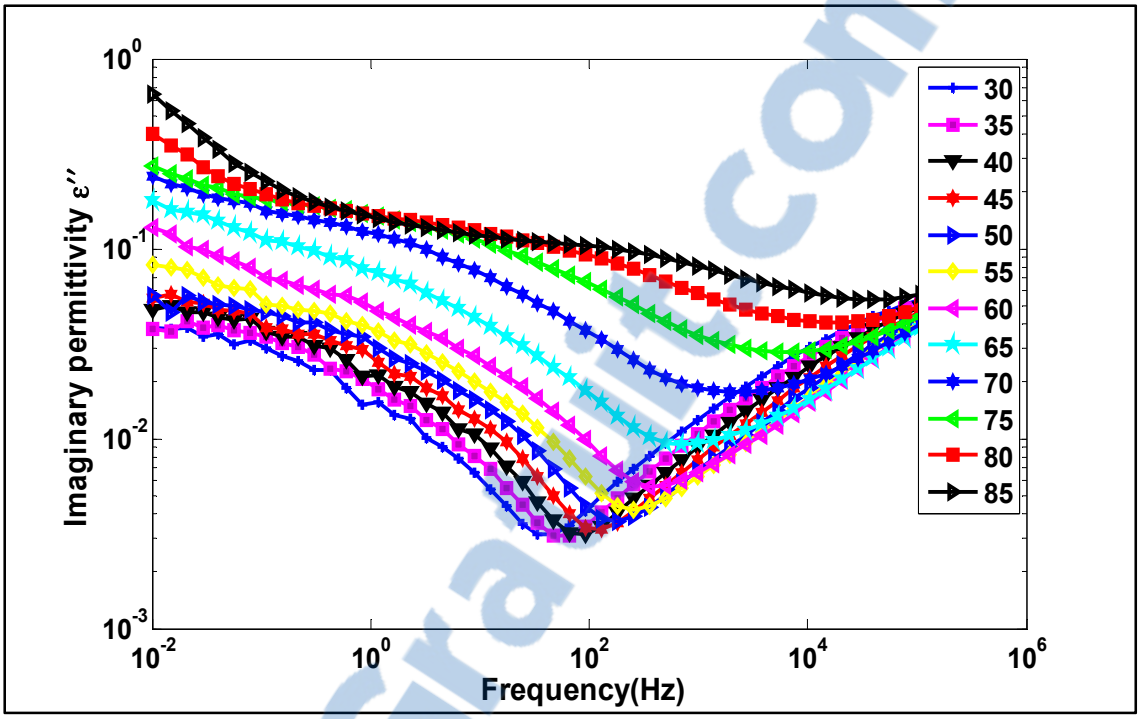

Figure 5.20 2D plot of the dependence of the imaginary permittivity (ε") of the recycled PETGF2 composite on frequency at different temperatures

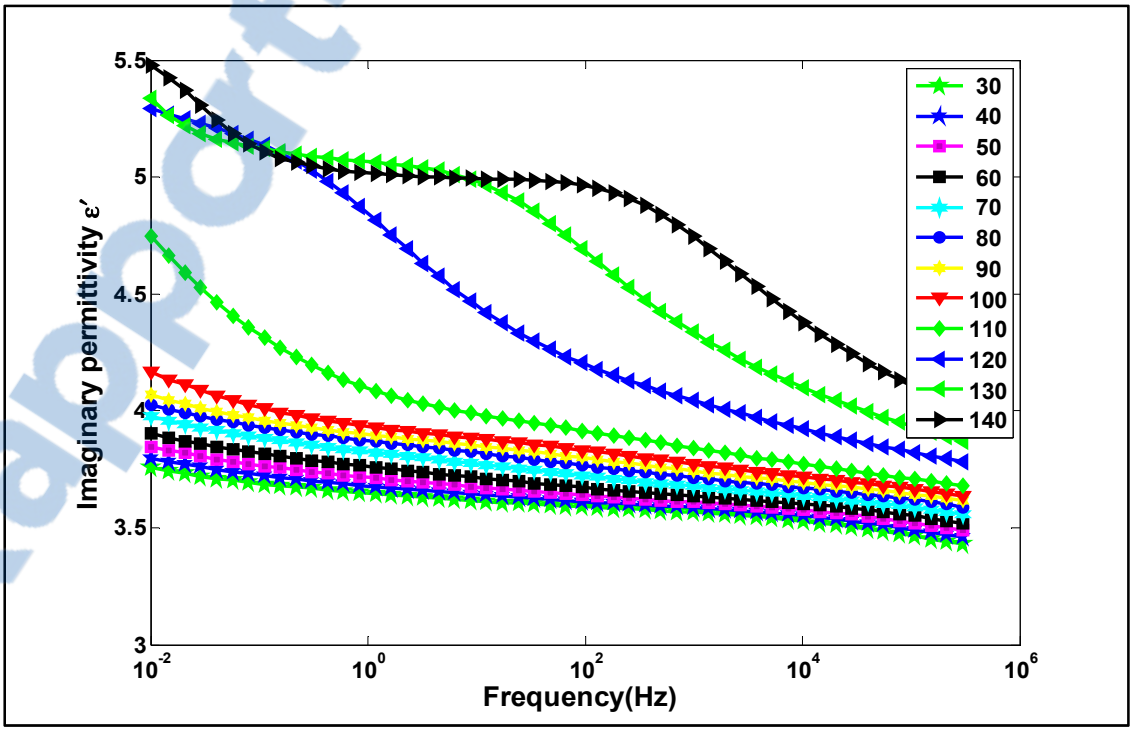

Figure 5.21 2D plot of the dependence of the real permittivity (ε') of the PEN polymer on frequency at different temperatures

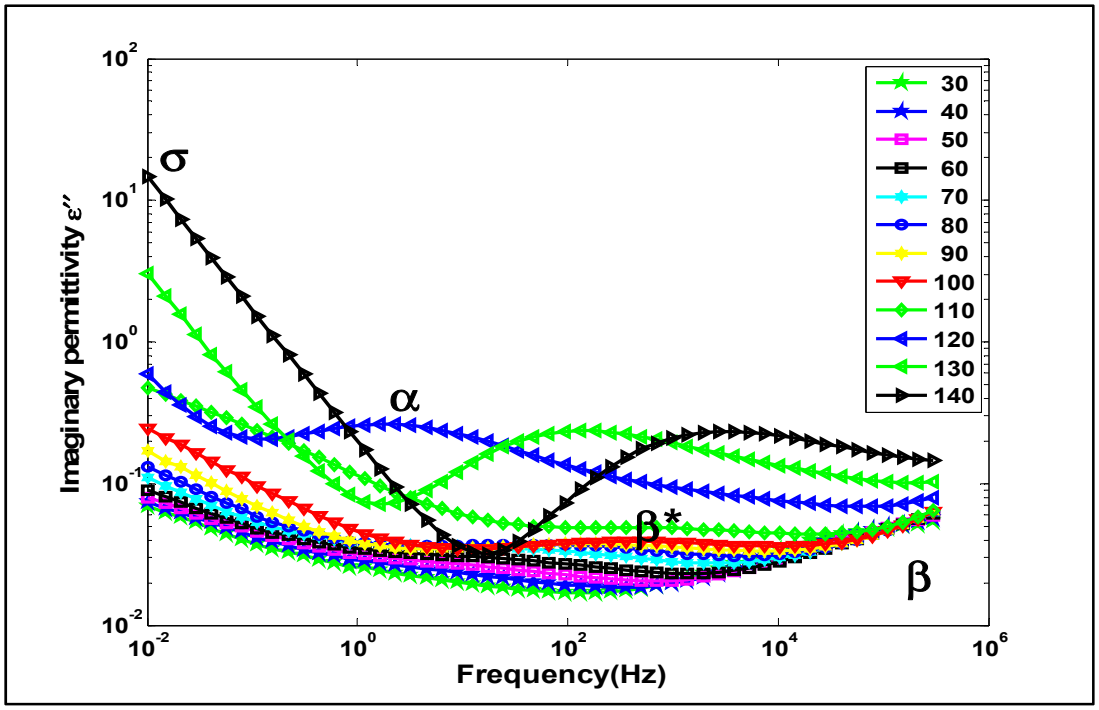

Figure 5.22 2D plot of the dependence of the imaginary permittivity (ε") of the PEN polymer on frequency at different temperatures

Figures 5.19 and 5.20 illustrate the 2D BDS plots of the real part ε' and the imaginary part ε" of dielectric permittivity versus the frequency and temperature for the glass fiber-filled RPET (RPETGF2). It should be noted that the RPETGF2 composite shows an almost identical evolution of the dielectric losses as the RPETGF composite. However, increasing the glass fiber content has a remarkable change in the increase in the real dielectric permittivity of the recycled PET and in the decrease in the conductivity (see the slope in Figure 5.19).

The isothermal plots of the real (ε') and imaginary (ε") parts of the complex permittivity of the PEN polymer as a function of frequency at different temperatures from 30 to 140 °C are shown in Figures 5.21 and 5.22 for selected temperatures. Figure 5.22 indicates that three relaxation processes could be identified in the dielectric spectra of the polyethylene naphthalate, namely, the α, β* and β processes. The β*-relaxation, which is located between the main relaxation α and the secondary relaxation β denotes the naphthalene rigid ring motion. It should be

mentioned that no obvious changes were observed for the glass fiber-filled PEN polymer, similarly to its PET counterpart.

Only the imaginary part (ε") of the dielectric permittivity was selected for the fitting. Figure 5.23 describes an example of the fitted imaginary part (ε") of the recycled PET as a function of frequency at 78 °C, which is the glass transition temperature of the specimen. As is common for the PET polymer, two main relaxation peaks were identified in these spectra. The characteristic segmental α process, which is associated with the glass transition of the amorphous phase and the local β process, which is related to the motion of the carbonyl group of the PET polymer, are clearly visible. At the glass transition temperature, the α dielectric relaxation, which denotes the glass transition of the amorphous phase, is clearly observed as a very large relaxation pic in the 10^{-1} to 10^{4} Hz frequency domain.

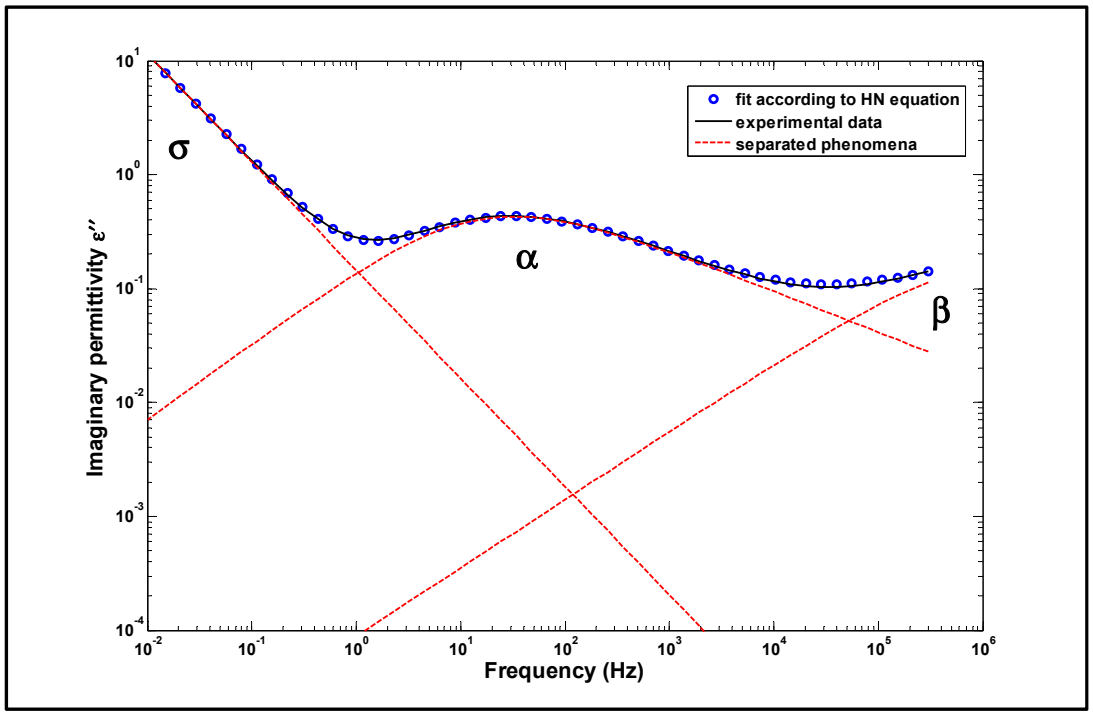

Figure 5.23 Imaginary dielectric permittivity (ε") vs. frequency for recycled PET polymer at its glass transition temperature (the dashed lines are the separated main relaxations and the circle line is the fit using H-N relaxation functions)

Figure 5.24 gives the corresponding relaxation times obtained after the fitting of the relaxation peaks of the non-filled recycled PET using the HN equation. The evolution of the relaxation time for the β-relaxation has an Arrhenius evolution. However, the α-relaxation relating to the main polymer chains occurs above the glass temperature, and their mobility increases with increasing temperature, with a non-Arrhenius temperature dependence. Figure 5.25 gives the relaxation times corresponding to a fitting according to the HN procedure, for the semi-crystalline recycled PET filled with mica. The evolution of the relaxation time for the interfacial peak shows that the frequential position of this peak is not strongly affected by the change of temperature, with the surprising result that we have a slight decrease in the relaxation frequency with an increase in temperature. This is commonly found for hydrophic fillers that release absorbed water as the temperature increases (Couderc, David, Frechette, & Medjdoub, 2013).

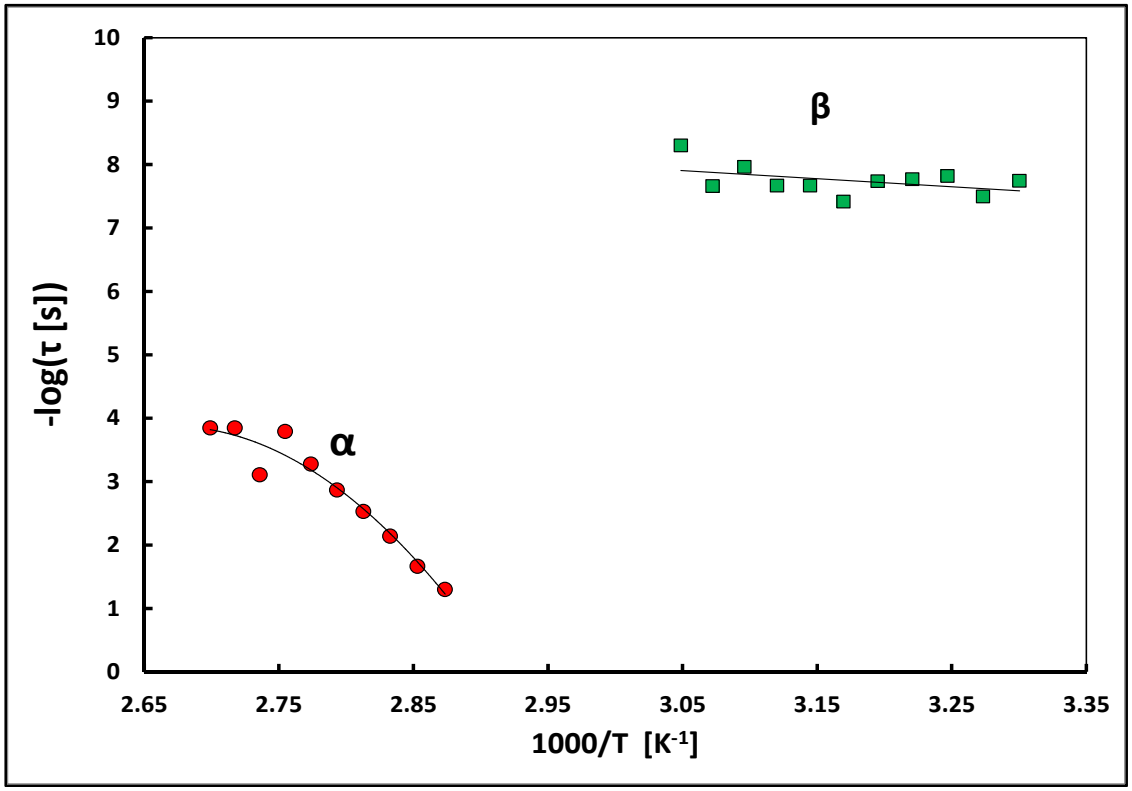

Figure 5.24 Relaxation times τ (s) for the non-filled semi-crystalline recycled PET

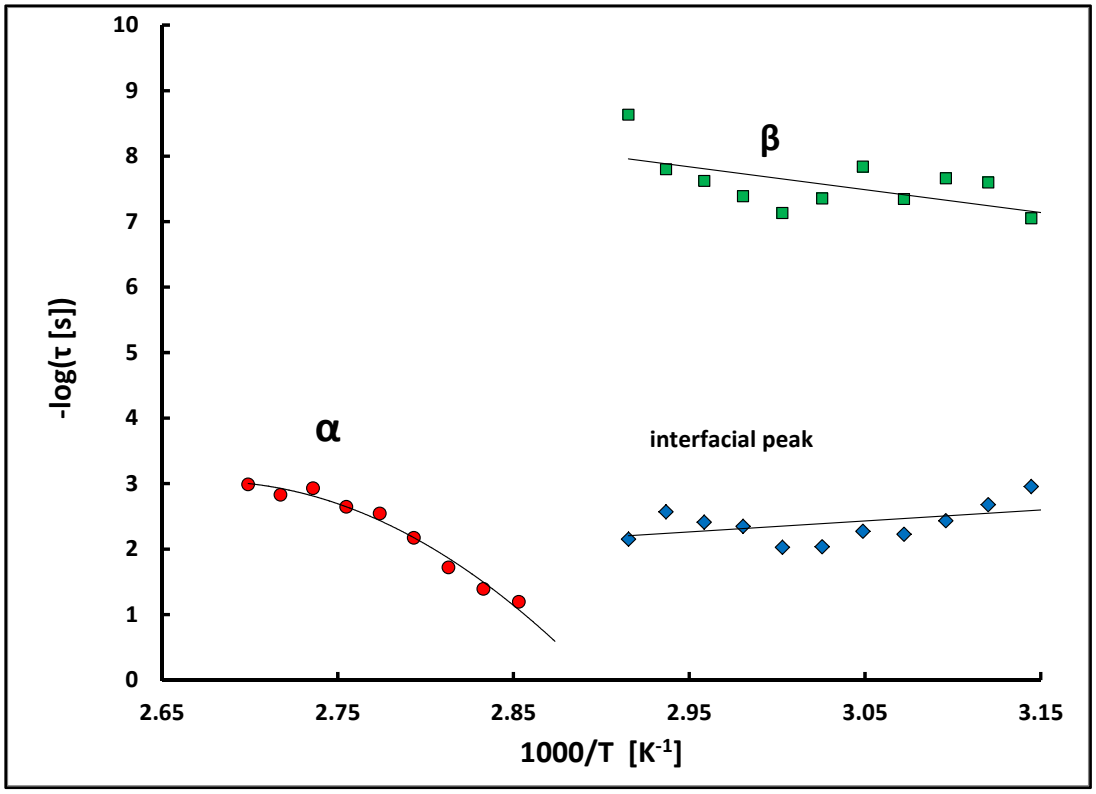

Figure 5.25 Relaxation times τ (s) for the semi-crystalline recycled PET -filled mica

5.3.6 Dielectric failure statistic analysis

The aim of this section is to compare the dielectric breakdown behavior of the unfilled recycled PET and PEN and to check the effect of inorganic fillers added to the tested polymers. Figures 5.28 and 5.29 show the dielectric-breakdown Weibull distributions obtained for the two types of polymer materials and their composites. The 90% confidence bounds (measured, but not shown in the figures) were obtained using the weighted least squares regression technique, as described in the IEEE Standard (ASTMD149, 2004). The statistical parameters for each sample are listed in Table 5.3. The relatively low values of the breakdown strength are due to the fact that the measurements were conducted on rather thick samples (Couderc, David, Corlu, Fréchette, & Savoie, 2011).

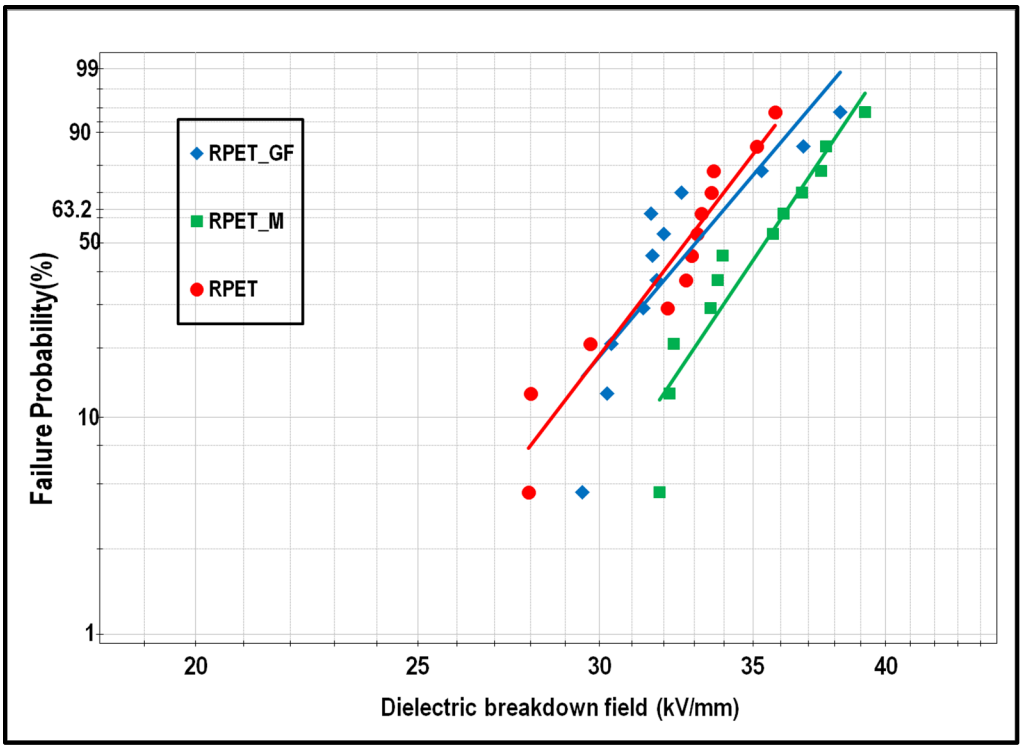

Figure 5.26 Dielectric breakdown strength of recycled PET and its composites

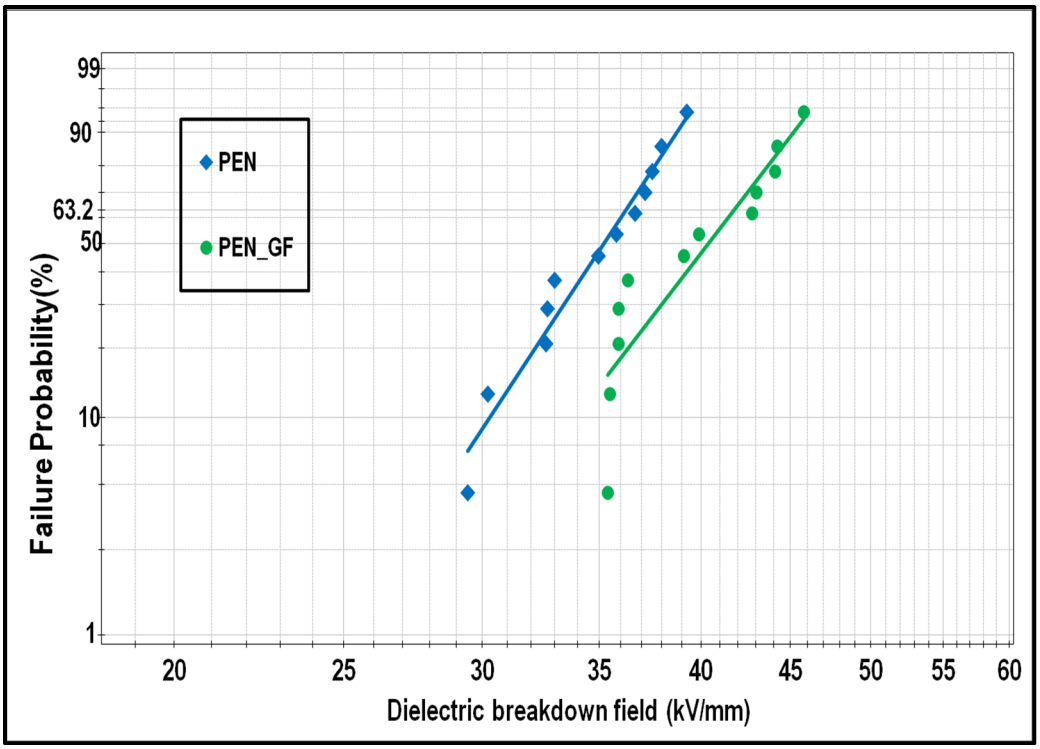

Figure 5.27 Dielectric breakdown strength of virgin PEN and glass fiber -filled PEN

Figure 5.26 displays the dielectric breakdown data for the unfilled recycled PET compared to the mica-reinforced recycled PET and glass fiber-reinforced recycled PET. It should be noted that the dielectric breakdown strength results obtained for the unfilled recycled PET polymer and the glass fiber-filled recycled PET indicate a near-equal dielectric behavior. However, a significant increase in the dielectric breakdown strength was observed when the mica fillers were added. Figure 5.27 shows the dielectric breakdown data for the unfilled PEN compared to those for the glass fiber-reinforced PEN. A significant effect was observed when the glass fibers were added to the PEN polymer.

Tableau 5.3 Breakdown parameter and its 95% confidence Interval calculated from the two-parameter Weibull distribution

Material	**Weibull parameters**			
	α_l	α	α_u	β
RPET	32.4	33.4	34.4	16.2
RPETGF	32.1	33.6	34.9	12.1
RPETM	34.8	36.1	37.3	14.6
PEN	34.7	36.2	37.7	12.3
PENGF	39.4	41.6	43.6	10.1

The statistical parameter α found for the two unfilled polymers indicates that the recycled PET polymer exhibits a good dielectric breakdown strength as compared to the high-performance polymer. Therefore, the dielectric reliability (in terms of dielectric strength) of the recycled PET and its composites was confirmed. However, glass fiber reinforcements were found to have a significant effect in enhancing the dielectric breakdown strength of the PEN polymer. This enhancement can be seen through a good adhesion and compatibility with the glass fibers fillers. In addition, our morphological study reveals that glass fiber-filled PEN material has a better surface finish than a recycled PET reinforced with glass fibers. On the other hand, the thermal analysis reveals that the crystallinity growth rate was less significant when glass fibers were added to the PEN polymer. This indicates that the recycled PET becomes more sensitive

to dielectric breakdown when filled with glass fibers, as compared to the PEN polymer. Consequently, both matrix and fillers type contribute to the resistance to the electric field.

5.4 Conclusion

In this work, the dielectric behavior of the recycled PET and the recycled PET reinforced with short glass fibers or mica platelets was evaluated in terms of breakdown strength and dielectric response. Moreover, a dielectric investigation of an unfilled PEN and the glass fiber-filled PEN was carried out. The following conclusions can be drawn:

- The cold crystallization of the PET starts at a lower temperature than for the PEN. Moreover, glass fibers have no effect on the cold crystallization of the recycled PET, whereas they lead to a significant slowdown in the cold crystallization process of the PEN polymer. This may be attributed to the rigid ring existing in the main chain of the PEN polymer (absent in the recycled PET) making this polymer. Furthermore, both matrix and reinforcements types were found to affect the crystallinity rate in the composites.
- Glass fiber reinforcements were found to have a significant effect on the improvement of the dielectric breakdown strength of the PEN polymer as compared to the recycled PET. This behavior can be explained by the good surface finish, as well as the adhesion and compatibility between the PEN matrix and the glass fiber reinforcements.
- An FTIR analysis confirmed that the presence of some inorganic filler, such as mica and glass fibers, contributes to a molecular structure change in the recycled PET and PEN polymers. A remarkable change in intensity of some bands was observed, indicating that a molecular chain rearrangement occurred when the crystallinity rate was increased.
- Increasing the glass fiber content leads to a significant change in the crystallinity rate as well as in the dielectric properties of the recycled PET polymer (mainly the real permittivity). Moreover, the presence of inorganic fillers increases the thermal resistance degradation for the recycled PET and PEN polymers.

- A dielectric spectroscopy analysis of the different materials indicated that an additional interfacial relaxation peak occurred in the case of the glass fiber- and mica-filled recycled PET at an intermediate frequency. This peak was found to be relatively unaffected by the change of temperature in the 30-100 °C temperature range.

ACKNOWLEDGMENT

The authors would like to express their deepest gratitude to Patrick Lachance and Doru Davinscu from the Lavergne Group Company that kindly supplied materials used for this investigation. Financial support of this work by the National Sciences and Engineering Research Council of Canada (NSERC) is deeply appreciated.

CONFLICT OF INTERESTS

The authors declare that there is no conflict of interests regarding the publication of this paper.

CHAPITRE 6

ARTICLE IV: NUMERICAL MODELING OF THE EFFECTIVE COMPLEX PERMITTIVITY OF PET-BASED COMPOSITES MATERIALS

Fouzia Mebarki and Éric David

Département de génie mécanique École de Technologie Supérieure (ÉTS), 1100 Notre-Dame Ouest, Montréal QC, Canada H3C 1K3

Article soumis dans: Journal of Polymer Research en Avril 2017
Numéro de confirmation: JPOL-D-17-00602

ABSTRACT

Heterogeneous mixtures were prepared using a homogeneous background (polyethylene terephthalate) in which fibers or platelets of a two-component mixtures were randomly embedded, glass fibers or mica platelets. The main purpose of this paper is to check the effect of adding some different types of inclusions on the complex dielectric permittivity of some recycled PET based composites. Our study is made to assess experimentally the effective dielectric properties and then use the finite element method (FEM) to predict the effective complex dielectric permittivity of some heterogeneous systems such as polyethylene terephthalate based-composites. The effective complex permittivity has been measured using broadband dielectric spectroscopy (BDS) and both real and imaginary permittivities were used for the following analysis. Results obtained by experimental tests and different analytical calculations were compared to those obtained from numerical simulations.

6.1 Introduction

Heterogeneous mixtures consist of at least two types of visible homogeneous phases. These materials exhibit vastly superior performance to those of homogeneous materials. Their effective properties are defined as variables representing a specific behavior of the heterogeneous mixture and their effective parameters depend on all properties of each phase. Microstructure of heterogeneous medium is complex and the effective properties are still difficult to obtain accurately. Hence, effective properties of random heterogeneous media have been the subject of extensive researches and studies in various domains particularly in mechanical, thermal and electrical applications (Castañeda, 1991; Jylha & Sihvola, 2005; Kikuchi, Kang, Kawasaki, Nishida, & Ichida, 2004; Scheller, Wietzke, Jansen, & Koch, 2009; S Torquato, 2000; F. Wu & Whites, 2001).

Over the past several years, the effective dielectric properties of heterogeneous mediums have been investigated in theoretical and experimental studies. Different theoretical models based on the law of mixtures, mean-field theory, the mean effective and integral methods have been reported (Banhegyi, 1986; Beran, 1965; Bergman, 1978; Salvatore Torquato, 2013). However, theoretical models have some limitations. It is only recently that new methods based on numerical calculations such as finite difference time domain (FDTD) (Karkkainen, Sihvola, & Nikoskinen, 2000; Yu & Mittra, 2001; Zivanovic, Yee, & Mei, 1991) and finite element method (FEM) (Brosseau & Beroual, 2003; Myroshnychenko & Brosseau, 2009; Serdyuk et al., 2004; Tuncer et al., 2002) were used. Numerical modeling methods are of a great importance for the improvement of the solutions obtained particularly for fairly complex microstructures.

Due to the complexity of the microstructure, there are relatively few situations in which one can evaluate the effective properties of heterogeneous materials exactly (Salvatore Torquato, 2013). Effective dielectric properties of most heterogeneous media such as permittivity vary considerably with several different factors. Concentration (Tuncer et al., 2001), geometry shape (Sillars, 1937), rearrangement of inclusions (Sareni, Krähenbühl, Beroual, & Brosseau,

1996)and interfacial interaction are very important to define effective properties of the composites (Chow, 1980; Tuncer, 2013). Several analytic models have been made in order to predict the effective dielectric properties (Golden & Papanicolaou, 1983; Hermann, 2010).

6.2 Different analytical approaches

Several analytical models based on mixtures law exist in the literature. These models are intended to express the permittivity of a multiphasic medium as a function of the permittivity and the volume fraction of each component. However, these models have limitations since they do not take account of the medium morphology. The mixing laws may include the law of Looyenga, Wiener's laws (for constituents in series (equa.2) and in parallel (equa.3)), the law of Böttcher and Lechtenecker formula:

$$(\hat{\varepsilon})^{1/3} = (\upsilon_2)(\widehat{\varepsilon_1})^{1/3} + (1-\upsilon_2)(\widehat{\varepsilon_2})^{1/3} \tag{6.1}$$

$$\frac{1}{\hat{\varepsilon}} = \frac{1-\upsilon_2}{\widehat{\varepsilon_1}} + \frac{\upsilon_2}{\widehat{\varepsilon_2}} \tag{6.2}$$

$$\hat{\varepsilon} = (1-\upsilon_2)\widehat{\varepsilon_1} + \upsilon_2\widehat{\varepsilon_2} \tag{6.3}$$

$$\frac{\hat{\varepsilon}-\widehat{\varepsilon_2}}{3\hat{\varepsilon}} = \upsilon_2 \frac{\widehat{\varepsilon_1}-\widehat{\varepsilon_2}}{\varepsilon_1+2\hat{\varepsilon}} \tag{6.4}$$

$$\ln \hat{\varepsilon} = \upsilon_1 \ln \hat{\varepsilon_1} + (1 - \upsilon_1) \ln \hat{\varepsilon_2} \tag{6.5}$$

where υ_1 and υ_2 are the volume fractions of the two phases, $\hat{\varepsilon}_1$ and $\hat{\varepsilon}_2$ are the complex dielectric permittivity of the two phases and $\hat{\varepsilon}$ is the composite effective complex permittivity.

A great deal of attention is being paid to the study of dielectric properties of heterogeneous materials. In 1986, (Banhegyi, 1986) presented a very good overview of the basic theoretical methods of calculating the dielectric properties of heterogeneous mixtures. The different formulas and theories to calculate the effective permittivity such as mean effective and integral methods were summarized. The complex effective dielectric permittivity of heterogeneous materials, $\hat{\varepsilon}$, is defined as (Beran, 1965):

$$\langle \widehat{\mathrm{D}} \rangle = \langle \widehat{\mathrm{E}} \rangle \hat{\varepsilon} \varepsilon_0 \tag{6.6}$$

Where$\langle \quad \rangle$ means the volume averaging, ε_0 denotes the vacuum permittivity and $\widehat{E}$ and $\widehat{D}$ are respectively the complex electrical field and the complex electrical displacement. For a two-phase material, (6.6) can obviously be re-written as:

$$\hat{\varepsilon} = \frac{\upsilon_1 \widehat{\varepsilon_1} \langle \widehat{\mathrm{E}_1} \rangle + \upsilon_2 \widehat{\varepsilon_2} \langle \widehat{\mathrm{E}_2} \rangle}{\langle \widehat{\mathrm{E}} \rangle} \tag{6.7}$$

With the mean electrical field given by:

$$\langle \widehat{\mathrm{E}} \rangle = \upsilon_2 \langle \hat{E}_2 \rangle + (1 - \upsilon_2) \langle \hat{E}_1 \rangle \tag{6.8}$$

where $\hat{E}_1$ and $\hat{E}_2$ are the complex electrical fields in the two phases and υ_2 and υ_1 are the volume fractions of the two phases.

The dielectric permittivity is defined as a complex quantity by:

$$\hat{\varepsilon}(\omega) = \varepsilon'(\omega) - i\varepsilon''(\omega) \tag{6.9}$$

where ε' denotes the real part. The imaginary part,ε", of the effective permittivity represents the energy losses caused by the polarization mechanisms, $\omega = 2\pi f$ is the angular frequency in rad/s and f is the frequency in Hz.

In the case of an ellipsoidal particle having a complex permittivity $\hat{\varepsilon}_2$ includedin a matrix having a complex permittivity$\hat{\varepsilon}_1$, the ratio of the average electrical fields in each phase may be given by (Banhegyi, 1986):

$$\frac{\langle\widehat{E_2}\rangle}{\langle\widehat{E_1}\rangle} = \sum_{k=1}^{3} \frac{\cos^2\alpha_k}{1 + \left(\frac{\widehat{\varepsilon_2}}{\widehat{\varepsilon_1}} - 1\right) A_k} \tag{6.10}$$

where A_k are the depolarization factors that depend on the geometry of the inclusion and direction of the applied field and α_k represent the angles between the applied field and k^{th} axes of the ellipsoid. This result can be obtained from the solution of the Laplace equation for an ellipsoidal inclusion for which a constant field is applied far away from the particle. It is also known as the mean field approximation or the effective medium approximation, all leading to the same equation (6.10). For spherical inclusions, the depolarization parameters are given as:

$$\begin{cases} A_1 = A_2 = A_3 = 1/3 \\ \cos^2\alpha_1 = \cos^2\alpha_2 = \cos^2\alpha_3 = 1/3 \end{cases}$$

Thus, the previous equation leads to:

$$\frac{\langle\widehat{E_2}\rangle}{\langle\widehat{E_1}\rangle} = \frac{3 * \widehat{\varepsilon_1}}{2\widehat{\varepsilon_1} + \widehat{\varepsilon_2}} \tag{6.11}$$

In case of cylindrical particles perfectly oriented with their main axis perpendicular to the electrical field, the depolarization factors and the orientation cosines are equal to:

$$\begin{cases} A_1 = A_2 = {}^1/_2 \ and \ A_3 = 0 \\ \cos^2\alpha_1 = 1 \ \ and \ \cos^2\alpha_2 = \cos^2\alpha_3 = 0 \end{cases}$$

Thus, the ratio of the electric fields will be given by the following equation

$$\frac{\langle \widehat{E_2} \rangle}{\langle \widehat{E_1} \rangle} = \frac{2 * \widehat{\varepsilon_1}}{\widehat{\varepsilon_1} + \widehat{\varepsilon_2}} \tag{6.12}$$

Using equation (6.7), (6.8) and (6.12), a general expression for the effective permittivity of the mixture in the case of a cylindrical inclusion can be given as

$$\hat{\varepsilon} = \widehat{\varepsilon_1} + 2\upsilon_2\widehat{\varepsilon_1}\frac{\widehat{\varepsilon_2} - \widehat{\varepsilon_1}}{\widehat{\varepsilon_1} + \widehat{\varepsilon_2} - \upsilon_2(\widehat{\varepsilon_2} - \widehat{\varepsilon_1})} \tag{6.13}$$

And in the case of perfectly oriented cylindrical inclusions with their main axis parallel to the applied field, the effective permittivity is given by the Rayleigh's formula:

$$\frac{\hat{\varepsilon} - \widehat{\varepsilon_1}}{\hat{\varepsilon} + 2\widehat{\varepsilon_1}} = \upsilon_2\frac{\widehat{\varepsilon_2} - \widehat{\varepsilon_1}}{\widehat{\varepsilon_2} + \widehat{\varepsilon_1}} \tag{6.14}$$

In this paper, we intend to investigate the effect of adding different types of inclusions on the complex dielectric permittivity of recycled PET based composites. The mixture was a

homogeneous background in which cylinders or platelets of a two-component mixture were randomly embedded, glass fibers or mica. Composites obtained can offer much better dielectric, thermal and mechanical properties. Table 6.1 gives a brief description of some composites related to our investigation. Two different micrometric reinforcements, consisting of short glass fibers 3 mm in length and 10.5 μm in diameter, as well as mica platelets 89~254 μm in diameter and 0.001-1 μm in thickness, were used to form our composites.

Tableau 6.1 Brief description of the different materials

Specimen identification	Material	Additional information
PET	Recycled PET	No reinforcements were added
PETGF15	RPET reinforced with glass fibers	Contains 15 wt % of glass fibers
PETGF20	RPET reinforced with glass fibers	Contains 20 wt % of glass fibers
PETGF30	RPET reinforced with glass fibers	Contains 30 wt % of glass fibers
PETGF35	RPET reinforced with glass fibers	Contains 35 wt % of glass fibers
PETM15	RPET reinforced with mica	Contains 15 wt % of mica platelets
PETMGF	RPET reinforced with mica and glass fibers	Contains 15 wt % of mica platelets and 25wt % of glass fibers

6.3 Dispersion and microstructure

The microstructure and dispersion of glass fibers in the PET matrix were observed using electronic scanning microscopy (SEM). The morphology and the dispersion of the glass fibers reinforcements are clearly shown in Fig. 6.1. This two-phase composite contains 15wt% of glass fibers randomly dispersed in a recycled PET matrix. In this work, the complex dielectric permittivity at 10^3 Hz of the glass fibers fillers was taken to be 5.1- $i(\sigma_2/(\omega\varepsilon_0)$ and 6.0- $i(\sigma_3/(\omega\varepsilon_0)$ for the mica reinforcements. While the complex dielectric permittivity of the recycled PET matrix has been measured using the broadband dielectric spectroscopy (BDS) and it was taken to be 3.2-0.02i at the same frequency. The microstructure pictures were not only taken to check the dispersion but also to use them for the numerical simulation.

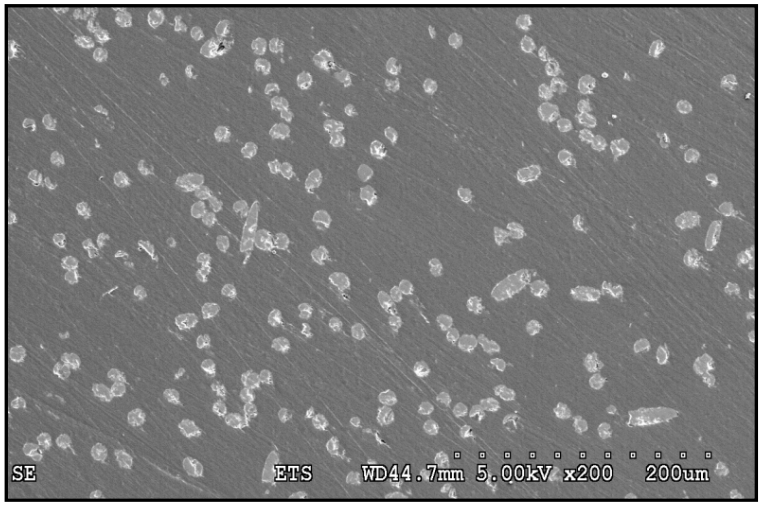

Figure 6.1 Scanning electron microscope (SEM) images of a cross section of a recycled PET based composite (15% glass fibers)

6.4 Numerical simulation

The finite element modeling process is mainly based on the assembly of the global matrix, knowledge of boundary conditions, choice of mesh and solving. In this work, finite element method (FEM) simulations using ***Comsol Multiphysics 5.2*** software have been used for

computing the effective dielectric permittivity of some PET polymer composites. The simplest approach for determining complex effective permittivity of a mixture is based on the application of a voltage *U* across a unit cell followed by the calculation of the averages of the dielectric displacement and of the electrical field in the material.

Our first 3D-model as illustrated by Fig. 6.2 is considered as a capacitor for which an AC electric field is applied along the z-axis into a biphasic polymer composite. Each phase is defined by its complex dielectric permittivity and its conductivity. The heterogeneous media studied is assumed to be made of uniformly periodically repeated cells. Each cell being made with a dielectric cylinder embedded into a dielectric background. The lower face of the square-parallelepiped was assumed to be grounded (V=0) and the upper side was sets to 1V. The complex dielectric permittivity of the PET material used for all numerical simulations was taken from the experimental data and complex dielectric permittivities for the inclusions were taken from the available technical datasheets.

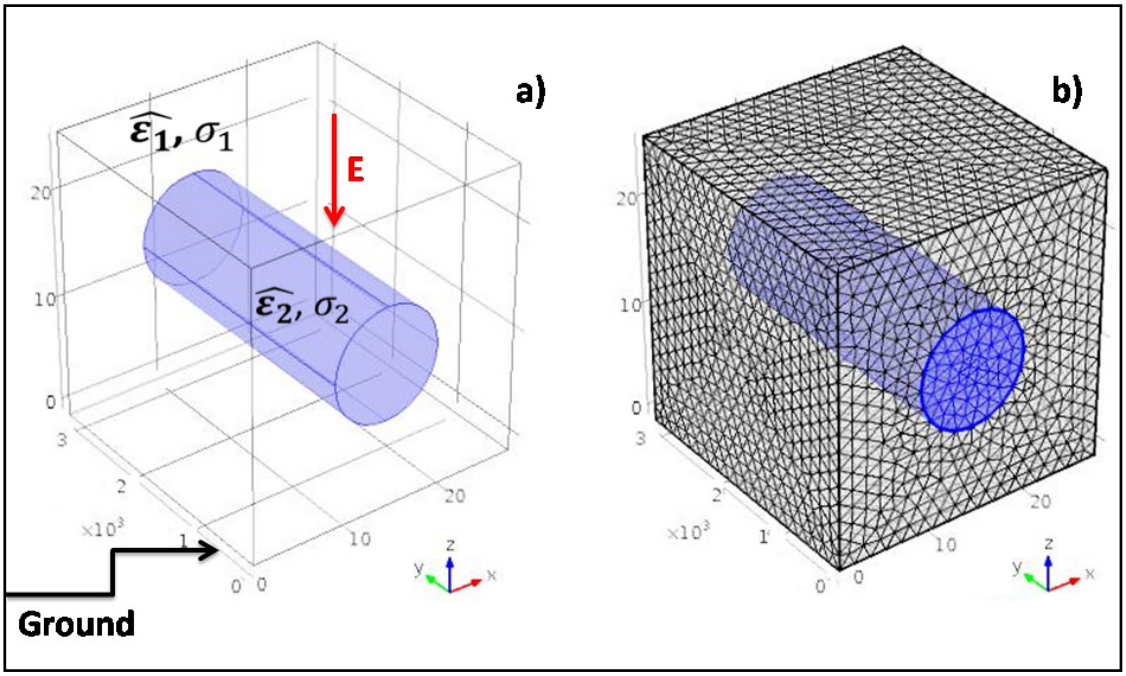

Figure 6.2 Illustration of a) the concept and b) the numerical model for defining the effective dielectric permittivity. The cylinder is the glass fiber inclusion with $\widehat{\varepsilon_2}$ =5.1- $(\sigma_2/(\omega\varepsilon_0)i$ and σ_2=10^{-13} S /m and the matrix medium with $\widehat{\varepsilon_1}$ =3.2-0.02i

Considering that glass fiber and mica filler are two different reinforcements, the effect of the inclusion type on the electric field and the complex effective permittivity of some PET composites was studied. Thus, two different geometries were created (see Fig. 6.3). The glass fiber is assumed to be horizontally disposed in the PET matrix ((with L<<<R) and the mica filler is vertically disposed in the PET matrix (with R>>>L). Both particles were assumed to be cylindrical shape and the real inclusion dimensions were taken for each geometry (R=127 µm and L=1 µm in case of the mica platelets and R=5.25 µm and L=3 mm in case of glass fibers).The volume of each unit cell was calculated to match the 15wt% of the inorganic reinforcements added to the manufactured PET polymer (the equivalent volume fraction is 0.0784). The resulting data of each case are listed in Table 6.2.

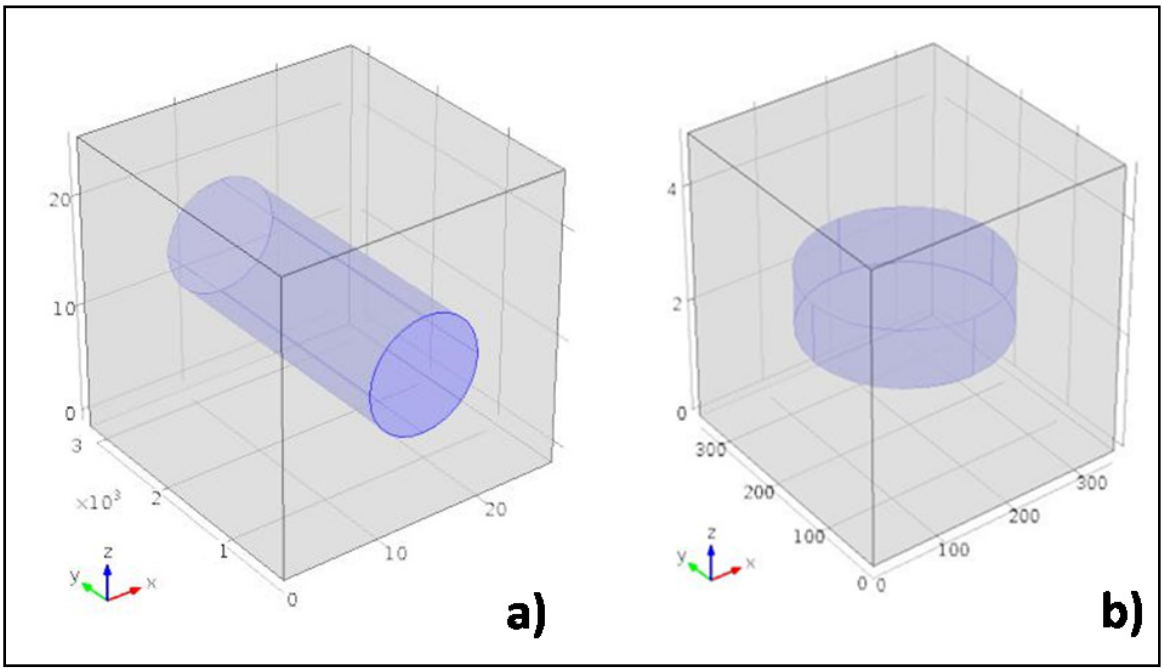

Figure 6.3 3D-geometries for a glass fiber horizontally disposed in the PET matrix (L<<<R) and b) a mica filler vertically disposed in the PET matrix (R>>>L)

As expected, the effective complex dielectric permittivity of the composite increases as the complex permittivity of the inclusion increases. In addition, the variation of the electrical field (the difference between the minimum and the maximum value) also increases as the complex permittivity of the reinforcement increases

Tableau 6.2 Effective complex permittivity dependence on the permittivity of the inclusion $\widehat{\varepsilon_1}$ =3.2-0.02i (matrix), $\widehat{\varepsilon_2}$ =5.1- $(\sigma_2/(\omega\varepsilon_0)i$ (glass fibers), $\widehat{\varepsilon_3}$ =6.0- $(\sigma_3/(\omega\varepsilon_0)i$ (mica), σ_2 =10^{-13}S /m (glass fibers), σ_3 =10^{-15}S /m (mica) (υ_2=0.0784 and f=10^3Hz)

Sample	Simulation	Analytic calculation		Experimental data
	$\widehat{\varepsilon_{eff}}$	$\widehat{\varepsilon_{eff}}$ (Eq. 2)	$\widehat{\varepsilon_{eff}}$ (Eq. 13)	$\widehat{\varepsilon_{eff}}$
PETGF15	3.327-0.018i	----	3.33-0.019i	3.32-0.02i
PETM15	3.438-0.018i	3.41-0.018i	-----	3.43-0.02i

In order to study the effect of both radius (R) and length (L) of inclusion on the field reinforcement and on the effective dielectric permittivity of some PET polymer composites, the ratio R/L was varied from 1000/1 to 1/1000. It should be noted that the same volume fraction (υ_2=0.0784) was used in every case. After the numerical simulations, the resulting data set is summarized in Table 6.3.

.

Tableau 6.3 Numerical simulation results

$\widehat{\varepsilon_1}$ =3.2-0.02i (matrix), $\widehat{\varepsilon_2}$ =5.1- $(\sigma_2/(\omega\varepsilon_0)i$ (glass fibers), σ_2 =10^{-13}S /m (glass fibers), υ_1=0.9216 and υ_2 =0.00784 , f=10^3 Hz		
Ratio R/L	$E_{max}/\langle E\rangle$	$\widehat{\varepsilon_{eff}}$
1000/1	1.17	3.361-0.018i
100/1	1.10	3.361-0.018i
10/1	1.16	3.361-0.017i
1/1	1.16	3.361-0.018i
1/10	1.28	3.361-0.018i
1/100	1.25	3.354-0.018i
1/1000	1.09	3.355-0.018i

Both the field reinforcement at the boundary polymer/particle and the effective complex permittivity are found to be related to the inclusion length more than its radius for the same concentration. Indeed, the electric field reinforcement ($E_{max}/\langle E\rangle$) decreases when the inclusion length is much higher compared to the diameter of the inclusion. Moreover, the effective complex dielectric permittivity seems to be dependent of the inclusion length mostly when the length exceeds 10 µm.

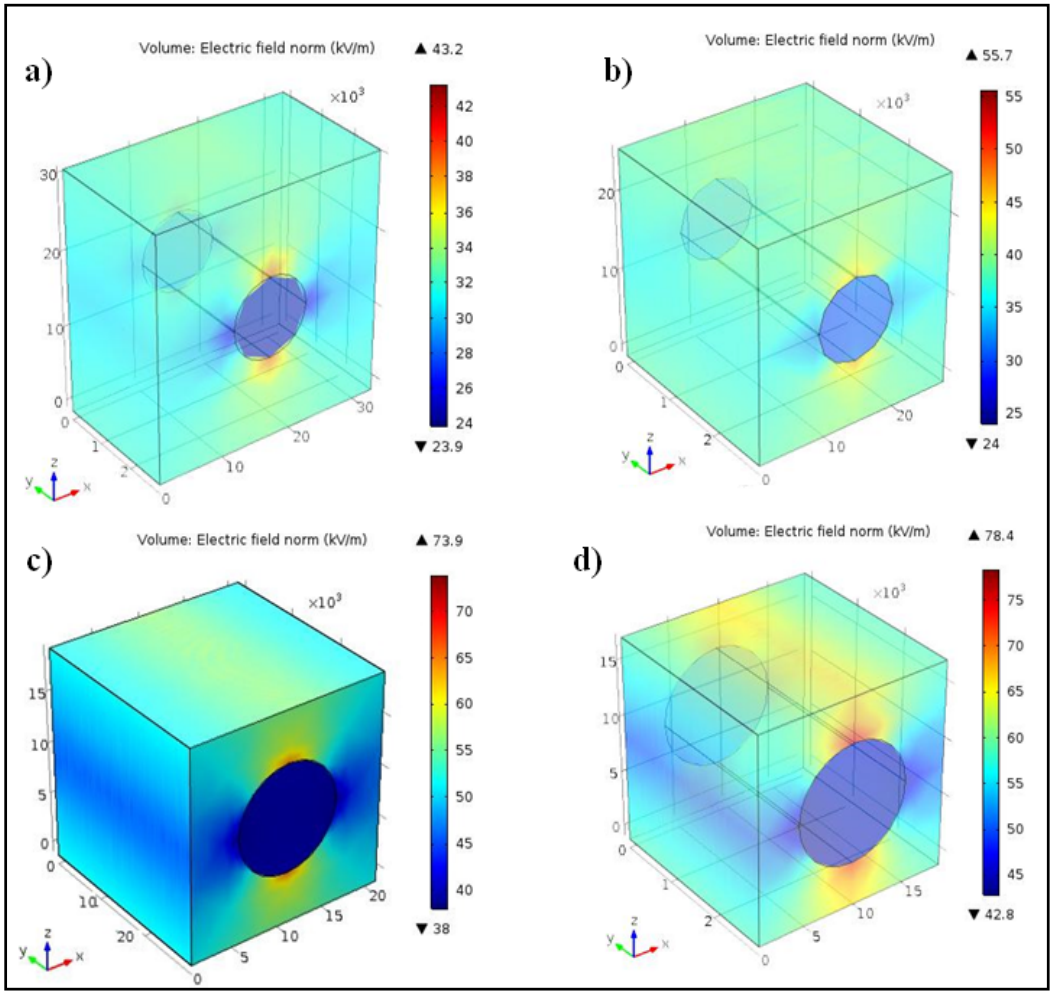

Figure 6.4 Volume fraction dependence on the electric field distribution for a biphasic composite with a) 15wt%, b) 20wt%, c) 30wt% and 35wt%

In order to check the volume fraction dependence on the effective complex dielectric permittivity of the glass fibers composite with the glass fibers oriented perpendicular to the electrical field, FEM simulation for four composites with different volume fractions $\upsilon_2$were

used (0.00784 , 0.1076, 0.1713 and 0.2061 respectively). The effect of the volume fraction on the electric field reinforcement was also computed. The resulting data set obtained from the FEM simulation is listed in Table 6.4.

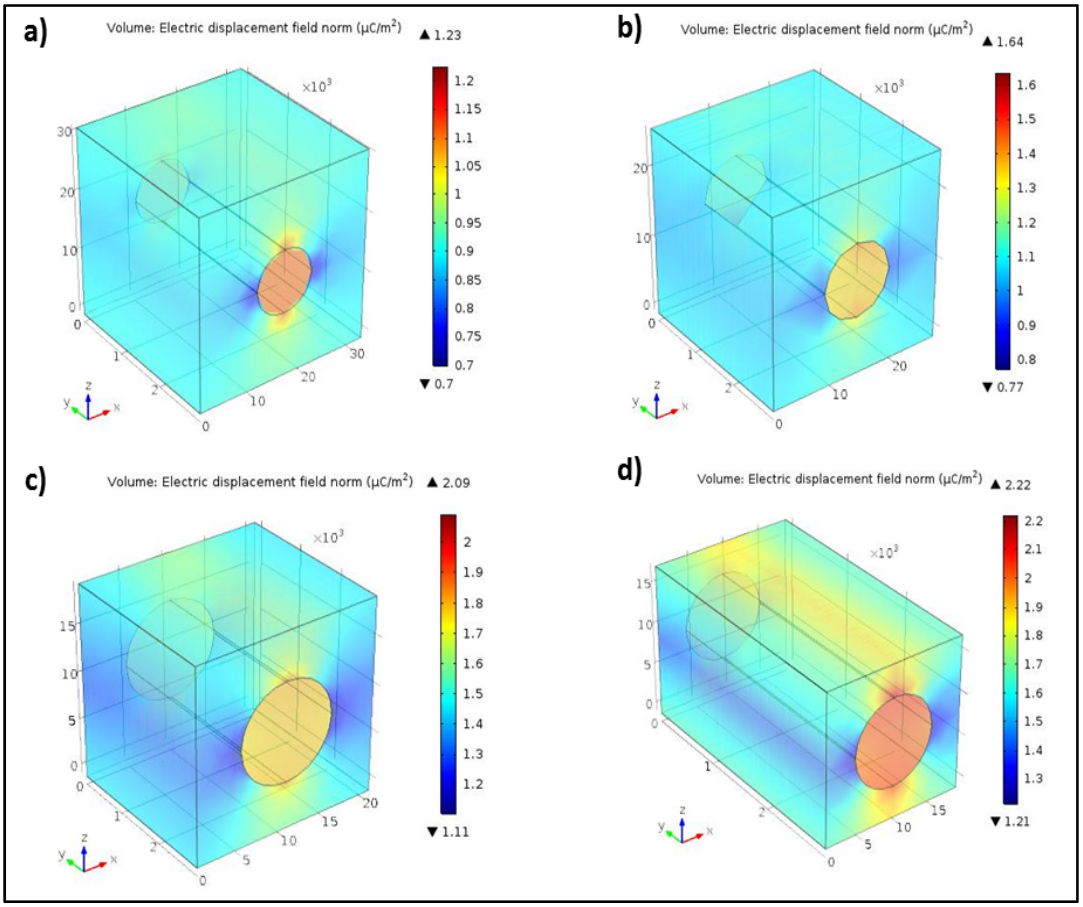

Figure 6.5 Volume fraction dependence on the dielectric displacement distribution for a biphasic composite with a) 15wt%, b) 20wt%, c) 30wt% and 35wt%

The volume plots of the electric field (kV/m) and the displacement (μC/m^2) distribution showing the volume fraction impact are illustrated in Fig. 4 and 5. As expected, an enhancement in the electric field was observed at the particle/polymer interface. Results obtained using both equations13and 14were found to be close to the experimental data. Moreover, the results obtained by the numerical calculations were found to also be in good agreement with the experimental data, especially when the amount of inclusions is higher than 15wt%.

Tableau 6.4 Volume fraction dependence on the effective complex permittivity for different PET composites filled with 15wt%, 20wt%, 30wt% and 35wt% of glass fibers

$\widehat{\varepsilon_1}$ =3.2-0.02i (matrix), $\widehat{\varepsilon_2}$ =5.1- $(\sigma_2/(\omega\varepsilon_0)i$ (glass fibers), $\widehat{\varepsilon_3}$ =6.0- $(\sigma_3/(\omega\varepsilon_0)i$ (mica); σ_2 =10^{-13}S /m (glass fibers), σ_3 =10^{-15}S /m (mica), f=10^3 Hz

Sample	Simulation	Analytic calculation (Eq. 13)	Experimental data
PETGF15	3.327-0.018i	3.33-0.019i	3.32-0.02i
PETGF20	3.378-0.018i	3.37-0.018i	3.36-0.02i
PETGF30	3.591-0.015i	3.48-0.017i	3.58-0.01i
PETGF35	3.692-0.014i	3.54-0.017i	3.68-0.01i

In this section, different formulas and analytical equations were used to calculate the effective complex dielectric permittivity of some polymer composites. The resulting data set obtained is listed in Table 6.5.

Tableau 6.5 Calculation of the $\widehat{\varepsilon_{eff}}$ using different analytical models

Sample	**Analytical calculation $\widehat{\varepsilon_1}$ =3.2-0.02i (matrix), $\widehat{\varepsilon_2}$ =5.1- $(\sigma_2/(\omega\varepsilon_0)i$ (glass fibers), $\widehat{\varepsilon_3}$ =6.0- $(\sigma_3/(\omega\varepsilon_0)i$ (mica); σ_2 =10^{-13}S /m (glass fibers), σ_3 =10^{-15}S /m (mica), f=10^3 Hz**					
	Lechtneker	**Looyenga**	**Wiener (eq. 2)**	**Wiener (eq. 3)**	**Rayleigh**	**Eq. 13**
PTGF15	3.33-0.019i	3.34-0.018i	3.30-0.019i	3.36-0.018i	3.34-0.019i	3.33-0.019i
PTGF20	3.38-0.018i	3.39-0.018i	3.34-0.019i	3.42-0.017	3.39-0.018i	3.37-0.018i
PTGF30	3.49-0.017i	3.51-0.017i	3.44-0.018i	3.55-0.016i	3.50-0.017i	3.48-0.017i
PTGF35	3.55-0.017i	3.57-0.016i	3.49-0.018i	3.62-0.015i	3.57-0.017i	3.54-0.017i
PTM15	3.35-0.019i	3.37-0.019i	3.31-0.019i	3.41-0.018i	3.35-0.019i	3.35-0.019i

The majority of results obtained using different analytical calculation models are either identical or close. Equations (6.13) and (6.14) give near equal values to the experimental data as compared to the other analytic calculation models. Simulation results were in very good agreement with experimental data. In addition, Wiener law (eq.6. 3) seems to be the most suitable formula for the calculation of the effective permittivity in case of a perfectly oriented cylindrical inclusions with their main axis parallel to the applied field and R>>>L (such as mica platelets).

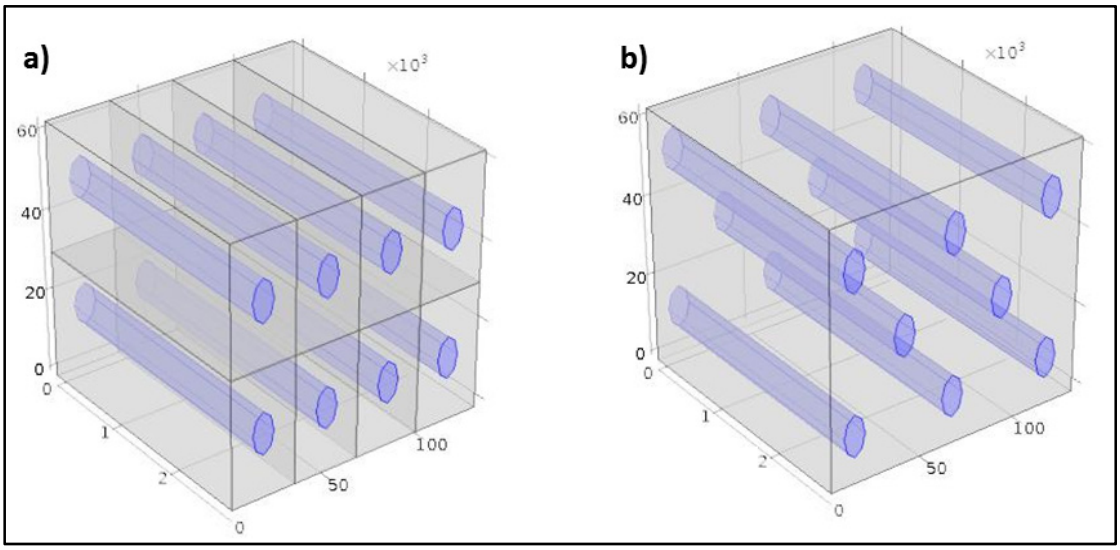

Figure 6.6 Different 3D- geometries: a) uniform type 1and b) uniform type 2

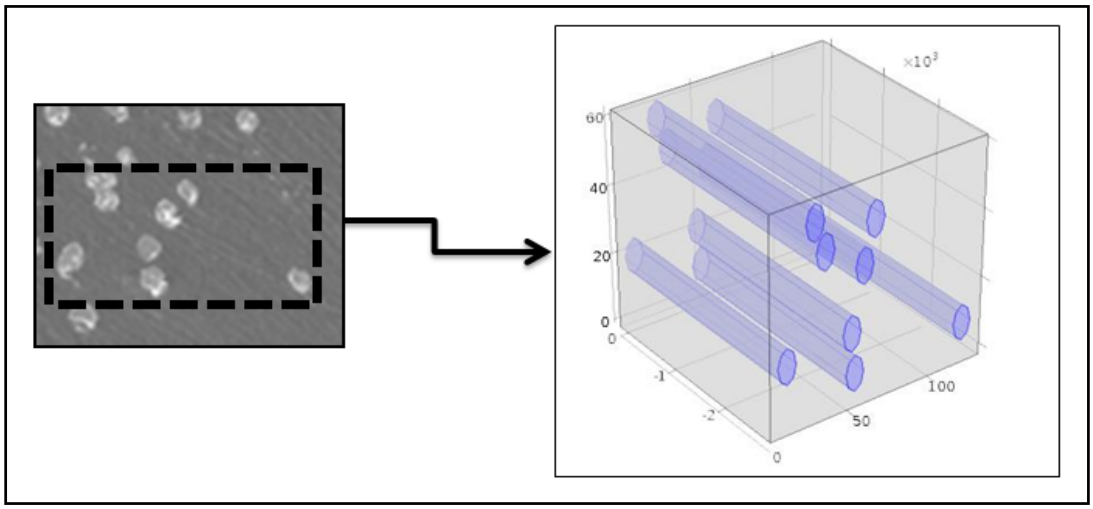

Figure 6.7 Geometry of a random dispersion based on the SEM image

As observed by the SEM image obtained for a biphasic composite, the dispersion is not uniform and can be classified as a random dispersion. Consequently, results obtained by a single cell have to be extended for a geometry more representative of the real microstructure. A new geometry with 8 unit cells was created in order to study the effect of the dispersion of the inclusions on the electrical field reinforcement and the effective complex dielectric permittivity of the PET composites. Two different uniform geometries with the same volume fraction were created, as illustrated in Fig. 6.6. A new geometry based on a SEM image was also added to the simulated a random dispersion of perfectly oriented fibres, as illustrated by Fig.6.7. The resulting data set obtained from the numerical simulations, is listed in Table 6.6.

.

Tableau 6.6 Numerical simulation results

$\widehat{\varepsilon_1}$ =3.2-0.02i (matrix), $\widehat{\varepsilon_2}$ =5.1- $(\sigma_2/(\omega\varepsilon_0)i$ (glass fibers) with σ_2 =10^{-13}S /m (glass fibers), υ_2 =0.00784, f=10^3 Hz		
Dispersion	$\frac{E_{max}}{\langle E \rangle}$	$\widehat{\varepsilon_{eff}}$
Ordered type1	1.44	3.361-0.018i
Ordered type2	2.27	3.344-0.018i
Random (real)	1.59	3.319-0.018i

In this part of simulation, we have treated three cases of statistically inhomogeneous systems; two ordered dispersion types and a random dispersion. In all cases, the particle volume fraction υ_2 was 0.0784. Fig.6.8 illustrates the contour plots of the electric field obtained by the numerical simulation. As expected, the electric field is attenuated inside the inclusions and enhanced at the interface inside the polymeric matrix. An enhancement in the electrical field at the interfaces was found in case of the randomly dispersed composite.

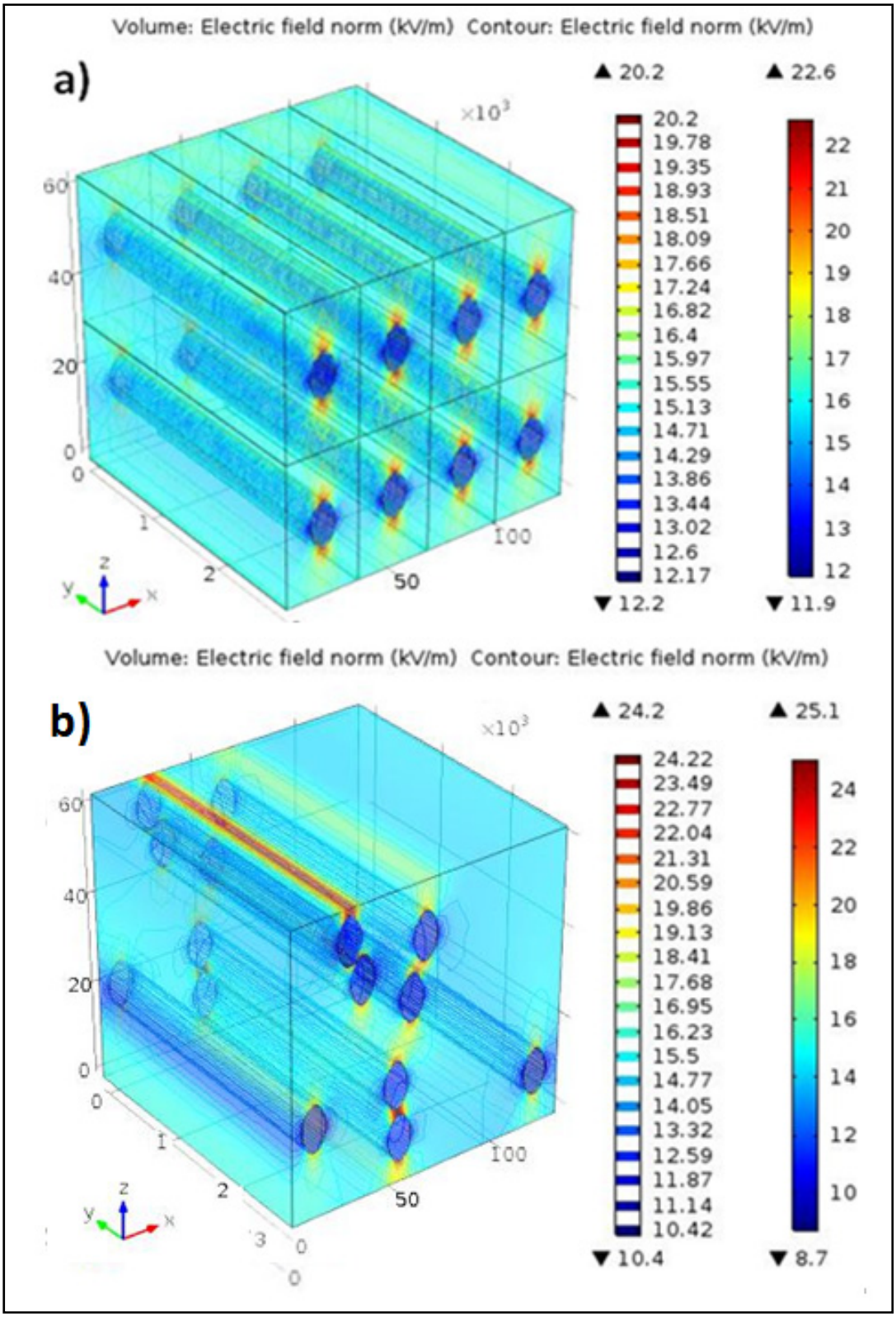

Figure 6.8 Contour plots of the electric field simulation in the case of the a) ordered and b) real dispersion

The dispersion type was found to influence the value of the calculated effective complex permittivity of the biphasic composite. For the same concentration, the ordered dispersion geometries give higher values as compared with the real geometry. Moreover, the effective complex permittivity obtained from the numerical simulation of the random dispersion based on the SEM image matches very well the experimental data. It should be noted that both the field reinforcement at the boundary polymer/particle and the effective complex permittivity are found to be related to the dispersion type of the inclusions. It was found that the field reinforcement is enhanced when the inclusions are closer.

The last part of our numerical simulation was to predict the effective complex dielectric permittivity of the PET filled by both glass fibers and mica. Thus, a new numerical geometry was created, as illustrated by Fig.6.9.The position of both inclusions can be clearly seen and the particle volume fractions are about 0.1694 for the glass fibers and 0.0894 for the mica. The volume of the unit cell was calculated to match the 15 wt % of glass fibers and the 25 wt % of mica that were added to the manufactured PET composites.

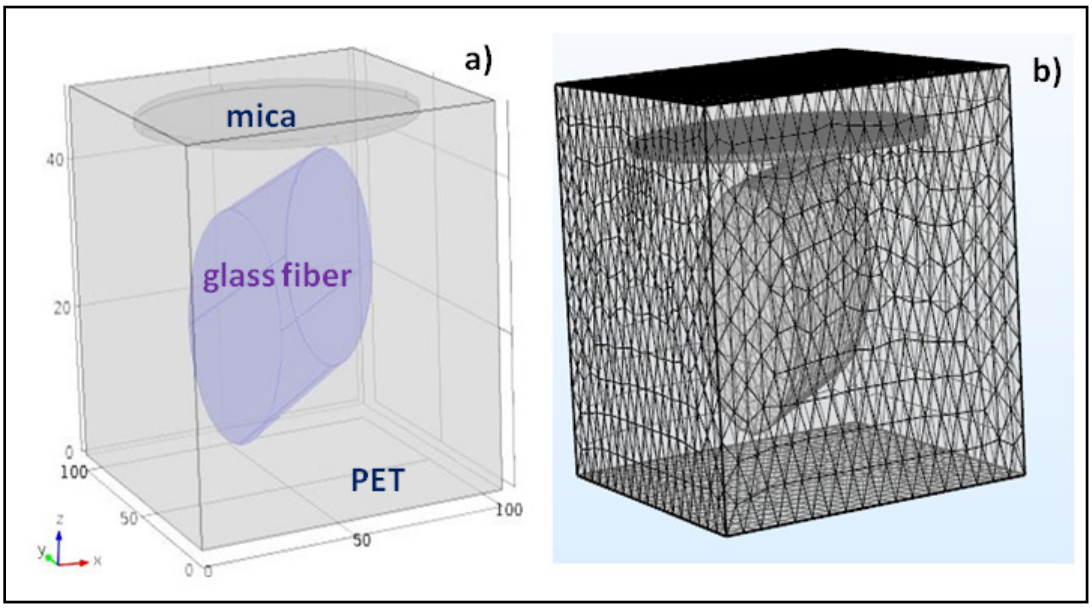

Figure 6.9 Scanning illustration of a) the concept and b) the numerical model to study the impact of the presence of both glass fibers and mica platelets on the effective complex permittivity of the PET polymer

Fig. 6.10 shows the electrical field and the dielectric displacement distribution when both inclusions are present. The presence of both inclusions leads to an increase in the effective complex permittivity. It increases from 3.43-0.018i for the PETM15 composite to 3.701-0.014i when 25wt% of glass fiber was also added to the composite. This value matches the experimental data.

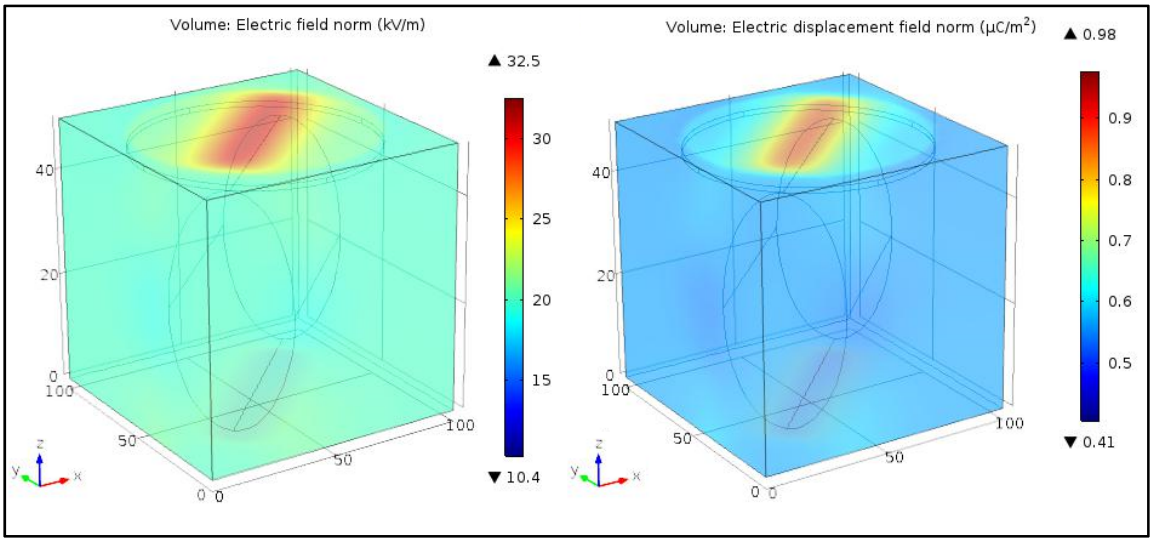

Figure 6.10 Electric field and displacement distribution in case of a multiphase composite

6.5 Conclusion

The variation of the electrical field enhancement and the effective complex dielectric permittivity of PET composites was related to several different parameters. The inclusion type and the volume fraction were found to be a significant factor. Moreover, the field reinforcement at the polymer/filler boundary and the effective complex permittivity were found to be related to the inclusion axis ratio for the same concentration. Consequently, the effective complex permittivity of the composites is related to both the inclusions properties and geometry. The dispersion is also a pertinent parameter to be considered in the design of the composite materials with specific dielectric properties.

The analytical models based on the mean field approximation were found to give a good estimate when computing the effective complex dielectric permittivity of multiphase composites. However, simulation results gave better agreements with our experimental data. Consequently, our numerical model can be used to optimise the dielectric properties of multiphasic composites of with complex geometries.

ACKNOWLEDGMENT

Financial help from the National Sciences and Engineering Research Council of Canada (NSERC) is acknowledged. The authors would like to express their deepest gratitude to Patrick Lachance and Doru Davinscu from the Lavergne Group Company that kindly supplied materials used for this investigation.

CONFLICT OF INTERESTS

The authors declare that there is no conflict of interests regarding the publication of this paper.

CONCLUSION GÉNÉRALE

Cette étude avait pour objectif d'évaluer la fiabilité de certains composites à base de matrice thermoplastique recyclée destinée à des applications impliquant certaines propriétés diélectriques comme le support mécanique des systèmes d'allumage dans les moteurs à combustion interne. Notre travail nous a permis de tirer diverses conclusions concernant le comportement diélectrique et thermique du polyéthylène téréphtalate recyclé renforcé de charges inorganiques, notamment au niveau de la dégradation que ces composites peuvent subir lorsqu'ils sont assujettis à certaines contraintes électriques, thermiques ou combinées. Les constatations suivantes doivent être soulignées :

- La fiabilité de certaines sources du polyéthylène téréphtalate recyclé et son endurance diélectrique et thermique a été confirmé grâce aux différents tests élaborés. Le polyéthylène Naphthalate (PEN) qui est un polymère ayant une rigidité diélectrique supérieure à celle du PET, tend à avoir un comportement similaire à celui du PET recyclé lorsqu'il est thermiquement vieilli à des températures supérieures ou égales à 170 ° C, limitant ainsi sa température de fonctionnement.
- Le changement causé par le vieillissement thermique sur certaines propriétés est en relation avec le comportement diélectrique des matériaux polymères tel que le polyéthylène téréphtalate (PET) recyclé et le polyéthylène Naphthalate (PEN). On peut citer le degré de cristallinité qui peut affecter la permittivité réelle du PET recyclé. Cette grandeur diélectrique diminue remarquablement avec l'augmentation de la température du vieillissement. De plus, une diminution significative de la rigidité diélectrique a été constatée après le vieillissement thermique du PET recyclé et de ses composites. La morphologie en est un autre exemple. Ces matériaux subissent une dégradation significative notamment pour des températures de vieillissement supérieures à 170 ^{o}C. En effet, l'endurance diélectrique du PET recyclé diminue avec la dégradation résultant du vieillissement thermique.
- Les résultats obtenus ont montré que le PET recyclé présente un comportement diélectrique similaire comparativement au PET industriel. Donc, l'endurance au

vieillissement électrothermique n’est pas affectée par l’utilisation d’une résine recyclée.

- La présence de certains renforts inorganiques augmente la cristallinité du PET recyclé et contribue également à la modification de la structure moléculaire des polymères PET et PEN. En effet, un changement remarquable de l'intensité de certaines bandes a été observé grâce aux mesures FTIR. Cela indique qu'un réarrangement de la chaîne moléculaire s'est produit lorsque le taux de cristallinité a été augmenté.
- Les fibres de verre améliorent la résistance au vieillissement thermique et les flocons de mica assurent l’endurance aux contraintes électriques. La présence des deux renforts inorganiques contribue grandement à la résistance au différent processus de vieillissement électrique, thermique et électrothermique. En outre, l'augmentation de la teneur en fibres de verre entraîne un changement significatif au niveau du taux de cristallinité ainsi qu’aux propriétés diélectriques du PET recyclé (principalement la permittivité réelle).
- L’ajout des flocons du mica au PET recyclé résulte en un pic de relaxation interfaciale. En plus de la conductivité de ces renforts, leur forme et hydrophilie peuvent affecter l'amplitude et la position fréquentielle de ce processus de relaxation interfaciale. En outre, la présence du mica aboutit à une certaine adhérence et compatibilité entre la résine du PET recyclé et les renforts.
- La forme, le type et la grosseur des renforts inorganiques comme les fibres de verre et le mica sont des facteurs pouvant affecter l’endurance diélectrique de certains polymères, tel que le PET recyclé, soit au niveau de la rigidité diélectrique ou au niveau des pertes diélectriques.
- Les plastifiants permettent d’améliorer l’aptitude du traitement ainsi que l’adhésion entre les renforts inorganiques et la matrice polymérique du PET recyclé et par conséquent augmentent la résistance au vieillissement électrothermique.
- La simulation par élément finis (MEF) nous a donné l’occasion de comprendre le comportement diélectrique au niveau de la permittivité effective complexe de certains composites à base de PET lorsque des renforts inorganiques comme le mica et les fibres de verre sont introduits. Le modèle numérique pour un composite biphasique a été

validé par les données expérimentales ainsi que par des calculs analytiques. Ainsi, notre modèle pourra servir à prédire la permittivité effective complexe d'un composite multiphasique ayant une microstructure plus complexe.

Bref, ce travail a révélé une bonne corrélation entre les différentes propriétés diélectriques, thermiques et structurales du PET recyclé notamment lorsque des renforts inorganiques comme le mica et les fibres de verre sont incorporés. Ces renforts contribuent grandement à l'endurance du polyéthylène téréphtalate recyclé lorsqu'il est assujetti aux contraintes électriques, thermiques ou combinées.

RECOMMANDATIONS

Les fibres de verre sont des renforts inorganiques servant dans la majorité des cas à augmenter la tenue mécanique d'un polymère. Ils peuvent être incorporés également pour améliorer d'autres propriétés comme la conductivité thermique des polymères. Ces renforts inorganiques ont également un champ de claquage inférieur par rapport aux polymères tels que le PET ou le PEN. Selon les résultats du chapitre 5, l'ajout des fibres de verre au PET et au PEN conduit à une baisse du champ de claquage du PET. Par contre, une amélioration de la rigidité diélectrique du PEN a été constatée. Le résultat a été expliqué par le bon fini de surface, l'adhérence et la bonne compatibilité entre le PEN et les fibres. Pour compléter cette étude, il serait très intéressant d'effectuer des mesures rhéologiques afin de vérifier l'effet des fibres de verre sur la variation de la viscosité dans le domaine fréquentiel. Ces mesures vont permettre de valider la bonne comptabilité et l'adhésion à l'interface entre les particules et la matrice et ainsi d'évaluer la dispersion des renforts.

Bien que plusieurs modèles analytiques servant à la prédiction des propriétés diélectriques comme la permittivité complexe effective d'un matériau hétérogène existent dans la littérature, la possibilité d'utiliser des modèles numériques est intéressante et mérite d'être développée. Les modèles analytiques ne tiennent pas en compte certains paramètres comme la dispersion et l'interaction entre les particules dans un composite hétérogène multiphasique. Les modèles numériques permettent de varier certains paramètres comme la dispersion des particules afin de vérifier leurs effets sur des propriétés effectives. Il serait donc intéressant de développer un modèle numérique basé sur la dispersion réelle qui permet de comparer la variation de la partie réelle et imaginaire de la permittivité effective dans le domaine fréquentiel avec les données expérimentales surtout dans le cas où les deux types de renforts (fibres de verre et mica) sont présents dans le composite.

ANNEXE I

PUBLICATIONS

ARTICLES DE JOURNAL:

1. Mebarki, F., & David, E. 2015. « *Characterization of the dielectric endurance of reinforced recycled PET using electro-thermal aging test* ». **IEEE Transactions on Dielectrics and Electrical Insulation**, vol. 22, nº 6. p. 3513-3520.
2. Mebarki, F., & David, E. 2016. « *Dielectric Characterization of Thermally-aged Recycled Polyethylene Terephthalate and Polyethylene Naphthalate Reinforced with Inorganic Fillers* ». Accepted, **Polymer Engineering & Science.** Article ID : PES-16-0801.
3. Mebarki, F., & David, E. 2017. « *Dielectric and Structural Properties of Recycled PET and PEN based Composites* ». Submitted, **Transactions on Electrical and Electronic Materials**. Article ID : 17-0026.
4. Mebarki, F., & David, E. 2017. « *Numerical Modeling of the Effective Complex Permittivity of PET-based Composite Materials*». Submitted, **Journal of Polymer Research.** Article ID JPOL-D-17-00602:

ARTICLES DE CONFÉRENCES:

1. Mebarki, Fouzia et David, Éric. 2012. « *Corona resistance and dielectric strength of recycled PET-based composites* ». In 2012 IEEE Conference on Electrical Insulation and Dielectric Phenomena (CEIDP) (Montreal, QC, Canada, Oct. 14-17, 2012), p. 407-411. Piscataway, NJ : Institute of Electrical and Electronics Engineers Inc.
2. Mebarki, F. et David, Eric. 2014. «*Aging under thermal and electrical stresses of recycled PET based composite materials*». In 2014 IEEE Conference on Electrical Insulation and Dielectric Phenomena (CEIDP) (Des Moines, IA, USA, Oct. 19-22, 2014), p. 518-521. Piscataway, N. J., USA : IEEE.

3. Mebarki, F., & David, É. (2015). «*Corona Discharges Aging of Recycled PET Filled with Inorganic Reinforcements*». In IEEE Conference on Electrical Insulation and Dielectric Phenomena (CEIDP 2015) (Ann Arbor, MI, USA, Oct. 18-21, 2015), p. 796-799. Institute of Electrical and Electronics Engineers Inc

LISTE DE RÉFÉRENCES BIBLIOGRAPHIQUES

164, I. S. (1991). IEEE Guide for Multifactor Stress Functional Testing of Electrical Insulation Systems *IEEE*

Abdi, C., Khemici, M., & Doulache, N. (2015). Crystallinity effect on the structural relaxation of polyethylene naphtalate (PEN) by TSDC and DSC experiments. *IEEE Transactions on Dielectrics and Electrical Insulation, 22*(3), 1406-1414.

Adhikari, D., Hepburn, D., & Stewart, B. (2011). *Comparison of PD characteristics and degradation in PET insulation with vented and unvented voids.* Paper presented at the Electrical Insulation and Dielectric Phenomena (CEIDP), 2011 Annual Report Conference on.

Adhikary, K. B., Pang, S., & Staiger, M. P. (2008). Dimensional stability and mechanical behaviour of wood–plastic composites based on recycled and virgin high-density polyethylene (HDPE). *Composites Part B: Engineering, 39*(5), 807-815.

Akram, M., Javed, A., & Rizvi, T. Z. (2005). Dielectric properties of industrial polymer composite materials. *Turkish Journal of Physics, 29*(6), 355-362.

Alves, N., Mano, J., & Ribelles, J. G. (2002). Molecular mobility in polymers studied with thermally stimulated recovery. II. Study of the glass transition of a semicrystalline PET and comparison with DSC and DMA results. *Polymer, 43*(13), 3627-3633.

ASTMD149. (2004). 149 Standard Test Method for Dielectric Breakdown Voltage and Dielectric Strength of Solid Electrical Insulating Materials at Commercial Power Frequencies. *Annual Book of ASTM Standards, American Society for Testing and Materials*.

ASTME1356-08. (2014). Standard Test Method for Assignment of the Glass Transition Temperatures by Differential Scanning Calorimetry.

Avenas, P. (1978). LE RÔLE DE LA CRISTALLINITÉ DANS LA MISE EN FORME DES POLYMÈRES. *Le Journal de Physique Colloques, 39*(C2), C2-37-C32-47.

Awaja, F., & Pavel, D. (2005). Recycling of PET. *European Polymer Journal, 41*(7), 1453-1477.

Badia, J., Vilaplana, F., Karlsson, S., & Ribes-Greus, A. (2009). Thermal analysis as a quality tool for assessing the influence of thermo-mechanical degradation on recycled poly (ethylene terephthalate). *Polymer Testing, 28*(2), 169-175.

Bahadoorsingh, S., & Rowland, S. (2008). A Framework Linking Knowledge of Insulation Aging to Asset Management-[Feature Article]. *IEEE Electrical Insulation Magazine, 3*(24), 38-46.

Banhegyi, G. (1986). Comparison of electrical mixture rules for composites. *Colloid and polymer science, 264*(12), 1030-1050.

Bansal, N. P., & Doremus, R. H. (2013). *Handbook of glass properties*: Elsevier.

Bárány, T., Földes, E., & Czigány, T. (2007). Effect of thermal and hygrothermal aging on the plane stress fracture toughness of poly (ethylene terephthalate) sheets. *Express Polym Lett, 1*(3), 180-187.

Beauguitte, D., Yahyaoui, H., Notingher, P., Agnel, S., & Kieffel, Y. (2012). *Dielectric properties of polyethylene terephtalate submitted to long-term thermo-electrical AC stress.* Paper presented at the Electrical Insulation and Dielectric Phenomena (CEIDP), 2012 Annual Report Conference on.

Bedia, E. L., Murakami, S., Kitade, T., & Kohjiya, S. (2001). Structural development and mechanical properties of polyethylene naphthalate/polyethylene terephthalate blends during uniaxial drawing. *Polymer, 42*(17), 7299-7305.

Bellomo, J., & Lebey, T. (1996). On some dielectric properties of PEN. *Journal of Physics D: Applied Physics, 29*(7), 2052.

Bellomo, J., Lebey, T., Oraison, J., & Peltier, F. (1995). *Comparative Study of the influence of Thermal Ageing on PET and PEN Polymers.* Paper presented at the Conduction and Breakdown in Solid Dielectrics, 1995. ICSD'95., Proceedings of the 1995 IEEE 5th International Conference on.

Bentchikou, M. (2008). Contribution à l'étude et à l'élaboration de matériaux composites pour l'isolation thermique: Cas de béton de fibres de papiers recyclés.

Beran, M. (1965). Statistical continuum theories. *Transactions of the Society of Rheology, 9*(1), 339-355.

Bergman, D. J. (1978). The dielectric constant of a composite material—a problem in classical physics. *Physics Reports, 43*(9), 377-407.

Bravard, S. P., & Boyd, R. H. (2003). Dielectric relaxation in amorphous poly (ethylene terephthalate) and poly (ethylene 2, 6-naphthalene dicarboxylate) and their copolymers. *Macromolecules, 36*(3), 741-748.

Brosseau, C., & Beroual, A. (2003). Computational electromagnetics and the rational design of new dielectric heterostructures. *Progress in Materials Science, 48*(5), 373-456.

Budrugeac, P., & Segal, E. (1998). Changes in the mechanical properties and thermal behaviour of LDPE in response to accelerated thermal aging. *Journal of thermal analysis and calorimetry, 53*(3), 801–808. doi: 10.1023/A:1010186610454

Calderas, F., Sanchez-Solis, A., Maciel, A., & Manero, O. (2009). *The Transient Flow of the PET-PEN-Montmorillonite Clay Nanocomposite.* Paper presented at the Macromolecular symposia.

Castañeda, P. P. (1991). The effective mechanical properties of nonlinear isotropic composites. *Journal of the Mechanics and Physics of Solids, 39*(1), 45-71.

Chen, H.-m., Du, X.-c., Yang, A.-s., Yang, J.-h., Huang, T., Zhang, N., . . . Zhang, C.-l. (2014). Effect of graphene oxides on thermal degradation and crystallization behavior of poly (l-lactide). *RSC Advances, 4*(7), 3443-3456.

Chiellini, E., Corti, A., D'antone, S., & Baciu, R. (2006). Oxo-biodegradable carbon backbone polymers–oxidative degradation of polyethylene under accelerated test conditions. *Polymer Degradation and Stability, 91*(11), 2739-2747.

Chow, T. (1980). The effect of particle shape on the mechanical properties of filled polymers. *Journal of Materials Science, 15*(8), 1873-1888.

Collette, W. N., Schmidt, S. L., & Krishnakumar, S. M. (1999). Multilayer preform and container with polyethylene naphthalate (PEN), and method of forming same: Google Patents.

Corradini, E., Ito, E. N., Marconcini, J. M., Rios, C. T., Agnelli, J. A., & Mattoso, L. H. (2009). Interfacial behavior of composites of recycled poly (ethyelene terephthalate) and sugarcane bagasse fiber. *Polymer Testing, 28*(2), 183-187.

Couderc, H., David, E., Corlu, Y., Fréchette, M., & Savoie, S. (2011). *Dielectric breakdown of amorphous and semicrystalline polymers.* Paper presented at the Electrical Insulation Conference (EIC), 2011.

Couderc, H., David, E., Frechette, M., & Medjdoub, A. (2013). *Influence of water on PE—SiO 2 nanocomposites dielectric properties.* Paper presented at the Electrical Insulation and Dielectric Phenomena (CEIDP), 2013 IEEE Conference on.

de la Fuente, J. L. (2009). An analysis of the thermal aging behaviour in high-performance energetic composites through the glass transition temperature. *Polymer Degradation and Stability, 94*(4), 664-669.

Debnath, S., De, P. P., & Khastgir, D. (1988). Ambient electrical properties of mica-styrene-butadiene rubber composites. *Rubber chemistry and technology, 61*(4), 555-567.

Degallaix, S. (2007). *Caractérisation expérimentale des matériaux: Propriétés physiques, thermiques et mécaniques* (Vol. 1): PPUR presses polytechniques.

Dissado, L., Mazzanti, G., & Montanari, G. (1997). The role of trapped space charges in the electrical aging of insulating materials. *IEEE Transactions on Dielectrics and Electrical Insulation, 4*(5), 496-506.

Dissado, L. A., & Fothergill, J. C. (1992). *Electrical degradation and breakdown in polymers* (Vol. 9): IET.

Duguet, E., Pariente, J.-L., & Conort, P. (2005). Aspects physico-chimiques des biomatériaux utilisés en Urologie. *Progrès en Urologie, 15*(5), 865-886.

Emmanuel WIRTH, F. G., Christophe MATHONAT (2014). Thermogravimétrie *Technique de l'ingénieur*.

Eriksson, P. A., Boydell, P., Eriksson, K., Månson, J. A., & Albertsson, A. C. (1997). Effect of thermal-oxidative aging on mechanical, chemical, and thermal properties of recycled polyamide 66. *Journal of applied polymer science, 65*(8), 1619-1630.

Etcheverry, M., & Barbosa, S. E. (2012). Glass fiber reinforced polypropylene mechanical properties enhancement by adhesion improvement. *Materials, 5*(6), 1084-1113.

F. Mebarki , E. D. (2016). *Dielectric Characterization of Thermally-aged Recycled PET and PEN Reinforced with Inorganic Fillers*. SPE.

Fang, P., Wegener, M., Wirges, W., Gerhard, R., & Zirkel, L. (2007). Cellular polyethylene-naphthalate ferroelectrets: Foaming in supercritical carbon dioxide, structural and electrical preparation, and resulting piezoelectricity. *Applied physics letters, 90*(19), 192908.

Farahani, M., Gockenbach, E., Borsi, H., Schafer, K., & Kaufhold, M. (2010). Behavior of machine insulation systems subjected to accelerated thermal aging test. *IEEE Transactions on Dielectrics and Electrical Insulation, 17*(5), 1364-1372.

Fermeglia, M., Cosoli, P., Ferrone, M., Piccarolo, S., Mensitieri, G., & Pricl, S. (2006). PET/PEN blends of industrial interest as barrier materials. Part I. Many-scale molecular modeling of PET/PEN blends. *Polymer, 47*(16), 5979-5989.

Fox, B., Moad, G., Van Diepen, G., Willing, I., & Cook, W. D. (1997). Characterization of poly (ethylene terephthalate) and poly (ethylene terephthalate) blends. *Polymer, 38*(12), 3035-3043.

Fregoso-Infante, A. G., Vega-Rangel, R., & Figueroa-Gomez-Crespo, M. (2011). Chemical process for recycling polyethylene terephthalate (PET) waste: Google Patents.

Fu, S.-Y., Lauke, B., Mäder, E., Yue, C.-Y., & Hu, X. (2000). Tensile properties of short-glass-fiber-and short-carbon-fiber-reinforced polypropylene composites. *Composites Part A: Applied Science and Manufacturing, 31*(10), 1117-1125.

Gan, D., Cao, W., Song, C., & Wang, Z. (2001). Mechanical properties and morphologies of poly (ether ketone ketone)/glass fibers/mica ternary composites. *Materials Letters, 51*(2), 120-124.

Ghadami, A., Ehsani, M., & Khonakdar, H. A. (2015). A comprehensive study on morphological and rheological behavior of poly (ethylene terephthalate) and poly (ethylene-2, 6-naphthalene) nanocomposite blends in presence of graphene. *Journal of Vinyl and Additive Technology*.

Golden, K., & Papanicolaou, G. (1983). Bounds for effective parameters of heterogeneous media by analytic continuation. *Communications in Mathematical Physics, 90*(4), 473-491.

Gonzalez, E., Barankin, M., Guschl, P., & Hicks, R. (2008). Remote atmospheric-pressure plasma activation of the surfaces of polyethylene terephthalate and polyethylene naphthalate. *Langmuir, 24*(21), 12636-12643.

Hamasha, M. M., Dhakal, T., Alzoubi, K., Albahri, S., Qasaimeh, A., Lu, S., & Westgate, C. R. (2012). Stability of ITO thin film on flexible substrate under thermal aging and thermal cycling conditions. *Journal of Display Technology, 8*(7), 385-390.

Haq, S. U., & Omranipour, R. (2011). *Accelerated life testing of high voltage stator coils with enhanced PET-mica insulation system.* Paper presented at the 2011 Electrical Insulation Conference (EIC).

Hassan, M. A. (2012). Physical and Thermal Properties Of Fiber(S-type)-Reinforced Composite Araldite Resin (GY 260) *Al-Qadisiya Journal For Engineering Sciences, 5*(4), 341-346.

Hermann, H. (2010). Effective dielectric and elastic properties of nanoporous low-k media. *Modelling and Simulation in Materials Science and Engineering, 18*(5), 055007.

Hong, T. P. (2005). *Caractérisation et modélisation du comportement diélectrique d'un matériau composite soumis à un vieillissement hydrothermique.*Université Joseph-Fourier-Grenoble I.

Jarukumjorn, K., & Suppakarn, N. (2009). Effect of glass fiber hybridization on properties of sisal fiber–polypropylene composites. *Composites Part B: Engineering, 40*(7), 623-627.

Jean GRENET, B. L. (2010). Analyse calorimétrique différentielle à balayage (DSC)

Technique de l'ingénieur.

Jylha, L., & Sihvola, A. H. (2005). Numerical modeling of disordered mixture using pseudorandom simulations. *IEEE transactions on geoscience and remote sensing, 43*(1), 59-64.

Kalaprasad, G., Joseph, K., & Thomas, S. (1997). Influence of short glass fiber addition on the mechanical properties of sisal reinforced low density polyethylene composites. *Journal of composite materials, 31*(5), 509-527.

Karkkainen, K. K., Sihvola, A. H., & Nikoskinen, K. I. (2000). Effective permittivity of mixtures: Numerical validation by the FDTD method. *IEEE transactions on geoscience and remote sensing, 38*(3), 1303-1308.

Kikuchi, K., Kang, Y.-S., Kawasaki, A., Nishida, S., & Ichida, A. (2004). Microstructural modeling and thermal property simulation of unidirectional composite. *Materials Transactions, 45*(2), 542-549.

Kremer, F., & Schönhals, A. (2012). *2 Broadband Dielectric Measurement Techniques (10–6 Hz to 1012 Hz)*: Springer.

Kyotani, M., Pudjiastuti, W., & Saeed, A. (1999). Rheological, thermal, and mechanical properties of poly (ethylene naphthalate)/poly (ethylene terephthalate) blends. *Journal of Macromolecular Science, Part B: Physics, 38*(3), 197-215.

Lan, T., & Pinnavaia, T. J. (1994). Clay-reinforced epoxy nanocomposites. *Chemistry of Materials, 6*(12), 2216-2219.

Laskarakis, A., Gravalidis, C., & Logothetidis, S. (2004). FTIR and Vis–FUV real time spectroscopic ellipsometry studies of polymer surface modifications during ion beam bombardment. *Nuclear Instruments and Methods in Physics Research Section B: Beam Interactions with Materials and Atoms, 216*, 131-136.

Laura, D., Keskkula, H., Barlow, J., & Paul, D. (2002). Effect of glass fiber surface chemistry on the mechanical properties of glass fiber reinforced, rubber-toughened nylon 6. *Polymer, 43*(17), 4673-4687.

Lawrence, E. N., & Robert, F. L. (1994). Mechanical properties of polymers and composites. *Marcel Dekker, New York*.

Lechat, C., Bunsell, A. R., Davies, P., & Piant, A. (2006). Mechanical behaviour of polyethylene terephthalate & polyethylene naphthalate fibres under cyclic loading. *Journal of Materials Science, 41*(6), 1745-1756.

Lee, S. M., Cho, D., Park, W. H., Lee, S. G., Han, S. O., & Drzal, L. T. (2005). Novel silk/poly (butylene succinate) biocomposites: the effect of short fibre content on their mechanical and thermal properties. *Composites Science and Technology, 65*(3), 647-657.

Lei, Y., Wu, Q., Yao, F., & Xu, Y. (2007). Preparation and properties of recycled HDPE/natural fiber composites. *Composites Part A: Applied Science and Manufacturing, 38*(7), 1664-1674.

Li, C., & Liu, X. (2007). Mechanical and thermal properties study of glass fiber reinforced polyarylene ether nitriles. *Materials Letters, 61*(11), 2239-2242.

Lillwitz, L. (2001). Production of dimethyl-2, 6-naphthalenedicarboxylate: precursor to polyethylene naphthalate. *Applied Catalysis A: General, 221*(1), 337-358.

Lu, X., & Hay, J. (2001). Isothermal crystallization kinetics and melting behaviour of poly (ethylene terephthalate). *Polymer, 42*(23), 9423-9431.

MacDonald, W. A. (2004). Engineered films for display technologies. *Journal of Materials Chemistry, 14*(1), 4-10.

MacDonald, W. A., Looney, M., MacKerron, D., Eveson, R., Adam, R., Hashimoto, K., & Rakos, K. (2007). Latest advances in substrates for flexible electronics. *Journal of the Society for Information Display, 15*(12), 1075-1083.

Mason, J. (1981). Assessing the resistance of polymers to electrical treeing. *IEE Proceedings A-Physical Science, Measurement and Instrumentation, Management and Education-Reviews, 128*(3), 193-201.

McCrum, N. G., Read, B. E., & Williams, G. (1967). Anelastic and dielectric effects in polymeric solids.

Mebarki, F. (2012). *Caractérisation des propriétés diélectriques de matériaux composites à base de polyéthylène téréphtalate recyclé.*École de technologie supérieure.

Mebarki, F., & David, E. (2015). Characterization of the dielectric endurance of reinforced recycled PET using electro-thermal aging test. *IEEE Transactions on Dielectrics and Electrical Insulation, 22*(6), 3513-3520.

Mebarki, F., & David, É. (2012). *Corona resistance and dielectric strength of recycled PET-based composites.* Paper presented at the Electrical Insulation and Dielectric Phenomena (CEIDP), 2012 Annual Report Conference on.

Ménégotto, J., Demont, P., & Lacabanne, C. (1999). *Study of dielectric relaxation processes of PET by dynamic dielectric and thermostimulated spectroscopies.* Paper presented at the Electrets, 1999. ISE 10. Proceedings. 10th International Symposium on.

Merrill, W. M., Diaz, R. E., LoRe, M. M., Squires, M. C., & Alexopoulos, N. G. (1999). Effective medium theories for artificial materials composed of multiple sizes of spherical inclusions in a host continuum. *IEEE Transactions on antennas and propagation, 47*(1), 142-148.

Miyairi, K. (1986). Low-frequency dielectric response of polyethylene terephthalate (PET) films. *Journal of Physics D: Applied Physics, 19*(10), 1973.

Miyake, A. (1959). The infrared spectrum of polyethylene terephthalate. I The effect of crystallization. *Journal of Polymer Science, 38*(134), 479-495.

Montanari, G., Mazzanti, G., & Simoni, L. (2002). Progress in electrothermal life modeling of electrical insulation during the last decades. *IEEE Transactions on Dielectrics and Electrical Insulation, 9*(5), 730-745.

Morel, J., Dung, P. N., & Joly, J. (1980). Thermal Aging of Bi-axially Orifnted Pet Films: Relation between Structural Changes and Dielectric Behavior. *IEEE Transactions on Electrical Insulation*(4), 335-339.

Mueller, D. H., & Krobjilowski, A. (2004). Improving the impact strength of natural fiber reinforced composites by specifically designed material and process parameters. *Int. Nonwovens J, 13*(4), 31-38.

Myroshnychenko, V., & Brosseau, C. (2009). Effective complex permittivity and continuum percolation analysis of two-phase composite media. *IEEE Transactions on Dielectrics and Electrical Insulation, 16*(4), 1209-1222.

Neagu, E., Pissis, P., Apekis, L., & Ribelles, J. G. (1997). Dielectric relaxation spectroscopy of polyethylene terephthalate (PET) films. *Journal of physics D: applied physics, 30*(11), 1551.

Ouchi, I., Hosoi, M., & Shimotsuma, S. (1977). Infrared spectra of poly (ethylene 2, 6-naphthalate) and some related polyesters. *Journal of Applied Polymer Science, 21*(12), 3445-3456.

Panthapulakkal, S., & Sain, M. (2007). Injection-molded short hemp fiber/glass fiber-reinforced polypropylene hybrid composites—Mechanical, water absorption and thermal properties. *Journal of Applied Polymer Science, 103*(4), 2432-2441.

Papageorgiou, G. Z., Tsanaktsis, V., & Bikiaris, D. N. (2014). Synthesis of poly (ethylene furandicarboxylate) polyester using monomers derived from renewable resources: thermal behavior comparison with PET and PEN. *Physical Chemistry Chemical Physics, 16*(17), 7946-7958.

Paquin, L., St-Onge, H., & Wertheimer, M. (1982). The Complex Permittivity of Polyethylene/Mica Composites. *IEEE Transactions on Electrical Insulation*(5), 399-404.

Pastore, C., & Kiekens, P. (2000). *Surface characteristics of fibers and textiles* (Vol. 94): CRC Press.

Patcheak, T. D., & Jabarin, S. A. (2001). Structure and morphology of PET/PEN blends. *Polymer, 42*(21), 8975-8985.

Paul, A., & Thomas, S. (1997). Electrical properties of natural-fiber-reinforced low density polyethylene composites: A comparison with carbon black and glass-fiber-filled low density polyethylene composites. *Journal of applied polymer science, 63*(2), 247-266.

Pietrasanta, A. S.-Y. (1996). RECYCLAGE DU POLY (ETHYLENE TEREPHTALATE) PAR GLYCOLYSE.

Poh, M. K. C. (2004). *Thermal and mechanical analysis of recycled glass filled PET for printer part.* Paper presented at the Asian Green Electronics, 2004. AGEC. Proceedings of 2004 International IEEE Conference on the.

Quintanilla, L., Alonso, M., Rodríguez-Cabello, J., & Pastor, J. (1996). Structural analysis of poly (ethylene terephthalate) reinforced with glass fiber: Thermal behavior and correlation between PA-FTIR and DSC measurements. *Journal of applied polymer science, 59*(5), 769-774.

Quintanilla, L., Rodríguez-Cabello, J., Jawhari, T., & Pastor, J. (1994). Structural analysis of poly (ethylene terephthalate) reinforced with glass fibre: 1. A photoacoustic Fourier transform infra-red study. *Polymer, 35*(3), 514-518.

Rand, B. P., & Richter, H. (2014). *Organic Solar Cells: fundamentals, devices, and upscaling*: CRC Press.

Richardson, G. C., & Sauer, J. A. (1976). Effect of reinforcement type on the mechanical properties of polypropylene composites. *Polymer Engineering & Science, 16*(4), 252-256.

Rothon, R. N. (2002). *Particulate fillers for polymers* (Vol. 12): iSmithers Rapra Publishing.

Roy, M., Nelson, J., MacCrone, R., Schadler, L., Reed, C., & Keefe, R. (2005). Polymer nanocomposite dielectrics-the role of the interface. *IEEE Transactions on Dielectrics and Electrical Insulation, 12*(4), 629-643.

Rueda, D., & Varkalis, A. (1995). Water sorption/desorption kinetics in poly (ethylene naphthalene-2, 6-dicarboxylate) and poly (ethylene terephthalate). *Journal of Polymer Science Part B: Polymer Physics, 33*(16), 2263-2268.

Sahu, S., & Broutman, L. (1972). Mechanical properties of particulate composites. *Polymer Engineering & Science, 12*(2), 91-100.

Sakamoto, S., & Sato, Y. (1988). Polyethylene naphthalate film: Google Patents.

Sanchez-Solis, A., Garcia-Rejon, A., & Manero, O. (2003). *Production of nanocomposites of PET-montmorillonite clay by an extrusion process.* Paper presented at the Macromolecular Symposia.

Sareni, B., Krähenbühl, L., Beroual, A., & Brosseau, C. (1996). Effective dielectric constant of periodic composite materials. *Journal of Applied Physics, 80*(3), 1688-1696.

Scheller, M., Wietzke, S., Jansen, C., & Koch, M. (2009). Modelling heterogeneous dielectric mixtures in the terahertz regime: a quasi-static effective medium theory. *Journal of physics D: applied physics, 42*(6), 065415.

Sellarès, J., Diego, J., Cañadas, J., Mudarra, M., Belana, J., Colomer, P., . . . Calventus, Y. (2012). Dielectric study of the glass transition of PET/PEN blends. *Journal of Physics D: Applied Physics, 45*(50), 505301.

Serdyuk, Y. V., Podoltsev, A. D., & Gubanski, S. M. (2004). Numerical simulations and experimental study of frequency-dependent dielectric properties of composite material with stochastic structure. *IEEE transactions on Dielectrics and Electrical Insulation, 11*(3), 379-392.

Shields, A., & Kemp, I. (2000). Degradation and breakdown of mica under partial discharge stressing: transverse discharges. *IEE Proceedings-Science, Measurement and Technology, 147*(5), 256-260.

Sillars, R. (1937). The properties of a dielectric containing semiconducting particles of various shapes. *Institution of Electrical Engineers-Proceedings of the Wireless Section of the Institution, 12*(35), 139-155.

Simoni, L. (1999). A general phenomenological life model for insulating materials under combined stresses. *IEEE transactions on dielectrics and electrical insulation, 6*(2), 250-258.

Singleton, A., Baillie, C., Beaumont, P., & Peijs, T. (2003). On the mechanical properties, deformation and fracture of a natural fibre/recycled polymer composite. *Composites Part B: Engineering, 34*(6), 519-526.

Sreekanth, M., Bambole, V., Mhaske, S., & Mahanwar, P. (2009). Effect of particle size and concentration of flyash on properties of polyester thermoplastic elastomer composites. *Journal of Minerals and Materials Characterization and Engineering, 8*(03), 237.

Std-930, I. (2004). IEEE guide for Statistical Analysis of Electrical Insulation Breakdown Data.

Stipho, H. (1998). Effect of glass fiber reinforcement on some mechanical properties of autopolymerizing polymethyl methacrylate. *The Journal of prosthetic dentistry, 79*(5), 580-584.

Sulyman, M., Haponiuk, J., & Formela, K. (2016). Utilization of Recycled Polyethylene Terephthalate (PET) in Engineering Materials: A Review. *International Journal of Environmental Science and Development, 7*(2), 100.

Tanaka, T. (2002). Aging of polymeric and composite insulating materials. Aspects of interfacial performance in aging. *IEEE Transactions on Dielectrics and Electrical Insulation, 9*(5), 704-716.

Torquato, S. (2000). Modeling of physical properties of composite materials. *International Journal of Solids and Structures, 37*(1), 411-422.

Torquato, S. (2013). *Random heterogeneous materials: microstructure and macroscopic properties* (Vol. 16): Springer Science & Business Media.

Tuncer, E. (2013). Dielectric mixtures: importance and theoretical approaches. *arXiv preprint arXiv:1304.5516*.

Tuncer, E., Gubański, S. M., & Nettelblad, B. (2001). Dielectric relaxation in dielectric mixtures: Application of the finite element method and its comparison with dielectric mixture formulas. *Journal of Applied Physics, 89*(12), 8092-8100.

Tuncer, E., Serdyuk, Y. V., & Gubanski, S. M. (2002). Dielectric mixtures--electrical properties and modeling. *arXiv preprint cond-mat/0111254*.

Ulrych, J., Polanský, R., & Pihera, J. (2014). *Dielectric analysis of polyethylene terephthalate (PET) and polyethylene naphthalate (PEN) films*. Paper presented at the Electric Power Engineering (EPE), Proccedings of the 2014 15th International Scientific Conference on.

Van Den Heuvel, C., & Klop, E. (2000). Relations between spinning, molecular structure and end-use properties of polyethylene naphthalate tyre yarns. *Polymer, 41*(11), 4249-4266.

Wang, C. S., Shieh, J. Y., & Sun, Y. M. (1998). Synthesis and properties of phosphorus containing PET and PEN (I). *Journal of applied polymer science, 70*(10), 1959-1964.

Wang, W., Yue, C., Gu, J., Du, J., Li, F., & Yang, K. (2015). Status assessment of polymeric materials in mineral oil under electro-thermal aging by frequency-domain dielectric spectroscopy. *IEEE Transactions on Dielectrics and Electrical Insulation, 22*(2), 831-841.

Ward, I. (1962). Optical and mechanical anisotropy in crystalline polymers. *Proceedings of the Physical Society, 80*(5), 1176.

Wei, Y., & Hsueh, K. F. (1989). Thermal analysis of chemically synthesized polyaniline and effects of thermal aging on conductivity. *Journal of Polymer Science Part A: Polymer Chemistry, 27*(13), 4351-4363.

Weick, B. L., & Bhushan, B. (1995). Shrinkage and viscoelastic behavior of alternative substrates for magnetic tapes. *IEEE transactions on magnetics, 31*(6), 2937-2939.

Willems, C. R. J. (1995). *A Dielectric study of melting and crystallization of semi-rigid and flexible-chain polymers.* TU Delft, Delft University of Technology.

Wu, F., & Whites, K. (2001). *Effective permittivity calculation for 2-D pseudorandom composite media.* Paper presented at the Antennas and Propagation Society International Symposium, 2001. IEEE.

Wu, S.-H., Wang, F.-Y., Ma, C.-C. M., Chang, W.-C., Kuo, C.-T., Kuan, H.-C., & Chen, W.-J. (2001). Mechanical, thermal and morphological properties of glass fiber and carbon fiber reinforced polyamide-6 and polyamide-6/clay nanocomposites. *Materials Letters, 49*(6), 327-333.

Yoshioka, T., Tsuji, M., Kawahara, Y., & Kohjiya, S. (2003). Morphological study by TEM on uniaxially oriented thin films of PET, PEN and their blends. *Polymer, 44*(26), 7997-8003.

Yu, W., & Mittra, R. (2001). A conformal finite difference time domain technique for modeling curved dielectric surfaces. *IEEE Microwave and Wireless Components Letters, 11*(1), 25-27.

Zhu, P., & Ma, D. (1997). Double cold crystallization peaks of poly (ethylene terephthalate)—1. Samples isothermally crystallized at low temperature. *European polymer journal, 33*(10), 1817-1818.

Zivanovic, S. S., Yee, K. S., & Mei, K. K. (1991). A subgridding method for the time-domain finite-difference method to solve Maxwell's equations. *IEEE Transactions on Microwave Theory and Techniques, 39*(3), 471-479.